

The Lifetimes and Time-Series of  
Chlorine and Fluorine Containing  
Gases from the Atmospheric Chemistry  
Experiment

Alexander Thomas Brown

Submitted for the degree of Doctor of Philosophy

Department of Physics

University of York

July, 2013



# Abstract

The research presented in this thesis is focused around environmentally important chlorine- and fluorine-containing species. The work in this thesis was carried out using data from the ACE-FTS. This work is divided into four principle areas of research.

The changes in the volume mixing ratio (VMR) of  $\text{CCl}_4$ ,  $\text{CF}_4$ , CFC-11, CFC-12, CFC-113,  $\text{CH}_3\text{Cl}$ ,  $\text{ClONO}_2$ ,  $\text{COF}_2$ ,  $\text{COCl}_2$ ,  $\text{COClF}$ , HCFC-22, HCFC-141b, HCFC-142b, HCl, HF and  $\text{SF}_6$  between 2004 and 2010 in the tropics are presented. In addition to calculating the changes in the VMR of these species during this time, this work allowed a quick comparison between profiles from the new Version 3 ACE-FTS retrieval and from the 3D chemical transport model SLIMCAT. This work acted as a rough validation of these new retrieval schemes. The trends calculated from SLIMCAT and ACE-FTS are in generally in good agreement. They show decreases in  $\text{CCl}_4$ , CFC-11, CFC-12, CFC-113 and  $\text{CH}_3\text{Cl}$  and increases in  $\text{CF}_4$ , HCFC-22, HCFC-141b and HCFC-142b. ACE-FTS shows no statistically significant change in  $\text{COCl}_2$  and  $\text{COClF}$ , whilst showing an increase in  $\text{COF}_2$ .

The total VMRs of stratospheric fluorine and chlorine have been calculated, allowing changes in the VMRs of total stratospheric fluorine and chlorine between 2004 and 2010 to be calculated. In addition to this, the changes in the global warming potential-weighted chlorine and fluorine are also presented. This value allows the radiative forcing effects of changes in the VMR of these species to be evaluated. In a similar manner the changes in the ozone depleting potential-weighted total chlorine are also presented.

Total fluorine is increasing in all latitudes. Global Warming Potential-weighted fluorine is increasing at a mean rate of  $3.85 \pm 0.07$  % per year in the

Northern Hemisphere and  $3.58 \pm 0.07$  % per year in the Southern Hemisphere. Radiative efficiency-weighted total fluorine show smaller increases of between  $0.23 \pm 0.11$  % per year and  $0.45 \pm 0.11$  % per year. In the short term the changes in fluorine-containing species is having a small climatological effect whilst in the long term these changes will have a more significant climatological effect.

Total chlorine is decreasing in all latitude bands. Both the global warming potential- and radiative forcing-weighted chlorine is decreasing. Global warming potential-weighted chlorine is decreasing by  $0.31 \pm 0.08$  % per year in the northern hemisphere and  $0.23 \pm 0.08$  % per year in the southern hemisphere. The changes in radiative efficiency-weighted chlorine are smaller with decreases of  $0.11 \pm 0.04$  % per year in the northern hemisphere and  $0.06 \pm 0.12$  % per year in the southern hemisphere. When considered together these results suggest that in the short term there has been very little, if any, change in climatologically effective chlorine. However, in the long term the reduction in the emissions of long lived CFCs and halons will produce a small reduction in the climatological effect of chlorine containing species.

Finally, the stratospheric lifetimes of CFC-12 (113  $\pm$  26 (18) years), CCl<sub>4</sub> (35  $\pm$  11 (7) years), CH<sub>4</sub> (195  $\pm$  75 (42) years), CH<sub>3</sub>Cl (69  $\pm$  65 (23) years) and N<sub>2</sub>O (123  $\pm$  53 (28) years) have been calculated, by correlating the stratospheric VMR of the species of interest against the VMR of CFC-11 at the same altitude.

# Table of Contents

|     |   |    |
|-----|---|----|
| 1   | Introduction  | 19 |
| 2   | The Atmosphere  | 28 |
| 2.1 | The Ever-changing Atmosphere                              | 29 |
| 2.2 | Atmospheric Structure                                     | 30 |
| 2.3 | Atmospheric transport                                     | 33 |
| 2.4 | Ozone Loss  | 39 |
| 2.5 | Greenhouse Effect   | 43 |
| 2.6 | The effect of the greenhouse effect on ozone depletion    | 47 |
| 2.7 | Summary   | 48 |
| 3   | The Atmospheric Chemistry Experiment                      | 50 |
| 3.1 | Introduction  | 50 |
| 3.2 | An introduction to the Atmospheric Chemistry Experiment   | 54 |
| 3.3 | Summary   | 68 |
| 4   | Trends in atmospheric halogen containing gases since 2004 | 69 |
| 4.1 | Introduction  | 69 |
| 4.2 | Measurements and Methods                                  | 73 |
| 4.3 | SLIMCAT 3D Chemical Transport Model                       | 80 |

|     |   |     |
|-----|---|-----|
| 4.4 | Results and Discussion  | 81  |
| 4.5 | Summary & Conclusion  | 100 |
| 5   | Global stratospheric fluorine inventories   | 105 |
| 5.1 | Introduction  | 105 |
| 5.2 | Fluorine Chemistry  | 108 |
| 5.3 | Fluorine Budget Method  | 110 |
| 5.4 | Results and Discussion  | 115 |
| 5.5 | Conclusions   | 132 |
| 6   | Global stratospheric chlorine inventories   | 134 |
| 6.1 | Introduction  | 134 |
| 6.2 | Chlorine Budget Calculation Method  | 136 |
| 6.3 | Results and Discussion  | 140 |
| 6.4 | Conclusion  | 161 |
| 7   | Stratospheric lifetimes of CFC-12, CCl <sub>4</sub> , CH <sub>4</sub> , CH <sub>3</sub> Cl and N <sub>2</sub> O | 164 |
| 7.1 | Introduction  | 164 |
| 7.2 | Calculating stratospheric lifetimes using correlations with CFC-11  | 167 |
| 7.3 | Results and Discussion  | 173 |
| 7.4 | Conclusion  | 192 |

|     |   |     |
|-----|---|-----|
| 8   | Conclusion  | 194 |
| 8.1 | Trends in atmospheric halogen containing gases since 2004   | 195 |
| 8.2 | Global stratospheric fluorine inventories for 2004 to 2009  | 197 |
| 8.3 | Global stratospheric chlorine inventories for 2004 to 2009  | 198 |
| 8.4 | Stratospheric lifetimes of CFC-12, CCl <sub>4</sub> , CH <sub>4</sub> , CH <sub>3</sub> Cl and N <sub>2</sub> O | 200 |
| 8.5 | Future Work   | 201 |
| 8.6 | Final Thoughts  | 204 |
|     | Appendix A  | 205 |
|     | Fluorine Budgets  | 205 |
|     | Appendix B  | 221 |
|     | Chlorine Budgets  | 221 |
|     | Appendix C  | 257 |
|     | CFC-11 correlation plots  | 257 |
|     | Appendix D  | 278 |
|     | Comparison plots of lifetimes and correlations  | 278 |
|     | Appendix E  | 281 |
|     | The derivation of the new equation for the steady-state correlations<br>for the lifetimes calculations          | 281 |
|     | References  | 283 |

# List of Figures

|   |    |
|---|----|
| Figure 1.1: The impact of the Montreal Protocol and Molina and Rowland seminal paper.....                                 | 25 |
| Figure 2.1: The composition of the atmosphere at the Earth's surface .....  | 30 |
| Figure 2.2: The vertical profile of the temperature of the Earth's atmosphere .....                                       | 31 |
| Figure 2.3: Vertical transport in the troposphere .....   | 36 |
| Figure 2.4: Atmospheric transport in the upper troposphere-lower stratosphere .....                                       | 37 |
| Figure 2.5: The main vibrational modes of water .....   | 44 |
| Figure 2.6: Changes in the mean global temperature between 1855 and 2005.....   | 45 |
| Figure 3.1: Top panel: The limb of the atmosphere .....   | 52 |
| Figure 3.2: A schematic of the Fourier Transform Spectrometer which is on board the Atmospheric Chemistry Experiment..... | 56 |
| Figure 3.3: The latitude coverage of ACE over the course of a year .....  | 58 |
| Figure 3.4: An ACE-FTS spectrum from December 2003.....   | 59 |
| Figure 4.1: Mean global surface mixing ratio of some halogen-containing species as measured by the NOAA and AGAGE .....   | 71 |
| Figure 4.2: The positions of the ACE-FTS occultations during 2005.....  | 73 |

|  |    |
|--|----|
| Figure 4.3: The positions of the occultations used in this study .....   | 74 |
| Figure 4.4: The vertical profile of CFC-12 in 2005 between the latitudes of 30° N and 30° S.....   | 77 |
| Figure 4.5: The difference between the mean CFC-11 profile from evening and morning profiles. The error bars shown are the standard deviation of the data..... | 79 |
| Figure 4.6: Average vertical profile of carbon tetrachloride, carbon tetrafluoride, methyl chloride & sulphur hexafluoride .....                               | 84 |
| Figure 4.7: Volume mixing ratio of carbon tetrachloride, carbon tetrafluoride, methyl chloride & sulphur hexafluoride .....                                    | 85 |
| Figure 4.8: Average vertical profile of CFC-11, CFC-12 and CFC-113.....  | 88 |
| Figure 4.9: Volume mixing ratio of CFC-11, CFC-12 & CFC-113.....   | 89 |
| Figure 4.10: Average vertical profile of HCFC-22, HCFC-141b and HCFC-142b .....  | 92 |
| Figure 4.11: Volume mixing ratio of HCFC-22, HCFC-141b & HCFC-142b.....  | 93 |
| Figure 4.12: Average vertical profile of phosgene from ACE and carbonyl chlorofluoride, carbonyl fluoride & chlorine nitrate.....                              | 96 |
| Figure 4.13: Volume mixing ratio of phosgene, carbonyl chlorofluoride, carbonyl fluoride & chlorine nitrate .....  | 97 |
| Figure 4.14: Average vertical profile of hydrogen fluoride & hydrogen chloride.....  | 99 |

|   |     |
|---|-----|
| Figure 4.15: Volume mixing ratio of hydrogen fluoride and hydrogen chloride.....  | 100 |
| Figure 5.1: The extended and un-extended ACE-FTS profiles of CFC-11 and COF <sub>2</sub> along with the accompanying SLIMCAT profile.....             | 113 |
| Figure 5.2: The profiles of the total fluorine contribution of species retrieved from ACE-FTS spectra and SLIMCAT to the total fluorine.....          | 118 |
| Figure 5.3: The fluorine budgets from 2004 to 2009 in latitude bands 30° N - 70° N and 0° - 30° N.....  | 119 |
| Figure 5.4: The fluorine budgets from 2004 to 2009 in latitude bands 0° - 30°S and 30°S - 70°S.....   | 120 |
| Figure 5.5: The mean profile of CFC-12, COF <sub>2</sub> , HCFC-22, HF, HCFCs & HFCs .....  | 123 |
| Figure 5.6: The trends in the mean total stratospheric fluorine between 2004 and 2009.....  | 126 |
| Figure 5.7: The trends in the radiative efficiency-weighted total fluorine mean between 2004 and 2009.....  | 130 |
| Figure 5.8: The trends in the GWP-weighted total fluorine mean between 2004 and 2009.....   | 131 |
| Figure 6.1: The extended and un-extended ACE-FTS profiles of CCl <sub>4</sub> and COCl <sub>2</sub> along with the accompanying SLIMCAT profile ..... | 139 |
| Figure 6.2: The profiles of the total chlorine contribution of species retrieved from ACE-FTS spectra and SLIMCAT to the total fluorine.....          | 142 |

|  |     |
|--|-----|
| Figure 6.3: The total chlorine, inorganic chlorine and organic chlorine profiles between 70° and 30° in the northern hemisphere. ....  | 143 |
| Figure 6.4: The mean morning profiles of inorganic chlorine species. ....  | 144 |
| Figure 6.5 The mean profile of CFC-12, CFC-11, CCl <sub>4</sub> , CH <sub>3</sub> Cl, HCFCs, HCl, ClONO <sub>2</sub> and ClO calculated from all morning data in the 70°N to 30°N latitude range. ....                               | 148 |
| Figure 6.6: The trends in the mean total stratospheric chlorine between 2004 and 2009 for different regions. ....  | 151 |
| Figure 6.7: The trends in the radiative efficiency-weighted total chlorine mean between 2004 and 2009. ....  | 156 |
| Figure 6.8: The trends in the GWP-weighted total chlorine between 2004 and 2009. ....  | 157 |
| Figure 6.9: The trends in the ODP weighted total chlorine between 2004 and 2009. ....  | 161 |
| Figure 7.1: Correlations between the VMRs of CFC-12, CCl <sub>4</sub> , CH <sub>4</sub> , CH <sub>3</sub> Cl and N <sub>2</sub> O and CFC-11 for the data from the northern hemisphere during the stratospheric winter of 2008. .... | 176 |

# List of Tables

|   |     |
|---|-----|
| Table 1.1: The Montreal Protocol: Phase-out dates .....   | 23  |
| Table 2.1: The Ozone Depleting Potential of a number of atmospheric species. ....   | 42  |
| Table 2.2: The global warming potential, on a 20-year timescale, radiative efficiencies and lifetimes of some of the species used in this research.....   | 46  |
| Table 4.1: The number of ACE v.3 vertical profiles used in this study for each year .....   | 75  |
| Table 4.2: The halogen containing species currently retrieved routinely from ACE-FTS data and their maximum and minimum retrieval altitudes and the altitudes between which means were calculated in this study ..... | 78  |
| Table 4.3: Results of trend analysis on ACE-FTS data of halogen containing molecules .....  | 101 |
| Table 5.1: The retrieval altitudes of the fluorine-containing species used in this study .....  | 111 |
| Table 5.2: The number of ACE-FTS occultations used for each latitude band and year .....  | 112 |
| Table 5.3: The slopes of the total fluorine profile and the mean stratospheric VMR of the fluorine budgets .....  | 117 |
| Table 5.4: The slopes of the correlation between fluorine source species .....  | 122 |

|   |     |
|---|-----|
| Table 5.5: The trends in mean VMR of stratospheric total fluorine, between 2004 and 2009 .....  | 125 |
| Table 5.6: The global warming potential-weighted trends in the total fluorine mass and the radiative efficiency-weighted trends in the total fluorine volume mixing ratio between 2004 and 2009 ..... | 129 |
| Table 6.1: The ACE-FTS retrieval altitude ranges of the chlorine containing species used in this study .....  | 137 |
| Table 6.2: The mean stratospheric total chlorine VMR in ppb .....   | 145 |
| Table 6.3: The vertical slopes of the total chlorine profiles for both evening and morning occultations in the 4 latitude bins used in this study.....  | 146 |
| Table 6.4: The correlation between organic chlorine species .....   | 147 |
| Table 6.5: The trends in the mean stratospheric total chlorine VMR between 2004 and 2009 for different regions and for morning, evening and combined morning and evening occultations .....           | 152 |
| Table 6.6 The trends in the mean stratospheric total chlorine VMR between 2004 and 2009 for different regions and for morning, evening and combined morning and evening occultations .....            | 154 |
| Table 6.7: The RE- and GWP-weighted trends in the total chlorine VMR between 2004 and 2009 .....  | 158 |
| Table 6.8: The ozone depletion potential-weighted trends in the total chlorine VMR between 2004 and 2009 .....  | 160 |
| Table 7.1: The slope of the age of air against the VMR of CFC-11 at the tropopause.....   | 171 |

|   |     |
|---|-----|
| Table 7.2: The effective linear growth rates ( $\gamma_0$ ) in % Year <sup>-1</sup> of CFC-11, CFC-12, CCl <sub>4</sub> , CH <sub>4</sub> , CH <sub>3</sub> Cl and N <sub>2</sub> O .....     | 172 |
| Table 7.3: The slopes of the correlations of CFC-12, CH <sub>3</sub> Cl, CCl <sub>4</sub> , N <sub>2</sub> O and CH <sub>4</sub> with CFC-11, extrapolated to the tropopause .....            | 178 |
| Table 7.4: The mean VMR at the tropopause ( $\sigma_0$ ). .....   | 180 |
| Table 7.5: The corrected slopes of the correlations of CFC-12, CCl <sub>4</sub> , CH <sub>4</sub> , CH <sub>3</sub> Cl and N <sub>2</sub> O with CFC-11, extrapolated to the tropopause. .... | 181 |
| Table 7.6: Mean atmospheric VMR ( $\sigma$ ). .....   | 184 |
| Table 7.7: The calculated lifetimes of CFC-12, CCl <sub>4</sub> , CH <sub>4</sub> , CH <sub>3</sub> Cl and N <sub>2</sub> O using a CFC-11 lifetime of 45 years.....                          | 185 |
| Table 7.8: The mean lifetimes of CFC-12, CH <sub>3</sub> Cl, CCl <sub>4</sub> , N <sub>2</sub> O and CH <sub>4</sub> using a CFC-11 lifetime of 45 years.....                                 | 188 |
| Table 7.9 The ratio of $\tau_{\text{CFC}} - \tau_{\text{CFC-11}}$ for CFC-12, CCl <sub>4</sub> , CH <sub>4</sub> , CH <sub>3</sub> Cl and N <sub>2</sub> O.....                               | 191 |

# Acknowledgements

My university education would not have been possible without the truly inspiring teaching of Mr Keith Owen Price, now sadly departed. Everything that has followed grew from the seeds of his teaching.

This work would not have been possible without the support and guidance of Professor Peter Bernath, who gave me the opportunity to work on such an enjoyable and exciting project, and Professor Sarah Thompson who has ensured that this work has continued to its end. I would also like to thank the many co-authors with whom I've had the pleasure of working, in particular Professors Martyn Chipperfield and Michael Volk who have been constant sources of advice and direction. The funding I received from the National Centre for Earth Observation not only allowed me to carry out my research, but also made it possible for me to visit conferences with some of the world's leading scientists; an opportunity that I'll always be grateful for.

The members of the physical chemistry office, together with Prof. Bernath, ensured that I always looked forward to coming to work. I would like to especially thank Dr Richard Lidster and Dr Robert Hargreaves without whose 'witticisms', life in the office would have been significantly duller. The friendship offered by Drs Allen, Gonzalez-Abad, Lidster and Hargreaves at the start of my PhD and the continued friendship of James Brooke was as good as I could ever have hoped for.

Outside of the world of science, the support of my family and friends has been more greatly valued than I can comfortably express. Will, Stell, Mick, Jen and John, this would not have been possible without your love and constant belief in me. That goes for Benjamin and Lisa Lefebvre as well.

Finally, I'd like to thank my wonderful wife Louise, your love and support have carried me through good and bad times. Without you this thesis would never have been completed. I can never fully repay you for this, but I will always value everything that you've done.

Thank you all!

# Declaration of Authorship

I declare that the work presented in this thesis, except where otherwise stated, is based on my own research and has not been submitted previously for a degree at this or any other university.

Chapter 4 has been published in the Journal of Quantitative Spectroscopy:

Brown, A. T., Chipperfield, M. P., Boone, C., Wilson, C., Walker, K. A., and Bernath, P. F.: Trends in atmospheric halogen containing gases since 2004, *Journal of Quantitative Spectroscopy and Radiative Transfer*, 112, 2552-2566, 10.1016/j.jqsrt.2011.07.005, 2011.

Chapter 5 has been published in Atmospheric Chemistry and Physics:

Brown, A. T., Chipperfield, M. P., Richards, N. A. D., Boone, C., and Bernath, P. F.: Global stratospheric fluorine inventories for 2004–2009 from Atmospheric Chemistry Experiment Fourier Transform Spectrometer (ACE-FTS) measurements, *Atmospheric Chemistry and Physics*, 14, 267-282, 2014, doi:10.5194/acp-14-267-2014

Chapter 6 has been submitted for publication as a discussion paper in Atmospheric Chemistry and Physics Discussions:

Brown, A. T., Chipperfield, M. P., Dhomse, S., Boone, C., and Bernath, P. F.: Global stratospheric chlorine inventories for 2004–2009 from Atmospheric Chemistry Experiment Fourier Transform Spectrometer (ACE-FTS) measurements, *Atmospheric Chemistry and Physics Discussions*, 13, 23491-23548, 2013, doi:10.5194/acpd-13-23491-2013

Chapter 7 has been published in Atmospheric Chemistry and Physics:

Brown, A. T., Volk, C.M., Schoeberl, M. R., Boone, C. D., and Bernath, P. F.: Stratospheric lifetimes of CFC-12, CCl<sub>4</sub>, CH<sub>4</sub>, CH<sub>3</sub>Cl and N<sub>2</sub>O from measurements made by the Atmospheric Chemistry Experiment-Fourier Transform Spectrometer (ACE-FTS), Atmospheric Chemistry and Physics, 13, 1-30, 2013 doi:10.5194/acp-13-1-2013

# 1

## Introduction

When historian J. R. McNeill came to write his history of the 20th Century he chose to do so by focusing on the environmental history of the century. McNeill (2001) wrote:

“In time, I think, this [human’s effect on the environment] will appear as the most important aspect to twentieth-century history, more so than World War II, the communist enterprise, the rise of mass literacy, the spread of democracy, or the growing emancipation of women.”

We are now over a decade into the 21<sup>st</sup> Century and mankind’s effects on the environment continues apace. In no area has the effect of man been better illustrated than the atmosphere.

The start of the industrial revolution represents the beginning of large scale changes in the atmosphere due to human actions. The driving force of the industrial revolution was the steam engine which allowed mechanical energy

## Introduction

to be produced from boiling water by burning coal. Carbon dioxide is one of the many particulates and gases which are released into the atmosphere when coal undergoes combustion (Wayne, 2000a). The use of coal in powering the steam engines also had an effect on the atmospheric concentrations of methane. Coal mining releases pockets of methane into the atmosphere which have previously been trapped beneath the ground. Both of these species act as potent greenhouse gases by absorbing infra-red radiation in the atmosphere (see Chapter 2) gradually causing the temperature of the atmosphere to warm. As steam engines became more widespread, coal was consumed in ever increasing quantities releasing greater amounts of these gases. At the same time developments in agricultural practices, such as the growing sizes of livestock herds and cultivated rice paddies, were increasing the emissions of methane. Forests naturally remove carbon dioxide from the atmosphere during photosynthesis (Baker et al., 2004). However throughout the industrial revolution major deforestation was occurring across the developing world (McNeill, 2001). This had the effect of further increasing the concentration of atmospheric carbon dioxide.

Throughout the 20th century human society continued to release a large number of species into the atmosphere. These chemicals could have varying effects on the environment. Some, such as sulphur dioxide, would dissolve in rain to form acid rain which would go on to destroy both plants and buildings. Some bromine- and chlorine-containing species of chemicals were found to be extremely unreactive making them perfect for use in industrial, commercial and domestic situations. These species would eventually be found to be destroying the ozone layer (Molina et al., 1974; Farman et al., 1985), with consequences for both human health and the environment. Most recently attention has turned to the effect of anthropogenic emission on the global climate. Within the last 50 years global temperatures have been rising at an average rate of  $0.13\text{ }^{\circ}\text{C}$  per decade (Solomon et al., 2007). Rising emissions of

## Introduction

greenhouse gases from human activity are thought to be to blame for this. The Intergovernmental Panel on Climate Change (IPCC) was set up by the United Nations Environmental Program (UNEP) and the World Metrological Organisation (WMO) in 1988. The aim of the program is to provide policy makers with scientific evidence of the changes in the global climate. In order to do this, the IPCC produces an assessment every six years which presents scientific evidence for the state of the climate. The next IPCC assessment report is due in late 2013.

In the 1930s the American scientist, Thomas Midgley, produced the first chlorofluorocarbon (CFC), which was known as Freon. This chemical proved to be chemically inert and rapidly replaced more flammable and toxic chemicals which were being used for a diverse number of jobs such as in aerosol propellants, refrigerators and foam manufacture. However, unbeknown to the scientific community, these chemicals were not chemically inert throughout the atmosphere. In fact, in 1973 a paper was published claiming that atmospheric CFC-11 posed “no conceivable hazards” (Lovelock et al., 1973). Once they reached the stratosphere they are broken down by ultraviolet (UV) light coming from the Sun. The breaking up of these chemicals releases chlorine atoms into the stratosphere. The chlorine atoms go on to catalyse reactions which result in the destruction of ozone. The ozone layer acts as a barrier to UV radiation which can have an extremely harmful effect on both humans, where it can cause skin cancer, cataracts and other medical ailments, and ecosystems, where it can kill phytoplankton (Smith et al., 1992) which act as the building block for many oceanic ecosystems. It was not until 1974 that the scientists Mario Molina and Sherwood Rowland published a paper in *Nature* which suggested that chlorine in chemicals emitted at ground level could be causing a reduction in the concentration of atmospheric ozone (Molina et al., 1974). The first evidence of atmospheric ozone loss came from observations made by Farman, Gardiner and Shanklin of the stratosphere

## Introduction

above Antarctica, published in 1985 (Farman et al., 1985). The international community reacted rapidly to these observations with the United Nations Environmental Programme's (UNEP) 1985 Vienna convention on ozone depletion (Anderson et al., 2002a). International efforts eventually led to the ratification of the Montreal Protocol on Substances which deplete the ozone layer in 1987.

The Montreal Protocol and its subsequent amendments were designed to reduce the uses, and thus the emissions, of chlorine- and bromine-containing chemicals. It is the most widely ratified treaty in the history of the United Nations with 197 nations as signatories. These nations are divided into two groups, Article 5 and non-Article 5 countries. Non-Article 5 countries are developing countries whose consumption of ozone depleting substances (ODS) was less than 0.3 kilograms per capita when the Montreal Protocol came into effect. This division ensured that these countries could continue to meet their domestic needs whilst gradually phasing out their use in these countries (Anderson et al., 2002b). The Montreal Protocol divides ODS into a number of different groups (annexes). Each group of gases has a particular phase out target which can be seen in Table 1.1. Grouping the species in this way allowed countries to reduce their production and consumption of some species whilst continuing to use other species depending on their economic needs. This gave the countries sufficient time to find replacement species whilst simultaneously reducing the total chlorine and bromine being emitted into the atmosphere. A country for which this was particularly important was Japan (Anderson et al., 2002b). An important part of the Japanese economy is its electronics industries, which used large amounts of CFC-113 as a solvent. Grouping CFC-113 with other similar CFCs in Annex A Group 1 (see Table 1.1) allowed Japan to reduce its overall uses of this group of substances by reducing the production and consumption of other CFCs from this group whilst continuing to use CFC-113 until a replacement could be found (Anderson et al., 2002b).

## Introduction

Table 1.1: The Montreal Protocol: Phase-out dates. The phase-out dates in the consumption and production of some of the species controlled under the Montreal Protocol used in this work (Retrieved from <http://www.unep.org/ozone/issues.shtml>)

| Annex A Group 1 |                 |                 |
|-----------------|-----------------|-----------------|
|                 | Non-Article 5   | Article 5       |
| Freeze          | July 1, 1989    | July 1, 1999    |
| 100 % Reduction | January 1, 1996 | January 1, 2010 |
| Annex B Group 2 |                 |                 |
|                 | Non-Article 5   | Article 5       |
| 85 % Reduction  | January 1, 1995 | January 1, 2005 |
| 100 % Reduction | January 1, 1996 | January 1, 2010 |
| Annex A Group 2 |                 |                 |
|                 | Non-Article 5   | Article 5       |
| Freeze          | January 1, 1992 | January 1, 2002 |
| 100 % Reduction | January 1, 1994 | January 1, 2010 |
| Annex C Group 1 |                 |                 |
|                 | Non-Article 5   | Article 5       |
| Freeze          | 1996            | 2016            |
| 100 % Reduction | January 1, 2030 | January 1, 2040 |

|                 |  |
|-----------------|--|
| Annex A Group 1 | CFC-11, CFC-12, CFC-113, CFC-114 & CFC-115 |
| Annex A Group 2 | Halon-1211, Halon-1301 & Halon-2402        |
| Annex B Group 2 | Carbon Tetrachloride                       |
| Annex C Group 1 | HCFCs                                      |

## Introduction

This treaty has proved highly effective in reducing the atmospheric concentrations of chlorine- and bromine-containing species. Figure 1.1 shows the success that the Montreal Protocol has had in reducing both the production and the atmospheric volume mixing ratio (VMR) of CFC-11 and CFC-12 (Velders et al., 2007). In Velders et al.'s seminal paper on the "Importance of the Montreal Protocol on protecting climate" the production and atmospheric VMRs of these species were simulated in worlds without Molina and Rowland's paper where the world remained oblivious to the ozone destruction, and without the strictures of the Montreal Protocol. Since these species are also powerful greenhouse gases the Montreal Protocol has had considerably more impact on reducing greenhouse gas emissions than the Kyoto Protocol (Velders et al., 2007).

One of the implications of the Montreal Protocol was the gradual replacement of chlorine-containing species with fluorine-containing species which did not contain chlorine. Initially CFCs were replaced with hydrochlorofluorocarbons (HCFCs) which are similar chemically to CFCs but contain additional hydrogen. This hydrogen allows HCFCs to react with hydroxyl radicals (OH) in the troposphere; these reactions decrease the amount of chlorine that reaches the stratosphere relative to CFCs. HCFCs are now being replaced by hydrofluorocarbons (HFCs) which do not contain chlorine and so are not considered to be ozone-depleting substances. These HFCs are extremely powerful greenhouse gases and their emissions have been growing in recent years (e.g Stohl et al. (2009); Miller et al. (2010); Grealley et al. (2007)). According to Velders et al. (2009) rising HFC emissions could have a serious impact on climate change; by 2050 the global warming potential weighted HFC emissions could be between 9 % and 19 % of carbon dioxide emissions.

## Introduction

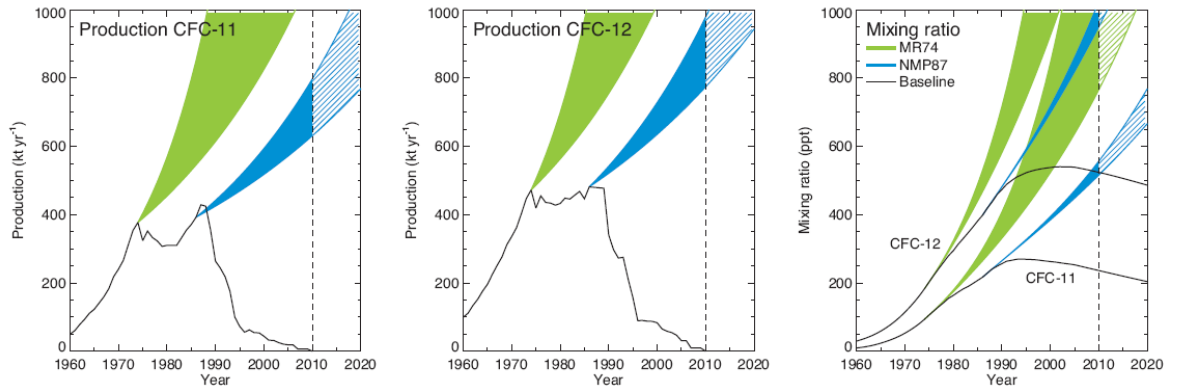


Figure 1.1: The impact of the Montreal Protocol and Molina and Rowland seminal paper. The scenarios used by Velders et al. (2007) when assessing CFC-11 and CFC-12 production and atmospheric mixing ratio (ppt). The green shaded region represents the possible outcome in a world without the 1974 paper of Molina and Rowland, and the Montreal Protocol. The blue shaded area represents the possible outcome in a world with Molina and Rowland's paper but without the implementation of the Montreal Protocol. The baseline data comes from model simulations used for the 2006 scientific assessment of ozone depletion.

The Montreal Protocol stipulates that every four years a scientific assessment be carried out into ozone depletion. This assessment is carried out by the World Metrological Organisation (WMO). Due to the potentially large scale ecological and health effects of the loss of the ozone layer. One of the results, presented in each of these reports, is the expected date for the recovery of the ozone layer. Their predictions come from the analysis of atmospheric models which require high quality data in order that they can accurately predict changes in ozone. A full budget for the VMR of chlorine in the stratosphere and, more importantly, how this VMR is changing over time, is vital for accurate simulation. In addition to this, accurate lifetimes for the ozone

## Introduction

depletion species are also required so that their changes over time can be accurately simulated.

This thesis presents four related investigations which use measurements taken by the Atmospheric Chemistry Experiment Fourier Transform Spectrometer (ACE-FTS) of long-lived halogen-containing species. Trends in the atmospheric concentrations of halogen-containing species between 2004 and 2010 were calculated using ACE-FTS data and compared with those from the SLIMCAT Chemical Transport Model (CTM). As has been discussed previously, in order that predictions can be made on the recovery of the ozone layer it is necessary that the total stratospheric chlorine is accurately known. ACE-FTS is ideally suited to this task as it has a high vertical resolution in the stratosphere and measures a large number of chlorine containing species. A stratospheric chlorine budget has therefore been calculated and is presented here. The effect of changes in chlorine over this time on ozone has been evaluated using ozone depleting potential weighted trends. Chlorine containing species are not only ozone destroying substances they are also powerful greenhouse gases (see Section 2.5). The changes in chlorine have also been evaluated in terms of their effect on the climate using their radiative efficiencies and their global warming potentials. Alongside this work a fluorine budget has been calculated. Fluorine containing species are extremely potent greenhouse gases which, with the implementation of the Montreal Protocol, are increasing in volume mixing ratio in the atmosphere. It is therefore important to evaluate how the changes in the volume mixing ratio of fluorine have affected the climate. Once more global warming potential- and radiative efficiency-weighted trends have been calculated to do just this. Finally there has been a global effort to better evaluate the lifetime of chlorine species (for the reasons described above and in Chapter 7) which are involved in ozone loss. Once more ACE-FTS is ideally positioned to carry out this work. The stratospheric lifetimes of CFC-12, carbon tetrachloride, methyl chloride,

## Introduction

nitrous oxide and methane have been calculated using tracer-tracer correlations with CFC-11. This work contributed to the Stratospheric Processes And their Role in Climate (SPARC) reassessment of the stratospheric lifetimes of halogen source gases. Some of the work presented here will feature in the 2014 WMO assessment on ozone depletion.

# 2

## The Atmosphere

The atmosphere is in a perpetual state of change. Dynamic meteorological events, such as winds and storms, perturb the atmosphere at a number of altitudes. Convective transport carries air parcels from the ground to the tropopause. Breaking large scale planetary waves within the stratosphere mix the air parcels in this region. The atmosphere is not simply changing dynamically; its atmospheric constituents are also changing. This chapter presents a brief description of the physical processes which ensure this continuing dynamism alongside a description of the changes in the composition of the atmosphere. The chapter begins with a short description of the evolution and the current composition of the atmosphere. Subsequently the temperature profile which gives the atmosphere its structure is discussed. The dynamics of the main atmospheric layers (the troposphere and stratosphere) measured in this work are then discussed. The chapter concludes with a discussion on ozone loss and the greenhouse effect.

## ***2.1 The Ever-changing Atmosphere***

The Earth's primordial atmosphere was formed from the gases trapped by the accretion of small rocks and dust which formed the Earth. This primordial atmosphere was comprised almost entirely of hydrogen and helium with only trace amounts of other gases (Freedman et al., 2005). The Earth did not have sufficient mass to prevent the escape of hydrogen and helium and so these gases were mostly lost into space. As the molten surface of the Earth cooled, some of the atmospheric hydrogen bonded with oxygen forming water. As will be discussed in Section 2.5 water is a powerful greenhouse gas and so the atmosphere was warmed by its presence. As the Earth cooled further, water began to condense in the atmosphere forming oceans, lakes and rivers. The reduction in atmospheric water vapour led to a decrease in the greenhouse effect, in turn leading to further condensation, which caused further condensation and precipitation. This was a self-propagating process, which caused the Earth to enter the 'snowball Earth' phase. During this time the temperature of the Earth was such that all surface water froze.

The Earth would have remained in its frozen state had it not been for the large scale volcanic activity which was on-going at this time. This volcanic activity had the effect of releasing large amounts of carbon dioxide into the atmosphere. Carbon dioxide is a powerful greenhouse gas, and so an increase in the atmospheric concentration of this gas began to warm the atmosphere once more. As the atmosphere warmed, the ice began to melt releasing water vapour into the atmosphere, which also contributed to the warming of the atmosphere. At this point Earth had a carbon dioxide rich atmosphere, very similar to the atmosphere of the planet Venus today.

The advent of life once more changed the composition of the atmosphere. Rudimentary life relied on the process of photosynthesis to produce energy. In this process carbon dioxide and water react in the presence of sunlight to form

## The Atmosphere

sugar and oxygen. This oxygen was released into the atmosphere. At first the oxygen was trapped within rocks, however eventually, as the number of living organisms increased, the amount of oxygen being released was too great for it all to be trapped within rocks. In this way the concentration of oxygen in the atmosphere increased over time. Life continues to affect the concentration of gases in the atmosphere to this day. For example in the 10 years between 1995 and 2005 the concentration of atmospheric carbon dioxide has increased at a rate of 1.9 ppm per year, as an effect of human activity (Solomon, 2007).

The atmosphere is currently composed of 78.08 % nitrogen and 20.95 % oxygen, the remaining 0.97 % is composed primarily of argon, carbon dioxide and neon (see Fig. 2.1). Anthropogenic, biogenic and metrological cycles are constantly releasing and removing gases to and from the atmosphere.

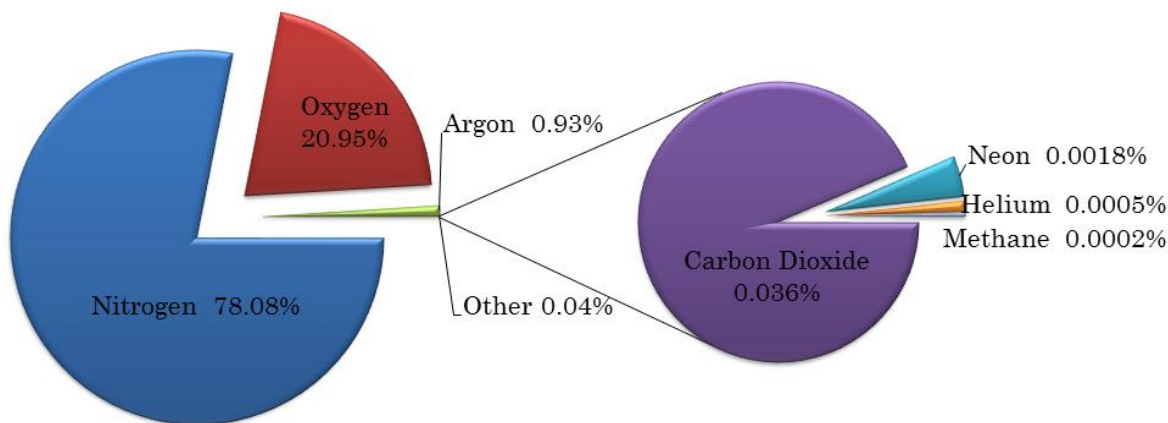


Figure 2.1: The composition of the atmosphere at the Earth's surface

## 2.2 Atmospheric Structure

The vertical profile of the temperature of the atmosphere varies with altitude. This variation with altitude allows the atmosphere to be divided into four distinct bands: the troposphere, stratosphere, mesosphere and thermosphere. These bands can be seen in Fig. 2.2. The areas of interest in this study are the troposphere and stratosphere.

## The Atmosphere

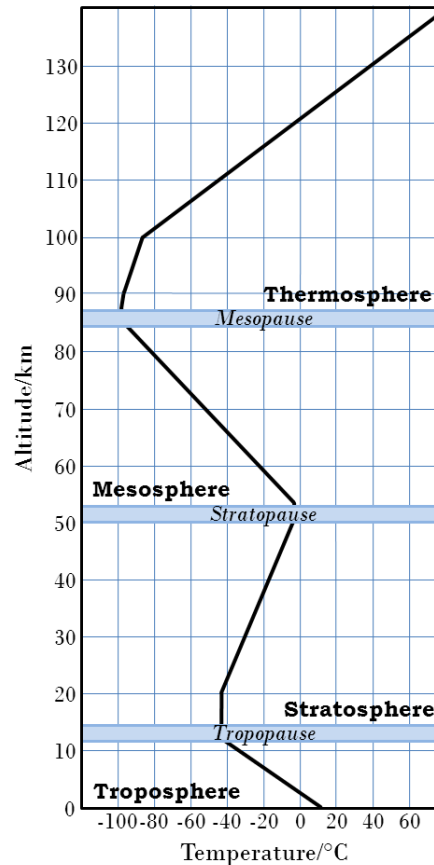


Figure 2.2: The vertical profile of the temperature of the Earth's atmosphere. This figure is based on an original figure from <http://www.srh.noaa.gov/jetstream/atmos/atmprofile.htm>

### 2.2.1 The Troposphere

The troposphere contains around 75 % of the mass of the atmosphere (Barry, 2007a). The lowest region of the troposphere is known as the boundary layer. The upper altitude limit of this region is between 30 m above oceans and 2-3 km above land in the summer. In this layer the motion of the air is due to the friction effects from the surface of the Earth. Above this layer is the free tropopause, an area where air mass transport is convective.

The surface of the Earth is warmed by the radiation coming from the Sun; the surface in return warms air in the lowest levels of the atmosphere. This

## The Atmosphere

warming causes the air to rise up through the troposphere. Since atmospheric pressure decreases with altitude as the air packet rises, its volume increases. This increase in volume causes the temperature of the air packet to decrease. This leads to a decrease in atmospheric temperature with altitude. The temperature of the atmosphere is not solely determined by adiabatic cooling of the air packet. The photolysis of ozone ( $O_3$ ) by ultraviolet (UV) radiation at higher altitudes releases energy warming the surrounding atmosphere (Holton, 2004a). This causes the temperature of the atmosphere to begin to increase rather than decrease. The point where this inversion occurs marks the upper limit of the troposphere and is known as the tropopause. The height of the tropopause is driven by the amount of convection in the troposphere. Since the surface temperature is higher in the tropics than at the poles there is far greater convection in these latitudes which increases the altitude of the tropopause.

### 2.2.2 The Stratosphere

The area of the atmosphere above the tropopause where the temperature continues to rise with altitude is the stratosphere. Since temperature increases with altitude, the air parcels do not mix vertically through convection. This makes the stratosphere extremely stable; it also produces the stratified nature which gives this region of the atmosphere its name. In the stratosphere vertical mixing occurs through the breaking of planetary scale Rossby waves (Plumb, 2002). This process is described in Section 2.3.3. This area of the atmosphere is of particular interest to atmospheric scientists as it is in this location that the ozone layer can be found. Above around 15 km above the poles and around 25 km at the equator, the VMR of ozone decreases. The warming of the atmosphere due to the photolysis of ozone can no longer compete with the adiabatic cooling of the atmosphere and so, once more, temperature decreases with altitude. The point at which the temperature

## The Atmosphere

begins to decrease is known as the stratopause. This denotes the boundary between the stratosphere and the mesosphere.

### **2.2.3 The Mesosphere and Thermosphere**

Above the stratopause, the temperature once more decreases with altitude. It is in the mesosphere that we find the coldest average temperatures in the atmosphere. Eventually the temperature profile of the atmosphere begins to increase once more, at the point called the mesopause. Above the mesopause, the temperature increases again. High energy UV radiation ionises and dissociates the few particles which are in this region causing a warming of the surrounding atmosphere. This region is known as the thermosphere (Barry, 2007a).

## ***2.3 Atmospheric transport***

Since ozone depleting substances (ODS) – see section 2.4 - have the most significant environmental effect in the stratosphere, this section will concentrate on vertical transport rather than horizontal transport. This section is divided into two: the vertical transport in the troposphere and in the stratosphere. There is a stark contrast in the vertical transport mechanism in the troposphere and stratosphere. Generally, vertical transport in the troposphere is driven by convection; whilst in the stratosphere it is wave-driven (Plumb, 2002). This section gives a brief description of both mechanisms, for a more detailed discussion the reader is directed to Barry (2007b) – for tropospheric transport, Plumb (2002) and Holton (2004a) – for stratospheric transport.

### 2.3.1 Troposphere

As can be clearly seen in Fig. 2.2, temperature decreases with altitude in the troposphere. The inversion of this temperature gradient at the tropopause prevents further convective transport above this height. Instead the air parcel will move towards the pole where the temperature is lower. This description suggests that air rising in the warm tropical troposphere would be carried polewards before subsiding in the poles due to the cooling of the air. This does not occur however, since in the model described above does not account for the Coriolis Effect.

When air moves from high- to low-pressure systems it does not travel directly between the two systems. Instead the air deflects, moving in curved paths, clockwise in the northern hemisphere and anti-clockwise in the southern hemisphere. This deflection is the result of the Coriolis Effect which is caused by the rotation of the Earth. The Earth revolves once every 24 hours; however the speed at which the Earth is rotating depends on latitude. The circumference of the Earth at the equator is larger than the circumference of the Earth at the poles. The whole of the Earth rotates in 24 hours, thus a point at the equator must rotate at a greater velocity than a point at the poles. This difference in rotation velocity causes particles, which are moving from the equator to the North Pole, to appear to deflect to the right. Particles moving equatorward from the North Pole also appear to deflect to the right. This occurs since the ground at the equator has rotated further during movement of the particle than the ground at the poles.

The Coriolis Effect increases with latitude causing the flow of air from the tropics to the pole to become unstable and break down. This occurs at 30° latitude (both north and south), where the air parcel will descend. This descending air produces a high pressure region and is in contrast to the low pressure region at the equator produced by the upwards vertical movement of

## The Atmosphere

the air parcels. This difference in atmospheric pressure between these two regions causes the air parcel to return to the equator. The deviation of this returning air towards the west by the Coriolis Effect produces the trade winds seen in this region.

The structure formed by the cycle, described above, between the equator and roughly 30° is known as a Hadley cell. A second cell-like structure can be seen at the poles where air at 60° is once more warmed by the surface and ascends through the troposphere. The vertical movement of this air is limited by the tropopause and at this altitude will move towards the pole. As the air moves towards the poles it cools and descends. Air flowing back towards the low pressure region, at 60°, from the pole will be deviated towards the west producing the polar easterlies. In between the polar and Hadley cells lies the mid-latitude cell. Air ascending with the ascending branch of the polar cell can be drawn towards the low pressure area produced by the descending branch of the Hadley cell.

The average time taken for an air parcel to be transported from the ground to the tropopause is approximately one month. The majority of the species studied in this work (excluding the HCFCs and CH<sub>3</sub>Cl) have extremely long tropospheric lifetimes since they are chemically inert. These species are therefore uniformly vertically mixed in the troposphere. Due to the temperature inversion at the tropopause, transport from the troposphere into the stratosphere takes significantly more time than transport through the troposphere, between five and ten years (Jacob, 1999).

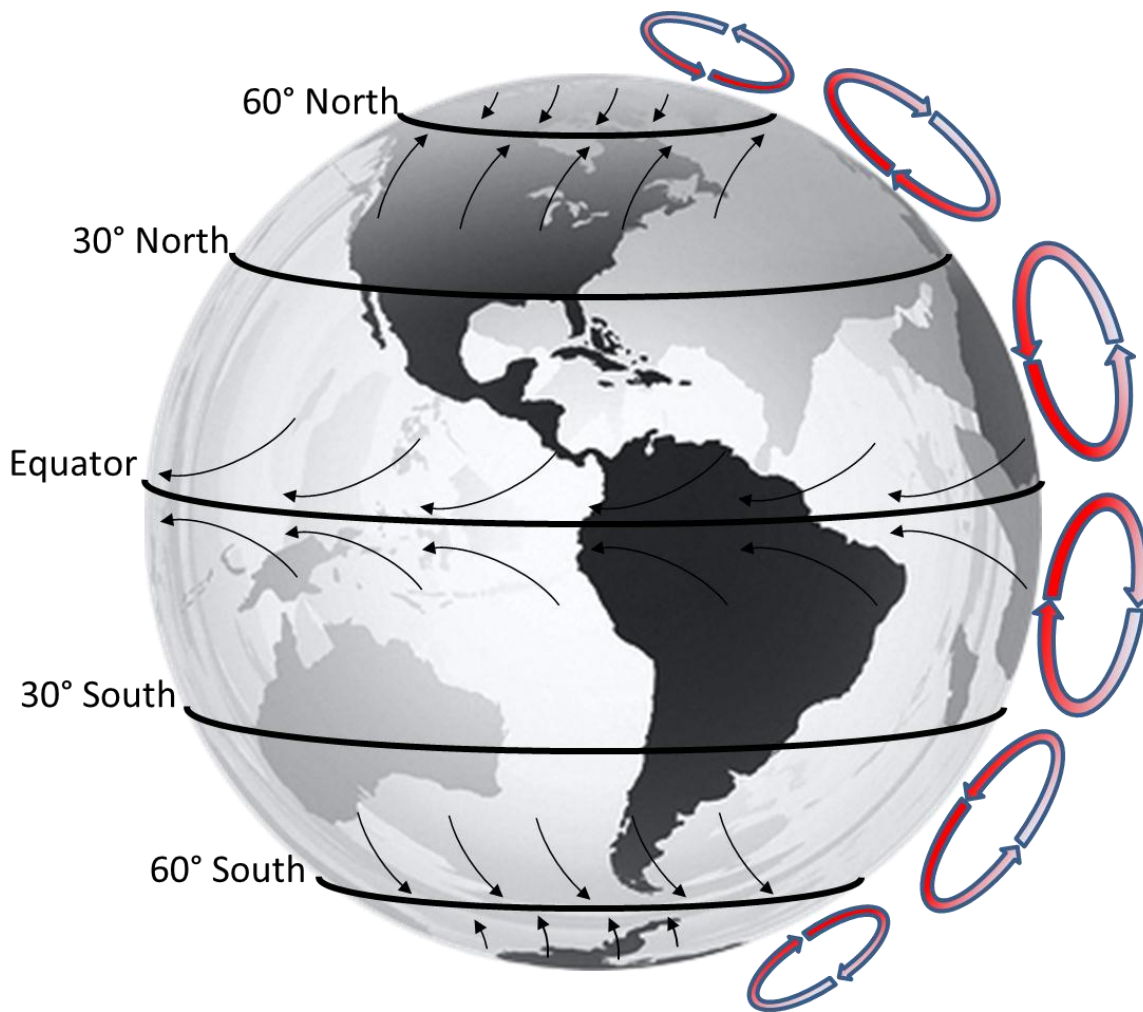


Figure 2.3: Vertical transport in the troposphere. There are three main convective cells which exist between the equator and 30° (Hadley cell), 30° and 60° (Ferrel cell) and 60° and 90° (Polar cell). The black arrows represent the surface wind direction at these points. (This figure is based on a figure from <https://courseware.e-education.psu.edu/courses/earth540/nasa.6-cell-model.jpg>)

### 2.3.2 Troposphere-Stratosphere Exchange

Since the majority of the species studied in this thesis are released at the surface it is now necessary to discuss how these species transfer from the troposphere into the stratosphere. As has been noted previously the majority of the species reach the stratosphere through powerful convective upwelling in the tropics. There are however a

## The Atmosphere

number of different ways by which species can enter (and exit) the stratosphere.

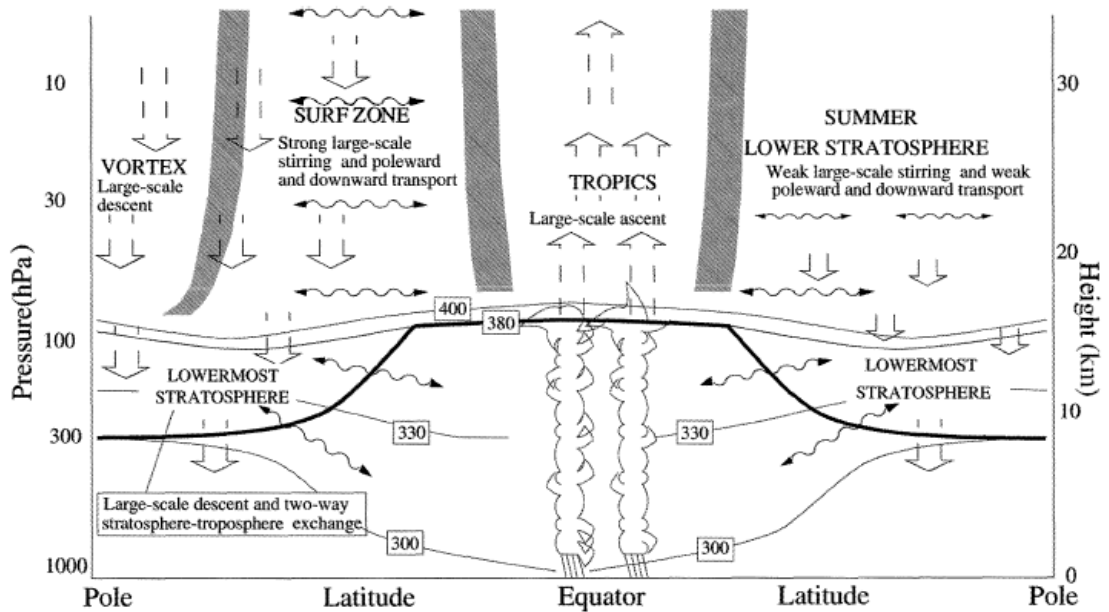


Figure 2.4: Atmospheric transport in the upper troposphere-lower stratosphere. The thick black line shows the tropopause whilst the thin lines show potential temperature isentropes. The wavy arrows represent stirring along these isentropic surfaces. This diagram is taken from the 1998 Scientific Assessment of Ozone Depletion (Ravishankara et al., 1999).

To fully understand this transport the concept of potential temperature must first be introduced. Potential temperature is the temperature of an air parcel if it were at a reference pressure of 1000 mb (Holton, 2004b). This value is conserved within the atmosphere, producing surfaces of constant potential temperature along which parcels of air can move without expending energy (and thus work). In the mid-latitudes these surfaces transect the tropopause (see Fig. 2.4). In this region there is therefore a slow motion of air parcels along these surfaces through the tropopause. This process is significantly slower

than convection through the tropopause in the tropics. Fig. 2.4 illustrates transport in the upper troposphere-lower stratosphere.

### 2.3.3 Stratosphere

Vertical transport through the stratosphere is not driven by convection due to its inverted temperature profile. The increasing temperature with altitude makes this region extremely stable and vertical mixing is driven by the complex mechanism of wave breaking (Plumb, 2002). The movement of air in the stratosphere from the tropical to the high latitudes is known as the Brewer-Dobson circulation.

Atmospheric waves, which break in the stratosphere, are formed by the movement of air over extremely large objects such as mountain ranges, such as the Himalayas or the Rockies, and large scale temperature formations. Mixing in the stratosphere is caused by a particular variant of the Rossby wave, known as stationary planetary waves.

As the air moves up over the obstacle, the vertical movement of air causes a wave to propagate upwards through the atmosphere above the object. As the waves propagate higher into the atmosphere, their amplitude increases as the density of the atmosphere decreases. This process of vertically propagating waves with ever increasing amplitudes eventually leads to the waves breaking. This process of wave breaking deposits momentum into the stratosphere and warms the stratosphere. The now warmed area of the stratosphere rapidly cools becoming denser, and sinks. This causes a movement of air poleward to replace the air which has sunk, thus establishing the Brewer-Dobson circulation. The upward movement of air in the tropics is known as tropical upwelling and is responsible for the transport of long-lived species, such as CFC-11 and CFC-12, into the stratosphere. The area within the mid-latitude stratosphere in which this mixing occurs is known as the surf-zone (McIntyre et al., 1983).

## The Atmosphere

The winter stratosphere has a westerly background movement of air whilst the summer hemisphere has an easterly background movement of air. This has an effect on the vertical mixing of the stratosphere. Stratospheric mixing is weak in the summer hemisphere since the vertical propagation of planetary waves requires a westerly general background motion (Plumb,2002). Thus the vertical propagation of stationary planetary waves can only occur in the winter hemisphere.

Much of the Earth's landmass is situated in the northern hemisphere. There are therefore more large scale geographical features (such as the Rockies or the Himalayas) in the northern hemisphere than the southern hemisphere. More of these waves are therefore formed in the northern hemisphere than in the southern hemisphere. This leads to significantly more wave activity in the northern hemisphere stratosphere than in the southern hemisphere stratosphere. The consequence of this is that Brewer-Dobson circulation is stronger during northern hemisphere winter than southern hemisphere winter. Since ozone is produced in the tropics and is transported by this circulation, the total ozone column in the mid to high latitudes is larger northern hemisphere than in the southern hemisphere. The stronger Brewer-Dobson circulation in the northern hemisphere causes more disturbances of the polar vortex and leads to a weaker polar vortex which dissipates far earlier than its southern counterpart.

### ***2.4 Ozone Loss***

The ozone layer is an area of the stratosphere where the VMR of ozone peaks (Dobson, 1931). The ozone layer is extremely important for life on Earth as it strongly absorbs solar ultra-violet (UV) radiation peaking 230 and 290 nm. It should be noted that UV radiation with wavelengths less than 230 nm is absorbed by molecular oxygen (Wayne, 2000b). UV radiation, with wavelengths less than 290 nm, can have extremely serious effects on health

which include skin cancers, a reduction in the response of the immune system and cancer of the eye. The political implications of the discovery of the ozone hole and the international treaty which was ratified to solve the problem have been described in Chapter 1. The photolysis of halogenated source gases by ultra violet radiation in the stratosphere releases reactive F, Cl and Br atoms. F rapidly forms the very stable HF molecule so only Cl and Br atoms lead to ozone destruction. Iodine-containing gases would also destroy stratospheric ozone, but these molecules have such a short atmospheric lifetime that they seldom reach the stratosphere (Montzka et al., 2011a).

This section briefly outlines the chemistry of stratospheric chlorine which leads to ozone destruction. This section does not consider ozone destruction due to bromine radicals since bromine-containing molecules are not currently retrieved from ACE-FTS spectra.

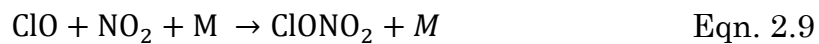
### 2.4.1 Chlorine catalysed ozone loss

CFCs and halogen-containing species are primarily released by human activities in the troposphere. Since CFCs are tropospherically inert, the main tropospheric removal mechanism for these species is transport into the stratosphere. Once in the stratosphere photolysis by ultraviolet radiation and reactions with O(<sup>1</sup>D) causes these CFCs to break down and release chlorine radicals into the stratosphere. Once released these chlorine radicals can catalyse ozone loss in a number of separate reactions; the overall result of which is the destruction of stratospheric ozone. The main cycle can be seen in Eqns. 2.1 and 2.2 (Wayne, 2000c). The overall effect of these reactions is to convert ozone into oxygen molecules (Eqn. 2.3).



## The Atmosphere

Standard atmospheric chemistry textbook, show that these equations are not the only processes in which chlorine can catalyse ozone destruction. For example, the presence of both HO<sub>x</sub> and NO<sub>x</sub> lead to the catalytic process laid out in Eqns. 2.4 through 2.12 (Wayne, 2000c). These reactions follow on directly from the reaction given in Eqn. 2.1.



Species such as HOCl and ClONO<sub>2</sub> (Eqns. 2.5 & 2.6 and Eqns. 2.9 & 2.10), which are easily photodissociated by UV radiation ( $h\nu$ ), act as both a temporary sink and a source for stratospheric chlorine.

The potential damage which a chlorine-containing species can do to the ozone layer is evaluated by its Ozone Depleting Potential (ODP).

## 2.4.2 Ozone Depleting Potential

The ODP of a number of halogen-containing species is given in Table 2.1. The ODP is a measure of the potential of a substance to deplete stratospheric ozone in comparison to the potential of CFC-11. The ODP is calculated using Eqn. 2.11 (Wayne, 2000d), where  $f_x(\text{CFC-11})$  is the fraction of species  $x$  (CFC-11) which is photodissociated,  $M_x$  (CFC-11) is the the molar mass of species  $x$  (CFC-11),  $n$  is the number of chlorine atoms contained in species  $x$ , and  $\tau_x$  (CFC-11) is the lifetime of species  $x$  (CFC-11). The ODP is calculated by multiplying the ratios of photodissociation, molar mass, number of chlorine atoms and lifetime (which can be seen in table 2.2) between species  $x$  and CFC-11. The dependence of ODP on lifetime is one of the key reasons for the SPARC lifetimes re-evaluation project (see Chapter 7). The factor of 3 in Eqn. 2.11 represents the number of chlorine atoms contained in the CFC-11 molecule.

$$\text{ODP} = \frac{f_x}{f_{\text{CFC-11}}} \cdot \frac{M_{\text{CFC-11}}}{M_x} \cdot \frac{n}{3} \cdot \frac{\tau_x}{\tau_{\text{CFC-11}}} \quad \text{Eqn. 2.11}$$

Table 2.1: The Ozone Depleting Potential (ODP) of a number of atmospheric species (Montzka et al., 2011b).

| Species            | Number of chlorine atoms | Ozone Depleting Potential |
|--------------------|--------------------------|---------------------------|
| CFC-11             | 3                        | 1.00                      |
| CCl4               | 4                        | 0.82                      |
| CFC-113            | 3                        | 0.85                      |
| CFC-114            | 2                        | 0.58                      |
| CFC-12             | 2                        | 0.82                      |
| CH <sub>3</sub> Cl | 1                        | 0.02                      |
| Halon-1211         | 1                        | 7.90                      |
| HCFC-141b          | 2                        | 0.12                      |
| HCFC-142b          | 1                        | 0.06                      |
| HCFC-22            | 1                        | 0.04                      |
| N <sub>2</sub> O   | 0                        | 0.017                     |

## The Atmosphere

It is clear from Eqn. 2.11 that, if all other variables are equal, species with a larger number of chlorine atoms will have a larger ODP. A species with a larger number of chlorine atoms is able to release more chlorine into the stratosphere and so has a larger effect on ozone loss.

### ***2.5 Greenhouse Effect***

The Earth's atmosphere is transparent to different wavelengths of radiation. Short wavelength radiation, such as gamma rays and x-rays, is absorbed in the upper atmosphere. The atmosphere is also opaque to the longest wavelengths of radio waves, those with wavelengths longer than around 10 m. However, the atmosphere is transparent to shorter radio waves, those with wavelengths between 1 mm and 10 m. The atmosphere is also almost transparent to visible light, with Rayleigh scattering at shorter wavelengths and small amounts molecular absorption by water at longer wavelengths. The surface of the Earth is warmed by the radiation which makes it through the atmosphere (Freedman et al., 2005). The Earth re-emits this radiation in the form of infra-red (IR) radiation. The incoming and outgoing radiation is in equilibrium which allows the effective temperature of the Earth to be calculated. These calculations produce a surface temperature of 255 K (Barry, 2007c). This temperature is significantly lower than the freezing point of water. However, liquid water exists on the Earth's surface and therefore an additional source of warming must exist.

Many atmospheric constituents can absorb some of the outgoing IR radiation, re-radiating it isotropically. IR radiation is absorbed only if it has a corresponding energy to one of the excited states of the molecule. For molecules within the atmosphere these excitations take the form of rotational and vibrational transitions. An example of vibrational modes of water can be seen in Fig. 2.5. The overall effect of this process is to retain some of the outgoing IR radiation within the Earth's atmosphere. This trapping of the IR

## The Atmosphere

radiation increases the temperature of the atmosphere which in turn increases the surface temperature of the Earth. This is the greenhouse effect. Species such as water, carbon dioxide, methane and CFCs which can absorb outgoing IR radiation are known as greenhouse gases (GHG).

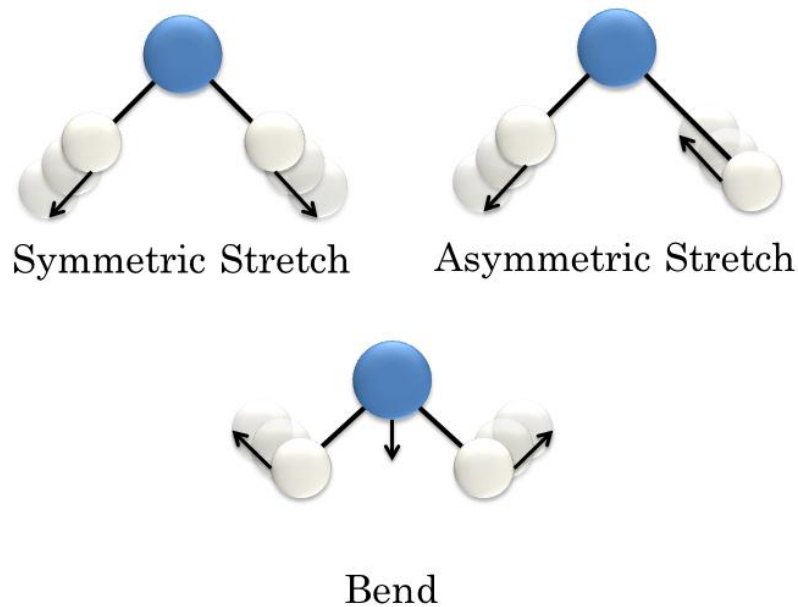


Figure 2.5: The main vibrational modes of water. The symmetric stretch is the  $\nu_1$  mode,  $\nu_2$  corresponds to the bending mode and the  $\nu_3$  mode to the asymmetric stretch

Figure 2.6 shows the long-term temperature data between 1850 and 2000 from the 2007 IPCC report on climate change (Solomon et al., 2007). The long-term increase in the Earth's temperature has been termed global warming. By increasing the concentration of greenhouse gases in the atmosphere more molecules are available for IR absorption to occur leading to further warming of the atmosphere. Different species of greenhouse gases are formed from different combinations of elements. Thus different species have different bonds and therefore have different rotational and vibrational excited states. The impact of a molecule on global warming is quantified using its Global Warming Potential (GWP).

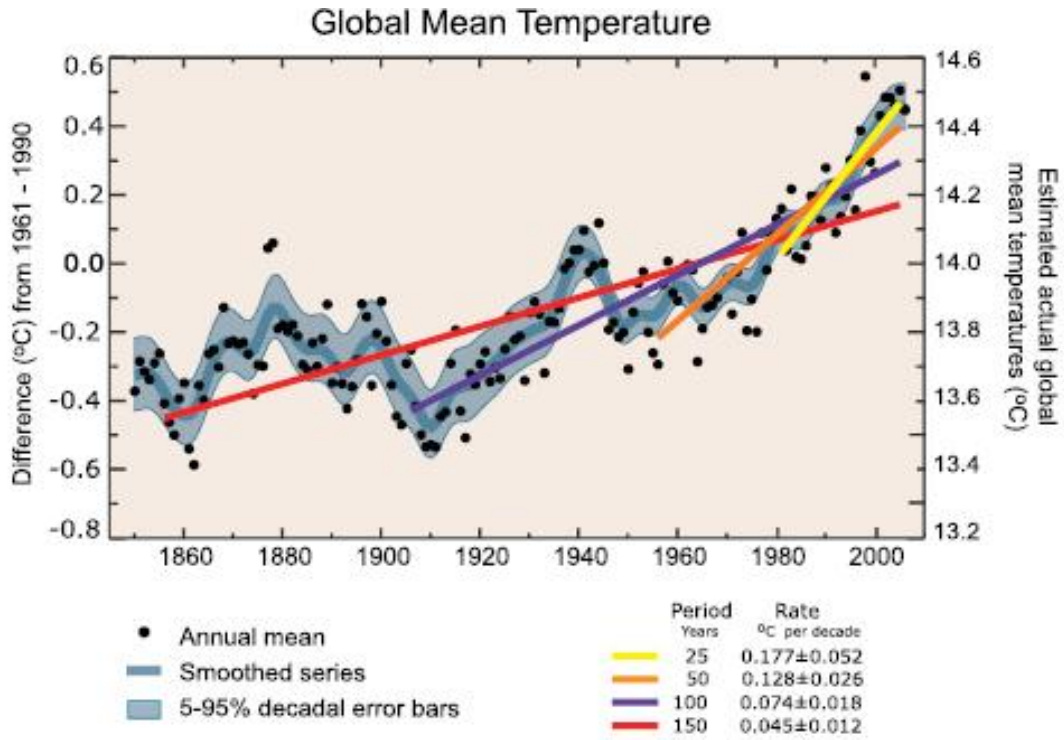


Figure 2.6: Changes in the mean global temperature between 1855 and 2005 (this chart is from the IPCC fourth assessment report: climate change 2007). This data shows an increasing rate of increasing temperature during this period (Solomon et al., 2007).

$$GWP_x = \frac{\int_0^{TH} RF_x(t) dt}{\int_0^{TH} RF_{CO_2}(t) dt} \tag{Eqn. 2.12}$$

The global warming potential of several molecules can be seen in Table 2.2. The first thing that should be noticed is that by definition the GWP of carbon dioxide over all timescales is 1. Like ODP, the value of the GWP of a species is a relative value. In this case the value is relative to the GWP of CO<sub>2</sub>. Eqn. 2.12 is used to calculate the GWP of a molecule (Solomon et al., 2007).

Table 2.2: The global warming potential, on a 20-year timescale (Solomon et al., 2007), the radiative efficiencies (Solomon et al., 2007) and the lifetimes (Montzka et al., 2010) of some of the species used in this research

| Species   | Global Warming Potential | Radiative Efficiency ( $\text{Wm}^{-2} \text{ppb}^{-1}$ ) | Stratospheric Lifetime (years) |
|---|--------------------------|---|--------------------------------|
| $\text{CF}_4$   | 5,210                    | 0.10  | >50,000                        |
| CFC-11 ( $\text{CCl}_3\text{F}$ )                       | 6,730                    | 0.25  | 45                             |
| CFC-12 ( $\text{CCl}_2\text{F}_2$ )                     | 11,000                   | 0.32  | 100                            |
| CFC-113 ( $\text{C}_2\text{Cl}_3\text{F}_3$ )           | 6,540                    | 0.30  | 85                             |
| CFC-114 ( $\text{C}_2\text{Cl}_2\text{F}_4$ )           | 8,040                    | 0.31  | 190                            |
| CFC-115 ( $\text{C}_2\text{ClF}_5$ )                    | 5,310                    | 0.18  | 1,020                          |
| Halon-1301 ( $\text{CBrF}_3$ )                          | 8,480                    | 0.32  | 65                             |
| Halon-1211 ( $\text{CBrClF}_2$ )                        | 4,750                    | 0.30  | -                              |
| HCFC-22 ( $\text{CHClF}_2$ )                            | 5,160                    | 0.20  | 186                            |
| HCFC-141b ( $\text{C}_2\text{H}_3\text{Cl}_2\text{F}$ ) | 2,250                    | 0.14  | 64.9                           |
| HCFC-142b ( $\text{C}_2\text{H}_3\text{ClF}_2$ )        | 5,490                    | 0.20  | 160                            |
| HFC-23 ( $\text{CHF}_3$ )                               | 12,000                   | 0.19  | 2,347                          |
| HFC-134a ( $\text{C}_2\text{H}_2\text{F}_4$ )           | 3,830                    | 0.16  | 232                            |
| HFC-152a ( $\text{C}_2\text{H}_4\text{F}_2$ )           | 437                      | 0.09  | 45.4                           |
| $\text{SF}_6$   | 16,300                   | 0.52  | 3,200                          |

RF is the global mean Radiative Forcing of 1kg of a species and TH is the time horizon over which the effect will occur (for example 20, 100 or 500 years in Table 2.2). The radiative forcing of a species is a combination of its concentration in the atmosphere and its ability to absorb IR radiation. The concentration of a species in the atmosphere over a specific time period is a function of its lifetime. Thus a species with a longer lifetime than  $\text{CO}_2$  but a comparable ability to absorb IR radiation will have a GWP greater than 1. The ability of a gas to absorb radiation is a function on the wavelengths that it absorbs and its ability to absorb IR radiation. A species with a greater ability to absorb IR radiation than  $\text{CO}_2$  but a comparable lifetime will have a GWP greater than 1. It should be noted that fluorine-containing species are particularly efficient greenhouse gas, since they absorb radiation in an area of

the electromagnetic spectrum in which most other molecules do not. This gives the CFCs replacement species (the HCFCs and HFC) extremely large GWPs ensuring that, despite their reduced ODP, these species remain extremely important in the atmosphere. A useful value is the radiative efficiency of a species; this is the effect of the species on the outgoing flux per ppb. This value is used in Chapters 5 and 6 to evaluate the effect of fluorine on the radiation budget between 2004 and 2009. These values are also shown (for comparison) in Table 2.2.

### ***2.6 The effect of the greenhouse effect on ozone depletion***

There is an interesting link between warming tropospheric temperatures and ozone recovery. Whilst the temperature of the atmosphere will have an impact on chemical reaction rates, the most important effect of changes in stratospheric temperature relate to its effect on polar stratospheric cloud.

#### **2.6.1 Polar Stratospheric Clouds**

Equations 2.1 and 2.2 are only one example of how stratospheric chlorine can catalyse ozone loss. There are many gas-phase reactions by which chlorine can catalyse stratospheric ozone loss of which some are more effective than others. Whilst these reactions do produce ozone loss, it would not be to the extent that is seen at the poles (Wayne, 2000e). The reactions which cause the large scale loss of ozone seen in the Antarctic (Kuttippurath et al., 2013) and, more recently, in the arctic (Sonkaew et al., 2013) are not gas-phase reactions at all. The reactions take place on the surface of polar stratospheric clouds (PSC). PSC form at extremely low temperatures that are only seen in the polar stratosphere. They are formed in the winter polar vortex where temperatures decrease significantly from the norm, Lower stratospheric temperatures produce greater PSC which in turn produces greater ozone loss. There is

## The Atmosphere

temperature decreasing feedback to ozone loss. It has already been mentioned that stratosphere is warmed by absorption of UV radiation, thus if there is less ozone there is less absorption of UV radiation. This leads to less warming of the stratosphere which leads to a cooling. As the stratosphere cools it allows further PSC to form increasing the rate of ozone loss. This is therefore a feedback loop with ozone loss leading to a reduction in temperature which in turn leads to an increased rate of ozone loss (Randel and Wu, 1999). This is not the only process which is cooling the stratosphere.

### **2.6.2 Greenhouse effect initiated stratospheric cooling**

The decrease in temperature of the stratosphere due to an increase in temperature of the troposphere may seem counter intuitive. To explain this phenomenon we must think of the troposphere and the stratosphere. Some of the IR radiation emitted from the surface is absorbed in the troposphere; some is absorbed in the stratosphere warming the region. Greenhouse gases in the stratosphere, such as CO<sub>2</sub>, will emit IR radiation from the stratosphere into space. As the levels of greenhouse gases in the troposphere increase less IR radiation reaches the stratosphere and so less is absorbed. The stratospheric gases continue to emit IR. Thus less IR is absorbed in the stratosphere and similar amounts continue to be emitted from the stratosphere. The net effect of this process is to cool the stratosphere whilst the troposphere warms (Shindell et al., 1998). This cooling in the stratosphere produces more PSC which produces further ozone loss. In this way there is an intrinsic link between ozone loss and the greenhouse effect.

## **2.7 Summary**

The atmosphere is a complex system in which dynamics and composition are intrinsically linked. The atmosphere has a layered

## The Atmosphere

structure which includes the troposphere, stratosphere, mesosphere and thermosphere. These layers are defined by their temperature profiles: increasing temperature with altitude in the troposphere and mesosphere and a decreasing temperature with altitude in the stratosphere. Transport through the troposphere is driven by the convection whilst transport in the stratosphere is driven by atmospheric waves produced by air moving over areas of powerful convection and mountain ranges.

Human activity is having an effect on both the troposphere and the stratosphere. In the troposphere, the release of gases which absorb infrared radiation is increasing the atmospheric temperature. These changes are expected to have a significant effect on the global climate. In the stratosphere, chlorine and bromine containing species react with the ozone converting ozone to diatomic oxygen. This process is extremely important as it is the ozone layer in the stratosphere which absorbs UV radiation which can have adverse health effects on both plants and animals. In order to fully understand the effects of these processes measurements of the atmospheric concentration of greenhouse gases, ODS and ozone are required. The next chapter will discuss one satellite which is designed to measure the concentrations of a number of greenhouse gases and ODS.

# 3

## The Atmospheric Chemistry Experiment

### ***3.1 Introduction***

#### **3.1.1 Atmospheric Measurements**

There are a number of experimental methods available to modern atmospheric scientists for measuring the chemistry and the physics of the atmosphere. These methods can be divided into two different categories, remote sensing and in situ measurements. In situ and remote sensing methods are complementary and together allow a more rigorous assessment of the atmosphere to be made. As the name suggests, in situ measurements are made through direct contact with the atmosphere. A common example of an in situ atmospheric measurement is gas chromatography-mass spectrometry (GC-MS). In atmospheric science GC-MS instruments are used to analyse the chemical composition of an atmospheric sample. Gas samples may be analysed directly or can be trapped in bottles to be analysed at a more convenient time.

## The Atmospheric Chemistry Experiment

This method is widely used in atmospheric science as it allows accurate concentrations to be measured against high quality reference samples. Remote-sensing instruments measure the atmosphere from a distance. Examples of this type of atmospheric measurement include satellite measurements (discussed in section 3.1.2) and radar. In situ measurements, when carefully calibrated, can produce accurate and precise measurements of the VMRs of atmospheric constituents at specific locations and times. However, in situ ground-based measurements are limited to the locations of the stations and do not offer true global vertical profiles. Satellite based instruments, which remotely measure the atmosphere, allow for a wide spatial coverage across the globe. Whilst individual satellite measurements lack the accuracy and precision of a well-calibrated in situ measurement, their truly global coverage allows regional or zonal averages to be calculated.

### **3.1.2 Remote-Sensing Instruments**

The field of atmospheric remote sounding is extremely diverse. Remote-sensing satellite instruments can be divided into two different categories: passive and active sounders. Atmospheric-sounders are instruments which measure a number of different characteristics of the atmosphere, for example the pressure, chemical constituents, temperature and density of the atmosphere at various different altitudes. Active-sounding instruments illuminate an area using particular wavelengths of electromagnetic radiation and then measure the backscattered and reflected returning radiation. Analysing this backscattered or reflected radiation can allow the topography of an area to be measured; it can also allow both the type and the concentrations of aerosols to be measured. Passive sounding instruments do not illuminate areas of the ground or atmosphere; instead they measure the radiation being emitted or reflected by the object that they are viewing. For the sake of brevity this section will only discuss passive satellite based remote sounding instruments. Active techniques such as LIDAR and GPS measurements are not considered

## The Atmospheric Chemistry Experiment

in this thesis as they were not used in the research that is documented in this work.

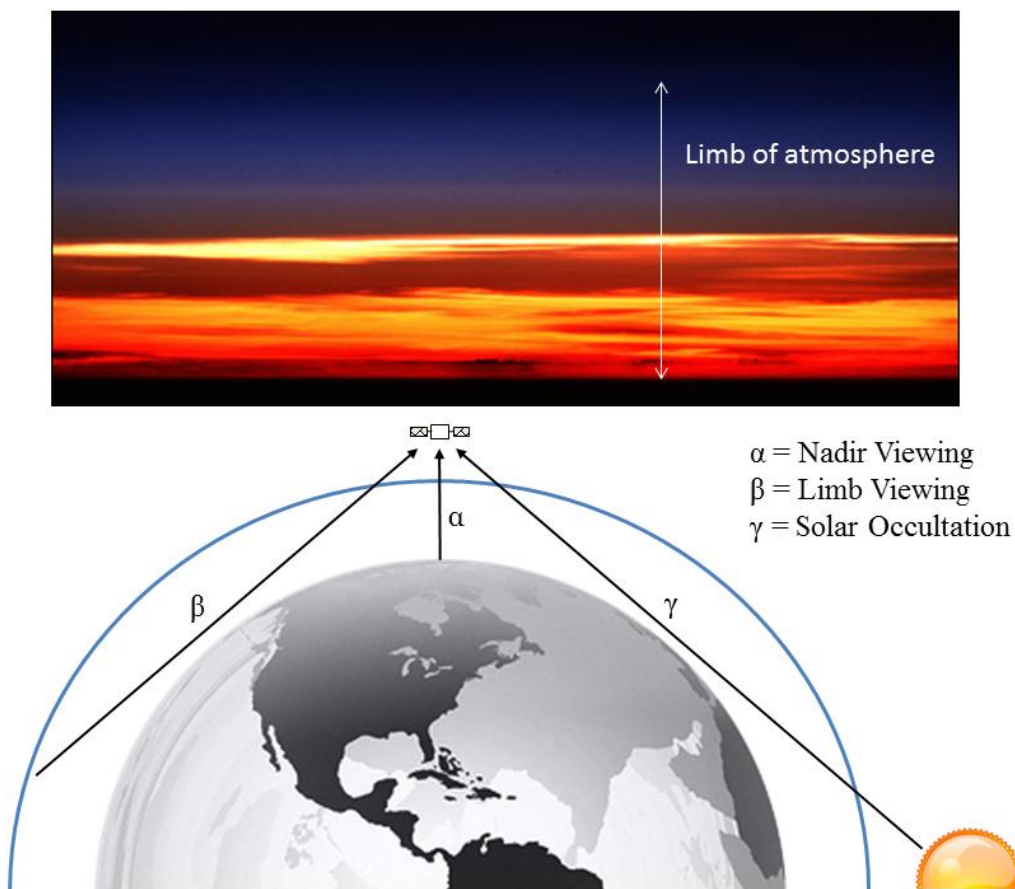


Figure 3.1: Top panel: The limb of the atmosphere as observed from the International Space Station (original image from NASA Earth Observatory). Bottom panel: The three major types of passive instruments used in remote-sensing. Nadir sounders detect the infra-red radiation which is being emitted by the surface of the Earth. Limb viewers detect radiation which is emitted from the limb of the atmosphere whilst solar occultation instruments detect the infra-red radiation which is emitted by the Sun.

There are three major types of passive instruments which are used to measure the atmospheric VMRs of gases: Nadir viewing ( $\alpha$  in Fig. 3.1), limb viewing ( $\beta$

## The Atmospheric Chemistry Experiment

in Fig. 3.1) and solar occultation ( $\gamma$  in Fig. 3.1). Nadir viewers look down towards the surface of the Earth and measure infra-red radiation being emitted upwards by the surface and the atmosphere. Nadir sounders have good horizontal resolution but relatively poor vertical resolution. Limb viewers observe radiation coming through the limb of the atmosphere. The limb of the atmosphere can be seen in the upper panel of Fig. 3.1, it is the outer edge of the atmosphere. The radiation coming through the limb of the atmosphere can be reflected or scattered sunlight, emissions from the atmosphere or in rare cases direct sunlight. By observing the limb of the atmosphere it is possible to observe a number of different altitudes and thus limb viewing instruments have good vertical resolution. The length of the path which the radiation has travelled through the atmosphere (the path length) is usually extremely long and causes the horizontal resolution of the instrument to be lower than that possible with nadir sounders.

Solar occultation instruments are a variety of limb sounders but they use the Sun as a source of radiation for observing the atmospheric limb. Like limb sounders, solar occultation sounders have good vertical resolution but relatively poor horizontal resolution. The main differences between these sounders are the signal-to-noise ratios of the spectra that they measure and the number of spectra which are measured each day. Solar occultations can only be made as the Sun travels through the limb of the atmosphere at sunrise and sunset (relative to the satellite). The number of measurements that can be made per day by a solar occultation instrument is therefore limited by the number of times the Sun can be observed rising and setting through the limb during the course of a single day's orbit. For a satellite in low Earth orbit, this is 30 measurements, 15 per sunrise/sunset.

Limb viewers do not require the Sun to be in the field of view to make measurements, and therefore make significantly more measurements over the course of a day. The number of measurements which can be made in a day is a

## The Atmospheric Chemistry Experiment

trade off with the signal-to-noise (S/N) ratio of the spectra that these instruments measure. The S/N is a measure of the power of the signal that is being measured compared to the background noise of an instrument. Since the Sun produces a strong radiation signal the S/N of solar occultation instruments is higher than conventional limb viewing instruments. This high S/N produces ‘cleaner’ spectra which allow weaker absorption lines to be observed more clearly. This allows the atmospheric VMRs of more species to be retrieved from the spectra.

The Atmospheric Chemistry Experiment-Fourier Transform Spectrometer (ACE-FTS) is a solar occultation instrument. As has been stated in previous chapters, the work presented in this thesis centres on the retrievals, carried out at the Science Operations Centre, University of Waterloo, of the VMRs of a number of fluorine and chlorine containing species from ACE-FTS spectra. The following section begins with an introduction to the ACE mission and its aims and objectives. Subsequently, the method used to retrieve VMR from ACE-FTS spectra is briefly described. Previous studies and validations of the fluorine- and chlorine-containing species retrieved from ACE-FTS spectra are then reviewed so as to give some perspective on the work presented in this thesis.

### ***3.2 An introduction to the Atmospheric Chemistry Experiment***

The ACE mission derives from the international support for, and strengthening of, the Montreal Protocol during the 1990s. The aim of the ACE mission is to study ‘the chemical and dynamical processes that control the distribution of ozone in the stratosphere and upper troposphere’ (Bernath, 2006). Selected for flight by the Canadian Space Agency in 1998, the instrument, carried on-board the satellite SCISAT-I, was launched in August

## The Atmospheric Chemistry Experiment

2003. The instrument concept is based on the Atmospheric Trace MOlecule Spectroscopy experiment (ATMOS) which has since been retired (Bernath et al., 2005a). ATMOS was a space-shuttle-borne IR Michelson Interferometer which operated in solar occultation mode to measure the VMR of long-lived gases from altitudes between the upper troposphere and the mesosphere (roughly 10 to 150 km) using spectra of the atmospheric limb (Gunson et al., 1996).

### **3.2.1 The Instrument**

ACE-FTS is a high-resolution ( $0.02\text{ cm}^{-1}$ ) Michelson Interferometer which operates between  $750$  and  $4400\text{ cm}^{-1}$ . A Michelson Interferometer is a simple instrument which produces interference fringes by splitting the incoming light beam and varying the path differences between the two new beams. The path difference between the beams causes them to constructively or destructively interfere depending on the path difference. A Fourier Transform can then be used to convert the interference pattern into a spectrum. A simple schematic of the Michelson Interferometer which constitutes ACE-FTS is shown in Fig. 3.2.

# The Atmospheric Chemistry Experiment

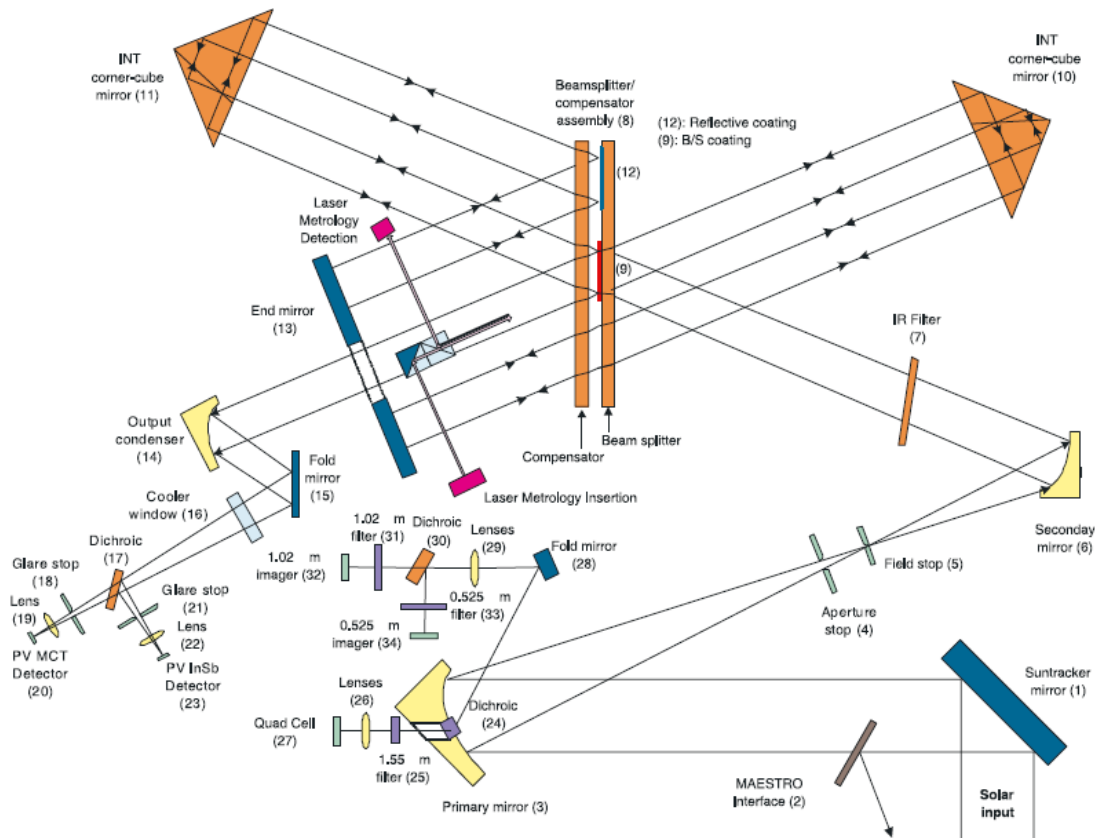


Figure 3.2: A schematic of the Fourier Transform Spectrometer which is on board the Atmospheric Chemistry Experiment (Bernath et al., 2005b).

Since the spectrometer requires the Sun as its light source, ACE-FTS includes a Sun tracker which, through the use of a detector and a small adjustable mirror, ensures that during the measurement phase the spectrometer is constantly aimed at the radiometric centre of the Sun. Incoming sunlight passes through a beam splitter which divides the light into two beams. Each of these beams is then incident onto a corner-cube which reflects the light parallel to the incident beam. The corner-cube mirrors pivot so as to introduce a varying path difference to the beams. The resolution of a spectrometer is governed by its optical path difference (OPD). A larger OPD corresponds to a higher resolution. Since a spectrometer on-board a satellite is limited by both space and weight, the spectrometer must be as compact as possible. In order to increase the optical path length, without greatly increasing the overall size of

## The Atmospheric Chemistry Experiment

the instrument, an end mirror was added into the design so that light would be reflected back towards the corner cubes before reaching the detector. These additional mirrors coupled with the pivoting corner cubes produce an OPD of  $\pm 25$  cm. The corner cubes have an additional role in the spectrometer. Cube mirrors reflect light parallel to the direction that it was incident on the mirror. The cube mirrors prevent light which may have been reflected from areas within the FTS from reaching the detector. This improves the quality of the spectrum.

The ACE-FTS instrument was chosen for a number of reasons chief among them being the high signal-to-noise ratio and the high spectral resolution. Since ACE-FTS is a solar occultation device, the source of the radiation which is detected is the sun. The intensity of this IR radiation which is received by the detectors is therefore very high producing significant signal (see Section 3.1.2). In addition to this the ACE-FTS's spectral resolution is extremely high compared to other passive limb sounders. Coupled with the high signal-to-noise the high resolution of the spectrometer allows weak absorption lines to be observed so that it is possible to retrieve the VMR of a large number of species from the spectra. The use of the sun as a radiation source has an additional advantage for ACE. It allows for a highly accurate pointing accuracy since the position of the measurement can be deduced from simple knowledge of the position of the satellite relative to the sun. Finally, ACE-FTS is able to take spectra of the Sun and of deep space which allows the instrument to self-calibrate. That is to say the contribution of the solar spectrum to an atmospheric spectrum can be removed simply by subtracting a solar spectrum (measured by ACE-FTS when there is no atmosphere between it and the sun) from said spectrum. This ensures that the retrieval program only has to fit atmospheric absorption lines. By taking spectra of deep space the background spectrum of the instrument itself can be gained. This can also be subtracted from the atmospheric spectrum, once again simplifying the retrieval process.

### 3.2.2 The Orbit

Since ACE-FTS was designed to concentrate on the study of ozone over Canada, SCISAT-1's orbit was chosen to give the maximum coverage over the poles and the upper latitudes. Despite this, a low circular orbit with an inclination of  $74^\circ$  and an altitude of 650 km (Bernath et al., 2005a) gives ACE-FTS almost global coverage from the Antarctic to the Arctic. The positions of the occultations are shown in Figure 3.3.

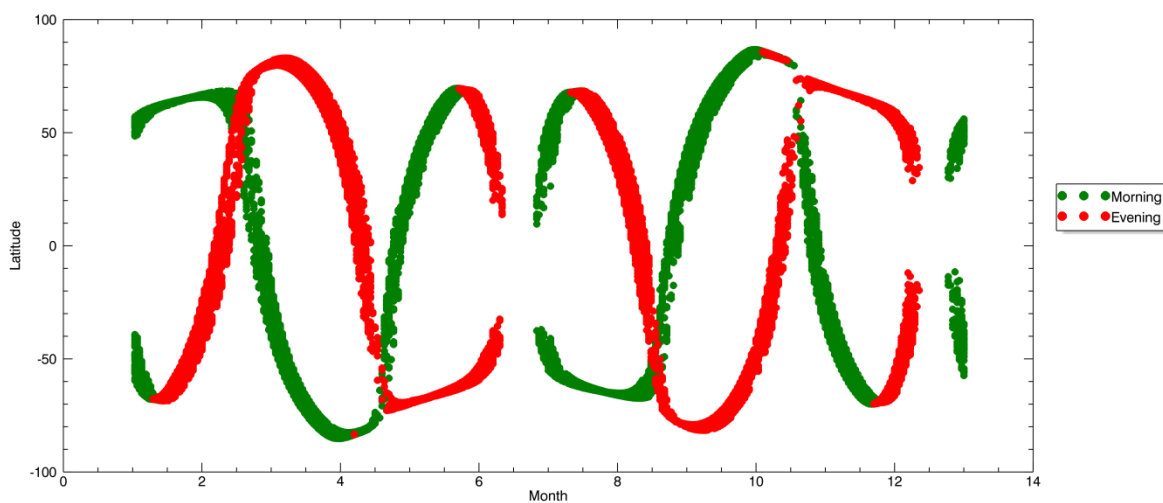


Figure 3.3: The latitude coverage of ACE over the course of a year. The red points are occultations made at local morning time, the green points are occultations made at local evening time

### 3.2.3 ACE retrieval method

The process of acquiring data for the state of the atmosphere from atmospheric spectra is known as the retrieval process. An example of an atmospheric spectrum taken by the ACE-FTS can be seen in Fig. 3.4.

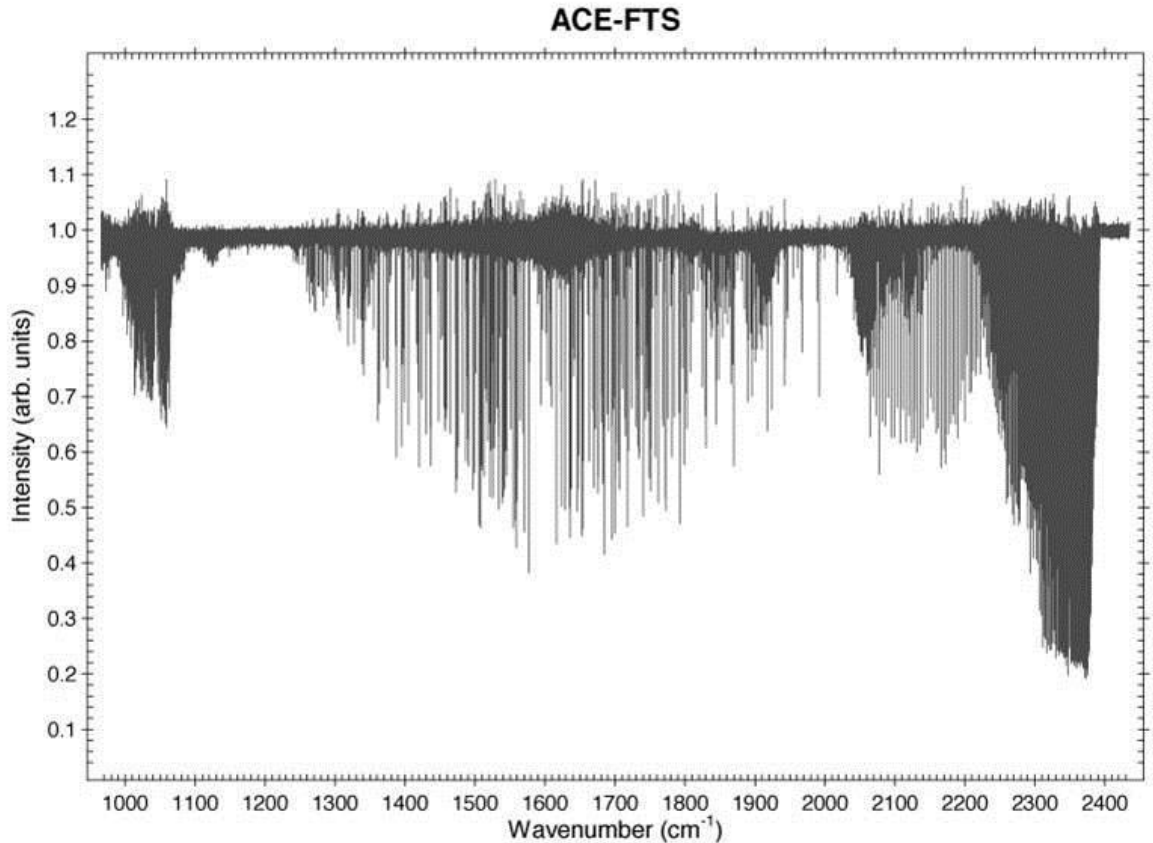


Figure 3.4: An ACE-FTS spectrum from December 2003. The feature between  $1000\text{cm}^{-1}$  and  $1100\text{cm}^{-1}$  is caused by ozone. The large feature running between  $1300\text{cm}^{-1}$  and  $2000\text{cm}^{-1}$  is a water absorption feature. The final feature running from  $2200\text{cm}^{-1}$  is produced by carbon dioxide.

Measured spectra are compared to a forward model, which is changed until the observed spectra match the simulated spectra. The process is complicated since each spectrum contains data from a range of different altitudes. Thus the contributions of different layers to the spectrum must be deduced so that vertical profiles can be calculated. In order to do this the shapes of the vertical profiles of the retrieved species are used as a starting point for the contribution of species to the overall atmospheric spectrum. The retrievals however are not constrained by this *a priori* information; they are simply used as initial guesses for the retrieval.

## The Atmospheric Chemistry Experiment

Prior to the retrieval of the VMR profile of any species from a set of occultation spectra, the atmospheric pressure and the temperature profiles of the occultation must be retrieved. ACE retrievals are carried out between 5 and 150 km (Boone et al., 2005). CO<sub>2</sub> absorption features are used to retrieve temperature and pressure. The VMR of CO<sub>2</sub> is considered to be constant up to 75 km between 60° North and South, and up to 65 km at latitudes greater than 60°. Accurate tropospheric measurements of the VMR of CO<sub>2</sub> can therefore be used as the *a priori* for the pressure and temperature retrieval. The atmospheric pressure and temperature can then be retrieved from the CO<sub>2</sub> absorption features over a range of altitudes. The pressure and temperature are varied until the magnitude and lineshapes of the retrieval model's CO<sub>2</sub> absorption feature matches that observed in the ACE-FTS spectrum.

Once the pressures and temperatures have been retrieved, it is possible to retrieve the VMRs of atmospheric constituents. To reduce the required computing power which is, rather than use the entire atmospheric spectrum to retrieve VMR profiles, small sections of the spectrum, between 0.3 and 1 cm<sup>-1</sup> wide, called microwindows, are used. The choice of microwindows depends on the species being retrieved. Microwindows are chosen to contain spectral features of the species of interest with minimal interference from other species. In practice it is not always possible to entirely minimise the interference from other species, so the target and the interfering species are retrieved simultaneously; this is known as the global fit method. The retrieval is carried out by fitting a simulated microwindow (the forward model) to the observed microwindow. The VMRs of the target and interfering species are varied within the forward model and the resulting calculated spectrum is subtracted from the observed spectrum, producing a residual spectrum. The better the agreement between the calculated and observed spectra, the smaller the residual. The process of fitting spectra is repeated using different atmospheric constituents until the residuals are minimised. In this way the VMRs of all species can be acquired.

### 3.2.4 Errors in the retrieval

There are a number of sources of error inherent in the ACE-FTS retrieval. From the description of the retrieval process above perhaps the most obvious source of error is in the pressure and temperature. Since these variables are retrieved assuming a prior knowledge of the CO<sub>2</sub> profile, any error in the CO<sub>2</sub> VMR will be translated into errors in the retrieved pressure and temperature profiles. This has become a problem for occultations made after September 2010. It has been found that after this date the CO<sub>2</sub> VMR used by the retrieval program was incorrect and was introducing a significant error into the retrieval process. Data before this date was largely unaffected with any errors thought to be less than the errors due to spectroscopic uncertainties. The new ACE-FTS version 4 data will correct this error in the VMR of CO<sub>2</sub> after September 2010. An additional source of error can come from thin clouds which lie in the path of incoming IR radiation, Thin clouds will change the absorption cross-section of the path in a way that the retrieval program is not designed to compensate. When working with sufficiently high numbers of data, this error can be minimised as retrieved VMR affected by this will appear as outliers in the data which will be removed when filtering.

The most significant source of systematic errors in the ACE-FTS retrieval program are spectroscopic errors. If the spectrum of the species is not well known then the retrieval will not correctly take spectroscopic features into account. For example, let us consider the case where the cross-section of a species is not well known such that the intensity of a particular line, which is used in the retrieval of a species, is thought to be lower than it is in reality. This would lead to an overestimation of the VMR of the target species as the retrieval program attempted to account for the stronger than expected line. It is

## The Atmospheric Chemistry Experiment

not only error in the line intensity which could introduce these spectroscopic errors. If the effects of broadening or line position are not well known then these will also cause errors in the retrieval. The pressure and temperature dependence of a spectrum can be a serious problem to overcome. In order that the parameters of a spectrum should be sufficiently known a number of spectra are measured in the lab at a selection of different pressures and temperatures which represent atmospheric conditions. However, it is not possible for these measurements to fully replicate the atmosphere. That is to say, it is impossible to make measurements at every pressure and temperature combination that exists in the atmosphere. Instead the data which is available is extrapolated. Naturally, this extrapolation introduces further systematic errors into spectroscopic parameters needed for the retrieval. This factor can introduce an altitude dependent error to the retrieval. The extrapolation of the spectroscopic parameter may be better at some altitudes than other. This would lead to an altitudinally varying error.

Spectroscopic effects are not just confined to the target species; they also apply to the species which absorb in the same microwindow. For example, the microwindow used in the HCFC-141b retrieval includes absorption features of PAN. PAN is not included in the ACE-FTS retrieval scheme thus its impact on the microwindow is not accounted for. This produces an overestimation of the VMR of HCFC-141b as, in the eyes of the retrieval program; HCFC-141b appears to have a larger absorption feature than it should. There interfering species can also lead to altitude dependent errors. Once more we can take the HCFC-141b retrieval as an example. The profile of PAN decreases with altitude reaching a minimum at around 20 km (Keim et al., 2008). Thus the impact of PAN on the spectrum of HCFC-141b also decreases with altitude.

## The Atmospheric Chemistry Experiment

As can be seen in Figure 3.3, ACE's orbit repeats annually. This will lead to similar occultations being made each year. The main sources of error on the retrieved VMR are from spectroscopic uncertainties. These will likely remain very similar annually as the profiles shapes do not change significantly and neither do the occultation locations. The errors mentioned here should not have a significant effect on trend calculations as they should affect all years (before September 2010) equally. It should be noted that these errors become more important when calculating the correlations used in the evaluations of lifetimes in Chapter 7. In this case the systematic errors on the retrievals have been estimated using previous comparison between retrievals from ACE-FTS and other instruments. These results are presented in the following section. Fluorine and Chlorine containing species

Currently 16 fluorine- and chlorine-containing species are regularly retrieved from ACE-FTS spectra. These species are important constituents of the atmosphere as many of them act as both powerful ozone-depleting substances and greenhouse gases. The ozone-depleting and global warming potentials of some of these species can be seen in Tables 2.1 and 2.2. The aim of this section is to discuss briefly some of the previous work carried out using each of the fluorine and chlorine containing species retrieved by ACE-FTS.

### **3.2.5 Carbon Tetrachloride - CCl<sub>4</sub>**

Carbon tetrachloride (CCl<sub>4</sub>) was first retrieved from ACE observations for the 2004 global stratospheric chlorine budget (Nassar et al., 2006a). This study found that, in 2004, 3 % of the total stratospheric chlorine budget was made up of CCl<sub>4</sub>. The production of CCl<sub>4</sub> is banned by the Montreal Protocol, and a study of measurements of this species from ground-based instruments shows decreasing atmospheric concentrations of this species in recent times (Montzka et al., 2011a). A study of the global atmospheric distribution of CCl<sub>4</sub> from ACE-

FTS data was published in 2009 and presented global mean distributions and comparisons with a number of different atmospheric models (Allen et al., 2009). This work found that the ACE-FTS retrieval of CCl<sub>4</sub> overestimated the VMR by 20 to 30%.

### **3.2.6 Carbon Tetrafluoride – CF<sub>4</sub>**

CF<sub>4</sub> is a powerful greenhouse gas (see Table 2.2), the emissions of which are primarily from aluminium production. First retrieved from ACE-FTS spectra for the 2004 stratospheric fluorine budget (Nassar et al., 2006b), the ACE-FTS retrieval was validated by comparison with non-coincident profiles made by the Mk-IV balloon-borne instrument. This study found that profiles from Mk-IV and ACE were within  $\pm 10\%$  (Velazco et al., 2011).

### **3.2.7 Methyl Chloride – CH<sub>3</sub>Cl**

The main sources of CH<sub>3</sub>Cl are emissions from the ocean and biomass burning. Measurements made by ACE-FTS of CH<sub>3</sub>Cl biomass plumes have been studied by Rinsland et al. (Rinsland et al., 2007). CH<sub>3</sub>Cl is the main source of natural chlorine in the atmosphere and was included in the 2004 global stratospheric chlorine budget (Nassar et al., 2006a). The ACE-FTS retrieval has been compared to that from non-coincident occultations made by the MkIV balloon borne instrument (Velazco et al., 2011). This study found that the ACE-FTS retrieval was consistently higher with a maximum difference of 30%.

### **3.2.8 Sulphur Hexafluoride – SF<sub>6</sub>**

SF<sub>6</sub> is used as an electrical insulating gas in power distribution equipment and as an inert chemical tracer. The long lifetime of 3200 years and strong infrared absorption cross sections, in an atmospheric window region near 950 cm<sup>-1</sup>, are responsible for making this molecule a potent greenhouse gas. ACE-FTS retrievals of SF<sub>6</sub> were validated by comparison with non-coincident Mk-IV

balloon profiles. This study found an agreement to within  $\pm 15\%$  between 12 and 19 km (Velazco et al., 2011).

### **3.2.9 CFC-11 – CCl<sub>3</sub>F**

CFC-11 is banned under the Montreal Protocol and is the second most abundant CFC in the atmosphere. Validation of ACE-FTS retrievals were carried out using the FIRS-2 instrument. These comparisons showed an agreement to within 10% below 16 km (Mahieu et al., 2008). Comparisons between ACE and Mk-IV profiles show agreement within 10% above 12 km and 20% below 12 km (Mahieu et al., 2008). Non-coincident Mk-IV balloon profiles were also used for validation, producing differences of less than  $\pm 20\%$  between 17 km and 24 km (Velazco et al., 2011).

### **3.2.10 CFC-12 – CCl<sub>2</sub>F<sub>2</sub>**

CFC-12 is the most abundant CFC in the atmosphere and is banned under the Montreal Protocol. ACE-FTS retrievals were compared to FIRS-2 measurements showing an agreement within 10% above 12 km and 20% below 12 km (Mahieu et al., 2008). Non-coincident retrievals from ACE-FTS were compared to measurements from the Mk-IV instrument. This study also found differences of around  $\pm 10\%$  (Velazco et al., 2011).

### **3.2.11 HCFC-22 – CHClF<sub>2</sub>**

HCFCs are transitional replacement compounds for CFCs under the Montreal Protocol. HCFC-22 is the most abundant HCFC in the atmosphere as it has been widely used since the 1950s. The HCFC-22 retrieval used in this paper is a new retrieval; a paper is currently in preparation which discusses this new retrieval.

### **3.2.12 Carbonyl Chlorofluoride - COClF**

COClF is produced from the atmospheric degradation of molecules which contain a single fluorine atom and chlorine, such as CFC-11. The first global observations of atmospheric COClF from ACE-FTS were made using data from between 2004 and 2007 (Fu et al., 2009). The ACE-FTS retrieval of COClF was used in both the stratospheric chlorine and fluorine budgets (Nassar et al., 2006b; Nassar et al., 2006a). A full validation of this species has yet to be carried out.

### **3.2.13 Carbonyl Fluoride - COF<sub>2</sub>**

COF<sub>2</sub> is produced from the atmospheric degradation of molecules which contain two fluorine atoms on the same carbon, such as CFC-12. Comparisons with measurements from Mk-IV show an agreement to within  $\pm 20\%$  (Velazco et al., 2011).

### **3.2.14 Phosgene - COCl<sub>2</sub>**

The first study of atmospheric phosgene from ACE-FTS spectra were made by Fu et al. (2007). This study showed lower concentrations of COCl<sub>2</sub> than observations made in the 1980s and 1990s. Once more a full validation of this species has yet to be carried out.

### **3.2.15 Chlorine Nitrate - ClONO<sub>2</sub>**

Chlorine nitrate (ClONO<sub>2</sub>) is a reservoir species for atmospheric chlorine, produced by the reaction of ClO with NO<sub>2</sub>. During the day ClONO<sub>2</sub> is photolysed and so its VMR decreases. In the absence of light the VMR of stratospheric ClONO<sub>2</sub> increases as it re-forms. This diurnal cycle must be accounted for when analysing data since ACE-FTS measures only at sunrise and sunset. The mean difference between ACE-FTS and MIPAS

## The Atmospheric Chemistry Experiment

measurements of ClONO<sub>2</sub> showed differences of 0.03 ppbv at the peak of the profile (Höpfner et al., 2007). Further comparisons have been made between ACE-FTS total column and ground-based FTS measurements. The largest difference between these measurements was 21%, within the uncertainty of the retrievals from both the ground instrument and ACE (Mahieu et al., 2005). ClONO<sub>2</sub> was included in the 2004 stratospheric chlorine budget (Nassar et al., 2006a).

### **3.2.16 Hydrogen Chloride - HCl**

Hydrogen chloride (HCl) is the main chlorine reservoir in the stratosphere. The concentration of stratospheric HCl from ACE-FTS data has been studied in both the Arctic and Antarctic (Dufour et al., 2006; Mahieu et al., 2005; Santee et al., 2008). The Microwave Limb Sounder (MLS) retrieval of HCl was validated using ACE-FTS measurements (Froidevaux et al., 2006). MLS HCl profiles were within 5 % of the ACE profiles. ACE-FTS measurements of HCl have also been compared to those taken by the balloon-borne Mk-IV instrument. The difference between these measurements was 7 %. Rinsland et al. (2005) sought to build on the legacy of the ATMOS instrument by calculating the trend in stratospheric HCl between 1985 and 2004 (Rinsland et al., 2005). This work found that between 1994 and 2004 there was a marked decrease in the mixing ratio of HCl. These results helped illustrate the success of the Montreal Protocol in reducing the concentration of stratospheric chlorine.

### **3.2.17 Hydrogen Fluoride - HF**

HF is the main fluorine reservoir in the stratosphere. Retrievals of ACE-FTS HF have been compared to retrievals from coincident measurements made by the HALogen Occultation Experiment (HALOE) instrument. The results of this analysis showed that the VMR of retrievals from ACE-FTS version 1 were around 10 % to 20 % higher than HALOE (McHugh et al., 2005). ACE-FTS

## The Atmospheric Chemistry Experiment

version 2, non-coincident, retrievals were compared once more to HALOE; these results showed that ACE-FTS retrievals were larger by between 5 % and 20 % (Mahieu et al., 2008). HF from ACE-FTS has also been compared to measurements from the balloon-borne FIRS-2 instrument. These results showed significant differences between ACE and FIRS-2 with differences between 60 % (below 16 km where the VMR of HF is at its lowest) and 20 % (above 16 km) (Mahieu et al., 2008). This study also compared Mk-IV and ground-based FTIR to ACE HF. These results showed a difference of  $\pm 10$  % between ACE and Mk-IV above 19 km, and an average difference of  $\pm 7.4$  % for the average partial columns from ground-based FTIRs.

### **3.3 Summary**

The Atmospheric Chemistry Experiment Fourier Transform Spectrometer (ACE-FTS) is a satellite bourn infrared spectrometer. It is designed to measure the concentration of ozone and ODP within the polar regions It is a passive limb viewing instrument which uses the sun as its source. This solar occultation allows ACE-FTS to produce spectra with both a high signal-to-noise ratio and a high spectral resolution. Vertical profiles for concentration of over 30 gases are retrieved from atmospheric spectra using a global fit method. ACE-FTS currently retrieves 16 fluorine- and chlorine-containing gases. In the subsequent chapters these retrievals are used to calculate changes in the atmospheric VMR of these species over time individually and as a group and to calculate the stratospheric lifetime of some of the most important ODS,

# 4

## **Trends in atmospheric halogen containing gases since 2004**

### ***4.1 Introduction***

In their seminal paper in 1974, Molina and Rowland suggested that chlorofluorocarbons (CFCs) would lead to the destruction of stratospheric ozone (Molina et al., 1974). In 1985 the destructive effect of long-lived halogenated gases was dramatically demonstrated with the discovery of the Antarctic ‘ozone hole’ (Farman et al., 1985). As has been discussed in chapter 2, these discoveries coupled with further observations and simulations led to the instigation of the 1987 Montreal Protocol and its subsequent amendments and adjustments (UNEP, 2009). This treaty has systematically phased out the production and emission of CFCs and halons (for a more in-depth description

## Trends in atmospheric halogen containing gases since 2004

of the Montreal Protocol refer to Chapter 1). As a temporary measure, CFCs have been replaced by hydrochlorofluorocarbons (HCFCs): have shorter atmospheric lifetimes because they react with OH radicals. However, HCFCs still destroy stratospheric ozone and are in turn being phased out and replaced by hydrofluorocarbons (HFCs). Because they contain no chlorine, HFCs have no direct chemical effect on stratospheric ozone.

HFCs do not destroy stratospheric ozone but they are not entirely without their environmental impact. As has been discussed in chapter 2, HFCs, along with HCFCs and CFCs, are very powerful greenhouse gases. In fact, taken as a group, halocarbons are almost equal to tropospheric ozone in terms of a positive anthropogenic radiative forcing, and only CO<sub>2</sub> and CH<sub>4</sub> are more important (Solomon et al., 2007). The Montreal Protocol has been successfully implemented since 1987 with the aim of eradicating the use of substances which are damaging to the ozone layer. Ground based stations have been measuring annually decreasing concentrations of the main gases prohibited under the Montreal Protocol (Montzka et al., 2011a). These trends can be clearly seen in ground-based measurements made by the Advanced Global Atmospheric Gases Experiment (AGAGE) which can be seen in Fig. 4.1. The Montreal Protocol has inadvertently had a greater impact on reducing greenhouse gas emissions than the first commitment period of the Kyoto Protocol (Velders et al., 2007). However, the reduction of CFCs and halons has bought about a rapid increase in the atmospheric concentrations of HFCs. This has serious implications for climate change. Recent papers have predicted that Global-Warming-Potential-weighted HFC emissions in 2050 could be between 9 and 19% of global CO<sub>2</sub> emissions (Velders et al., 2009).

## Trends in atmospheric halogen containing gases since 2004

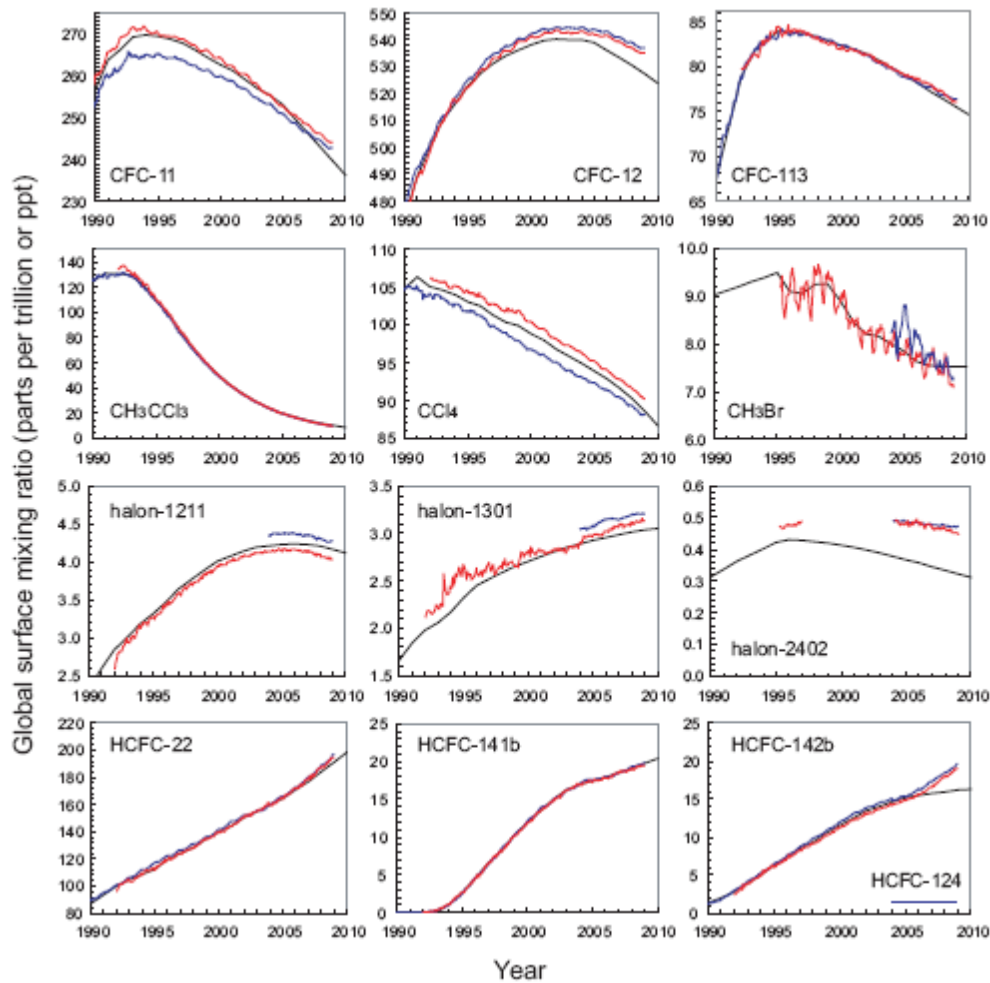


Figure 4.1: Mean global surface mixing ratio of some halogen-containing species as measured by the NOAA (red) and AGAGE (blue) and the A1 model scenario from the 2010 WMO ozone assessment (Montzka et al., 2011a)

The Montreal Protocol is continually evolving. Since its initial signing in 1987, the Montreal Protocol has been amended five times (in 1991, 1993, 1996, 1998, 2000 & 2008). These changes were driven as a reaction to updates in scientific knowledge. It is therefore crucial to assess the performance of the Montreal Protocol in reducing the concentrations of ODSs and to monitor the recovery of the ozone layer. Therefore, every four years the World Meteorological Organisation (WMO) and the United Nations Environmental Program (UNEP) publish a report on the “Scientific Assessment of Ozone Depletion” (SAOD), which is carried out by the Scientific Assessment Panel (SAP) of UNEP. The

## Trends in atmospheric halogen containing gases since 2004

2010 Scientific Assessment of Ozone Depletion report, released in early January 2011 (Montzka et al., 2011a), relied heavily on high precision in situ surface measurements of ODSs, with relatively modest contributions from satellite observations. High quality in situ measurements offer accurate and precise measurements of surface concentrations of ODS from a number of sites around the globe. Remote sensing from orbit allows the concentrations of these substances to be measured as a function of altitude, generally offering extensive spatial coverage, but with reduced accuracy and precision. Both spatial and temporal averaging of satellite data improves measurement precision, but often significant biases remain due to spectroscopic errors in the retrievals. Limb sounding satellite instruments such as MIPAS (Fischer et al., 2008) and solar occultation instruments such as ACE-FTS (Bernath, 2006; Bernath et al., 2005a) offer extensive four-dimensional (latitude, longitude, altitude and time) coverage of the atmosphere, which is only possible from orbit. Most importantly, these satellite instruments make routine measurements of atmospheric composition in the stratosphere where ozone depletion occurs.

In this chapter the changes in the VMR of 16 halogenated gases in the tropical atmosphere between 2004 and 2010 are presented. This work was carried out using Version 3 ACE-FTS retrievals of  $\text{CCl}_4$ ,  $\text{CF}_4$ ,  $\text{CCl}_3\text{F}$  (CFC-11),  $\text{CCl}_2\text{F}_2$  (CFC-12),  $\text{C}_2\text{Cl}_3\text{F}_3$  (CFC-113),  $\text{CH}_3\text{Cl}$ ,  $\text{ClONO}_2$ ,  $\text{COF}_2$ ,  $\text{COCl}_2$ ,  $\text{COClF}$ ,  $\text{CHF}_2\text{Cl}$  (HCFC-22),  $\text{CH}_3\text{CCl}_2\text{F}$  (HCFC-141b),  $\text{CH}_3\text{CClF}_2$  (HCFC-142b),  $\text{HCl}$ ,  $\text{HF}$  and  $\text{SF}_6$ . The purpose of this work was to give a general overview of global trends to demonstrate the utility of the ACE-FTS instrument observations rather than focus on details on the retrievals and global distributions of individual molecules which had been reported elsewhere. This chapter is divided into five sections. Section 4.2 focusses on the ACE occultations used in this study and the methods used in analysing the data. The SLIMCAT 3D chemical transport model is briefly described in Section 4.3. The results of the analysis and a

discussion of these results can be found in Section 4.4, before the work is summarised and final remarks are made in Section 4.5.

## ***4.2 Measurements and Methods***

As described in Chapter 2, the majority of halogenated source gases reach the stratosphere by powerful convective upwelling through the tropical tropopause. Therefore, this work focuses on changes in the tropical VMR of the halogen containing species measured by ACE. However, as can be seen in Fig. 4.2.,the number of tropical occultations which could be used in this study was limited by the observational geometry of SCISAT,

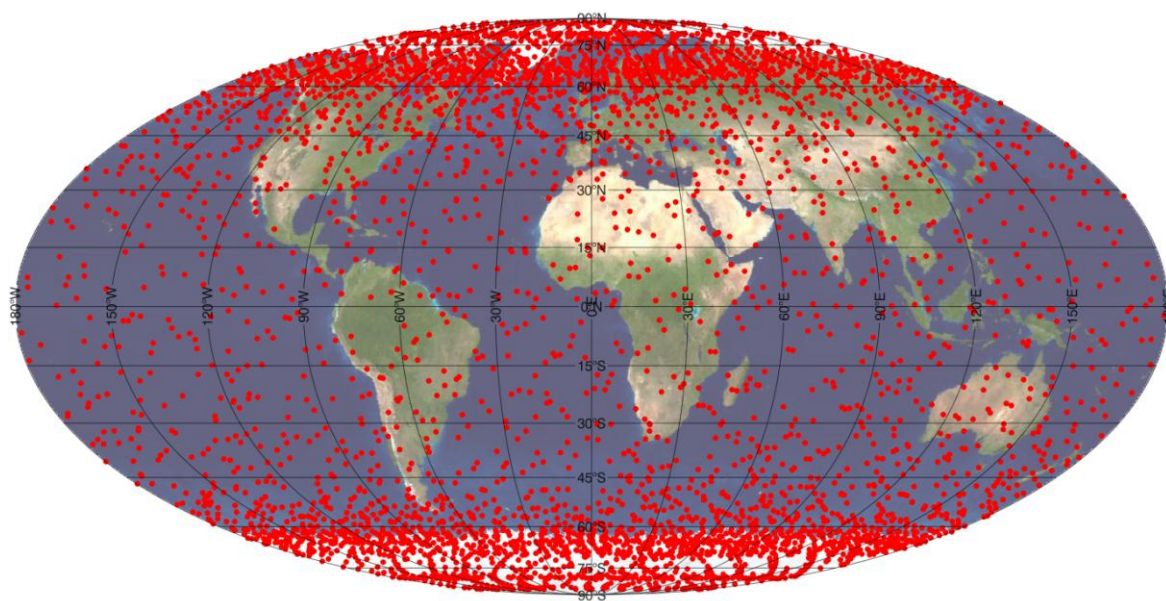


Figure 4.2: The positions of the ACE-FTS occultations during 2005. The occultations are clearly distributed with a greater number around the poles with fewer occultations occurring in the tropics. This imbalance is caused by the orbit of the satellite which is designed to observe the atmosphere in the polar regions.

## Trends in atmospheric halogen containing gases since 2004

This work follows the convention in atmospheric science of defining the tropics as the region around the equator which ranges from 30° N to 30° S (Barry, 2007d). The data does not present any significant grouping in this region (as can be seen in Fig. 4.3), thus the data from occultations in this region can be regarded as a fair representation of the whole 30° N to 30° S region.

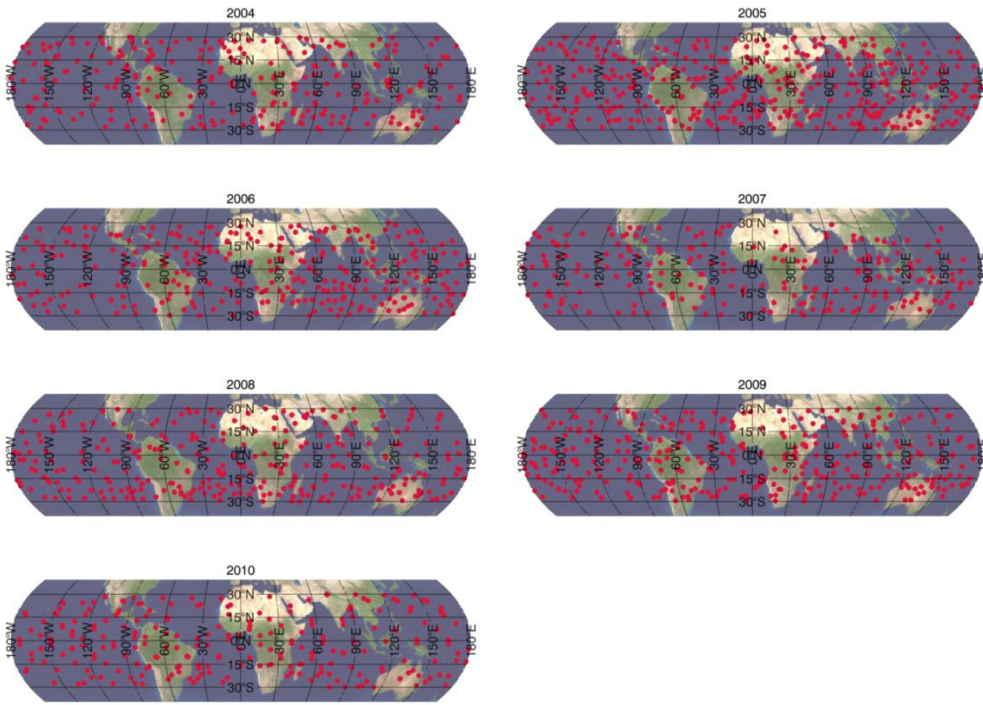


Figure 4.3: The positions of the occultations used in this study. These data do not exhibit any longitudinal or latitudinal grouping and so the mean VMRs of these data are representative of the region as a whole.

Occultations which did not lie within the tropical band were discarded, whilst the remaining occultations grouped according to the year in which they were made. The number of occultations from each year used in this study is shown in Table 4.1. Since the VMR of the species used in this work could be changing annually, the data from each year was filtered individually so that annual changes would not be filtered out.

Table 4.1: The number of ACE v.3 vertical profiles used in this study for each year

| Year | Number of Occultations |         |       |
|------|------------------------|---------|-------|
|      | Morning                | Evening | Total |
| 2004 | 57                     | 200     | 257   |
| 2005 | 159                    | 293     | 398   |
| 2006 | 127                    | 162     | 289   |
| 2007 | 99                     | 127     | 226   |
| 2008 | 122                    | 168     | 290   |
| 2009 | 180                    | 174     | 354   |
| 2010 | 94                     | 150     | 244   |

Filtering of the data required that the outliers were removed without removing significant amounts of the data. A median absolute deviation (MAD) filter was chosen to carry out this filtering. The MAD of a data set is calculated using Eq. 4.1. When calculating the standard deviation the difference between individual data points and the mean is squared; this gives added weight to outliers when calculating the standard deviation. When calculating the MAD however, the difference between the median ( $\tilde{x}$ ) and the data points ( $x_i$ ) is not squared; this prevents outliers from having a large effect on the MAD. The median of the absolute of this difference is the MAD. For this reason the MAD is a robust statistic and is ideal for filtering data which contains a number of large outliers.

$$\text{Median Absolute Deviation} = \text{Median}(|x_i - \tilde{x}_i|) \quad (4.1)$$

Outliers were removed by discarding individual points which were greater than 2.5 times the MAD from the median of the raw data (see Fig. 4.4). Individual points were removed rather than whole profiles since in a number of retrievals, only a small number of points are outliers. In many of these cases, the outliers are caused by failures within the retrieval program, caused

by high aerosols and clouds. This produces a localised effect within the profile and the retrieved VMR becomes excessively high (or low in the case of negatively retrieved VMRs) for a small number of points. The value of 2.5 times the MAD was chosen as a filter since, if data exhibits a Gaussian distribution, 95% of the data will be contained within 2.5 times the MAD away from the median. ACE data do not exhibit a truly Gaussian distribution and so this 2.5 MAD filter contains between 80 and 98% of the data; depending on the distribution of the data around the median. Nevertheless, as can be seen in Fig. 4.4, the filter is effective in removing the outlying data without removing significant amounts of data. Both a single MAD and 1.5 times the MAD removed too much data. In contrast a value of 3.5 MAD was too wide a window, as it allowed a number of outliers to be kept. Following this filtering, the remaining data were used to calculate a mean concentration at each altitude in the retrieval range; producing a mean vertical profile for each year. The altitude range over which these means are calculated are determined by the altitude limits of the retrieval. The tropical retrieval limits of the halogenated species in the ACE-FTS version 3 data product are displayed in Table 4.2. The retrieval of VMR from ACE-FTS level 2 data are carried out by Dr Chris Boone and Sean McLeod in the University of Waterloo, Canada. The work presented here is the analysis of the results of these retrievals by the author.

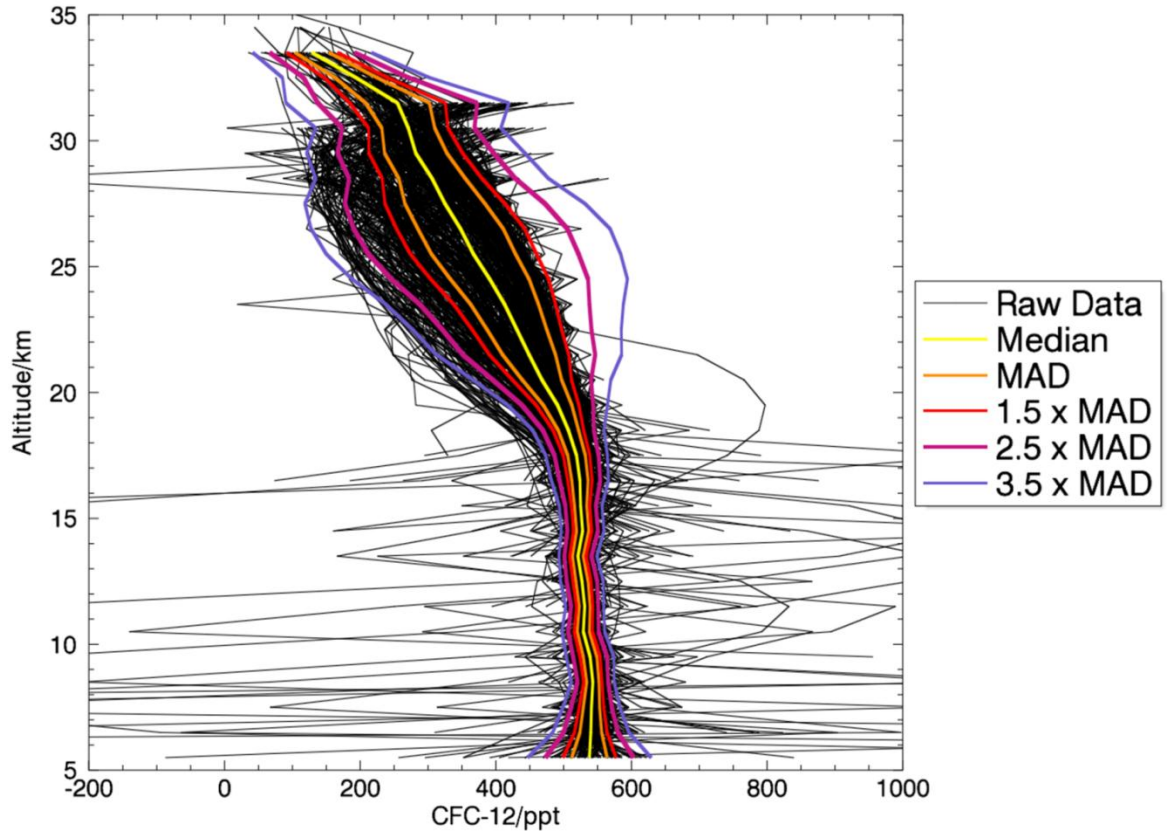


Figure 4.4: The vertical profile of CFC-12 in 2005 between the latitudes of 30° N and 30° S. The black lines are the raw unfiltered data. The yellow line is the median of that data. The orange, red, purple and blue lines are one MAD, one and a half MAD, two and a half MAD and three and a half MAD from the median respectively.

Once mean profiles had been calculated for each year, the profiles could be averaged between two altitudes depending on the species. Source species (such as CFC-11 and CFC-12), which are emitted at the surface and are photolysed in the stratosphere, were averaged in the region where their concentrations were roughly constant. For decomposition products (such as COClF and COCl<sub>2</sub>), which are produced from the decomposition of source species in the stratosphere, mean VMRs were calculated around the peak in VMR. Since the atmospheric VMR of CF<sub>4</sub> and SF<sub>6</sub> are roughly constant over their retrieval range, means for these species were calculated in regions where the retrieved

## Trends in atmospheric halogen containing gases since 2004

profiles were relatively flat. Mean HCl and HF VMR were calculated at the top of the retrieval range where their VMRs peak.

Table 4.2: The halogen containing species currently retrieved routinely from ACE-FTS data and their maximum and minimum retrieval altitudes and the altitudes between which means were calculated in this study.

| Species  | Altitude (km) |         |         |         |
|--|---------------|---------|---------|---------|
|  | Retrieval     |         | Means   |         |
|  | Minimum       | Maximum | Minimum | Maximum |
| CCl <sub>4</sub>   | 7             | 30      | 7       | 17      |
| CF <sub>4</sub>  | 15            | 55      | 25      | 40      |
| CFC-11 (CCl <sub>3</sub> F)                              | 6             | 28      | 7       | 16      |
| CFC-12 (CCl <sub>2</sub> F <sub>2</sub> )                | 5             | 36      | 5       | 17      |
| CFC-113 (C <sub>2</sub> Cl <sub>3</sub> F <sub>3</sub> ) | 7             | 20      | 7       | 17      |
| CH <sub>3</sub> Cl                                       | 12            | 40      | 12      | 17      |
| ClONO <sub>2</sub>                                       | 10            | 36      | 25      | 33      |
| COCl <sub>2</sub>  | 10            | 29      | 22      | 24      |
| COClF  | 15            | 32      | 23      | 28      |
| COF <sub>2</sub>   | 12            | 45      | 30      | 40      |
| HCFC-141b (CCl <sub>2</sub> F-CH <sub>3</sub> )          | 8             | 22      | 8       | 17      |
| HCFC-142b (CClF <sub>2</sub> -CH <sub>3</sub> )          | 5             | 21      | 7       | 17      |
| HCFC-22 (CHF <sub>2</sub> Cl)                            | 7             | 30      | 8       | 17      |
| HCl  | 7             | 63      | 50      | 54      |
| HF   | 12            | 57      | 50      | 54      |
| SF <sub>6</sub>  | 12            | 32      | 12      | 17      |

The windows in which the profiles were calculated are shown in brackets in Table 4.2. Chlorine nitrate (ClONO<sub>2</sub>) is a chlorine reservoir species produced by the reaction of ClO and NO<sub>2</sub>. ClONO<sub>2</sub> is photolysed during the day, so its concentration drops. During the night, the concentration of stratospheric

## Trends in atmospheric halogen containing gases since 2004

ClONO<sub>2</sub> rises once more as it reforms (Fig. 4.12). This diurnal cycle must be accounted for when analysing data because ACE measures only at morning and evening. There is no significant dependency in the retrieval program on morning or evening. This is exhibited by comparing the mean profile of CFC-11 from local evening and morning. Inspection of Fig. 4.5 shows that differences between evening and morning profiles of CFC-11 are smaller than the standard deviations of the profiles. Thus differences between the morning and evening profiles of chlorine nitrate are not due to bias in the retrieval program.

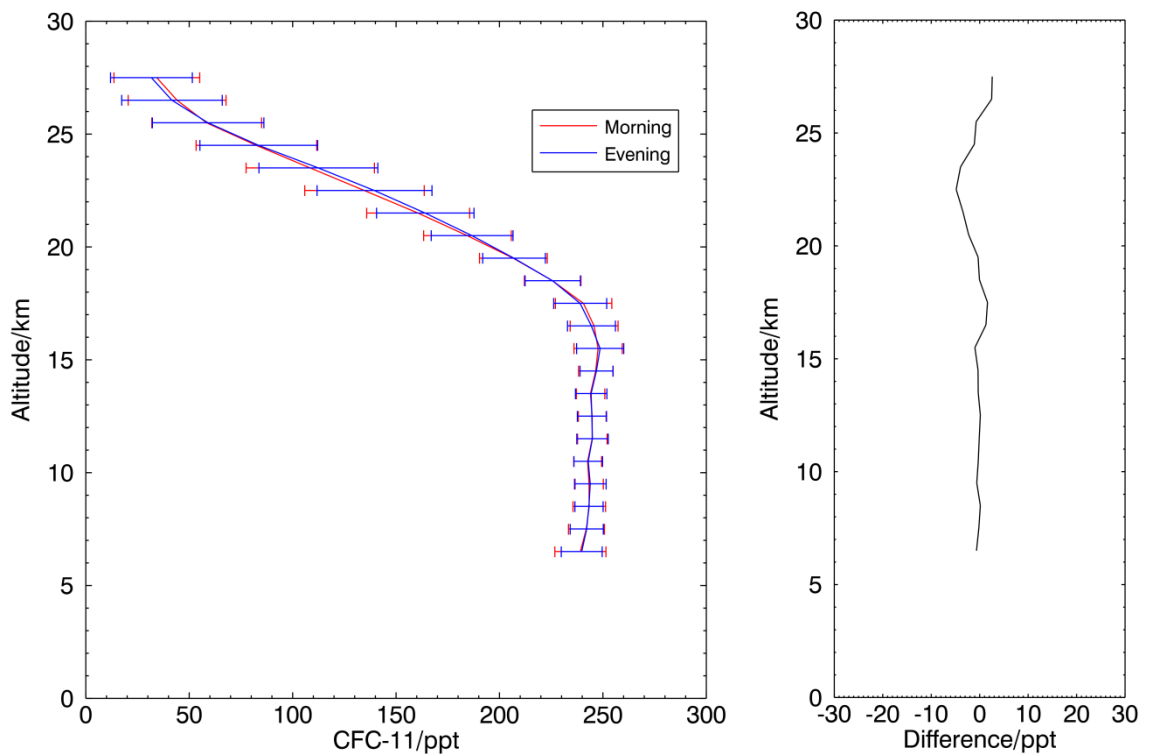


Figure 4.5: The difference between the mean CFC-11 profile (from all data) from evening and morning profiles. The error bars shown are the standard deviation of the data.

### ***4.3 SLIMCAT 3D Chemical Transport Model***

The ACE-FTS observations were compared to output from the SLIMCAT off-line three-dimensional (3-D) CTM. Since SLIMCAT is an off-line model, it does not calculate the winds and temperature fields that are used within the model. Instead, the model uses archived meteorological analyses. For this study, SLIMCAT used temperature and winds from the European Centre for Medium-Range Weather Forecasts (ECMWF) ERA-Interim reanalysis; which are available from 1989 onwards. Horizontal transport in the model is calculated using the wind from the meteorological data. Simulating vertical transport in the stratosphere is more complicated as it is calculated using heating rates which use the temperature from the meteorological data, along with the concentration of ozone and other stratospheric species. These variables are used to calculate the rate of solar absorption, and thus how much local heating occurs. This in turn is used to calculate vertical transport (Chipperfield, 2006; Monge-Sanz et al., 2007). SLIMCAT contains a detailed treatment of stratospheric chemistry including the major species in the  $O_x$ ,  $NO_y$ ,  $HO_x$ ,  $Cl_y$  and  $Br_y$  chemical families (Chipperfield, 1999; Feng et al., 2007). Whilst SLIMCAT does not include  $CF_4$  or  $COCl_2$ , all other species analysed in this study are included in the chemistry scheme.

For this study SLIMCAT was run at a horizontal resolution of  $5.6^\circ \times 5.6^\circ$  and 32 vertical levels from the surface to 60 km. The initial conditions for the surface VMR of source gases came from two sources. Species which contained chlorine or bromine came from the 2010 WMO/UNEP ozone report (Montzka et al., 2011a). Initial VMRs for HFCs came from annual mean surface observations such as AGAGE. These global mean surface values define the long-term tropospheric source gas trends in the model, which should therefore compare well with surface observations over the same time. For comparison with ACE, the model zonal mean monthly output was averaged to create annual means for latitudes between  $30^\circ$  S and  $30^\circ$  N on a 1 km altitude grid

ranging from 0 km to 60 km. For SF<sub>6</sub> comparisons, a separate model run was performed using the same setup but with an idealised SF<sub>6</sub> tracer. This run models tropospheric SF<sub>6</sub> based on estimated emission rates. The SLIMCAT model runs used in this study were carried out by Martyn Chipperfield and Chris Wilson at the University of Leeds.

## **4.4 Results and Discussion**

### **4.4.1 Carbon Tetrachloride, Carbon Tetrafluoride, Methyl Chloride & Sulphur Hexafluoride**

Carbon Tetrachloride (CCl<sub>4</sub>) was first retrieved from ACE-FTS spectra in 2004 for a stratospheric chlorine budget (Nassar et al., 2006a). This work found that CCl<sub>4</sub> contributed around 3% of the total stratospheric chlorine budget. CCl<sub>4</sub> is a potent ODS, with an ODP of 0.82. That is to say, CCl<sub>4</sub> has an ODP 18% smaller than CFC-11. CCl<sub>4</sub> has a GWP of 2,700 on a 20 year timeframe; CCl<sub>4</sub> is 2,700 times more powerful as a greenhouse gas than CO<sub>2</sub> (all GWP quoted in this chapter are given on a 20 year timeframe). An analysis of the global distribution of the Version 2.2 retrieval of CCl<sub>4</sub> from ACE-FTS data showed that ACE-FTS VMR were consistently higher than that from NASA's Global Modelling Initiative (GMI) CTM, the Atmospheric & Environmental Research (AER) group radiative transfer and SLIMCAT models (Allen et al., 2009). Those results are similar to those from this work, thus showing that ACE VMRs are consistently higher than those of SLIMCAT (Fig. 4.6). Once the mean CCl<sub>4</sub> VMR was calculated for each year (the altitudes of which are given in Table 4.2), a linear least squares fit was fitted to the annual data. The error on the time series quoted here is the error on the gradient calculated by the fitting program. These calculations show a linear decrease in the VMR of CCl<sub>4</sub> of  $1.32 \pm 0.09$  ppt ( $1.2 \pm 0.1\%$ ) per year since 2004. Simulations using the SLIMCAT model show a similar decrease of  $1.23 \pm 0.05$  ppt ( $1.4 \pm 0.1\%$ ) per year during

## Trends in atmospheric halogen containing gases since 2004

this time (Fig. 4.7). These values are in agreement with measurements made using AGAGE between 2007 and 2008 of a decrease of 1.1 ppt (1.3%) per year (Montzka et al., 2011a). The boundary conditions used by SLIMCAT are based on AGAGE measurements. Thus SLIMCAT values should agree with AGAGE measurements. SLIMCAT values at the surface are those of AGAGE, and the differences at higher altitude thus show the impact of atmospheric loss between the surface and the tropopause.

Atmospheric carbon tetrafluoride ( $\text{CF}_4$ ) is primarily emitted as a by-product during electrolytic aluminium production.  $\text{CF}_4$  is a powerful greenhouse gas with a GWP of 5,210. Previous comparisons between the retrieval of  $\text{CF}_4$  from spectra from the ATMOS in 1985 and from ACE in 2004, suggested a slowing of the rate of increase in atmospheric  $\text{CF}_4$  from  $2.77 \pm 0.47$  % per year in 1985 to  $1.14 \pm 0.68$  % per year in 2004 (Rinsland et al., 2006). Ground based observations between 1993 and 2008 in the northern hemisphere show  $\text{CF}_4$  increasing at a rate of  $0.686 \pm 0.002$  ppt per year (Muhle et al., 2010); a similar trend is seen in the southern hemisphere with a rate of  $0.702 \pm 0.001$  ppt per year. Annual stratospheric means from ACE data show  $\text{CF}_4$  increasing at a rate of  $0.54 \pm 0.03$  ppt ( $0.74 \pm 0.04\%$ ) per year between 2004 and 2010 (Fig. 4.6). The value calculated from ACE data appears significantly lower than the value from in situ ground based measurements. This is likely due to the altitude ranges between which the mean was calculated. These altitudes are firmly inside the stratosphere and therefore changes in the ground-based VMR of this species would take a number of years to affect the ACE calculated trends.

$\text{CH}_3\text{Cl}$  is the main source of natural chlorine in the atmosphere and whilst it is not as powerful a greenhouse gas as other halogen containing species, it is 45 times more effective in this regard than  $\text{CO}_2$  (Solomon et al., 2007). Similarly, the ODP of  $\text{CH}_3\text{Cl}$  is significantly smaller than other halons and CFCs, as it has a value of 0.02 (Montzka et al., 2011a). On the whole  $\text{CH}_3\text{Cl}$  emissions

## Trends in atmospheric halogen containing gases since 2004

emanate from oceans and biomass burning. ACE measurements of  $\text{CH}_3\text{Cl}$  are higher than those from SLIMCAT below 21 km (Fig. 4.6). Above 24 km, ACE measurements are lower than those from SLIMCAT. There has been a small increase in the concentrations of  $\text{CH}_3\text{Cl}$  during this time. ACE-FTS measures an annual increase of  $2.46 \pm 1.37$  ppt ( $0.4 \pm 0.2\%$ ) per year (Fig. 4.7). SLIMCAT data shows an increase of  $0.88 \pm 0.1$  ppt ( $0.17 \pm 0.1\%$ ) per year. Data from the 2010 WMO report showed an increase of  $2.5 \pm 1.2$  ppt ( $0.45 \pm 0.2\%$ ) per year between 2004 and 2008. The small SLIMCAT trend is a reflection of the constant surface VMR in the boundary condition files prepared for the WMO ozone report (Montzka et al., 2011a). The recent data (including ACE-FTS) points to a small positive trend; this is not reflected in the assumptions in the model.

Sulphur Hexafluoride ( $\text{SF}_6$ ) has an extremely long lifetime of 3200 years and a global warming potential of 16,300; thus making this molecule a potent greenhouse gas (Solomon et al., 2007). There are no natural sources of  $\text{SF}_6$ . Comparisons between the retrieval of  $\text{SF}_6$  from ATMOS and ACE observations showed an increasing trend of 0.22 ppt per year between 1985 and 2004 (Rinsland et al., 2005). The vertical profile of  $\text{SF}_6$ , as measured by ACE-FTS, is shown in Fig. 4.6. ACE-FTS measurements show the concentration of  $\text{SF}_6$  has increased between 2004 and 2010 at a rate of  $0.25 \pm 0.01$  ppt ( $4.2 \pm 0.1\%$ ) per year (Fig. 4.7). SLIMCAT data shows an increase of  $0.20 \pm 0.01$  ppt ( $3.5 \pm 0.18\%$ ) per year. These values, coupled with the calculations discussed previously, suggest a constant rate of increase between 1985 and 2010, and a possible increased rate of increase towards the end of this period.

## Trends in atmospheric halogen containing gases since 2004

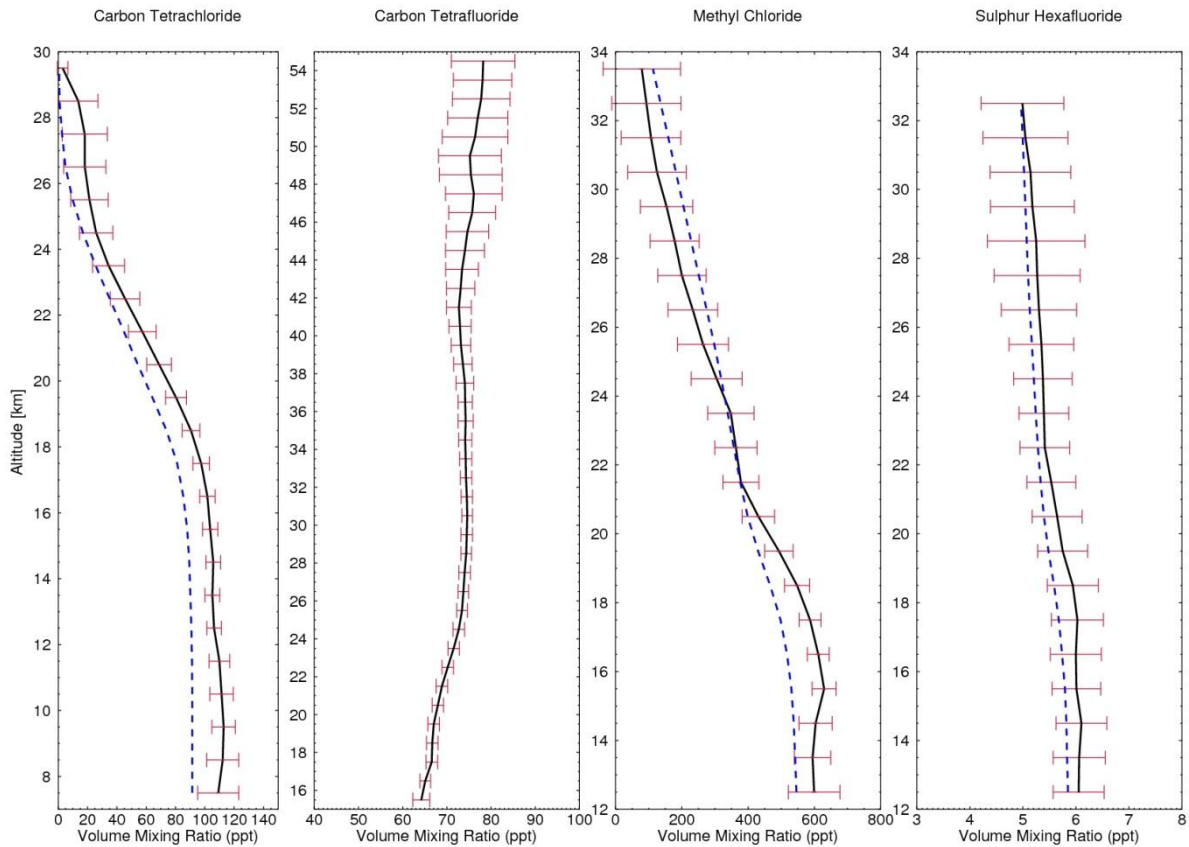


Figure 4.6: Average vertical profile of carbon tetrachloride, carbon tetrafluoride, methyl chloride & sulphur hexafluoride (ppt) between 30° N and 30° S from 2004 to 2010 from ACE (black) and SLIMCAT model (blue). The error bars represent one MAD of the ACE data. Note different y axis ranges.

## Trends in atmospheric halogen containing gases since 2004

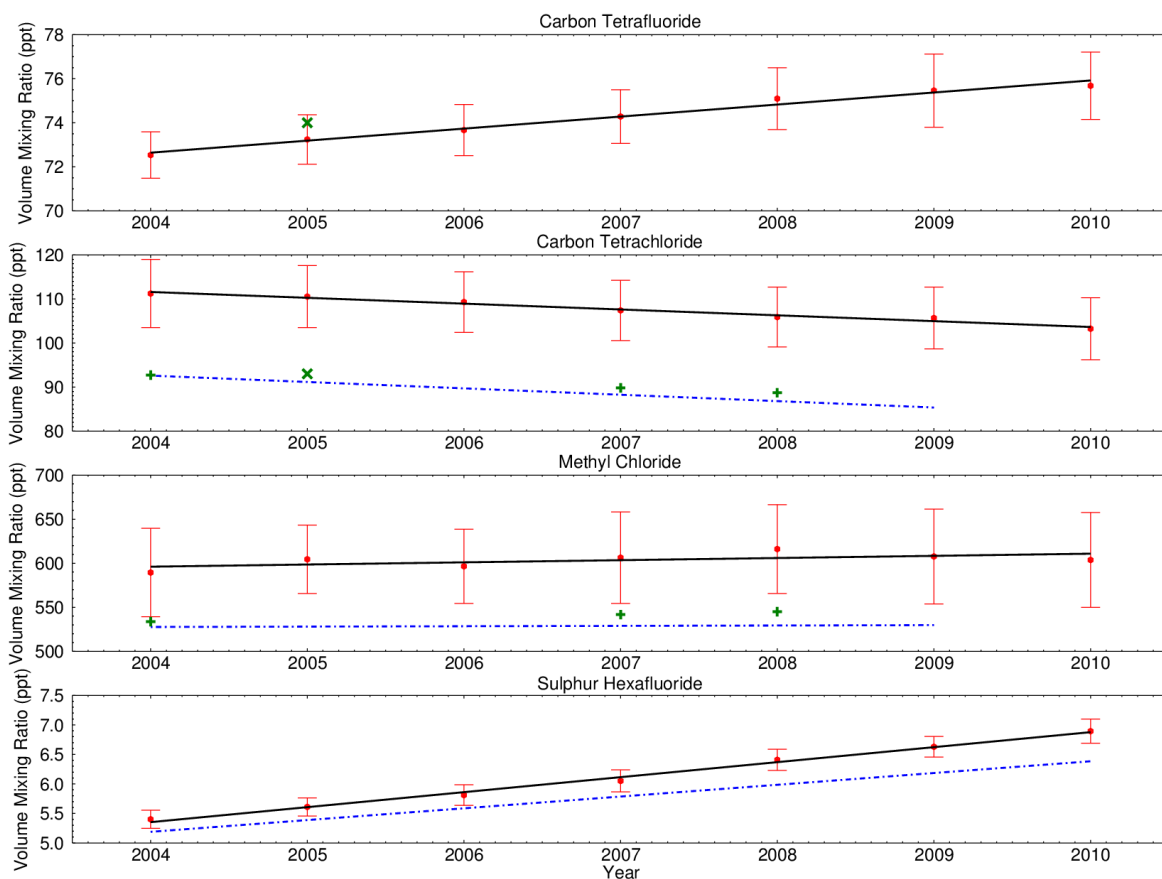


Figure 4.7: Volume mixing ratio of carbon tetrachloride, carbon tetrafluoride, methyl chloride & sulphur hexafluoride averaged between 30° N and 30° S for 2004 to 2010 from ACE (black line) and the SLIMCAT model (blue line). Also shown are surface mixing ratios from WMO (2010 - plus), IPCC (2007 – cross). The error bars represent one MAD of the ACE data and are shown for illustration. The errors on these means are significantly smaller than the MAD. Note different y axis ranges.

### 4.4.2 CFC-11, CFC-12 & CFC-113

CFC-11 is the second most abundant CFC in the atmosphere (Montzka et al., 2011a). Comparisons between measurements made in 1985, 1994 (ATMOS) and 2004 (ACE) showed a levelling off of emissions between 1994 and 2004 (Rinsland et al., 2005). This agrees with observations from the ground-based AGAGE and NOAA networks (Fig. 4.1) which show a stabilising of emissions

## Trends in atmospheric halogen containing gases since 2004

during this time (Montzka et al., 2011a). The vertical profile of CFC-11 from both ACE-FTS and SLIMCAT is shown in Fig. 4.8. There is good agreement between ACE and SLIMCAT profiles especially at lower altitudes. In the middle stratosphere, SLIMCAT underestimates ACE which could be due to a slightly too slow stratospheric circulation, too slow tropical upwelling in the Brewer-Dobson circulation. There has been a decrease in the concentrations of CFC-11 in the troposphere between 2004 and 2010. ACE-FTS measurements show an annual decrease of  $2.21 \pm 0.07$  ppt ( $0.9 \pm 0.1\%$ ) per year. SLIMCAT data show a decrease of  $3.03 \pm 0.13$  ppt ( $1.2 \pm 0.6\%$ ) per year (Fig. 4.9). There is good agreement between ACE and AGAGE measurements which show a decrease of 2.0 ppt (0.8%) per year between 2007 and 2008 (Montzka et al., 2011a). ACE observations also support observation of the VMR of CFC-11 in the troposphere decreasing over this time (Montzka et al., 2011a). It is to be expected that AGAGE and SLIMCAT would produce similar if not identical trends as CFC-11 does not have a tropospheric sink. The difference between the AGAGE and SLIMCAT trends is due to differences in the ground based VMR, which constrain these runs.

CFC-12 is the most abundant CFC in the atmosphere (Montzka et al., 2011a). Similarly to CFC-11, comparisons between measurements of the VMR CFC-12 made in 1985 and 1994, by ATMOS, and 2004, by ACE, showed a slowing rate of increase between 1985 and 2004 (Rinsland et al., 2005). When the profile of CFC-12 from SLIMCAT is compared to that from ACE, it is clear that there is good agreement at lower altitudes, but this agreement breaks down to a certain extent with increasing altitude (Fig. 4.8). This is probably due to a slow model circulation. There has been a decrease in the concentrations of CFC-12 in the upper troposphere and lower stratosphere between 2004 and 2010. ACE-FTS shows an annual decrease of  $1.90 \pm 0.12$  ppt ( $0.4 \pm 0.1\%$ ) per year, similarly SLIMCAT data shows a decrease of  $2.49 \pm 0.2$  ppt ( $0.5 \pm 0.1\%$ ) per year. These measurements suggest an increased rate of decrease in VMR when compared to measurements made by AGAGE between 2007 and 2008 of 2.2

## Trends in atmospheric halogen containing gases since 2004

ppt (0.4%) per year between 2007 and 2008 (Montzka et al., 2011a). Once more the difference between the AGAGE and SLIMCAT trends is due to differences in the ground based VMR, which constrain these runs.

CFC-113 was widely used in the late 1980s and early 1990s and is the third most abundant CFC in the atmosphere (Montzka et al., 2011a). Tropical measurements of CFC-113 using ACE-FTS show an unexpected increasing VMR with altitude below 12.5 km (Fig 4.8). This problem affects all years of data in a similar manner but does not affect occultations outside of the tropics. This suggests that this artefact is likely caused by a problem in the retrieval scheme of CFC-113 at high beta angles. That is to say when, the angle between the plane of the satellites orbit and the Sun is high (as occurs for tropical occultations), errors, are introduced into the retrieval scheme which form this unphysical increasing VMR with altitude. The precise nature of which are unknown at this time. Work is currently ongoing to produce an improved CFC-113 research product. A time series for this data can still be calculated, since the important factor in these calculations is the changing VMR relative to previous years. Since the problems in the retrieval should affect each year's data equally, a relative trend in the data should still be observed. The problems with the retrieval caused the mean of the ACE CFC-113 VMR to be lower than those from SLIMCAT. The CFC-113 profiles were averaged in the region between 6 km and 17 km, where the SLIMCAT profiles are roughly constant. ACE-FTS measures a decrease of  $0.65 \pm 0.08$  ppt ( $1.2 \pm 0.1\%$ ) per year in the VMR of CFC-113 since 2004. SLIMCAT simulations show a decrease of  $0.79 \pm 0.05$  ppt ( $1.1 \pm 0.1\%$ ) per year. The 2010 WMO report indicated an average decrease of 0.6 ppt (0.8%) per year (Montzka et al., 2011a). Despite problems with the ACE retrieval the trends calculated here show good agreement with both SLIMCAT and the AGAGE. These results suggest that the problem in the retrieval of CFC-113 does in fact impact on each year equally.

## Trends in atmospheric halogen containing gases since 2004

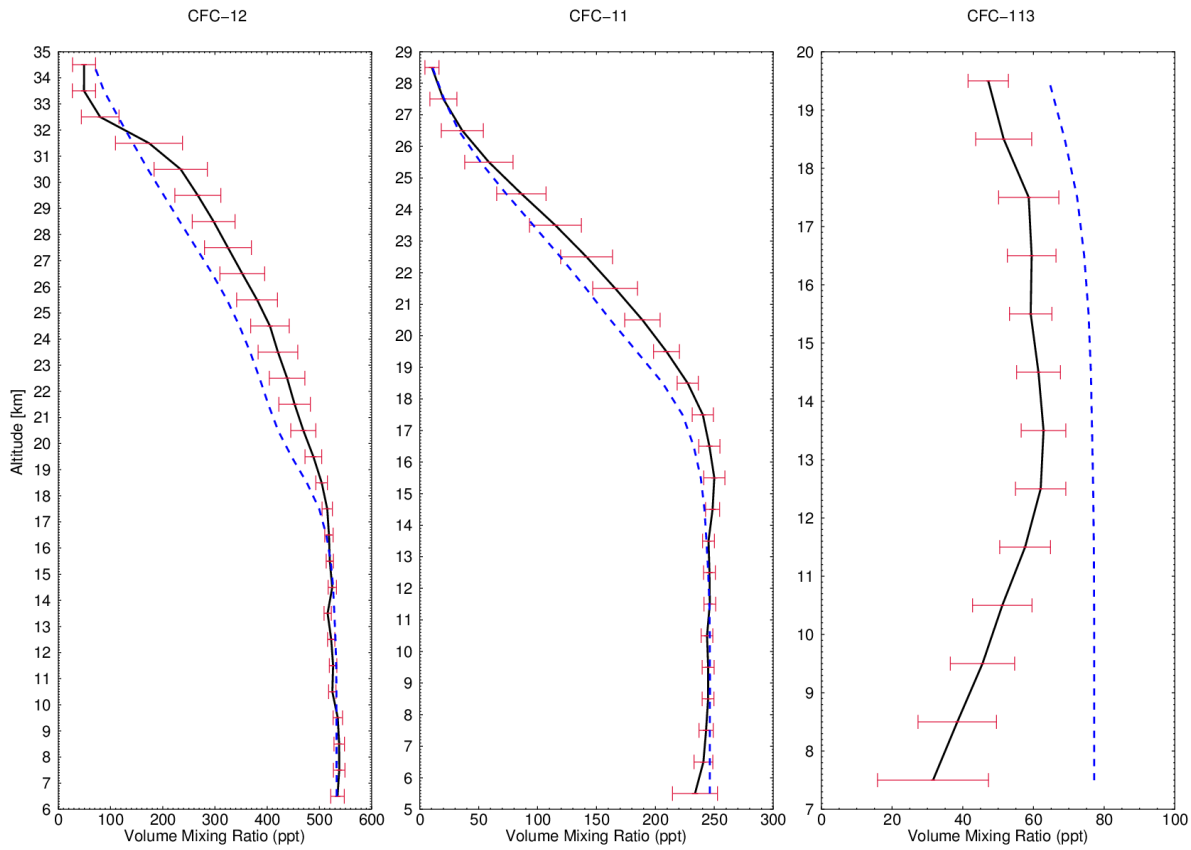


Figure 4.8: Average vertical profile of CFC-11, CFC-12 and CFC-113 (ppt) between 30° N and 30° S from 2004 to 2010 from ACE (black) and SLIMCAT (blue). The error bars represent one MAD of the ACE data. Note different y axis ranges.

## Trends in atmospheric halogen containing gases since 2004

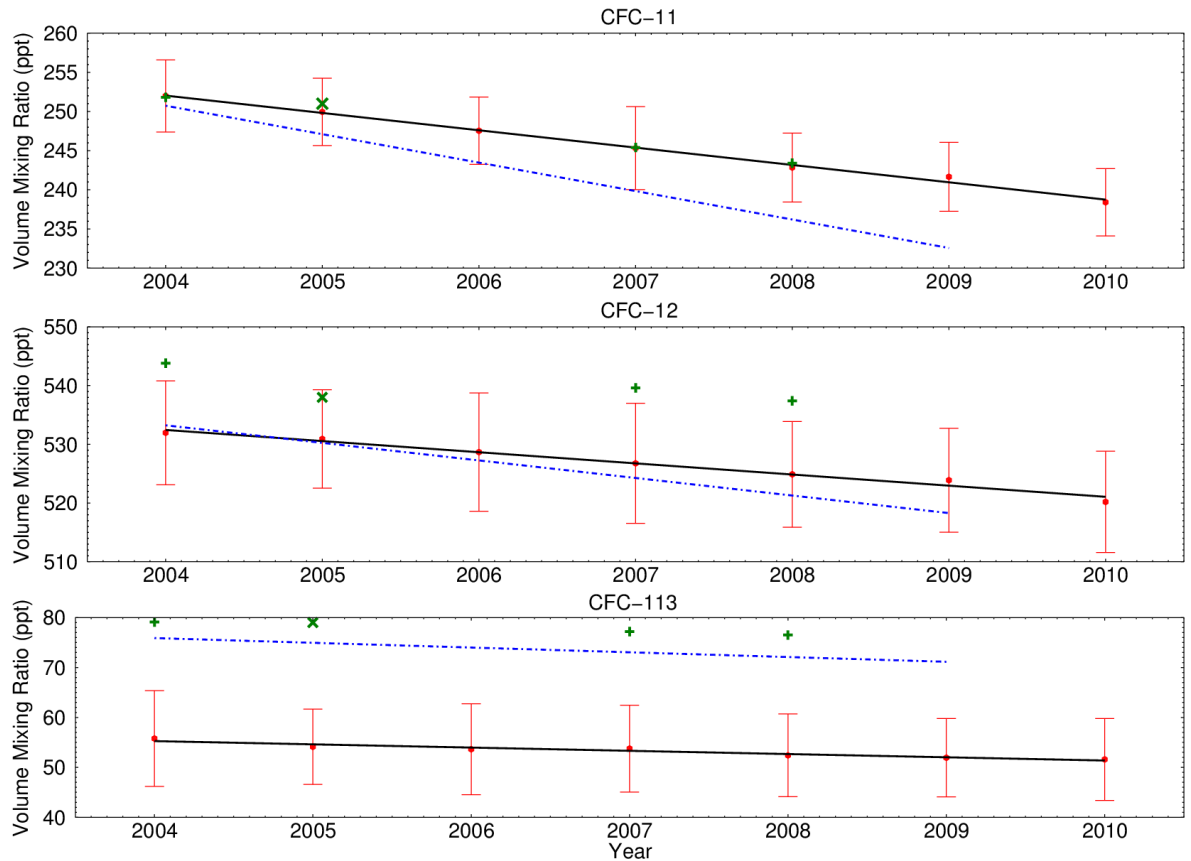


Figure 4.9: Volume mixing ratio of CFC-11, CFC-12 & CFC-113 averaged between 30° N and 30° S for 2004 to 2010 from ACE (black line) and the SLIMCAT model (blue line). Also shown are surface mixing ratios from WMO (2010 - plus) and IPCC (2007 - Cross). The error bars represent one MAD of the ACE data and are shown for illustration. The errors on these means are significantly smaller than the MAD. Note different y axis ranges.

### 4.4.3 HCFC-22, HCFC-141b & HCFC-142b

HCFCs are transitional replacement compounds for CFCs under the Montreal Protocol, and will in turn be phased out because they also deplete stratospheric ozone. HCFC-22 is the most abundant HCFC in the atmosphere, as it has been widely used since the 1950s. Measurements taken by ATMOS on two flights in 1985 and 1994 have been compared to measurements made by ACE-FTS in 2004 (Rinsland et al., 2005). These measurements showed that the

## Trends in atmospheric halogen containing gases since 2004

concentration of HCFC-22 in the lower stratosphere increased throughout this time. Tropical tropospheric measurements of HCFC-22 show an increasing VMR with altitude below the tropopause due to errors in the retrievals at high beta angle (Fig. 4.10). Whilst this effect appears to be similar to that exhibited by CFC-113, the source of the problem is entirely different. The version 3.0 retrievals for HCFC-22 employ two spectral regions, near 820 and 1115  $\text{cm}^{-1}$ . Investigation of the retrievals has found that retrievals using only the region near 820  $\text{cm}^{-1}$  do not exhibit this increasing VMR. Since there is no structure in the HCFC-22 spectral feature near 1115  $\text{cm}^{-1}$ , it is thought that retrievals in this region are more susceptible to errors from other atmospheric constituents such as aerosols. In subsequent chapters, data from a new retrieval of HCFC-22 was used which was unavailable at the time of this study. These problems had not been seen before this work. Despite these problems, there seems to be some agreement between the ACE and SLIMCAT VMRs. Measurements made since 2004 show that the concentration of HCFC-22 in the troposphere has increased annually. ACE-FTS measurements show an increase of  $6.56 \pm 0.20$  ppt ( $3.7 \pm 0.1\%$ ) per year. SLIMCAT shows an increase of  $6.24 \pm 0.11$  ppt ( $3.6 \pm 0.1\%$ ) per year (Fig. 4.11). AGAGE measured an increase of 8.6 ppt (4.6%) per year between 2007 and 2008 (Montzka et al., 2011a). ACE and SLIMCAT exhibit smaller trends in comparison to data from the AGAGE network. The difference in the trends between ACE, SLIMCAT and AGAGE are produced by the loss of HCFC-22, reacting with OH radicals in the troposphere, between the surface and the tropopause.

HCFC-141b is a new species available in the version 3.0 ACE-FTS data. There is again an unexpected slope to the VMR profile in the troposphere, which suggests that there may be problems with the retrievals at low altitudes. At low altitudes additional molecules, which are not part of the forward model, such as CFC-114, HFC-23 and PAN, contribute to the spectrum in the same region as HCFC-141b. Since these molecules are not included in the calculation of the VMR, errors are introduced into this calculation. The

contribution of these molecules to the spectrum decreases with altitude, allowing for better retrievals at higher altitudes. There is a large and varying difference between ACE and SLIMCAT profiles up to 15 km (Fig. 4.10). ACE VMRs are considerably higher than those from SLIMCAT above 15 km. ACE measurements show an annual increase of  $0.17 \pm 0.12$  ppt ( $0.74 \pm 0.5\%$ ). SLIMCAT data show an increase of  $0.55 \pm 0.01$  ppt ( $3.1 \pm 0.1\%$ ) per year (Fig. 4.11). Once more losses between the surface and the tropopause produce smaller trends than in the measurements made by AGAGE between 2007 and 2008, which showed an increase of 0.7 ppt (3.6%) per year (Montzka et al., 2011a). The large difference between the ACE retrieved HCFC-141b trends and SLIMCAT and AGAGE trends suggest that there are significant problems with the HCFC-141b retrieval.

The use of HCFC-142b in industry has greatly increased since the early 1990s because of the implementation of the Montreal Protocol (Montzka et al., 2009). The ACE V.2.0 retrieval of HCFC-142b shows an agreement to 15% between ground-based AGAGE and ACE measurements. SLIMCAT VMRs are generally within one MAD of the ACE measurements below 13 km. The VMR from SLIMCAT are slightly lower than ACE measurements above 13 km, but are always within two MAD of the ACE measurements (Fig. 4.10). ACE-FTS tropical measurements of HCFC-142b exhibit an unexpected increasing VMR with altitude below 17.5 km; this is similar to that for the CFC-113 profile. This is probably due to a similar problem in the retrievals as CFC-113 and work is on-going to produce an improved research product. Measurements taken since 2004 show that there has been an increase of  $1.17 \pm 0.05$  ppt ( $7 \pm 0.4\%$ ) per year. SLIMCAT data show a smaller increase of  $0.26 \pm 0.02$  ppt ( $1.7 \pm 0.1\%$ ) per year (Fig. 4.11). ACE-FTS measurements are in relatively good agreement with the rate of 1.1 ppt (5.9%) per year measured by AGAGE between 2007 and 2008 (Montzka et al., 2011a). As has been noted previously, a small difference between the SLIMCAT and ACE trends and AGAGE trends is to be expected. In this case however, the difference between the SLIMCAT

## Trends in atmospheric halogen containing gases since 2004

and AGAGE trend is larger than expected. The surface data file, prepared for WMO ozone report (Montzka et al., 2011a) which is used in the model, appears to underestimate the observed trend.

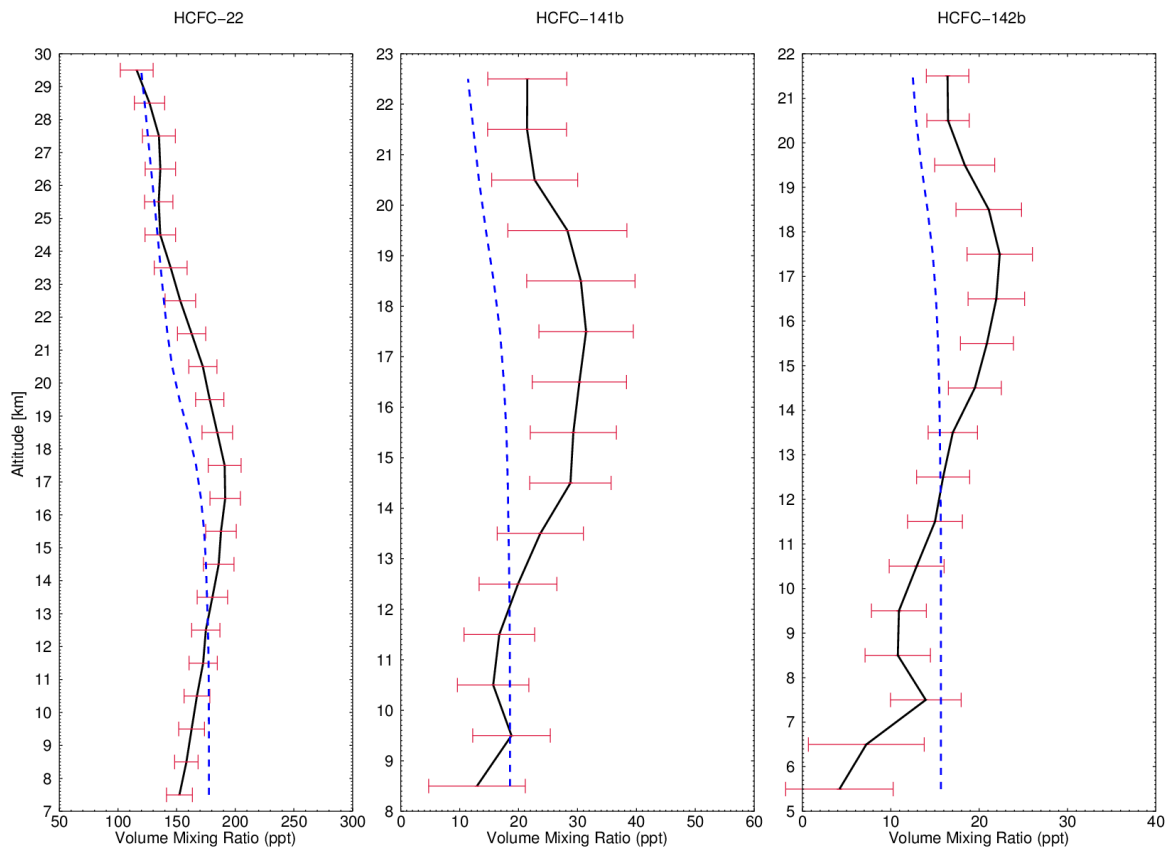


Figure 4.10: Average vertical profile of HCFC-22, HCFC-141b and HCFC-142b (ppt) between 30° N and 30° S from 2004 to 2010 from ACE (black) and SLIMCAT (blue) . The error bars represent one MAD of the ACE data. Note different y axis ranges.

## Trends in atmospheric halogen containing gases since 2004

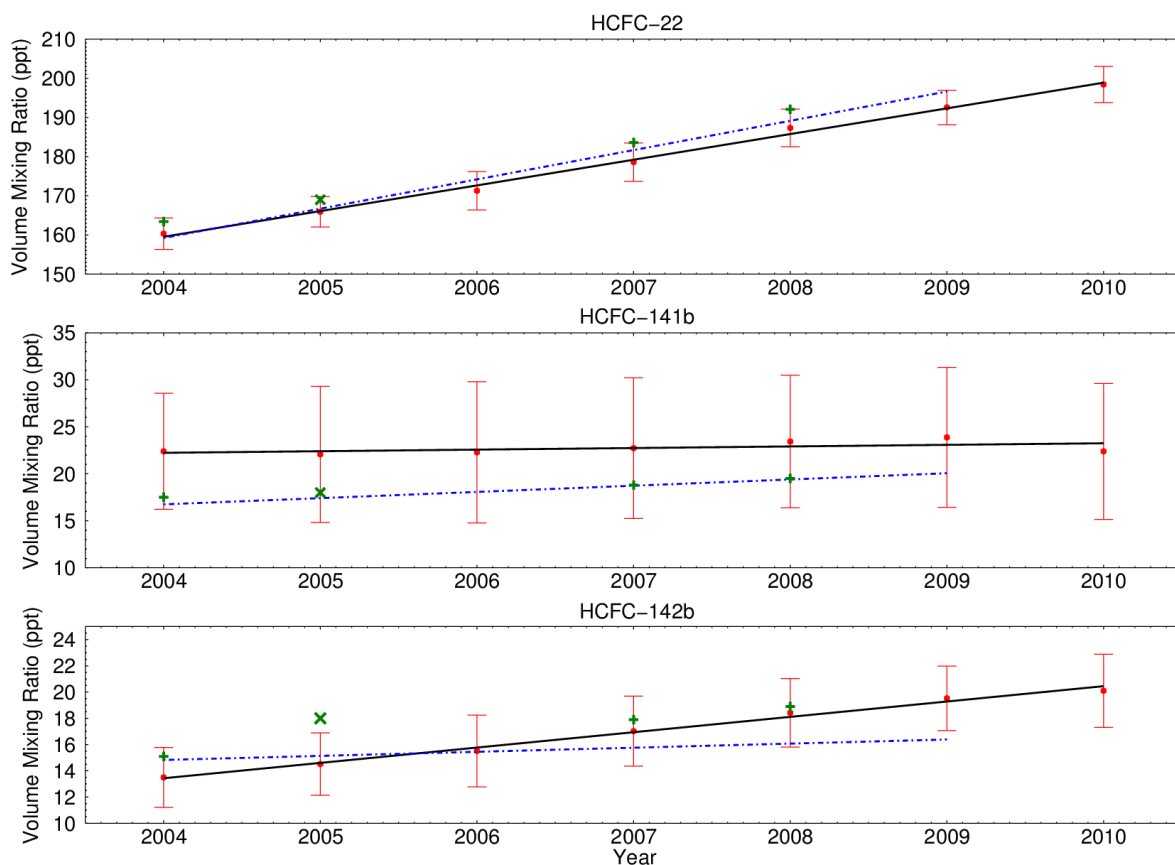


Figure 4.11: Volume mixing ratio of HCFC-22, HCFC-141b & HCFC-142b averaged between 30° N and 30° S for 2004 to 2010 from ACE (black line) and the SLIMCAT model (blue line). Also shown are surface mixing ratios from WMO (2010 - plus) and IPCC (2007 - cross). The error bars represent one MAD of the ACE data and are shown for illustration. The errors on these means are significantly smaller than the MAD. Note different y axis ranges.

### 4.4.4 Phosgene, Carbonyl Chlorofluoride, Carbonyl Fluoride & Chlorine Nitrate

Phosgene ( $\text{COCl}_2$ ) is created in the atmosphere by the decomposition of chlorocarbons such as tetrachloroethene, methyl chloroform and carbon tetrachloride. Phosgene is rained out in the troposphere, so the concentration increases with altitude within the troposphere. In the stratosphere, the main source of phosgene is the photolysis of carbon tetrachloride. The main sink for

## Trends in atmospheric halogen containing gases since 2004

stratospheric phosgene is photolysis which results in HCl formation and ozone depletion. The first analysis of phosgene from ACE-FTS was made by Fu et al. (2007), which found a reduction in phosgene concentration in the stratosphere between the 1980s and 1990s. This was attributed to the decrease in the concentrations of methyl chloroform and carbon tetrachloride due to the phase-out mandated by the Montreal Protocol. The ACE vertical profile of phosgene can be seen in Fig. 4.12. The phosgene profiles were averaged in the region between 22 km and 24 km, where the peak in the profile occurs. There does not appear to be any statistically significant change in the VMR of stratospheric phosgene during this time with a change of  $0.28 \pm 0.24$  ppt ( $0.9 \pm 0.8\%$ ) per year since 2004 (Fig. 4.13) being observed.

Carbonyl chlorofluoride (COClF) is a significant reservoir species for both atmospheric chlorine and fluorine. COClF is produced from the decomposition of CFC-11, and thus the mixing ratio of atmospheric COClF is a good indicator for the emissions of anthropogenic chlorine. Both SLIMCAT and ACE data show a peak in concentration between 24 km and 28 km. SLIMCAT assumes COClF is produced from the decomposition of CFC-11 and CFC-113 and its VMRs are higher than those from ACE (Fig. 4.12). The COClF profiles were averaged in the region between 23 km and 28 km where the peak in the profile occurs. Measurements made between 2004 and 2010 suggest that the VMR of COClF has decreased slightly during this time. ACE-FTS measurements show a statistically insignificant decrease of  $0.56 \pm 0.57$  ppt ( $0.9 \pm 0.9\%$ ) per year. SLIMCAT data show a more significant decrease of  $1.98 \pm 0.44$  ppt ( $2.3 \pm 0.5\%$ ) per year. This is in line with the decrease in CFC-11 (and CFC-113) during this time (Fig. 4.13). The observed trend in COClF indicates that the model may be overestimating the decline in CFCs.

Atmospheric carbonyl fluoride (COF<sub>2</sub>) is a stratospheric decomposition product produced mainly by the decomposition of CFC-12. Additional COF<sub>2</sub> formation is believed to come from the decomposition of HCFC-22 and -142b and HFC-32,

## Trends in atmospheric halogen containing gases since 2004

-125, -134a and -152a. The vertical profile has a maximum in the mid-stratosphere (Fig. 4.12).  $\text{COF}_2$  was retrieved for the 2004 global stratospheric fluorine budget (Nassar et al., 2006b). At its peak,  $\text{COF}_2$  accounts for 32% of the total 'inorganic' stratospheric fluorine budget (Nassar et al., 2006b). There is good agreement between SLIMCAT and ACE profiles below 27 km. However, SLIMCAT underestimates the ACE profile above 28 km as it assumes that  $\text{COF}_2$  is produced from CFC-12, CFC-113 and HCFC-22. HFC decomposition in this run of SLIMCAT is assumed to lead directly to HF. There has been a gradual increase of  $2.32 \pm 1.05$  ppt ( $0.8 \pm 0.4\%$ ) per year in the VMR of  $\text{COF}_2$  between 2004 and 2010. SLIMCAT data however seems to contradict the observations made by ACE-FTS and shows a decrease of  $2.98 \pm 0.98$  ppt ( $1.3 \pm 0.4\%$ ) per year (Fig. 4.13). This discrepancy is most likely due to the modelling of the sources of  $\text{COF}_2$ . SLIMCAT assumes mainly CFC sources, the VMR of which are declining. It does not include the HFC sources (HFC-32, -125, -134a and -152a) which are still increasing. The decrease in concentration during this time is probably caused by the decreasing concentration of CFC-12 in the model.

For evening measurements, the VMR of  $\text{ClONO}_2$  has decreased between 2004 and 2010 at a rate of  $9.4 \pm 7.4$  ppt ( $1.2 \pm 0.9\%$ ) per year in contrast to an increase of  $10.2 \pm 5.4$  ppt ( $1.7 \pm 0.9\%$ ) per year for morning data (Fig. 4.13). Although only marginally significant, the reason for this difference is not known at this time. When this work was carried out SLIMCAT was not outputting diurnal data for  $\text{ClONO}_2$ . Although SLIMCAT simulates the full diurnally varying chemistry, in this study, output was not saved at local sunrise and sunset. Therefore, only 24-hour mean fields are available for  $\text{ClONO}_2$ . This SLIMCAT data shows a decrease of  $3.83 \pm 2.73$  ( $0.6 \pm 0.4\%$ ) per year.

## Trends in atmospheric halogen containing gases since 2004

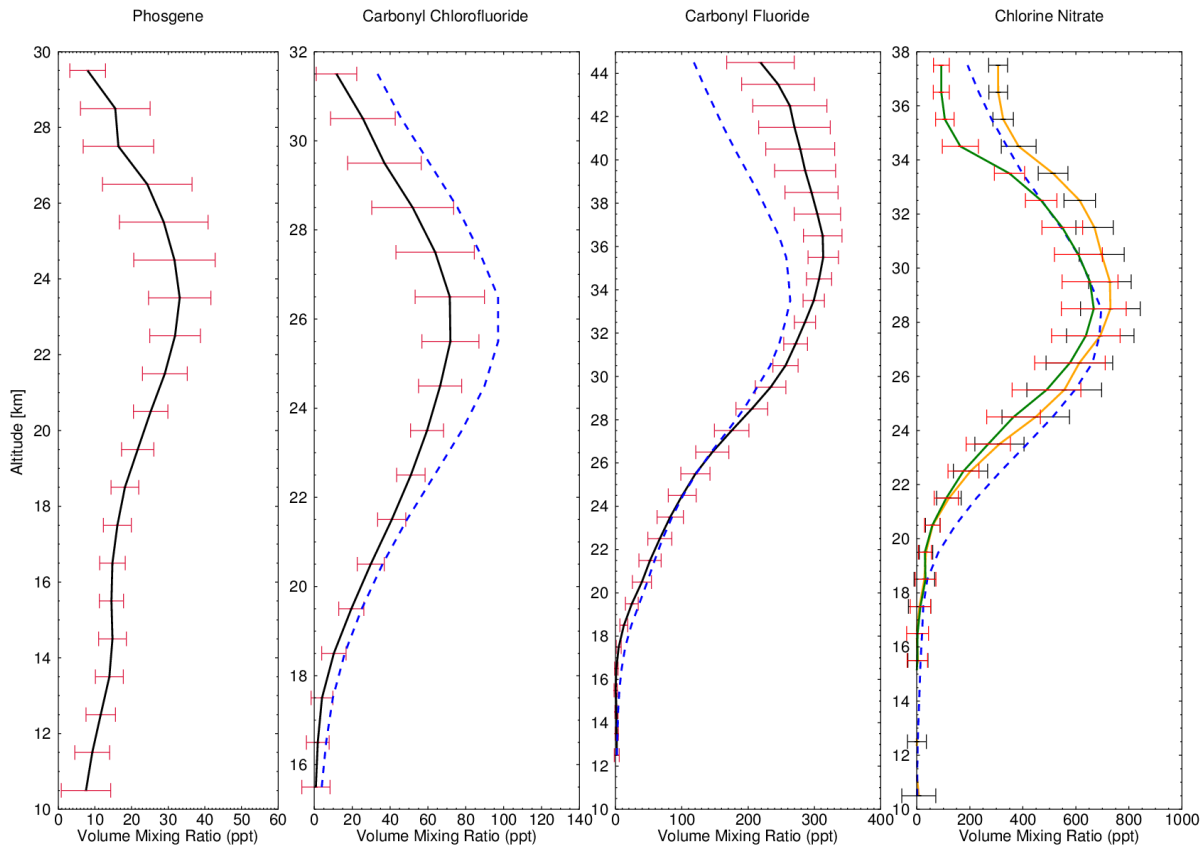


Figure 4.12: Average vertical profile of phosgene from ACE and carbonyl chlorofluoride, carbonyl fluoride & chlorine nitrate (ppt) between 30° N and 30° S from 2004 to 2010 from ACE (black) and SLIMCAT (blue). Measurements made in the morning of ClONO<sub>2</sub> by ACE are shown in orange. Measurements made in the evening are shown in green. The error bars represent one MAD of the ACE data. Note different y axis ranges.

## Trends in atmospheric halogen containing gases since 2004

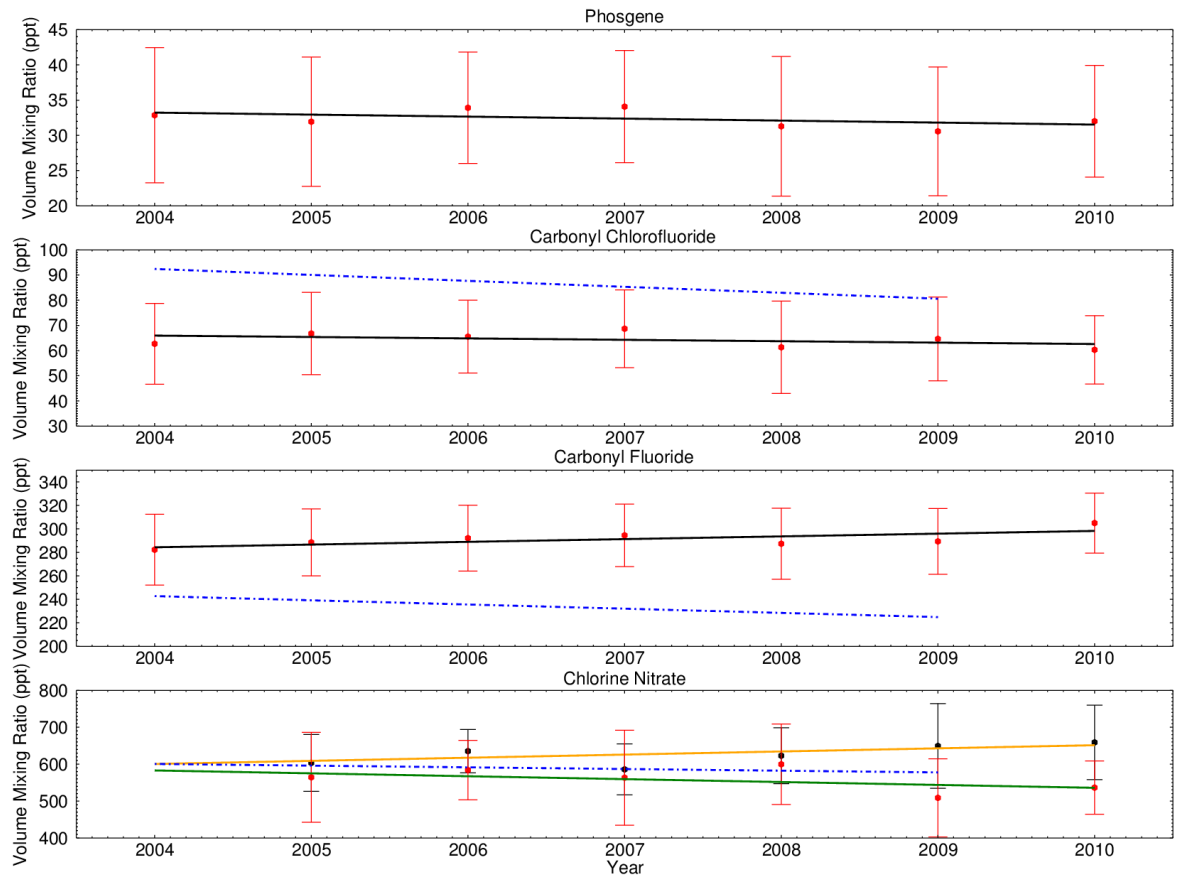


Figure 4.13: Volume mixing ratio of phosgene, carbonyl chlorofluoride, carbonyl fluoride & chlorine nitrate averaged between 30° N and 30° S for 2004 to 2010 from ACE (black line) and the SLIMCAT model (blue line). ACE  $\text{ClONO}_2$  measurements made in the morning are shown in orange. Measurements made in the evening are shown in green. The error bars represent one MAD of the ACE data and are shown for illustration. The errors on these means are significantly smaller than the MAD. Note different y axis ranges.

### 4.4.5 Hydrogen Chloride & Hydrogen Fluoride

Hydrogen chloride (HCl) is the main chlorine reservoir in the stratosphere. Rinsland et al. (2005) sought to build on the legacy of the ATMOS instrument by calculating the trend in stratospheric HCl between 1985 and 2004. This work found, that between 1994 and 2004, there was a marked decrease in the

## Trends in atmospheric halogen containing gases since 2004

mixing ratio of HCl. These results helped illustrate the success of the Montreal Protocol in reducing the concentration of stratospheric chlorine. There is good agreement between ACE VMRs and those from SLIMCAT in middle altitudes. In the lower and upper atmosphere, the agreement is worse (Fig. 4.14). At altitudes between 17 km and 32 km, SLIMCAT underestimates the concentrations of the major CFCs (CFC-11 and CFC-12), possibly due to a slightly too slow circulation. This results in more conversion of the source gases to HCl, the main inorganic chlorine reservoir. The model profile is constant above about 45 km; implying that all of the source gases which release Cl in the model have done so. The ACE observations continue to increase which suggests that there exists long-lived sources of chlorine which contribute to HCl production at these high altitudes. The HCl profiles were averaged in the region between 50 km and 54 km, where the profile peaks. Hydrogen chloride appears to have decreased between 2004 and 2010 by  $26.2 \pm 2.3$  ppt ( $0.7 \pm 0.1\%$ ) per year in the stratosphere (Fig. 4.15). This is larger than the decrease of  $18.9 \pm 0.9$  ppt ( $0.6 \pm 0.1\%$ ) per year shown in the SLIMCAT data. Froidevaux et al. (2006b) observed a decrease of  $27 \pm 3$  ppt ( $0.78 \pm 0.08\%$ ) per year for MLS from measurements made between August 2004 and July 2006 and 0.9% for ACE-FTS for the period between January 2004 and September 2009 (Montzka et al., 2011a; Froidevaux et al., 2006b).

Hydrogen fluoride (HF) is the main fluorine reservoir in the stratosphere. When fluorine-containing species undergo photolysis in the stratosphere, the resulting intermediates (which include  $\text{COF}_2$  and  $\text{COFCl}$ ) go on to form HF. Rinsland et al. compared measurements of HF made by ATMOS in 1985 and 1994 with those made by ACE in 2004 (Rinsland et al., 2005). These results showed a reduction in the rate of increase of HF in the atmosphere over this time. There is good agreement between SLIMCAT and ACE VMR. Generally the SLIMCAT VMRs are higher than ACE VMRs (Fig. 4.14). Once again, as for HCl, the model underestimates the major CFC sources of this species in the mid stratosphere and therefore overestimates the decomposition product. The

## Trends in atmospheric halogen containing gases since 2004

assumption that HFC decomposition leads only to HF, and not to  $\text{COF}_2$ , will also contribute to the overestimate of HF in the region where  $\text{COF}_2$  is underestimated (30 km and above). Hydrogen fluoride is increasing rapidly at a rate of  $20.6 \pm 4.5$  ppt ( $0.74 \pm 0.2\%$ ) per year. This is consistent with an increase in other fluorinated species. SLIMCAT data shows an increase of  $25.2 \pm 6.0$  ppt ( $1.4 \pm 0.3\%$ ) per year (Fig. 4.15).

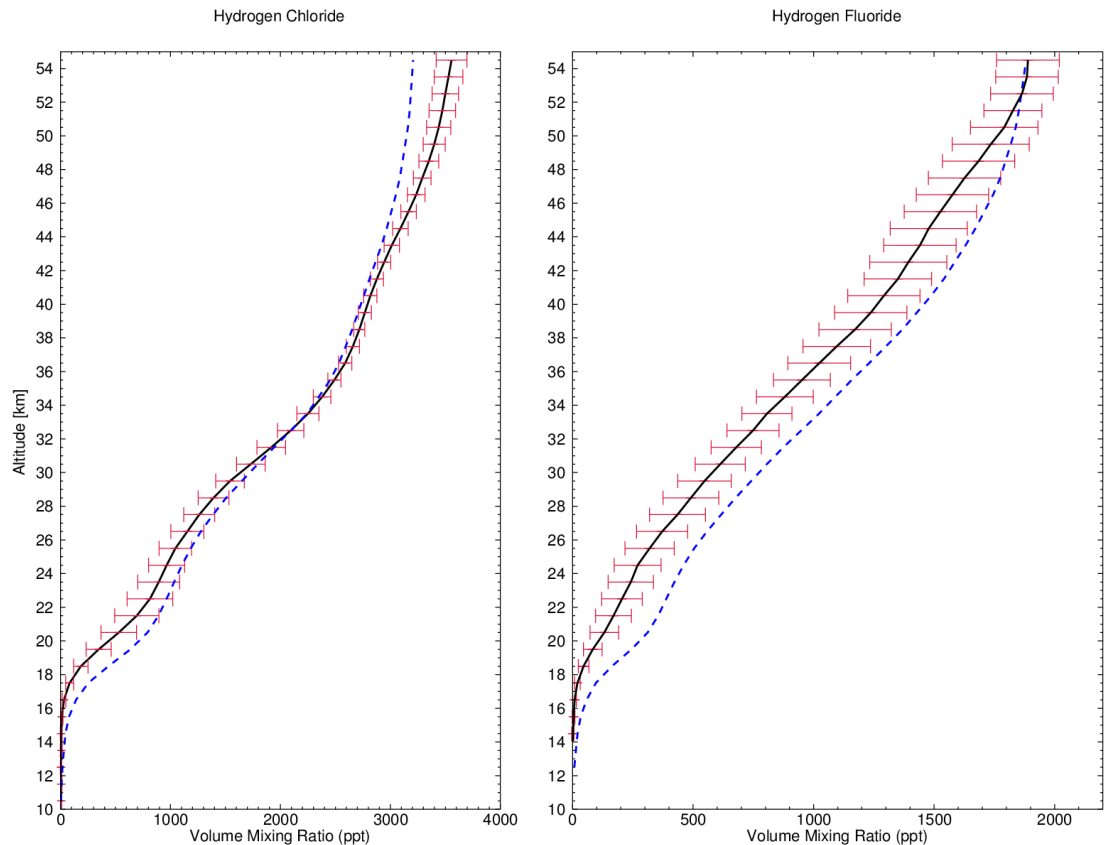


Figure 4.14: Average vertical profile of hydrogen fluoride & hydrogen chloride (ppt) between  $30^\circ$  N and  $30^\circ$  S from 2004 to 2010 from ACE (black) and SLIMCAT (blue). The error bars represent one MAD of the ACE data.

## Trends in atmospheric halogen containing gases since 2004

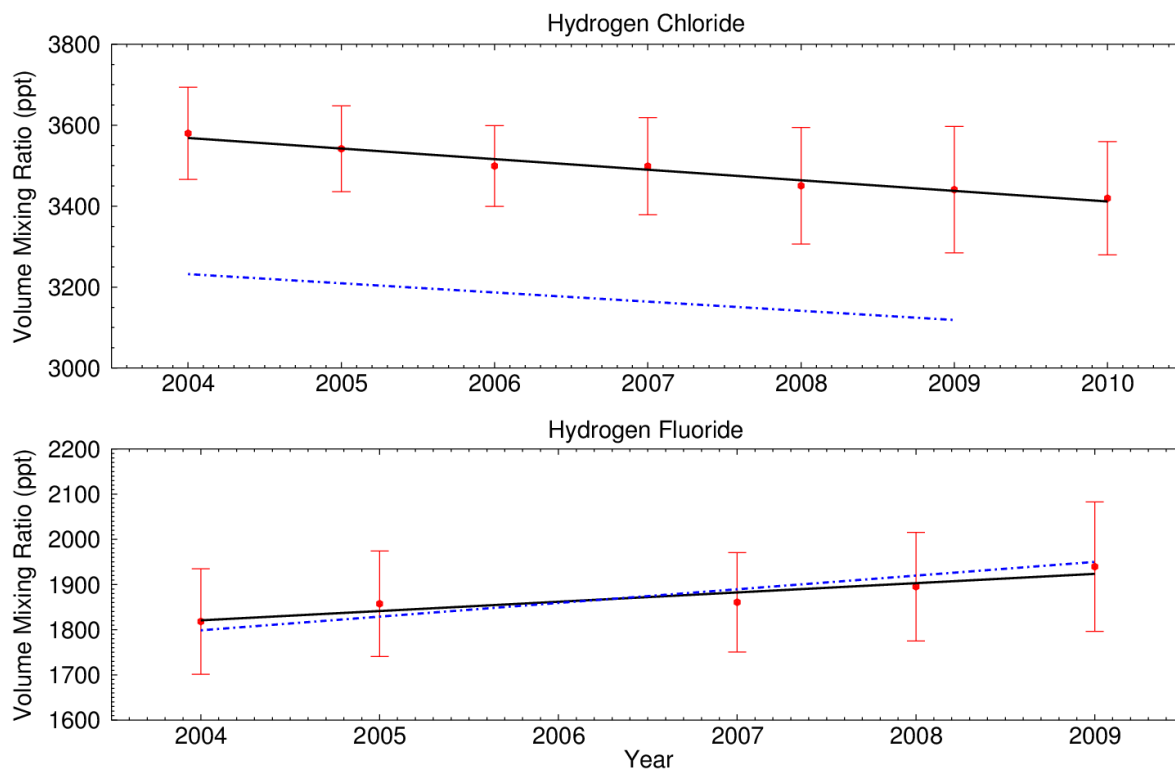


Figure 4.15: Volume mixing ratio of hydrogen fluoride and hydrogen chloride averaged between 30° N and 30° S for 2004 to 2010 from ACE from ACE (black line) and the SLIMCAT model (blue line). The error bars represent one MAD of the ACE data and are shown for illustration. The errors on these means are significantly smaller than the MAD. Note different y axis ranges.

### 4.5 Summary & Conclusion

Measurements were made by ACE-FTS of 16 halogen-containing species: CCl<sub>4</sub>, CF<sub>4</sub>, CFC-11, CFC-12, CFC-113, CH<sub>3</sub>Cl, ClONO<sub>2</sub>, COF<sub>2</sub>, COCl<sub>2</sub>, COClF, HCFC-22, HCFC-141b, HCFC-142b, HCl, HF and SF<sub>6</sub>. Tropical data for these molecules from 2004 to 2010 were analysed for trends. These data were filtered to remove values larger than two and a half median absolute deviations were removed. An annual mean was calculated, allowing the annual

## Trends in atmospheric halogen containing gases since 2004

variation of each species to be calculated. These results were compared to those from the SLIMCAT 3D chemical transport model and surface measurements made by the AGAGE network. The annual trends for each of the studied halogen-containing species are summarised in Table 4.3.

Table 4.3: Results of trend analysis on ACE-FTS data of halogen containing molecules (<sup>1</sup> average of northern and southern hemisphere (Muhle et al., 2010))

| Species            | Annual Trend (ppt (%) per year) |                             |                                |
|--------------------|---------------------------------|-----------------------------|--------------------------------|
|                    | ACE                             | Ground based                | SLIMCAT                        |
| CCl <sub>4</sub>   | - 1.32 ± 0.09<br>(- 1.2 ± 0.1)  | - 1.1<br>(- 1.3)            | - 1.23 ± 0.05<br>(- 1.4 ± 0.1) |
| CF <sub>4</sub>    | 0.54 ± 0.03<br>(0.74 ± 0.04)    | 0.69 <sup>1</sup>           | -                              |
| CFC-11             | - 2.21 ± 0.07<br>(- 0.9 ± 0.1)  | - 2.0<br>(- 0.8)            | - 3.03 ± 0.13<br>(- 1.2 ± 0.6) |
| CFC-12             | - 1.90 ± 0.12<br>(- 0.4 ± 0.1)  | - 2.2<br>(- 0.4)            | - 2.49 ± 0.20<br>(- 0.5 ± 0.1) |
| CFC-113            | - 0.65 ± 0.08<br>(- 1.2 ± 0.1)  | - 0.6<br>(-0.8)             | - 0.79 ± 0.05<br>(-1.1 ± 0.1)  |
| CH <sub>3</sub> Cl | 2.46 ± 1.37<br>(0.4 ± 0.2)      | 2.5 ± 1.2<br>(0.45 ± 0.20 ) | 0.88 ± 0.1<br>(0.17 ± 0.1)     |
| COCl <sub>2</sub>  | - 0.28 ± 0.24<br>(-0.9 ± 0.8)   | -                           | -                              |
| COClF              | - 0.56 ± 0.57<br>(- 0.9 ± 0.9)  | -                           | - 1.98 ± 0.44<br>(- 2.3 ± 0.5) |
| COF <sub>2</sub>   | 2.32 ± 1.05<br>(0.8 ± 0.4)      | -                           | - 2.98 ± 0.98<br>(- 1.3 ± 0.4) |
| HCFC-141b          | 0.17 ± 0.12<br>(0.74 ± 0.5)     | 0.7<br>(3.6)                | 0.55 ± 0.01<br>(3.1 ± 0.1)     |

Table 4.3 Continued

| Species                         | Annual Trend (ppt (%) per year)      |              |  |
|---------------------------------|--------------------------------------|--------------|--|
|                                 | ACE                                  | Ground based | SLIMCAT                                |
| HCFC-142b                       | $1.17 \pm 0.05$<br>( $7 \pm 0.4$ )   | 1.1<br>(5.9) | $0.26 \pm 0.02$<br>( $1.7 \pm 0.1$ )   |
| HCFC-22                         | $6.56 \pm 0.20$<br>( $3.7 \pm 0.1$ ) | 8.6<br>(4.6) | $6.24 \pm 0.11$<br>( $3.6 \pm 0.1$ )   |
| HF                              | $20.6 \pm 4.5$<br>( $0.74 \pm 0.2$ ) | -            | $25.2 \pm 6.0$<br>( $1.4 \pm 0.3$ )    |
| SF <sub>6</sub>                 | $0.25 \pm 0.01$<br>( $4.2 \pm 0.1$ ) |              | $0.20 \pm 0.01$<br>( $3.5 \pm 0.1$ )   |
| ClONO <sub>2</sub><br>(evening) | $-9.4 \pm 7.4$<br>( $-1.2 \pm 0.9$ ) | -            | -                                      |
| ClONO <sub>2</sub><br>(morning) | $10.2 \pm 5.4$<br>( $1.7 \pm 0.9$ )  | -            | -                                      |
| ClONO <sub>2</sub><br>(24-hour) | -                                    | -            | $-3.83 \pm 2.73$<br>( $-0.6 \pm 0.4$ ) |

Measurements of the trends made by ACE in the upper troposphere and lower stratosphere are generally in agreement with those from ground-based stations. Only three species (CH<sub>3</sub>Cl, HCFC-22 and HCFC-141b) have a difference of greater than 14% from ground-based measurements. The overall agreement is worse between ACE and SLIMCAT. Five species differed by more than 35% from ACE measurements at the sampled altitudes, namely COClF, HCFC-141b, HCFC-142b, HCl and CH<sub>3</sub>Cl. The VMR of the three CFCs measured in this study have decreased over time as has the VMR of CCl<sub>4</sub>. The HCFCs in this study, by contrast, have increased during this time. The VMR of CF<sub>4</sub> has also increased during this time. These results illustrate the success of the Montreal Protocol in reducing ozone depleting substances. The reduction in anthropogenic chlorine emissions has led to a decrease in the VMR of stratospheric HCl. The replacement of CFCs with HCFCs has led to an increase in the VMR of HF in the stratosphere. As chlorine-containing

## Trends in atmospheric halogen containing gases since 2004

compounds are phased out and replaced by fluorine-containing molecules, it is unlikely that total atmospheric fluorine will decrease in the near future.

The retrieved ACE-FTS profiles of HCFC-22, HCFC-141b, HCFC-142b and CFC-113 exhibit an unexpected and unphysical, increasing VMR with increasing altitude in the troposphere mainly because of spectral interferences in the retrieval. Work is on-going to improve the retrievals for these molecules. A research version of HCFC-22 has already been produced whilst work continues on the other species. Nevertheless, ACE HCFC-22, HCFC-141b, HCFC-142b and CFC-113 observations still show clear trends because of the systematic nature of the effect. The sloped portion of the VMR profile will introduce small offsets in the annual averages, and the resulting offsets in the trend slopes will be much smaller than the statistical regression errors. There is a noticeable difference between the morning and evening ACE trends of chlorine nitrate that is not understood at this time.

ACE measurements are useful in deriving global trends in atmospheric composition. In general, a single ACE measurement lacks the accuracy and precision of a careful, well-calibrated ground-based measurement. ACE measurements, however, offer extensive spatial coverage which is difficult to obtain in any other way. Converting ground-based measurements into the globally-averaged values, which are needed by policy makers using an atmospheric model, is not a trivial task and it is difficult to give reliable error estimates for the results. ACE also measures halocarbon abundances in the stratosphere where ozone depletion actually occurs, rather than on the ground where halocarbons are released. Averaging ACE measurements improves their precision although biases often remain because of systematic errors in the spectroscopy and in the retrievals. The sparse coverage of ACE data in the tropics requires larger latitude bands to increase the number of measurements which may be averaged. The ACE results reported here are only a preliminary

## Trends in atmospheric halogen containing gases since 2004

report on more extensive analyses of individual species, and the determination of complete atmospheric fluorine and chlorine budgets.

# 5

## Global stratospheric fluorine inventories

### *5.1 Introduction*

Many fluorine-containing chemicals are widely used in industry and elsewhere because they are chemically inert, non-toxic and odourless. A number of these species are controlled under the Montreal Protocol (UNEP, 2009) because they are ozone depleting substances. Whilst fluorine atoms do not play a direct part in ozone destruction, many of these species, such as CFCs and HCFCs, also contain chlorine and therefore are active ozone depleting substances. The C – F bonds in these molecules typically absorb infrared radiation between 1000 and 1300  $\text{cm}^{-1}$  (Lide, 1990); a “window” region in which the atmosphere is almost transparent. Below 1000  $\text{cm}^{-1}$  incoming radiation is absorbed by  $\text{CO}_2$  and  $\text{H}_2\text{O}$ , above 1400  $\text{cm}^{-1}$  incoming radiation is absorbed by  $\text{CH}_4$  and  $\text{H}_2\text{O}$ . Fluorine-containing species are therefore very powerful greenhouse gases and

as such their emissions are limited under the Kyoto Protocol (Solomon, 2007). The GWPs of some of the species used in this work are shown in Table 2.2. Many of these species, such as CFCs and hydrofluorocarbons (HFCs), are very stable and inert, thus they have extremely long atmospheric lifetimes. These species can therefore have a long-term effect on the global climate. HFC-23, for example, has an atmospheric lifetime of 222 years and a 100 year GWP of 14,800 (Montzka et al., 2011). Long-term monitoring of the VMRs of these species is therefore important for climate prediction.

Fluorine budgets are useful metrics for checking the atmospheric chemistry of fluorine-containing species. Previously fluorine budgets have used changes in the VMR of total fluorine as a proxy for changes in VMR of chlorine since many of these species contained both fluorine and chlorine containing species (Nassar et al., 2006b). In recent years, with the increased emissions of HFCs and decreases in purely chlorine containing species such as  $\text{CCl}_4$  and  $\text{CH}_3\text{CCl}_3$ , this approach can no longer be used. However, coupled with stratospheric chlorine budgets, the total fluorine calculation allows the effects of the Montreal Protocol to be quantified, with chlorine-containing species being replaced by fluorine-containing species.

A small number of fluorine budgets have been calculated previously. Measurements made by the ATMOS instrument were used to calculate a stratospheric fluorine budget using VMR profiles of  $\text{CF}_4$ , CFC-11, CFC-12,  $\text{COF}_2$ , HCFC-22, HF and  $\text{SF}_6$  at  $30^\circ \text{N}$  for 1985 (Zander et al., 1992). Further work was carried out using the Jet Propulsion Laboratory's MkIV balloon-borne Fourier Transform Spectrometer retrievals of  $\text{CF}_4$ , CFC-11, CFC-12, CFC-113,  $\text{COF}_2$ , HCFC-22, HF and  $\text{SF}_6$  (Sen et al., 1996). The most recent fluorine budget was carried out using data from the ACE-FTS (Nassar et al., 2006b). This budget used V2.2 ACE-FTS retrievals of  $\text{CF}_4$ , CFC-11, CFC-12, CFC-113,  $\text{COClF}$ ,  $\text{COF}_2$ , HCFC-22, HCFC-141b, HCFC-142b, HFC-134a, HF and  $\text{SF}_6$ . When considered together these works show increasing stratospheric

fluorine VMRs between 1985 and 2004. In the upper atmosphere the majority of the fluorine-containing species have been photolysed. Most of the fluorine which is present at these altitudes is therefore in the form of HF and COF<sub>2</sub>. In this case changes in the VMR of HF and COF<sub>2</sub> can be used as a proxy for overall changes in the VMR of fluorine-containing species. Total column measurements of these species from the ground based Fourier Transform Infra-red Spectrometers (FTIR) showed stratospheric fluorine increased at a rate of 0.4% per year between 2005 and 2008 (WMO, 2011). Ground-based FTIR measurements from Kiruna, Sweden show HF column increasing at a rate of  $1.0 \pm 0.3$  % per year between 1996 and 2008 (Mikuteit, 2008).

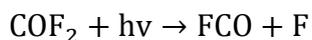
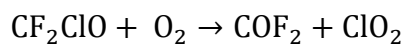
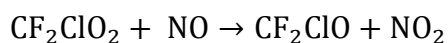
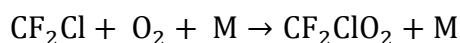
This chapter presents fluorine budgets calculated from ACE-FTS measurements which have been supplemented with data from the SLIMCAT 3D CTM. The budgets have been calculated using 18 fluorine-containing species (a list of which is given in Section 5.3), and represents the most comprehensive fluorine budget in the upper atmosphere to date. These budgets were calculated in 4 latitude bands between 70° N and 70° S. Since the ACE-FTS instrument has been active since 2004 we are able to chart the long-term changes in the atmospheric VMR of fluorine-containing species during this time. As such an individual fluorine budget has been calculated for every year, from 2004 to 2009. The large number of fluorine-containing species used in this work allows the calculation of the contribution of each species to the total fluorine VMR. It was shown in chapter 4 that the rate of decrease of the VMRs of CFC-11, CFC-12 and CFC-113 is significantly smaller than the rate of increase in the VMRs of the 3 most common HCFCs, HCFC-22, HCFC-141b and HCFC-142b. The effect that changes in the atmospheric VMR of a particular species will have on the total fluorine budget is dependent on the overall impact of each species on the budget. The climatological impact of the changing VMR of fluorine containing species is quantified using radiative efficiency- (RE) and GWP-weighted trends in total fluorine.

## **5.2 Fluorine Chemistry**

There are two principal reaction paths for the breakdown of fluorine-containing species in the atmosphere. The reaction path for a particular compound is determined by the number of fluorine atoms in the molecule.

### **5.2.1 CFCs and HCFCs which contain two fluorine atoms (COF<sub>2</sub> formation)**

The source gas molecule will first be broken down into CF<sub>2</sub>Cl and will then follow the following path (Tressaud, 2006):

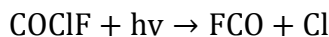
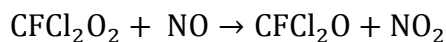


Above around 30 km the VMR of COF<sub>2</sub> decreases as photolysis becomes more effective. The primary source of COF<sub>2</sub> in the atmosphere is the decomposition of HCFC-22 and CFC-12. Contributions from HFCs, whilst smaller, are significant ensuring that, as was shown in chapter 4, the concentration of stratospheric COF<sub>2</sub> has been increasing since 2004.

### **5.2.2 CFCs which contain a single fluorine atom (COClF formation)**

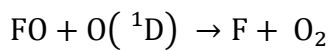
The source gas molecule will first be broken down by photodissociation into CFCl<sub>2</sub> and will then proceed along the following path (Tressaud, 2006):

## Global Stratospheric fluorine inventories



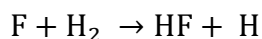
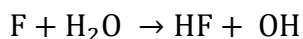
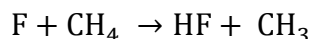
Carbonyl chlorofluoride (COClF) is less stable than  $\text{COF}_2$  and can be photolyzed more easily. It is therefore present in far smaller concentrations and peaks at lower altitudes than  $\text{COF}_2$ . The primary source for atmospheric COClF is CFC-11.

The production of FCO from the decomposition of COClF and  $\text{COF}_2$  leads to the formation of free fluorine atoms, in the following manner:



### 5.2.3 Production of Hydrogen Fluoride

The fluorine produced in both series of reactions will react with methane ( $\text{CH}_4$ ), water ( $\text{H}_2\text{O}$ ) or molecular hydrogen ( $\text{H}_2$ ) to form HF.



Photolysis of HF does not readily occur in the stratosphere, making HF an almost permanent reservoir of stratospheric fluorine (Tressaud, 2006). This means that the atmospheric concentrations of F and FO are very small, preventing fluorine from causing significant ozone loss. HF is ultimately

removed from the stratosphere by slow transport to, and rainout in, the troposphere or by upward transport to the mesosphere where its mixing ratio remains constant up to high altitudes.

### **5.3 Fluorine Budget Method**

#### **5.3.1 Fluorine-containing species included in the study**

Eight fluorine-containing species, CF<sub>4</sub>, CFC-12 (CCl<sub>2</sub>F<sub>2</sub>), CFC-11 (CCl<sub>3</sub>F), COF<sub>2</sub>, COClF, HCFC-22 (CHF<sub>2</sub>Cl), HF and SF<sub>6</sub>, are currently retrieved from ACE-FTS spectra. The retrieval limits of these species are shown in Table 5.1. Version 3.0 of the ACE-FTS retrieval has retrievals for CFC-113 (C<sub>2</sub>Cl<sub>3</sub>F<sub>3</sub>), HCFC-142b (C<sub>2</sub>H<sub>3</sub>ClF<sub>2</sub>), HCFC-141b (C<sub>2</sub>H<sub>3</sub>Cl<sub>2</sub>F) (Brown et al., 2011) and HFC-23 (CHF<sub>3</sub>) (Harrison et al., 2012), but the retrieved concentrations have substantial biases so it was decided to use model data instead. ACE data was supplemented with data from the SLIMCAT 3D chemical transport model. This study used the following SLIMCAT species to supplement ACE data: CFC-113, CFC-114, CFC-115, H-1211, H-1301, HCFC-141b, HCFC-142b, HFC-23, HFC-134a and HFC-152a. SLIMCAT was run using the same conditions as were previously described in chapter 4.3. The model zonal mean monthly output was averaged to create annual means for 4 latitude bins (70° N - 30° N, 30° N - 00° N, 00° N - 30° S and 30° S - 70° S) on a 1 km altitude grid.

Table 5.1: The retrieval altitudes of the fluorine-containing species used in this study

| Species                                   | Altitude (km) |            |
|---|---------------|------------|
|   | Polar         | Equatorial |
| CFC-11 (CCl <sub>3</sub> F)               | 5 – 23        | 6 – 28     |
| CFC-12 (CCl <sub>2</sub> F <sub>2</sub> ) | 5 – 28        | 5 – 36     |
| HCFC-22 (CHF <sub>2</sub> Cl)             | 5 – 30        | 7 – 30     |
| COClF                                     | 13 – 25       | 15 – 32    |
| COF <sub>2</sub>                          | 12 – 34       | 12 – 45    |
| SF <sub>6</sub>                           | 8 – 32        | 12 – 32    |
| CF <sub>4</sub>                           | 15 – 55       | 15 – 55    |
| HF  | 12 – 52       | 12 – 57    |

### 5.3.2 Total fluorine calculations

In total 16,186 ACE-FTS occultations were used in this study. For this analysis the globe was divided into 4 latitude bands (70° N - 30° N, 30° N - 0° N, 0° N - 30° S and 30° S - 70° S) chosen to represent the different transport regimes in the stratosphere. Outside of the tropics and the polar regions the stratosphere is well mixed by breaking planetary scale waves. Within the tropics powerful convective transport can penetrate the tropopause, mixing the lower layers of the stratosphere. In the polar regions the polar vortex has a significant effect on the VMR profiles of many of the species used in this work and so this region was excluded from the total fluorine calculations. The latitudes therefore represented the mid-latitude stratosphere (30° – 70° N/S) and the tropical stratosphere (0° – 30° N/S). Occultations were distributed by latitude and year; the number of occultations in each band is shown in Table 5.2. As would be expected from a satellite designed for polar observations, there are significantly more occultations in the mid latitude bands (70° - 30°

N/S) than in the tropical band (30° - 0° N/S). Despite this there are sufficient occultations in all bins to carry out budget calculations.

Once more (as in chapter 4) data in each band was filtered using the median absolute distribution (MAD) of the data. Any value which was greater than 2.5 times the MAD from the median of the raw data was discarded. Once the outliers had been removed a mean profile of each species was produced by calculating the mean mixing ratio at each altitude. The error on this profile is calculated using the standard deviation of the data used to calculate each mean mixing ratio. This produces a profile with errors which vary with altitude, dependent on the variation of the data at each altitude.

Table 5.2: The number of ACE-FTS occultations used for each latitude band and year

| Year | 70° - 30° N | 30° - 00° N | 00° - 30° S | 30° - 70° S | Total |
|------|-------------|-------------|-------------|-------------|-------|
| 2004 | 788         | 171         | 153         | 960         | 2072  |
| 2005 | 1631        | 278         | 301         | 1592        | 3802  |
| 2006 | 1166        | 164         | 178         | 1038        | 2546  |
| 2007 | 887         | 116         | 129         | 804         | 1936  |
| 2008 | 1449        | 134         | 197         | 1427        | 3207  |
| 2009 | 1162        | 168         | 202         | 1091        | 2623  |

ACE-FTS retrievals of the species used in this work extend between the limits set out in Table 5.1. These altitudes do not always coincide with the altitudes at which the VMR of the species in question is zero. A thorough fluorine budget requires that the mean profiles be extended to the limit of the budget. Profiles were extended by using the SLIMCAT profiles of the corresponding species scaled to match the ACE-FTS data at its highest and lowest retrieved altitude point. SF<sub>6</sub> and CF<sub>4</sub> did not have corresponding SLIMCAT data and so were extended vertically upwards at a constant VMR from the final retrieved altitude. An example of an extended profile can be seen in Fig. 5.1. All profiles

## Global Stratospheric fluorine inventories

were extended up to 54.5 km corresponding to the maximum altitude to which HF is retrieved by ACE-FTS.

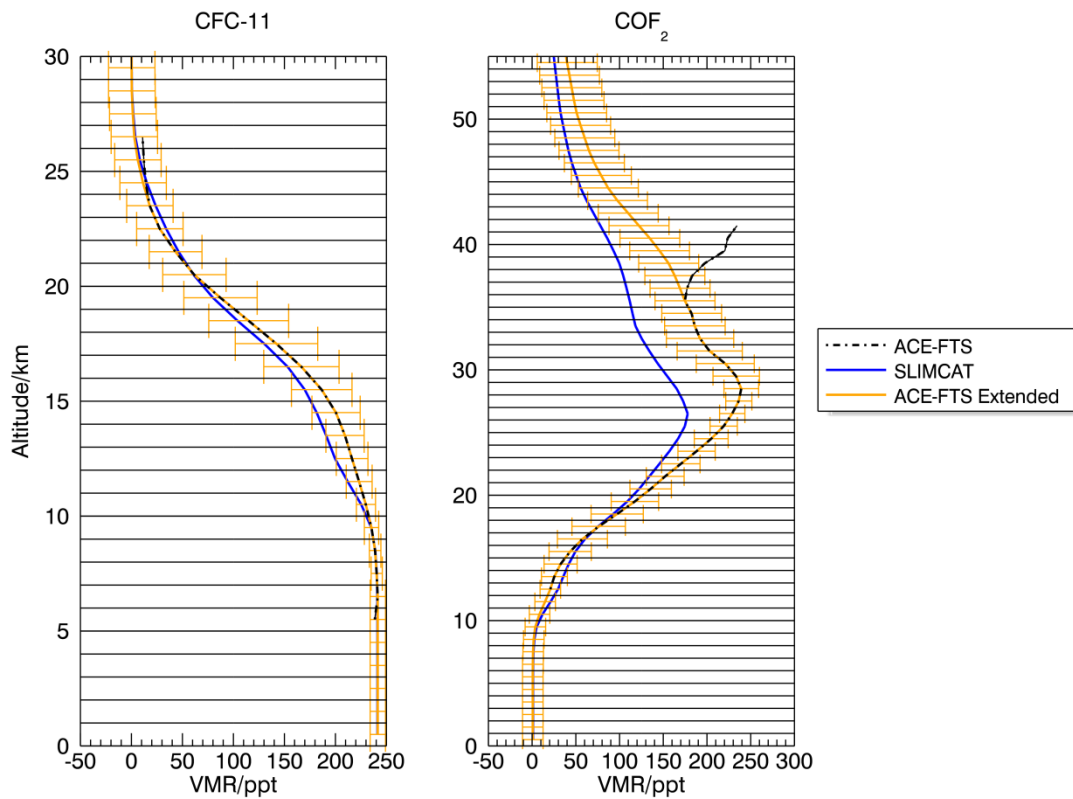


Figure 5.1: The extended and un-extended ACE-FTS profiles of CFC-11 and  $\text{COF}_2$  along with the accompanying SLIMCAT profile. The ACE-FTS profiles have been extended using a scaled SLIMCAT profile. The profiles shown in this figure are from the  $70^\circ - 30^\circ$  North 2008 latitude bin.

The total fluorine VMR was calculated at 54 levels between 0.5 km and 53.5 km corresponding to the ACE retrieval altitude grid. The equations used for this calculation are given below, where square brackets indicate the VMR. Following the convention of previous fluorine budgets (Nassar et al., 2006b; Zander et al., 1992), the total fluorine VMR can be expressed as the sum of the total inorganic fluorine and the total organic fluorine. The terms inorganic and organic are not used in the conventional sense in these works. Instead the term organic fluorine can be loosely interpreted as those fluorine species which

## Global Stratospheric fluorine inventories

are emitted from the surface. Inorganic fluorine species are fluorine containing molecules which are produced from the decomposition of the organic fluorine species (with the exception of SF<sub>6</sub>).

$$[\text{Total Fluorine}] = [\text{Total Inorganic Fluorine}] + [\text{Total Organic Fluorine}]$$

$$[\text{Total Inorganic Fluorine}] = [\text{HF}] + 2[\text{COF}_2] + [\text{COClF}] + 6[\text{SF}_6]$$

$$[\text{Total Organic Fluorine}] = 4[\text{CF}_4] + 2[\text{CFC-12}] + [\text{CFC-11}] + 2[\text{HCFC-22}] + 3[\text{CFC-113}] + 4[\text{CFC-114}] + 5[\text{CFC-115}] + 2[\text{HCFC-142b}] + [\text{HCFC-141b}] + 3[\text{HFC-23}] + 4[\text{HFC-134a}] + 2[\text{HFC-152a}] + 2[\text{H-1211}] + 3[\text{H-1301}]$$

### 5.3.3 Changes in the total fluorine VMR

Changes in the total fluorine VMR were calculated by calculating the mean total fluorine VMR in the stratosphere. In order to do this the mean position of the tropopause was calculated for each data group using the ACE-FTS Derived Metrological Products (DMPs). Each occultation has a corresponding DMP featuring various metrological variables which includes the altitude of the tropopause at that location. Total fluorine values below 2 km above the mean tropopause height were discarded leaving only stratospheric data. The mean and the standard deviation of this data were then plotted for each year allowing a linear least squares fit to be fitted to the data. The slope of this data represents the annual change in the total stratospheric fluorine whilst the error in the fitting was used as the error on this value.

The main environmental impact of the increasing VMR of atmospheric fluorine will be on warming in the troposphere and lower stratosphere regions. The different species analysed for this work have different GWPs and REs (see Table 2.2) and therefore have different effects on climate. A more useful quantity is therefore the trend in the atmospheric fluorine- weighted GWP. Since the GWP is a measure of the global warming potential of 1 kg of substance compared to 1 kg of CO<sub>2</sub>, the GWP total fluorine cannot be

calculated by simply weighting the fluorine source species by their GWP. Instead, the total fluorine must be weighted by the mass of the species and the GWP. The method used in this work to calculate this value was to weight each source species by its GWP and relative molecular mass. The VMR of these species was also weighted by the pressure, which is a measure of the atmospheric mass, at the corresponding altitude. Since the effect of these species is concentrated in the troposphere, data above the tropopause was not included in the calculations of the GWP weighted total fluorine.

### ***5.4 Results and Discussion***

This section is divided into 5 subsections. Section 5.4.1 presents the vertical profiles of the total fluorine calculations, with a focus on the gradient on the line and its implications for the long-term changes in the total fluorine VMR. Subsequently the slopes of the correlation plots between source fluorine species and reservoir fluorine species are presented and discussed in Section 5.4.2. The impacts of the individual species included in the total fluorine calculations on the total fluorine VMR are presented in Section 5.4.3. The final two sections present the changes in total fluorine between 2004 and 2009. Section 5.4.4 presents the changes in total stratospheric fluorine during this time and Section 5.4.5 discusses the implications of these changes on climate forcing using weighted total fluorine budget. The immediate effect of the total fluorine of radiative forcing was evaluated by weighting the total fluorine VMR by the radiative efficiency of each species. The mean total fluorine mass was weighted by the 20-year GWP to evaluate the climate forcing impact of total fluorine, due to the varying atmospheric lifetimes of the fluorine-containing species, over a 20-year time period.

### 5.4.1 Vertical Profiles

The results of the total fluorine calculations are shown in Fig. 5.3 and 5.4. Each point on the mean vertical profile of a species retrieved by ACE has an error, which represents the standard deviation of the data at that altitude. The error bars shown on the plots represent the linear combination of the standard deviations of the contributing species for that particular altitude. The SLIMCAT profiles have been given a flat 5 % error on their VMR. This value was chosen as it is an overestimation of the error on the surface measurements used to force SLIMCAT, and allows for some error in model transport. The total fluorine profiles seem to follow a straight line with the majority of the deviations from this line coming from the HF retrieval. The mean total stratospheric fluorine and the slope of the total fluorine profile can be seen in Table 5.3. There does not appear to be any statistically significant difference between extra-tropical and tropical total fluorine VMR. In most cases the differences between corresponding tropical and extra-tropical stratospheric means are smaller than the error on the values. This suggests that these differences are likely to be due to fluctuations in the retrieval of HF (the main source of atmospheric fluorine at higher altitudes) as opposed to a true feature.

The slopes of the total fluorine profiles are more negative in the tropical stratosphere than in the extra-tropical stratosphere. As has been discussed in Chapter 2, vertical transport through the atmosphere is not instantaneous. Thus at higher altitudes the air is older than air at lower altitudes. The slope of the total fluorine therefore represents the changes in the emissions of fluorine-containing species over time. The negative slopes of the total fluorine show that the VMR of fluorine-containing species has been increasing. Additionally the slopes suggest that the rate of increase is faster in the tropics than in the extra-tropics. ACE-FTS data accounts for between around 77 % of the total fluorine in the lower altitudes to around 96 % at the highest altitudes, this can be seen in Fig. 5.2.

Global Stratospheric fluorine inventories

Table 5.3: The slopes of the total fluorine profile and the mean stratospheric VMR of the fluorine budgets

| Year | 70° N - 30° N                            |                                   |  | 30° N - 00° N                            |                                   |  |
|------|--|-----------------------------------|--|--|-----------------------------------|--|
|      | Slope of total fluorine profile [ppt/km] | Mean Stratospheric Fluorine [ppt] |  | Slope of total fluorine profile [ppt/km] | Mean Stratospheric Fluorine [ppt] |  |
| 2004 | -1.76 ± 0.38                             | 2478 ± 33                         |  | -6.94 ± 0.45                             | 2429 ± 115                        |  |
| 2005 | -2.21 ± 0.36                             | 2501 ± 33                         |  | -4.29 ± 0.31                             | 2508 ± 68                         |  |
| 2006 | -2.68 ± 0.34                             | 2529 ± 43                         |  | -5.41 ± 0.28                             | 2513 ± 82                         |  |
| 2007 | -1.46 ± 0.27                             | 2573 ± 25                         |  | -3.84 ± 0.39                             | 2551 ± 65                         |  |
| 2008 | -1.78 ± 0.41                             | 2603 ± 38                         |  | -4.51 ± 0.53                             | 2577 ± 82                         |  |
| 2009 | -2.03 ± 0.35                             | 2607 ± 32                         |  | -4.37 ± 0.47                             | 2604 ± 78                         |  |

| Year | 00° N - 30° S                            |                                   |  | 30° S - 70° S                            |                                   |  |
|------|--|-----------------------------------|--|--|-----------------------------------|--|
|      | Slope of total fluorine profile [ppt/km] | Mean Stratospheric Fluorine [ppt] |  | Slope of total fluorine profile [ppt/km] | Mean Stratospheric Fluorine [ppt] |  |
| 2004 | -4.54 ± 0.39                             | 2455 ± 62                         |  | -1.28 ± 0.22                             | 2494 ± 24                         |  |
| 2005 | -5.17 ± 0.62                             | 2451 ± 89                         |  | -1.42 ± 0.23                             | 2510 ± 25                         |  |
| 2006 | -6.23 ± 0.51                             | 2488 ± 76                         |  | -0.95 ± 0.38                             | 2521 ± 33                         |  |
| 2007 | -5.49 ± 0.46                             | 2508 ± 71                         |  | -0.29 ± 0.39                             | 2559 ± 38                         |  |
| 2008 | -5.90 ± 0.40                             | 2569 ± 69                         |  | -1.42 ± 0.38                             | 2569 ± 31                         |  |
| 2009 | -4.53 ± 0.42                             | 2592 ± 64                         |  | -1.21 ± 0.26                             | 2621 ± 28                         |  |

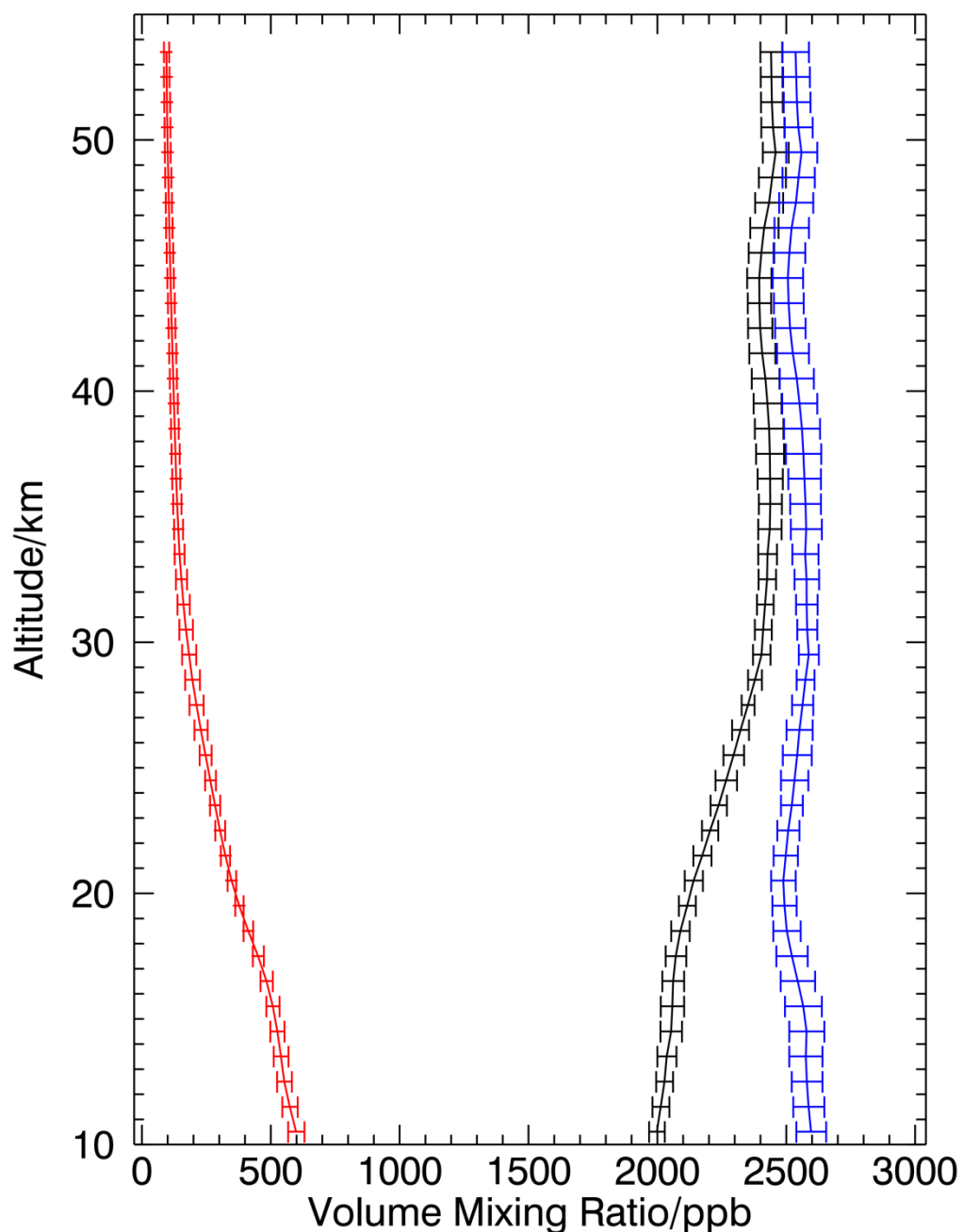


Figure 5.2: The profiles of the total fluorine contribution of species retrieved from ACE-FTS spectra (black) and SLIMCAT (red) to the total fluorine (blue). The profiles plotted here are means calculated from data from the 70° N to 30° N latitude band. The error bars represent the combination of the standard deviation of this data.

# Global Stratospheric fluorine inventories

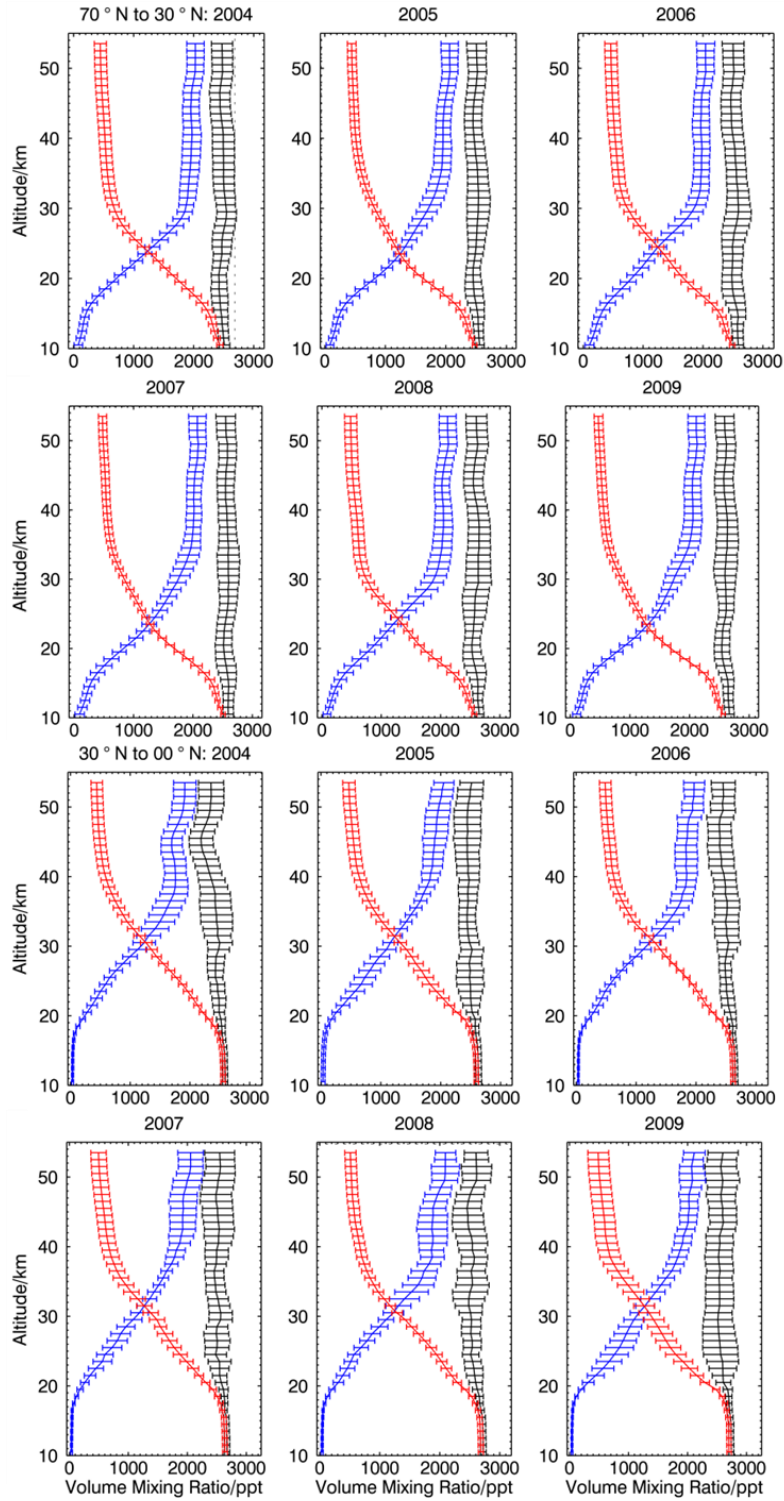


Figure 5.3: The fluorine budgets from 2004 to 2009 in latitude band 30° N - 70° N and 0° - 30° N (black). The inorganic (blue) and organic (red) fluorine profiles are also shown. The error bars are the result of combinations of standard deviations of the mean profiles of the relevant fluorine containing species

# Global Stratospheric fluorine inventories

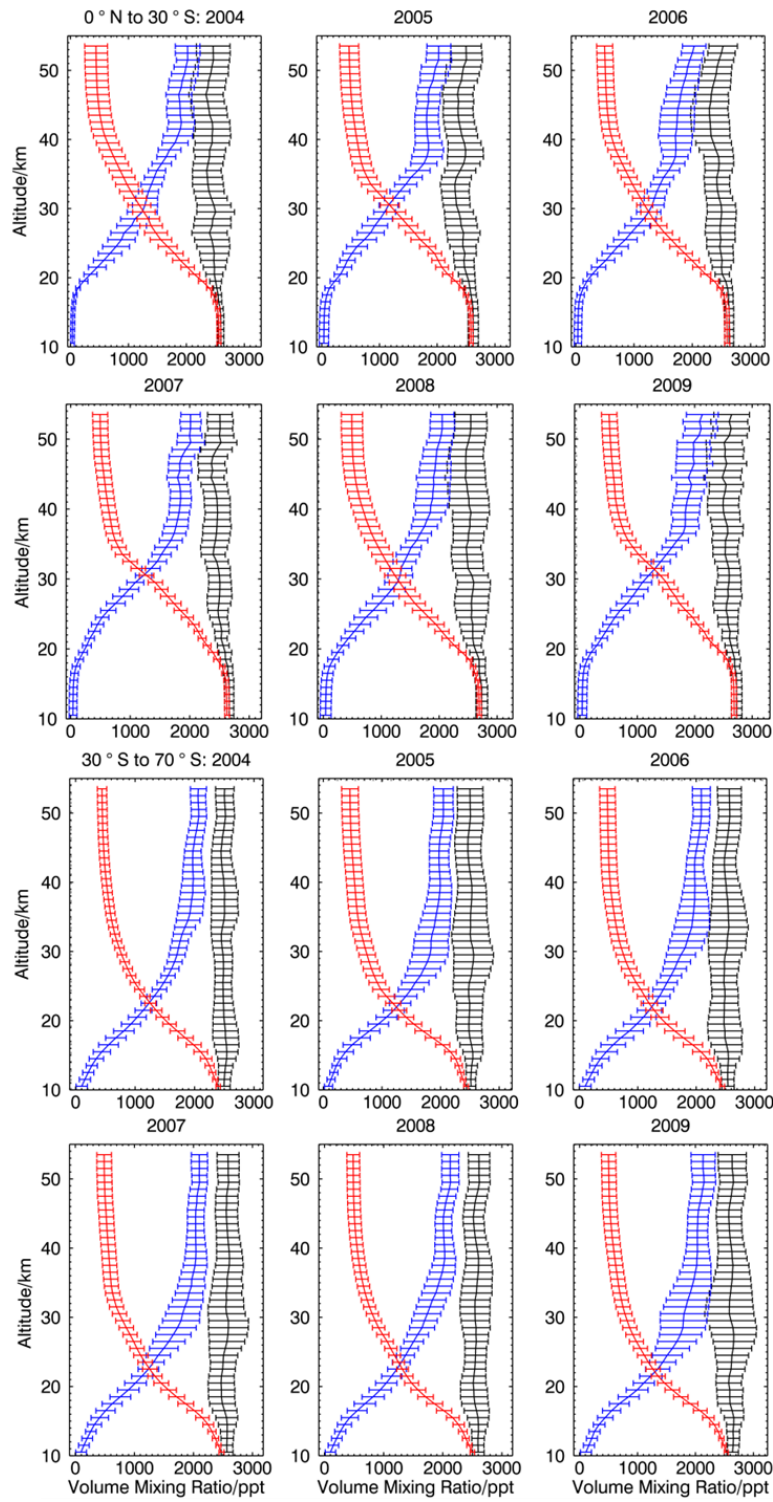


Figure 5.4: As Figure 5.3 but for latitude bands 0° - 30°S and 30°S - 70°S

### 5.4.2 Fluorine source and reservoir species correlations

The fluorine-containing species used in this analysis can be divided into source and reservoir species, reservoir species being produced from the decomposition of source species. In this work HF, COF<sub>2</sub> and COClF are considered to be reservoir species; all other species (CF<sub>4</sub>, CFC-12, CFC-11, HCFC-22, SF<sub>6</sub>, CFC-113, CFC-114, CFC-115, H-1211, H-1301, HCFC-141b, HCFC-142b, HFC-23, HFC-134a and HFC-152a) are source species. Correlating the source and reservoir species therefore gives an indication as to whether the major fluorine-containing species have been considered in the budget. It should be noted that this method cannot be used to check if all long lived fluorine species (such as SF<sub>6</sub>) have been included in the study. Instead this method is a test of whether the major source and reservoir species have been included in the budget. A slope close to one would show that most of the major fluorine-containing species were included in the budget.

The results of these plots can be seen in Table 5.4. All calculated slopes are greater than 0.9 with the lowest values coming in the tropical regions. The mean of the slope in the extra-tropics in the northern hemisphere is  $-0.97 \pm 0.01$  and  $-0.98 \pm 0.01$  southern hemisphere. In the northern tropics the mean slope of the correlation is  $-0.91 \pm 0.02$ , in the southern tropics the mean slope is  $-0.90 \pm 0.01$ . These values suggest that the most important fluorine-containing species have been included in this budget. Whilst many short-lived species are not included in this budget their overall contribution to stratospheric fluorine is small, and so their addition to the budget calculations would not have a significant effect the final fluorine budget. The slopes from the tropical latitudes are smaller than those from extra-tropical latitudes. This is likely to be an artefact from the smaller number of occultations which are available at tropical latitudes.

Table 5.4: The slopes of the correlation between fluorine source species (CF<sub>4</sub>, CFC-12, CFC-11, HCFC-22, SF<sub>6</sub>, CFC-113, CFC-114, CFC-115, H-1211, H-1301, HCFC-141b, HCFC-142b, HFC-23, HFC-134a and HFC-152a) and fluorine reservoir species (HF, COF<sub>2</sub> and COClF)

| Year | 70° N - 30° N |        | 30° N - 00° N |        | 00° N - 30° S |        | 30° S - 70° S |        |
|------|---------------|--------|---------------|--------|---------------|--------|---------------|--------|
| 2004 | -0.97         | ± 0.01 | -0.88         | ± 0.01 | -0.92         | ± 0.01 | -0.97         | ± 0.01 |
| 2005 | -0.96         | ± 0.01 | -0.92         | ± 0.01 | -0.90         | ± 0.01 | -0.97         | ± 0.01 |
| 2006 | -0.96         | ± 0.01 | -0.91         | ± 0.01 | -0.89         | ± 0.01 | -0.97         | ± 0.01 |
| 2007 | -0.97         | ± 0.01 | -0.93         | ± 0.01 | -0.90         | ± 0.01 | -0.99         | ± 0.01 |
| 2008 | -0.97         | ± 0.01 | -0.92         | ± 0.01 | -0.90         | ± 0.01 | -0.97         | ± 0.01 |
| 2009 | -0.96         | ± 0.01 | -0.92         | ± 0.01 | -0.92         | ± 0.01 | -0.98         | ± 0.01 |
| Mean | -0.97         | ± 0.01 | -0.91         | ± 0.02 | -0.90         | ± 0.01 | -0.98         | ± 0.01 |

### 5.4.3 The contributions of species to the total fluorine budget

The contributions of individual species to the total fluorine budget were calculated by producing a mean fluorine budget for each latitude band from annual data. Once these budgets had been produced the impact of each species on the fluorine budget could be calculated. The contribution of individual species to the total fluorine budgets can be found in Appendix A. At the lower altitudes of this study, between 11 and 20 km in the extra-tropics (ET) and 11 and 29 km in the tropics (T), the total fluorine VMR is dominated by CFC-12. At its peak CFC-12 accounts for almost 40% of atmospheric fluorine. This occurs despite a decrease in the VMR of atmospheric CFC-12 during this time. Up to 34 km in the tropics (29 km in ET), the VMR of total fluorine from CFCs and halons is larger than that from HFCs and HCFCs. The contribution of HCFCs and HFCs to atmospheric fluorine is dominated by HCFC-22, which, at its peak at 10.5 km, accounts for between 14% and 15 % of the total atmospheric fluorine depending on the latitude band. The combined contribution of the HCFCs (excluding HCFC-22) and HFCs used in this study

## Global Stratospheric fluorine inventories

peaks between 9.8 % (ET) and 10.1% (T). These values are significantly smaller than the combined contribution of the CFCs and halons (excluding CFC-12) which peak between 22 % (ET) and 23% (T). Above 20 km in the ET and 29 km in the T, HF dominates reaching between 74% (ET) and 77 % (T) of total fluorine at 53.5 km.

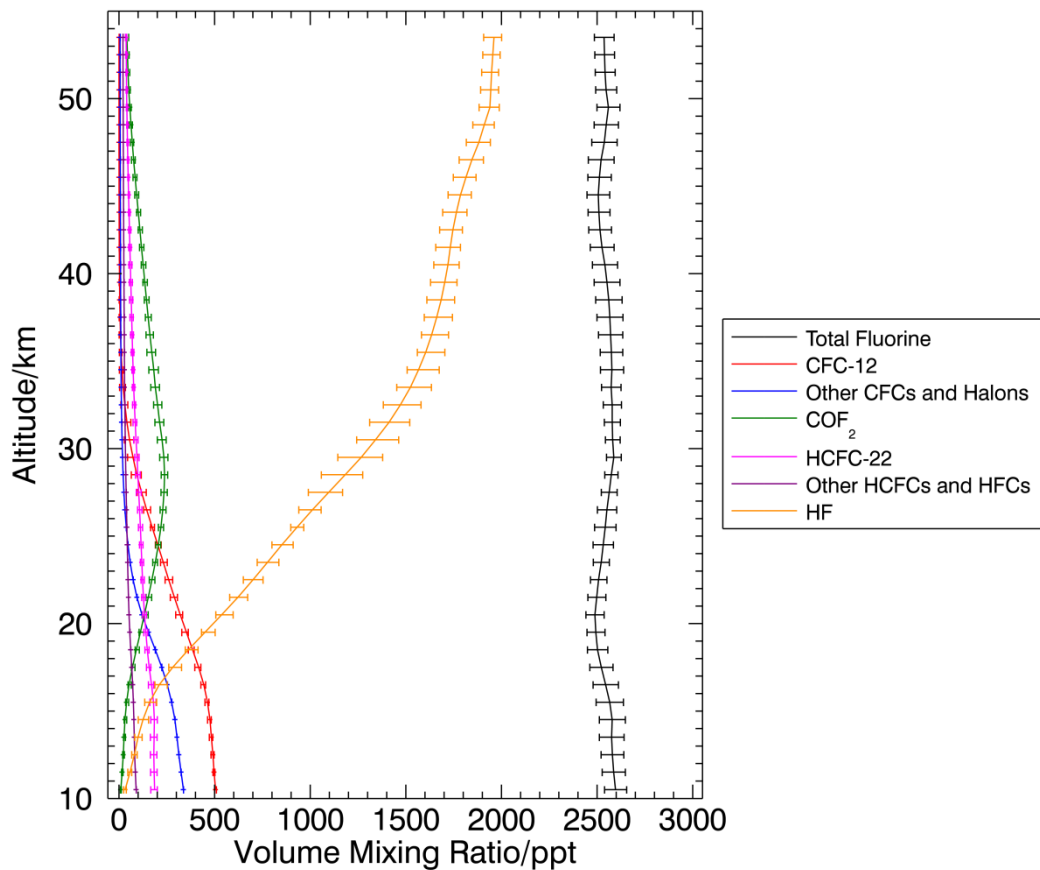


Figure 5.5: The mean profile of CFC-12,  $\text{COF}_2$ , HCFC-22, HF, HCFCs & HFCs (HCFC-142b, -141b, HFC-23, -134a & 152a) and CFCs & Halons (CFC-11, -113, -114, -115, H-1211, H-1301) calculated from all data in the 70°N to 30°N latitude range. The error bars on the profiles are the maxima and minima of the individual profiles used to calculate the mean.

An average total fluorine profile from all the data in the 70° N to 30° N latitude can be seen in Fig. 5.4. In addition to this the profiles of CFC-12,  $\text{COF}_2$ , HCFC-

22, and HF are also plotted. The remaining CFCs and halons, and HFCs and HCFCs are grouped separately so that their effect can also be seen.

#### **5.4.4 Trends in stratospheric fluorine**

Since the fluorine budget has been calculated for the years between 2004 and 2009 it is possible to calculate trends in the annual changes of the mean total stratospheric fluorine. Figure 5.4 shows the trend plots for each of the four latitude bands and the results of the analysis can be seen in Table 5.5. The errors quoted here are the 1- $\sigma$  fitting error of a linear least squares fit to the data. Systematic errors are not considered in this work as they have not been calculated for ACE-FTS at this time. Systematic errors should not have a significant effect on the trends as they are consistent annually for each species used in this budget. In addition, altitude dependent systematic errors will be identical annually, thus as long as the same altitudes are used to calculate an average they will cancel for the annual trends. The VMR of total stratospheric fluorine is increasing at a similar rate at all latitudes; the VMR of total stratospheric fluorine is increasing at a rate of  $1.12 \pm 0.11$  %/year in the northern extra-tropical stratosphere, and  $0.96 \pm 0.12$  %/year in the southern extra-tropical stratosphere. The rate of increase in stratospheric fluorine is also similar in the northern tropical stratosphere ( $1.31 \pm 0.20$  %/year), and in the southern tropical stratosphere ( $1.21 \pm 0.22$  %/year). Northern and southern hemispheric trends were calculated using the averages of the fluorine budgets of the relevant latitude bands. This method was preferred to calculating a budget from all the individual occultations within each hemisphere so that the budget is more representative of the whole hemisphere. As can be seen from Table 5.2 there are significantly more measurements at higher latitudes than in the tropics. A budget calculated from all the occultations in a particular hemisphere would therefore produce an average budget which was biased towards the higher latitudes. Total fluorine in the northern hemisphere and southern hemisphere is increasing at a similar rate,  $1.21 \pm 0.11$  %/year in the

## Global Stratospheric fluorine inventories

northern hemisphere, and  $1.07 \pm 0.15$  %/year in the southern hemisphere. Once more the errors quoted here are the statistical 1- $\sigma$  fitting error of a linear least squares fit to the data. Globally the VMR of fluorine in the stratosphere is increasing at a rate of  $1.14 \pm 0.06$  %/year. Despite the lower altitudes of the budget being dominated by CFC-12, a strong increase in the VMR of total fluorine is still seen. This is due to increases in the VMR of HCFCs and HFCs being significantly larger than the decreases in CFCs and halons during this time.

Table 5.5: The trends in mean VMR of stratospheric total fluorine, between 2004 and 2009 for different latitude bands and the NH and SH

|                     | ppt/year |           | % / year |            |
|---------------------|----------|-----------|----------|------------|
| 70° N - 30° N       | 28.3     | $\pm 2.7$ | 1.12     | $\pm 0.11$ |
| 30° N - 0° N        | 32.5     | $\pm 4.9$ | 1.31     | $\pm 0.20$ |
| 0° N - 30° S        | 29.6     | $\pm 5.4$ | 1.20     | $\pm 0.22$ |
| 30° S - 70° S       | 24.3     | $\pm 3.1$ | 0.96     | $\pm 0.12$ |
| Northern Hemisphere | 30.3     | $\pm 2.7$ | 1.21     | $\pm 0.11$ |
| Southern Hemisphere | 26.8     | $\pm 3.7$ | 1.07     | $\pm 0.15$ |

## Global Stratospheric fluorine inventories

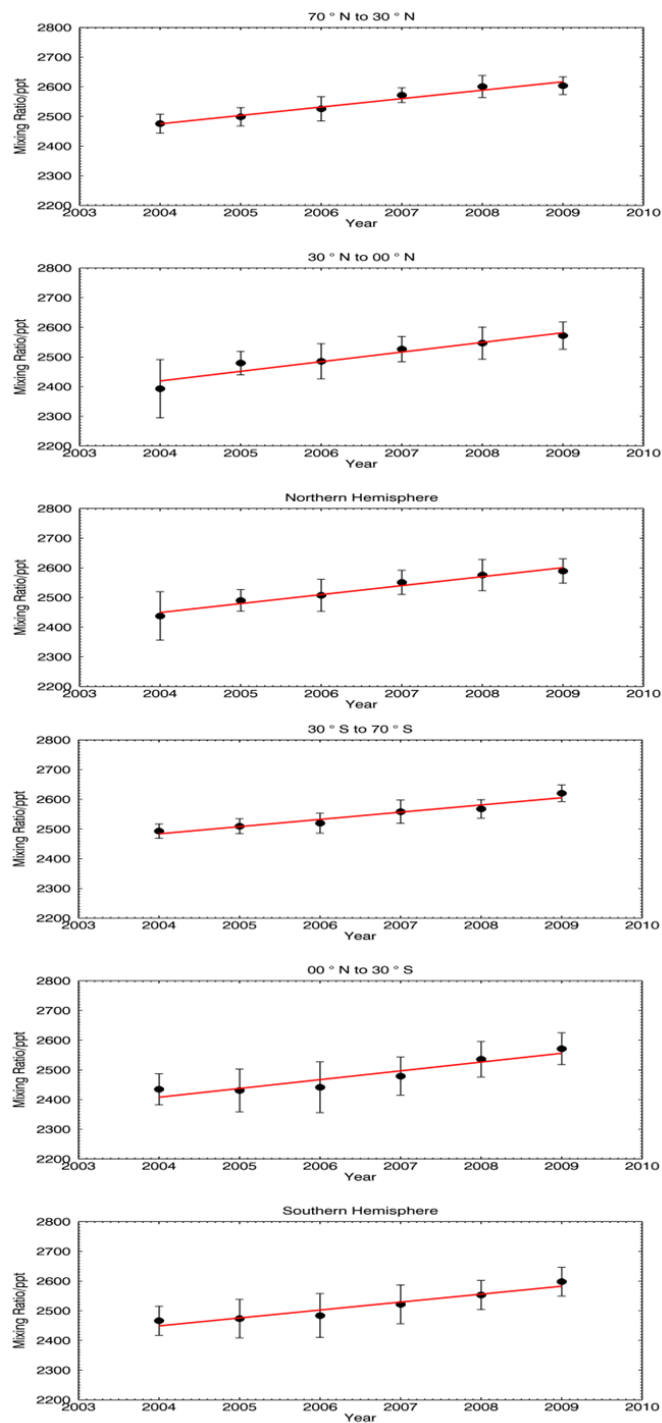


Figure 5.6: The trends in the mean total stratospheric fluorine (ppt) between 2004 and 2009. The red line represents the line of best fit for the mean stratospheric total fluorine VMR (the black circles). The error bars shown in the plots are calculated from the standard deviation of the data used to calculate the mean total fluorine VMRs

#### **5.4.5 Radiative Efficiency- and Global Warming Potential-weighted fluorine budget trends**

The increase in fluorine discussed in Section 5.4.4 will have a direct impact on warming temperatures in the troposphere. In order to evaluate this effect the total fluorine was weighted using the radiative efficiencies (Solomon et al., 2007) of the individual species to calculate the change in radiative forcing due to changes in fluorine VMR during this time. These changes in radiative forcing were calculated by removing VMR above the tropopause and multiplying the VMR (in ppb) of each species by its radiative efficiency giving the radiative forcing for each species. These values were summed together and the mean was calculated for each year. A least squares fit to the means then allowed the changes in radiative forcing to be calculated. The results of this analysis can be seen in Table 5.6 and Figure 5.7. Both hemispheres exhibit a similar increase in radiative forcing due to fluorine species. In the northern hemisphere the rate are  $0.23 \pm 0.11$  % per year in the extra-tropics and  $0.45 \pm 0.11$  % per year in the tropics. Similarly in the southern hemisphere radiative forcing due to fluorine-containing species appeared to increase by  $0.29 \pm 0.20$  % per year in the tropics and  $0.45 \pm 0.09$  % per year in the extra-tropics. Once more the same calculations were carried out without including CFCs and halons. These results are shown for comparison in Table 8. Without CFCs and halons the increase in radiative forcing would be significantly higher ranging between  $3.84 \pm 0.02$  % per year in the extra-tropical southern hemisphere and  $4.45 \pm 0.02$  % per year in the extra-tropical northern hemisphere. Thus at the present time the climate impact of fluorine is increasing.

Weighting the total VMR does not allow the long term impact of these species to be evaluated as radiative efficiencies do not take the lifetime of species into account. GWPs take lifetimes into account and the different species analysed for this work have different Global Warming Potentials (GWPs) (see Table 2.2) and therefore have different effects on climate. A more useful quantity is

therefore the trend in the atmospheric fluorine-weighted GWP. These calculations represent the climatological influence of the emission of a hypothetical packet of gas with the relevant burden of fluorine containing species over a 20-year timeframe. GWP-weighted fluorine appears to be stable in all regions cf. Fig. 5.8. Similar statistically insignificant increases are seen in both hemispheres with increases of  $0.10 \pm 0.10$  % per year in the northern hemisphere tropics, and  $0.11 \pm 0.13$  % per year in the southern hemisphere tropics. Once more the error on these values was calculated using a 1- $\sigma$  fitting error of a linear least squares fit to the data. Extra-tropical latitudes also show statistically insignificant trends. In the northern hemisphere extra-tropical region the GWP-weighted fluorine appears to be decreasing at a rate of  $-0.06 \pm 0.09$  % per year. Whilst in the southern hemisphere extra-tropical region GWP-weighted fluorine is increasing at a rate of  $0.02 \pm 0.03$  % per year. The errors on all of these GWP-weighted trends are larger than the reported GWP-weighted trends. These results suggest that it is likely that the GWP-weighted fluorine will remain roughly constant over a 20 year time period. These results are markedly different to the radiative efficiency-weighted trends. These differences are caused by the dependence of GWPs on lifetime. Thus, whilst in the short term fluorine is having an increasing effect on the climate, when these effects are extrapolated into the future the climate impact of these species will become less. The replacement of CFCs and Halons with HFCs and HCFCs which have significantly shorter tropospheric lifetimes reduces the climatological effect of these species in the long term. Since use of these species is prohibited under the Montreal Protocol the VMR of these species has been decreasing during the time frame of this study (Brown et al., 2011). HCFCs and, increasingly, HFCs have been replacing the species banned under the Montreal Protocol. The decrease in CFCs and halons has, in effect, suppressed the GWP-weighted fluorine trend which would otherwise have risen during this time. Carrying out the same calculations without including CFCs and halons shows the effects of this suppression. The trends in the weighted total fluorine range between  $3.51 \pm 0.16$  % and  $3.92 \pm 0.19$  % per year when CFCs

## Global Stratospheric fluorine inventories

and halons are not included (see Table 5.6). These results suggest that the Montreal Protocol has had a positive effect on reducing global warming (on a 20 year timeframe). By banning the use of a number of ozone-depleting substances which were also potent greenhouse gases the Montreal Protocol has inadvertently slowed the rate of increase in the VMR of greenhouse gases in the atmosphere. This agrees with the work of Velders et al. (2007), which stated that the Montreal Protocol had had a significant effect in reducing the emission of greenhouse gases.

Table 5.6: The global warming potential-weighted trends in the total fluorine mass and the radiative efficiency- (RE) weighted trends in the total fluorine volume mixing ratio between 2004 and 2009. The weighted total fluorine budgets were also calculated without including CFCs and halons so that the impact of the Montreal Protocol on global warming potential weighted fluorine could be quantified.

| Latitude band | RE-weighted total fluorine trend (%/year)  |        | RE-weighted total fluorine trend without CFCs and halons included (%/year)  |   |      |
|---------------|--|--------|---|---|------|
| 70° N - 30° N | 0.23                                       | ± 0.11 | 4.45  | ± | 0.05 |
| 30° N - 0° N  | 0.45                                       | ± 0.11 | 4.33  | ± | 0.2  |
| 0° N - 30° S  | 0.45                                       | ± 0.09 | 3.94  | ± | 0.15 |
| 30° S - 70° S | 0.29                                       | ± 0.20 | 3.84  | ± | 0.02 |
| Latitude band | GWP-weighted total fluorine trend (%/year) |        | GWP-weighted total fluorine trend without CFCs and halons included (%/year) |   |      |
| 70° N - 30° N | -0.06                                      | ± 0.09 | 3.78  | ± | 0.34 |
| 30° N - 0° N  | 0.1  | ± 0.1  | 3.92  | ± | 0.19 |
| 0° N - 30° S  | 0.11                                       | ± 0.13 | 3.65  | ± | 0.27 |
| 30° S - 70° S | 0.02                                       | ± 0.03 | 3.51  | ± | 0.16 |

## Global Stratospheric fluorine inventories

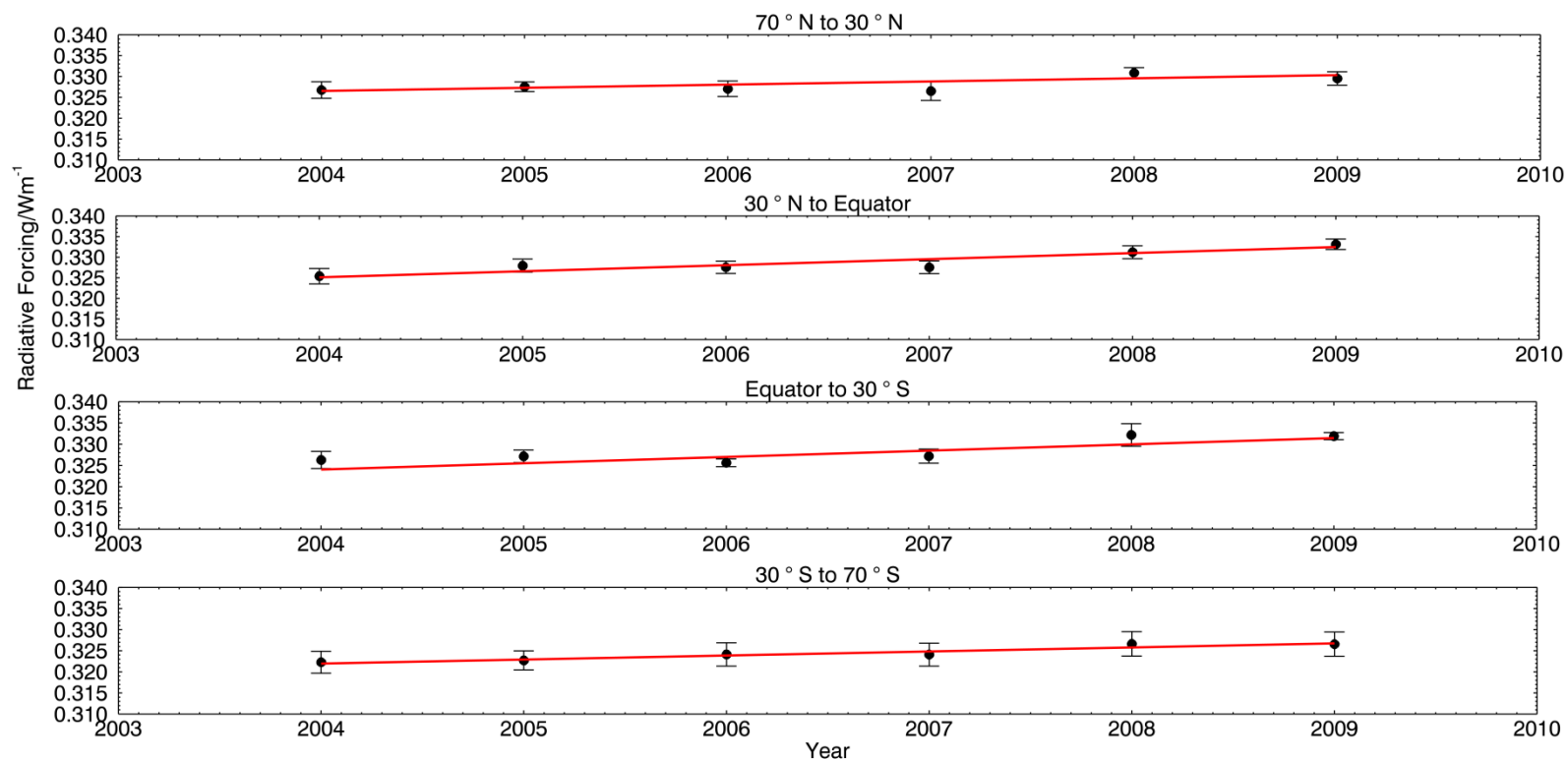


Figure 5.7: The trends in the radiative efficiency-weighted total fluorine mean between 2004 and 2009. The red line represents the line of best fit for the GWP-weighted mean volume mixing ratio (the black circles). The error bars shown in the plots are calculated from the standard deviation of the data used to calculate the means.

## Global Stratospheric fluorine inventories

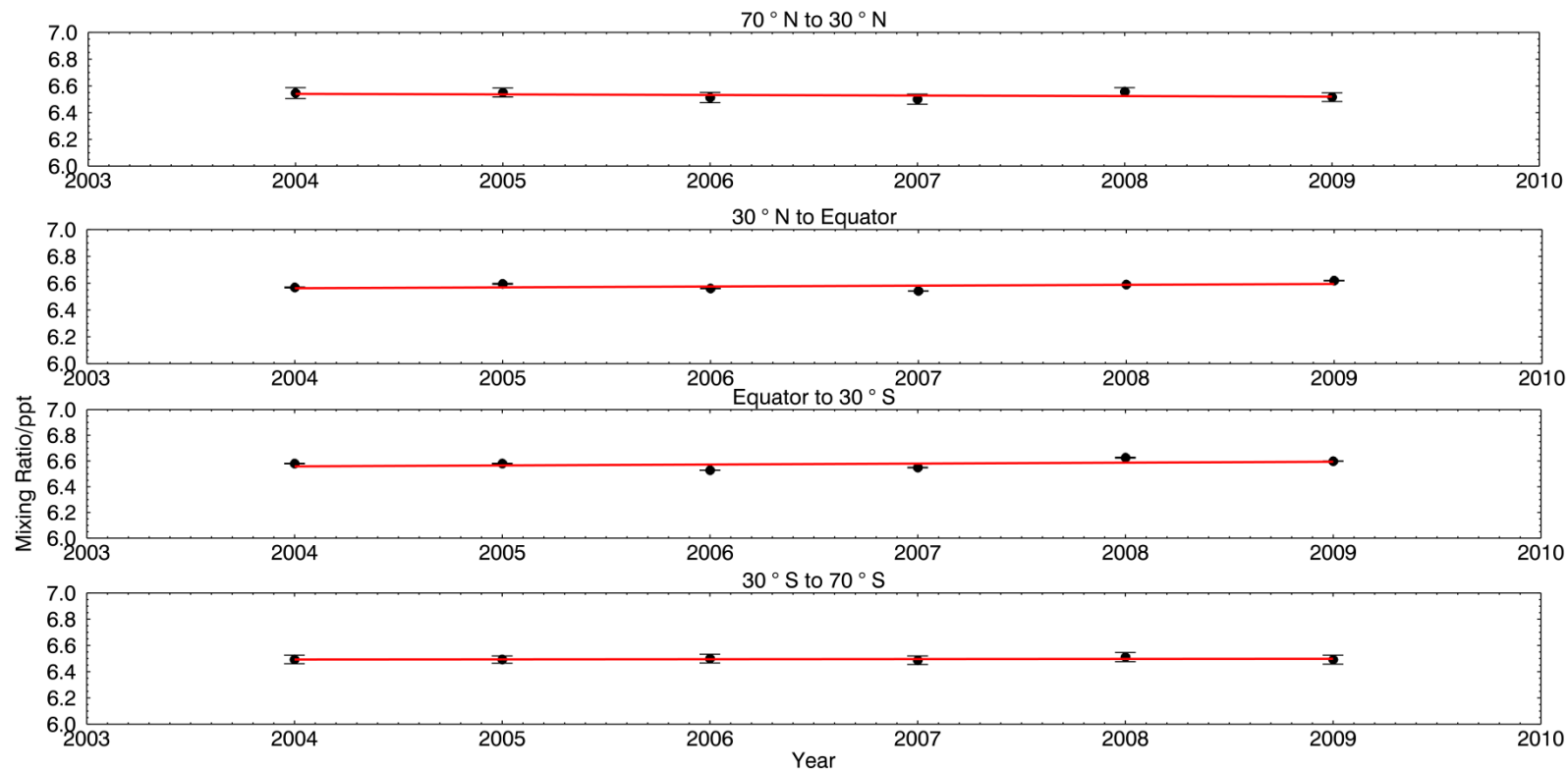


Figure 5.8: The trends in the GWP-weighted total fluorine mean between 2004 and 2009. The red line represents the line of best fit for the GWP-weighted mean VMR (the black circles). The error bars shown in the plots are calculated from the weighted standard deviation of the data used to calculate the means.

## **5.5 Conclusions**

In this chapter a series of stratospheric fluorine budgets have been presented for the years between 2004 and 2009. These budgets were calculated for 4 latitude bands which represent the extra-tropical and tropical latitudes. The fluorine budgets were calculated using species retrieved by ACE-FTS. ACE-FTS measurements were supplemented with data from the SLIMCAT 3D chemical transport model. This fluorine budget therefore includes all the major fluorine-containing species currently in the atmosphere. In the lower altitudes these budgets are dominated by the large VMR of CFC-12. At its peak CFC-12 contributes around 39% of total fluorine. Other species are much less important. HCFC-22 contributes 15% at its maximum and the combined contribution of the other HCFCs and HFCs used in this study peaks around 10%. The remaining CFCs and halons used in this study contribute a maximum of about 23%. As altitude increases HF overtakes CFC-12 as the most dominant species in the total fluorine budget.

The gradient of the total fluorine profiles offer an indication of the long-term changes in total fluorine. All budgets exhibit a negative slope with altitude. Since air at higher altitudes is older than air at lower altitudes, these results suggest that fluorine emissions have been increasing with time with higher concentrations at lower altitudes. Stratospheric fluorine is increasing in all the latitude bands used in this study.

By comparing the results of this fluorine budget with the budgets mentioned in the introduction it is possible to track the long term changes in atmospheric fluorine. When this work is considered alongside Zander et al. (1992) and Sen et al. (1996), a clear long term increase in stratospheric fluorine is seen. The VMR of total fluorine increases from a mean total fluorine value of  $1.15 \pm 0.12$  ppb in 1985 (Zander et al., 1992), to 1.48 ppb in 1993 (Sen et al., 1996) reaching between  $2.59 \pm 0.06$  ppb and  $2.62 \pm 0.03$  in 2009. Whilst the budgets

## Global Stratospheric fluorine inventories

of Zander and Sen do not include as many fluorine species as the work presented in this chapter they include the major fluorine contributors and are therefore good estimations for the total fluorine VMR at the times reported. The annual increases calculated in this work of between  $0.96 \pm 0.12$  and  $1.31 \pm 0.2$  % per year compare very well to the trend in HF between 1996 and 2008 from the ground-based FTIR measurements from Kiruna, Sweden. These results show an increase in the VMR of HF of  $1.0 \pm 0.3$  % per year between 1996 and 2008 (Mikuteit, 2008).

Total atmospheric fluorine trends have been produced which have been weighted by radiative efficiencies and the GWPs of the individual species used in this study. Radiative efficiency weighting allow the climatological implication of the increase in fluorine during this time to be quantified. Changes in climate forcing due to changes in the VMR of fluorine-containing species have also been calculated. These results show small increases of between  $0.23 \pm 0.11$  % per year and  $0.45 \pm 0.11$  % per year. GWP-weighted trends allow the longer term impact of these species to be evaluated. These calculations did not show any statistically significant trends. Analysis carried out without using data for the CFCs or halons show GWP-weighted fluorine increasing by a mean of  $3.85 \pm 0.07$  % per year in the Northern Hemisphere and  $3.58 \pm 0.07$  % per year in the Southern Hemisphere. When CFCs and halons are included in the calculations it appears that changes in the VMR of these species will not have a significant effect on the GWP of these species as a group over a 20 year timeframe. It appears that in the short term the climate forcing effects atmospheric fluorine are increasing. In the longer term, the decrease in species banned under the Montreal Protocol has limited the climatological effects of a general increase in the VMR of fluorine-containing species, in particular HCFCs and HFCs, during this time.

# 6

## Global stratospheric chlorine inventories

### *6.1 Introduction*

In the stratosphere chlorine-containing molecules can undergo photolysis or react with  $O(^1D)$  and produce chlorine species which can catalyse a cycle, resulting in the destruction of ozone. In an atmosphere without significant anthropogenic emissions this process of ozone loss is not significant since non-anthropogenic species of chlorine exist in relatively low VMRs in the stratosphere. As has been discussed previously, anthropogenic emissions of chlorine-containing species grew from the early-20<sup>th</sup> century until the mid-1990s. The publication of the work of Molina & Rowland (1974), and Farman, Gardiner and Shanklin (1985), forced the global community into action, prompting the development of the Montreal Protocol which came into force in 1987 (UNEP, 2009).

## Global Stratospheric fluorine inventories

The Montreal Protocol has successfully reduced the emissions of ozone depleting substances (Montzka et al., 2011a). Globally stratospheric ozone is predicted to return to the same levels as 1980 by 2050 in both the tropics and the poles (Montzka et al., 2011b). Rigorous assessments of ozone depletion require measurements of the stratospheric total chlorine and its change over time. A number of chlorine budgets have already been calculated. Measurements made by the ATMOS instrument were used to calculate a stratospheric chlorine budget at 30° N for 1985 using VMRs of HCl, CH<sub>3</sub>Cl, ClONO<sub>2</sub>, CCl<sub>4</sub>, CFC-12, CFC-11 and HCFC-22. A value of  $2.58 \pm 0.1$  ppb was calculated at that time (Zander et al., 1992). A second chlorine budget was produced using ATMOS in 1994 which, in addition to the species used in the previous study, used ClO, CH<sub>3</sub>CCl<sub>3</sub>, CFC-112, HOCl and COClF. This calculation produced a value of  $3.53 \pm 0.1$  ppb, representing a growth rate of 3.3% per year in the VMR of total chlorine during this time (Zander et al., 1996). Measurements of HCl from the HALOE between 1991 and 1995 showed concentrations rising at a rate of  $0.102 \pm 0.006$  ppb per year (Russell et al., 1996). Measurements made by the MK-IV balloon-borne instruments in 1997 showed a total chlorine VMR of  $3.7 \pm 0.2$  ppb suggesting further increases in atmospheric chlorine between the chlorine budgets (Sen et al., 1999). Data from the ACE-FTS were used to calculate a stratospheric chlorine budget using measurements made in 2004. This work calculated a mean stratospheric total chlorine VMR of  $3.65 \pm 0.13$  ppb (Nassar et al., 2006a) and provided evidence of the beginning of a slow decline in total stratospheric chlorine. Measurements made by the Microwave Limb Sounder (MLS) between August 2004 and February 2006 also displayed a reduction in stratospheric total chlorine of  $0.78 \pm 0.08$  % per year (Froidevaux et al., 2006b). A long-term stratospheric chlorine trend was produced from measurements made by 7 space-borne instruments (ACE-FTS, ATMOS, Aura MLS v1, Cryogenic Limb Array Etalon Spectrometer (CLAES), Cryogenic Infrared Spectrometer & Telescope for the Atmosphere (CRISTA), HALOE and Upper Atmosphere Research Satellite (UARS) MLS v5), for the years between 1991 and 2006. This series showed a general

increase in the concentration of stratospheric chlorine until the late 1990s, after this the concentration slowly began to decrease (Lary et al., 2007).

The chlorine budgets presented in this chapter were calculated using ACE-FTS measurements supplemented with data from the SLIMCAT 3D CTM. 18 chlorine-containing species, which are listed in Section 6.2, were used to calculate vertical profiles of total chlorine in 4 latitude bands between 70° N and 70° S. These budgets represent the most comprehensive stratospheric chlorine budget to date. The long-term changes in atmospheric VMRs of chlorine-containing species during this time have also been calculated. As such an individual chlorine budget has been calculated for every year, from 2004 to 2009. Since atmospheric chlorine will go on to catalyse ozone destruction in the stratosphere the long-term changes in atmospheric chlorine are important for forecasting the recovery of the ozone layer. The large number of chlorine-containing species used in this study allows the calculation of the contribution of each species on the total chlorine VMR. The RE, GWP and ODP weighted trends in total chlorine are also presented and illustrate how changes in atmospheric chlorine have affected both climate forcing and ozone depletion.

## ***6.2 Chlorine Budget Calculation Method***

### **6.2.1 Chlorine-containing species**

The ACE-FTS retrieves the VMRs of 9 chlorine-containing species, CCl<sub>4</sub>, CCl<sub>2</sub>F<sub>2</sub> (CFC-12), CCl<sub>3</sub>F (CFC-11), COCl<sub>2</sub>, COClF, CHF<sub>2</sub>Cl (HCFC-22), CH<sub>3</sub>Cl, HCl and ClONO<sub>2</sub> with version 3.0 retrievals and 10 years of data (2004-2013). The retrieval limits of these species can be seen in Table 6.1. Once more the ACE-FTS version 3.0 retrievals of CFC-113, HCFC-142b, and HCFC-141b are not used in these calculations due to the substantial biases in the retrieved VMR (see Chapter 4). ACE-FTS data was supplemented with data from the SLIMCAT 3D CTM. This study used the following SLIMCAT species to

## Global Stratospheric fluorine inventories

supplement ACE-FTS data: CFC-113, CFC-114, CFC-115, H-1211, H-1301, HCFC-141b, HCFC-142b, ClO and HOCl.

Table 6.1: The ACE-FTS retrieval altitude ranges of the chlorine containing species used in this study

| Species                                   | Altitude (km) |            |
|---|---------------|------------|
|   | Polar         | Equatorial |
| CFC-11 (CCl <sub>3</sub> F)               | 5 – 23        | 6 – 28     |
| CFC-12 (CCl <sub>2</sub> F <sub>2</sub> ) | 5 – 28        | 5 – 36     |
| HCFC-22 (CHF <sub>2</sub> Cl)             | 5 – 30        | 7 – 30     |
| COClF                                     | 13 – 25       | 15 – 32    |
| COCl <sub>2</sub>                         | 8 – 24        | 10 – 29    |
| CH <sub>3</sub> Cl                        | 9 – 40        | 12 – 40    |
| CCl <sub>4</sub>                          | 6 – 25        | 7 – 30     |
| HCl                                       | 6 – 57        | 7 – 63     |
| ClONO <sub>2</sub>                        | 10 – 41       | 10 – 36    |

SLIMCAT was run by Martyn Chipperfield and Sandip Dhomse in the University of Leeds using the same conditions as those outlined in Chapter 4. Zonal mean monthly outputs were used to produce latitudinal means for 4 different latitude bins (70° N - 30° N, 30° N - 0° N, 0° N – 30° S and 30° S - 70° S). Two species, ClO and HOCl, were sampled at the local space and time coordinates of the ACE-FTS occultations. This was carried out so that the profiles of ClO and HOCl from SLIMCAT would correspond to the profiles of ClONO<sub>2</sub> from ACE-FTS. These species exhibit strong diurnal cycles and so the evening and morning profiles of these species should not be mixed in the overall total chlorine calculations.

## 6.2.2 Chlorine Budget Calculations

Chlorine budgets were calculated using an almost identical method to that outlined in Chapter 5.3.2. The method given here is therefore a brief overview. In this study the globe has been divided into four latitude bands: 70° N - 30° N, 30° N - 0° N, 0° N - 30° S and 30° S - 70° S. 16,186 ACE-FTS occultations were used in this study; the distribution of these occultations in terms of year of occultation and latitude band are shown in Table 5.2. The data within each band was separated by year and then filtered to remove outlying data using 2.5 times the MAD of the data.

Once the outliers had been removed an average profile of each species was calculated. Profiles were extended by using the SLIMCAT profiles of the corresponding species scaled to match the ACE-FTS data at its highest and lowest retrieved altitude point. Examples of two of these extensions are shown in Fig. 6.1.  $\text{COCl}_2$  did not have corresponding SLIMCAT data and so was extended vertically upwards using a scaled  $\text{COClF}$  SLIMCAT profile from the final retrieved altitude. This can be seen in Fig. 6.1. SLIMCAT runs for  $\text{HOCl}$  and  $\text{ClO}$  were sampled for local ACE-FTS occultation time and location. This ensured that the total chlorine concentrations would be calculated correctly for these photosensitive molecules. Some of the profiles of these species ( $\text{HOCl}$  and  $\text{ClO}$ ) from 2004 appeared to peak at a higher altitude, to a significantly higher maximum VMR than the profiles from the other years. In this case the value for the mixing ratio in 2005 was used instead. Data from 2004 contained only a small number of occultations and so small atmospheric anomalies had a large effect on these profiles. All profiles were extended up to 54.5 km corresponding to the maximum altitude of the corresponding fluorine budget produced from ACE-FTS data (Chapter 5).

## Global Stratospheric fluorine inventories

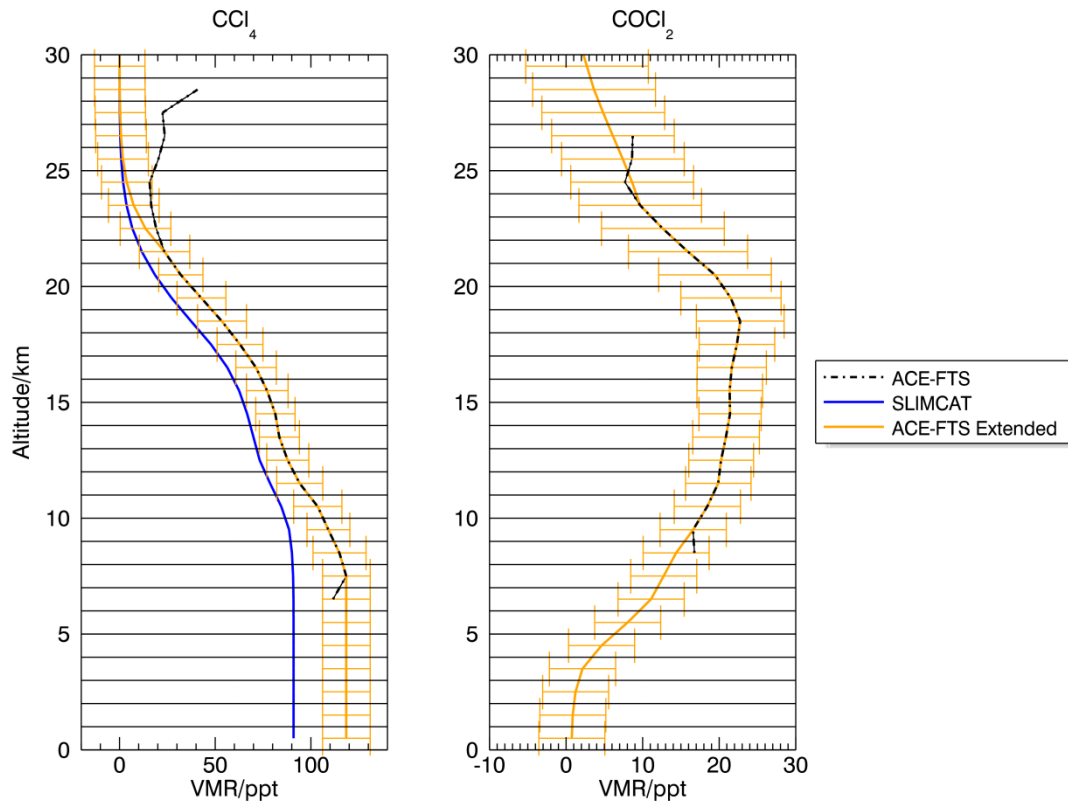


Figure 6.1: The extended and un-extended ACE-FTS profiles of  $\text{CCl}_4$  and  $\text{COCl}_2$  along with the accompanying SLIMCAT profile. The ACE-FTS profiles have been extended using a scaled SLIMCAT profile. The profiles shown in this figure are from the  $70^\circ - 30^\circ$  North 2007 latitude bin.

The local time of an occultation was calculated using the universal time and the longitude ( $\lambda$ ) of the occultation and Eq.6.1. This equation produces a local time which is relative to the date of the universal time of the occultation. A negative local time represents an occultation whose local time is a day before the universal time, in this case 24 hours should be added to the calculated time for a true local time. A positive local time represents an occultation whose local time is a day ahead of the universal time, in this case 24 hours should be subtracted from the calculated time for the true local time. Occultations with local times greater than twelve were considered to be evening occultations. Occultations with local times less than twelve were considered to be morning

occultations. Both morning and evening stratospheric chlorine budgets have been constructed as part of this work.

$$Local\ Time = Universal\ Time + \left(\frac{24}{360}\right)\lambda \quad 6.1$$

The total chlorine VMR was calculated at 54 levels between 0.5 km and 53.5 km. This spacing reflected the ACE retrieval altitude grid. The equation used for this calculation can be seen below, where square brackets indicate VMR. The total chlorine VMR can be expressed as the sum of the total inorganic and organic chlorine, in a similar manner to that laid out by Nassar et al. (2006) and Zander et al. (1992,1996) . These values are defined below.

$$[Total\ Chlorine] = [Total\ Inorganic\ Chlorine] + [Total\ Organic\ Chlorine]$$

$$[Total\ Inorganic\ Chlorine] = [ClONO_2] + [COClF] + 2[COCl_2] + [HCl] + [ClO] + [HOCl]$$

$$[Total\ Organic\ Chlorine] = 4[CCl_4] + 2[CFC-12] + 3[CFC-11] + [CH_3Cl] + [HCFC-22] + 3[CFC-113] + 2[CFC-114] + [CFC-115] + [HCFC-142b] + 2[HCFC-141b] + [H-1211]$$

### **6.3 Results and Discussion**

This section is divided into six subsections in a similar manner to Chapter 5.4. Once more in the first sub-section the vertical profiles of the total chlorine calculations are presented with a focus on the gradient of the line and its implications for the changes in total chlorine VMR in the atmosphere. The slope of the correlation plot between inorganic chlorine species and organic chlorine species are presented and discussed in Section 6.3.2. The impact of the individual species included in the total chlorine calculations on the total

chlorine VMR are presented in Section 6.3.3. The subsequent sections present the changes in total chlorine between 2004 and 2009. Section 6.3.4 presents the changes in total stratospheric chlorine during this time. Section 6.3.5 and 6.3.6 discuss the implications of these changes on climate and ozone loss using weighted total chlorine budgets. These budgets were calculated by weighting the VMR of each species not with the number of chlorine atoms contained within the molecule (as described in Section 6.2.2), but by their RE, 20-year GWP or their ODP following the method laid out in Chapter 5.3.3.

### 6.3.1 Total Chlorine Profiles

An example of a total chlorine profile is shown in Fig. 6.3 (additional plots can be found in Appendix B). The error bars shown on the plots are the errors calculated from the standard deviation of each species which was included in the budget. Once more (as in Chapter 5) the SLIMCAT profiles have been given a flat 5 % error on their VMR. This value was chosen as it is an overestimation of the error on the ground-based measurements, on which SLIMCAT is based, and accounted for slight errors in transport. The percentage of the total chlorine which comes from ACE-FTS measurements varies between 80% and 96%. At lower altitudes ACE-FTS measurements account for around 90% of the total chlorine VMR. This percentage contribution rises until it peaks at between 23 and 28 km which corresponds to a peak in the percentage contribution of ClONO<sub>2</sub>. Above this altitude the percentage contribution from ACE-FTS decreases slightly to around 80% as the percentage contributions of HOCl and ClO (SLIMCAT) increases. As the VMRs of HOCl and ClO decrease, the percentage contribution to the total chlorine from ACE-FTS increases to around 96% at 53 km (Fig. 6.2). The total chlorine profiles follow a straight line with small deviations around 40 km. The mean morning profiles of the inorganic chlorine species between 25 and 55 km, between 30° N and the equator, can be seen in Fig. 6.4. It appears that this decrease in the VMR of HCl (that can be seen in Fig. 6.4) is not compensated

## Global Stratospheric fluorine inventories

for by an increase in the VMR of ClO. It is possible that these dips may be due to a peak in stratospheric OH at this altitude. Stratospheric OH reacts with HCl to form chlorine atoms and water.

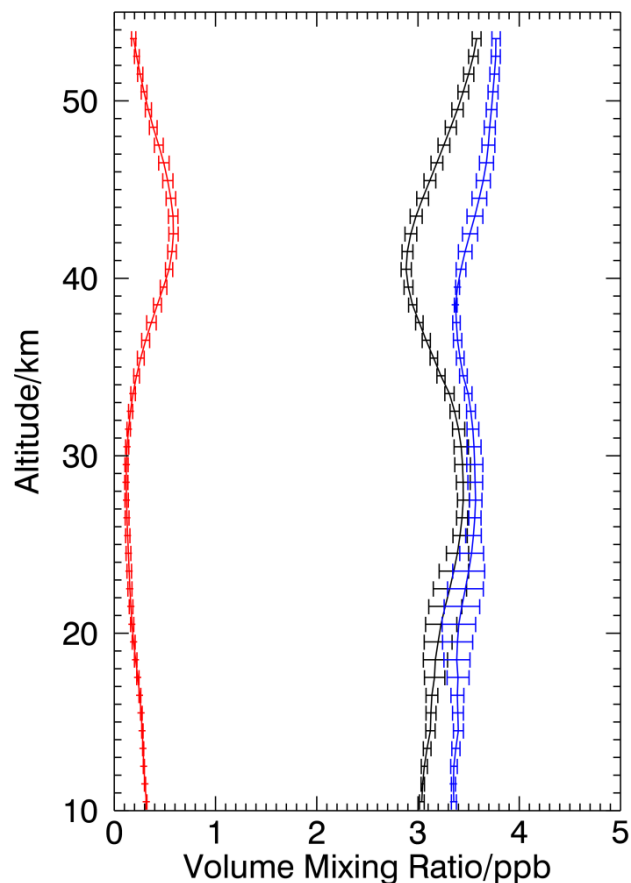


Figure 6.2: The profiles of the total chlorine contribution of species retrieved from ACE-FTS spectra (black) and SLIMCAT (red) to the total fluorine (blue). The profiles plotted here are means calculated from data from the 70° N to 30° N latitude band. The error bars represent the combination of the standard deviation of this data.

## Global stratospheric chlorine inventories

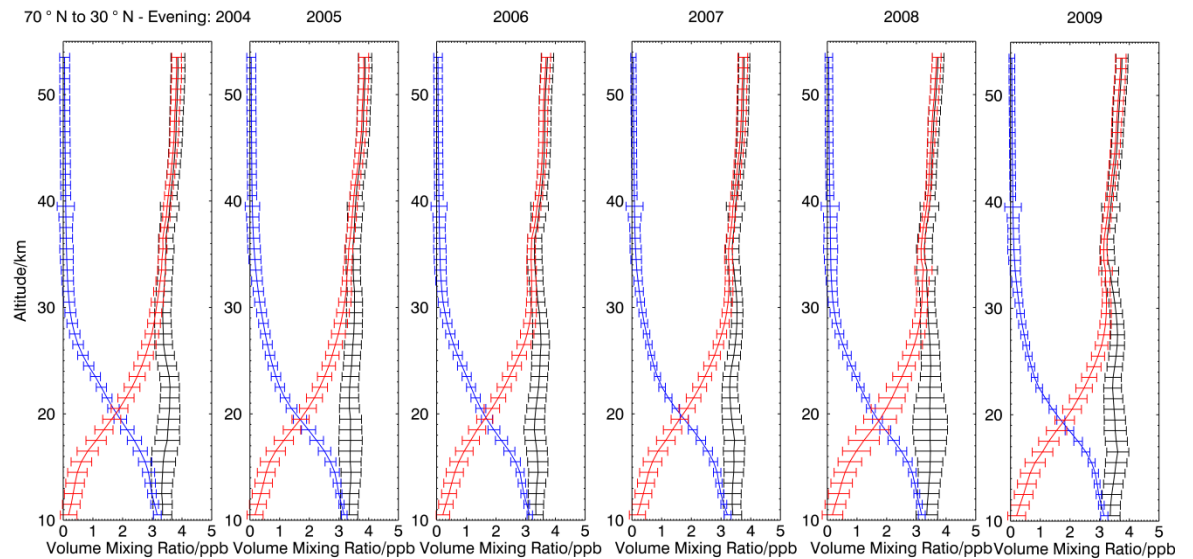


Figure 6.3: The total chlorine (black), inorganic chlorine (blue) and organic chlorine (red) profiles between 70° and 30° in the northern hemisphere. The error bars on the profiles are a linear combination of the standard deviations of the data which was used to calculate these profiles. These profiles were calculated using evening profiles of ClO, ClONO<sub>2</sub> and HOCl.

## Global stratospheric chlorine inventories

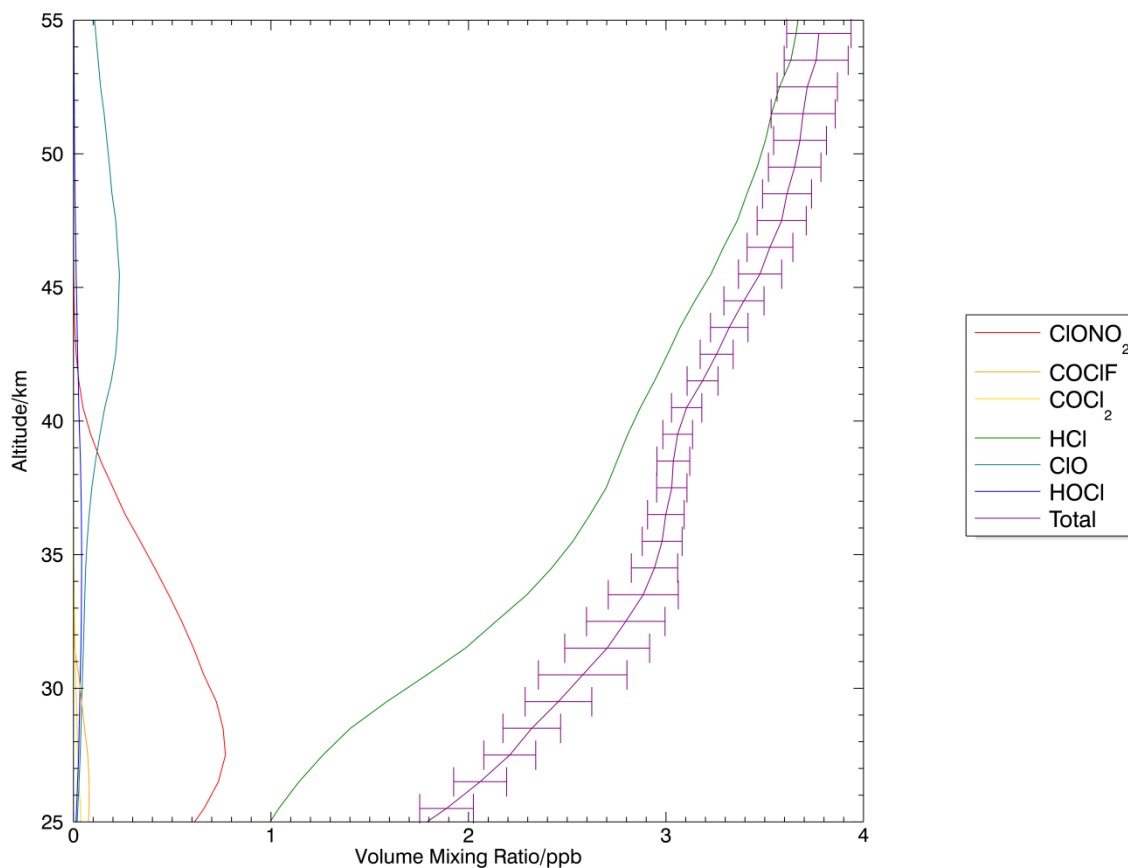


Figure 6.4: The mean morning profiles of inorganic chlorine species ( $\text{ClONO}_2$ ,  $\text{COClF}$ ,  $\text{COCl}_2$ ,  $\text{HCl}$ ,  $\text{ClO}$  and  $\text{HOCl}$ ) between 25 and 55 km between  $30^\circ \text{N}$  and the equator.

The mean total stratospheric chlorine and the slope of the total chlorine profile can be seen in Tables 6.2 and 6.3. There is no significant latitudinal difference between the mean total chlorine in the different latitude bands. All total chlorine profiles exhibit a positive slope, showing the VMR of total chlorine generally increases with altitude. Since age-of-air also increases with altitude (Waugh and Hall, 2002), this slope suggests that the concentration of chlorine has been decreasing over time. There does not appear to be a systematic difference between the slopes of the total chlorine profiles in the tropical and sub-tropical latitudes. This analysis suggests that there has been a global decrease in atmospheric chlorine over time.

Global stratospheric chlorine inventories

Table 6.2: The mean stratospheric total chlorine VMR in ppb

| Morning |               |   |      |              |   |      |              |   |      |               |   |      |
|---------|---------------|---|------|--------------|---|------|--------------|---|------|---------------|---|------|
| Year    | 70° N - 30° N |   |      | 30° N - 0° N |   |      | 0° N - 30° S |   |      | 30° S - 70° S |   |      |
| 2004    | 3.53          | ± | 0.18 | 3.46         | ± | 0.15 | 3.54         | ± | 0.13 | 3.60          | ± | 0.09 |
| 2005    | 3.54          | ± | 0.14 | 3.46         | ± | 0.12 | 3.47         | ± | 0.14 | 3.53          | ± | 0.11 |
| 2006    | 3.52          | ± | 0.13 | 3.44         | ± | 0.12 | 3.42         | ± | 0.14 | 3.51          | ± | 0.19 |
| 2007    | 3.51          | ± | 0.10 | 3.43         | ± | 0.12 | 3.42         | ± | 0.14 | 3.47          | ± | 0.19 |
| 2008    | 3.52          | ± | 0.12 | 3.41         | ± | 0.13 | 3.41         | ± | 0.14 | 3.43          | ± | 0.16 |
| 2009    | 3.44          | ± | 0.18 | 3.40         | ± | 0.13 | 3.47         | ± | 0.08 | 3.46          | ± | 0.22 |

| Evening |               |   |      |              |   |      |              |   |      |               |   |      |
|---------|---------------|---|------|--------------|---|------|--------------|---|------|---------------|---|------|
| Year    | 70° N - 30° N |   |      | 30° N - 0° N |   |      | 0° N - 30° S |   |      | 30° S - 70° S |   |      |
| 2004    | 3.55          | ± | 0.18 | 3.46         | ± | 0.14 | 3.53         | ± | 0.13 | 3.57          | ± | 0.15 |
| 2005    | 3.55          | ± | 0.18 | 3.49         | ± | 0.10 | 3.49         | ± | 0.15 | 3.50          | ± | 0.17 |
| 2006    | 3.47          | ± | 0.13 | 3.43         | ± | 0.12 | 3.44         | ± | 0.13 | 3.46          | ± | 0.15 |
| 2007    | 3.51          | ± | 0.15 | 3.46         | ± | 0.12 | 3.44         | ± | 0.11 | 3.45          | ± | 0.14 |
| 2008    | 3.47          | ± | 0.11 | 3.39         | ± | 0.13 | 3.41         | ± | 0.11 | 3.43          | ± | 0.18 |
| 2009    | 3.50          | ± | 0.13 | 3.44         | ± | 0.10 | 3.42         | ± | 0.14 | 3.44          | ± | 0.22 |

Table 6.3: The vertical slopes of the total chlorine profiles for both evening and morning occultations in the 4 latitude bins used in this study

| Morning |               |         |              |         |               |         |                |         |  |
|---------|---------------|---------|--------------|---------|---------------|---------|----------------|---------|--|
| Year    | 70° N - 30° N |         | 30° N - 0° N |         | 0° N to 30° S |         | 30° S to 70° S |         |  |
| 2004    | 0.010         | ± 0.001 | 0.004        | ± 0.002 | 0.006         | ± 0.001 | 0.003          | ± 0.001 |  |
| 2005    | 0.009         | ± 0.001 | 0.004        | ± 0.001 | 0.006         | ± 0.001 | 0.007          | ± 0.001 |  |
| 2006    | 0.007         | ± 0.001 | 0.005        | ± 0.001 | 0.005         | ± 0.001 | 0.010          | ± 0.002 |  |
| 2007    | 0.004         | ± 0.001 | 0.005        | ± 0.001 | 0.003         | ± 0.002 | 0.011          | ± 0.002 |  |
| 2008    | 0.006         | ± 0.001 | 0.004        | ± 0.002 | 0.004         | ± 0.002 | 0.010          | ± 0.001 |  |
| 2009    | 0.011         | ± 0.002 | 0.005        | ± 0.001 | 0.006         | ± 0.000 | 0.013          | ± 0.002 |  |
| Evening |               |         |              |         |               |         |                |         |  |
| Year    | 70° N - 30° N |         | 30° N - 0° N |         | 0° N - 30° S  |         | 30° S - 70° S  |         |  |
| 2004    | 0.011         | ± 0.001 | 0.006        | ± 0.001 | 0.009         | ± 0.001 | 0.007          | ± 0.001 |  |
| 2005    | 0.013         | ± 0.001 | 0.006        | ± 0.001 | 0.008         | ± 0.001 | 0.010          | ± 0.001 |  |
| 2006    | 0.008         | ± 0.001 | 0.006        | ± 0.001 | 0.006         | ± 0.001 | 0.011          | ± 0.001 |  |
| 2007    | 0.010         | ± 0.001 | 0.008        | ± 0.001 | 0.006         | ± 0.001 | 0.010          | ± 0.001 |  |
| 2008    | 0.005         | ± 0.001 | 0.004        | ± 0.001 | 0.004         | ± 0.001 | 0.012          | ± 0.001 |  |
| 2009    | 0.004         | ± 0.001 | 0.006        | ± 0.001 | 0.006         | ± 0.001 | 0.014          | ± 0.002 |  |

### 6.3.2 Inorganic chlorine against organic chlorine correlations

Inorganic chlorine species are produced by the breakdown of the organic chlorine species. Therefore, correlating the inorganic and organic species gives an indication as to whether the major chlorine containing species have been included in the budget; a slope close to one would show that all of the major chlorine containing species were included in the budget. The results of these plots can be seen in Table 6.4. All calculated slopes are greater than 1.01 and smaller than 1.11. These values suggest that the most important chlorine containing species have been included in this budget.

## Global stratospheric chlorine inventories

Table 6.4: The correlation between organic chlorine species (CCl<sub>4</sub>, CFC-12, CFC-11, HCFC-22, CH<sub>3</sub>Cl, CFC-113, CFC-114, CFC-115, H-1211, HCFC-141b and HCFC-142b) and inorganic chlorine species (HCl, COCl<sub>2</sub>, ClONO<sub>2</sub>, ClO, HOCl and COClF)

| Morning |               |        |              |        |              |        |               |        |  |  |
|---------|---------------|--------|--------------|--------|--------------|--------|---------------|--------|--|--|
| Year    | 70° N - 30° N |        | 30° N - 0° N |        | 0° N - 30° S |        | 30° S - 70° S |        |  |  |
| 2004    | -1.07         | ± 0.01 | -1.02        | ± 0.01 | -1.05        | ± 0.01 | -1.06         | ± 0.01 |  |  |
| 2005    | -1.08         | ± 0.01 | -1.02        | ± 0.01 | -1.07        | ± 0.02 | -1.08         | ± 0.01 |  |  |
| 2006    | -1.07         | ± 0.01 | -1.03        | ± 0.01 | -1.03        | ± 0.01 | -1.11         | ± 0.01 |  |  |
| 2007    | -1.03         | ± 0.01 | -1.03        | ± 0.01 | -1.00        | ± 0.01 | -1.10         | ± 0.01 |  |  |
| 2008    | -1.06         | ± 0.01 | -1.01        | ± 0.01 | -1.01        | ± 0.01 | -1.09         | ± 0.01 |  |  |
| 2009    | -1.07         | ± 0.01 | -1.01        | ± 0.01 | -1.05        | ± 0.01 | -1.11         | ± 0.02 |  |  |
| Mean    | -1.06         | ± 0.02 | -1.02        | ± 0.01 | -1.04        | ± 0.03 | -1.09         | ± 0.02 |  |  |

| Evening |               |        |              |        |              |        |               |        |  |  |
|---------|---------------|--------|--------------|--------|--------------|--------|---------------|--------|--|--|
| Year    | 70° N - 30° N |        | 30° N - 0° N |        | 0° N - 30° S |        | 30° S - 70° S |        |  |  |
| 2004    | -1.08         | ± 0.01 | -1.03        | ± 0.01 | -1.06        | ± 0.01 | -1.05         | ± 0.01 |  |  |
| 2005    | -1.09         | ± 0.01 | -1.04        | ± 0.01 | -1.09        | ± 0.02 | -1.07         | ± 0.01 |  |  |
| 2006    | -1.06         | ± 0.01 | -1.03        | ± 0.01 | -1.04        | ± 0.01 | -1.08         | ± 0.01 |  |  |
| 2007    | -1.05         | ± 0.01 | -1.05        | ± 0.01 | -1.04        | ± 0.01 | -1.08         | ± 0.01 |  |  |
| 2008    | -1.03         | ± 0.01 | -1.01        | ± 0.01 | -1.01        | ± 0.01 | -1.10         | ± 0.01 |  |  |
| 2009    | -1.04         | ± 0.01 | -1.03        | ± 0.01 | -1.03        | ± 0.01 | -1.11         | ± 0.02 |  |  |
| Mean    | -1.06         | ± 0.02 | -1.03        | ± 0.01 | -1.05        | ± 0.03 | -1.08         | ± 0.02 |  |  |

### 6.3.3 The contribution of species to the total chlorine budget

Total chlorine profiles are dominated by CFCs in the lower altitudes, with CFCs and halons contributing around 58% of the total chlorine. Most of this contribution comes from CFC-11 and CFC-12 which contribute around 20% and 30% respectively. In contrast HCFCs account for 7% of the total chlorine

## Global stratospheric chlorine inventories

in this region. As expected, above 24 km in the tropics and 19 km in the extra-tropics HCl rapidly dominates the chlorine budget. At its peak, at around 53 km, HCl accounts for around 95% of the total stratospheric chlorine. The second largest contribution from the chlorine reservoir species comes from ClONO<sub>2</sub> which peaks at between 20 and 25% of stratospheric chlorine between 26 and 28 km (dependent on the latitude). The full contribution of each species to the total chlorine VMR can be found in Appendix B. Figure 6.5 shows the average total fluorine profile from all the morning data in the 70° N to 30° N latitude range.

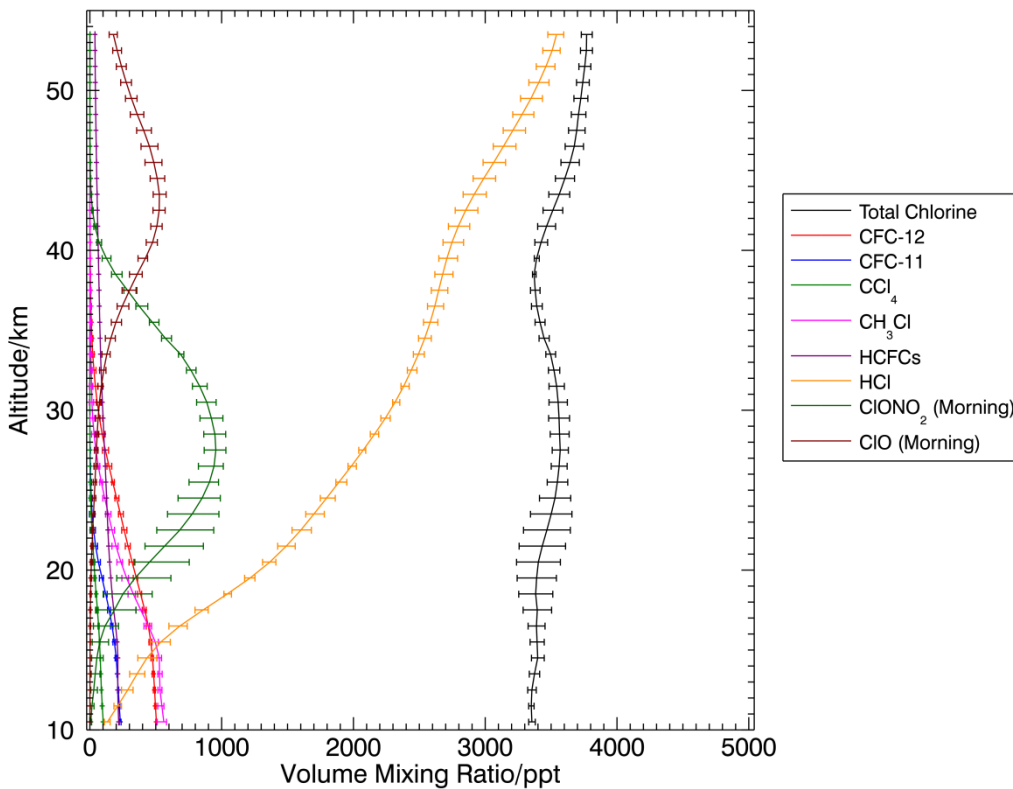


Figure 6.5 The mean profile of CFC-12, CFC-11, CCl<sub>4</sub>, CH<sub>3</sub>Cl, HCFCs (HCFC-22, -142b, -141b,) HCl, ClONO<sub>2</sub> and ClO calculated from all morning data in the 70°N to 30°N latitude range. The error bars on the profiles are the maxima and minima of the individual profiles used to calculate the mean.

### 6.3.4 The change in stratospheric chlorine between 2004 and 2009

The mean of the total stratospheric chlorine was calculated for the years between 2004 and 2009 to form a time series; these plots can be seen in Fig. 6.6. There does not seem to be significant latitudinal dependence to these time series. The difference between the morning and evening means are also not truly statistically significant. The VMR of the mean total chlorine is decreasing in every latitude band for both the evening and morning measurements. This rate is similar in the Northern and Southern Hemisphere tropics (30°N - 0°N and 0°N - 30°S respectively). In the Northern Hemisphere morning occultations show total chlorine decreasing at a rate of  $-0.40 \pm 0.05$  % per year and evening occultations show a decrease at a rate of  $-0.30 \pm 0.22$  % per year. The errors quoted here are the 1- $\sigma$  fitting error of a linear least squares fit to the data. Both southern and northern tropical occultations show a similar means with overlapping error ranges. In the southern tropics morning occultations show total chlorine decreasing at a rate of  $-0.43 \pm 0.31$  % per year and evening occultations show total chlorine decreasing at a rate of  $-0.65 \pm 0.14$  % per year.

Measurements from the northern extra-tropical stratosphere exhibit a trend very similar to the tropical trends. Morning occultations show mean stratospheric VMR decreasing at a rate of  $-0.40 \pm 0.17$  % per year, with evening occultations exhibiting a similar  $-0.36 \pm 0.21$  % per year. The rate of decrease appears to be slightly higher in the southern mid-latitude stratosphere. This is exhibited by both the evening and morning results,  $-0.69 \pm 0.17$  % per year and  $-0.84 \pm 0.17$  % per year respectively. This increased rate of change is due to a slightly higher mean total chlorine value for 2004 (yellow and purple points in Fig. 6.6). If this value is removed then the rate of change becomes  $-0.62 \pm 0.18$  % per year for morning occultations and  $-0.44 \pm 0.13$  % per year for evening occultations. These values show stratospheric chlorine is

## Global stratospheric chlorine inventories

decreasing at a very similar rate independent of latitude, and have been used in the calculation of the global trends.

The global trend for morning occultations is  $-0.47 \pm 0.1\%$  per year, the evening data produces a trend of  $-0.44 \pm 0.12\%$  per year. The mean trend (calculated using both morning and evening data) from the northern hemisphere is a decrease of  $-0.37 \pm 0.05\%$  per year. The southern hemisphere data exhibits a mean decrease of  $-0.70 \pm 0.08\%$  per year. The difference between these two rates is likely due to the difference in emissions of chlorine containing molecules from the different hemispheres. The temporary replacement HCFC molecules contain chlorine which can enter the stratosphere in the tropics before it is transported throughout the stratosphere. Whilst these species are rapidly being phased out in the European Union and the United States, their atmospheric concentrations continue to increase (O'Doherty et al., 2004; Montzka et al., 2009; Brown et al., 2011). The emission of these additional chlorine containing molecules in the northern hemisphere would slow the loss rate of chlorine in the northern hemisphere producing the different rates seen in this work. The global mean value is a decreasing VMR of total chlorine of  $-0.46 \pm 0.02\%$  per year. These results are presented in Table 6.5.

## Global stratospheric chlorine inventories

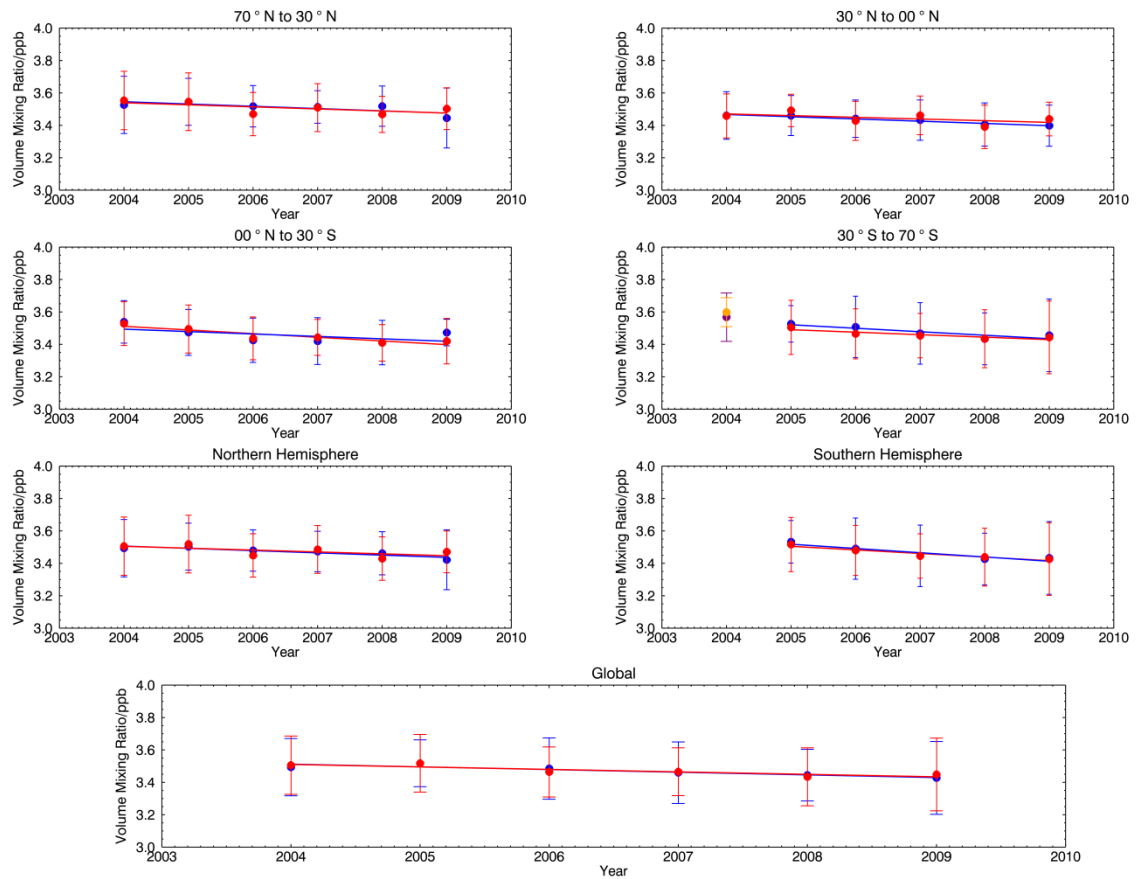


Figure 6.6: The trends in the mean total stratospheric chlorine between 2004 and 2009 for different regions. The red line represents the line of best fit for the evening occultations mean stratospheric total chlorine VMR (the red circles). The blue line represents the line of best fit for the morning occultations mean stratospheric total chlorine VMR (the blue circles). The error bars shown in the plots are calculated from the standard deviation of the data used to calculate the mean total chlorine VMRs.

## Global stratospheric chlorine inventories

Table 6.5: The trends in the mean stratospheric total chlorine VMR (ppb) between 2004 and 2009 for different regions and for morning, evening and combined morning and evening occultations. The errors quoted here are the 1- $\sigma$  fitting error of a linear least squares fit to the data.

|                     | Morning  |         |         |        |
|---------------------|----------|---------|---------|--------|
|                     | ppb/year |         | % /year |        |
| 70° N - 30° N       | -0.014   | ± 0.006 | -0.40   | ± 0.17 |
| 30° N - 0° N        | -0.014   | ± 0.002 | -0.40   | ± 0.05 |
| 0° N - 30° S        | -0.015   | ± 0.011 | -0.43   | ± 0.31 |
| 30° S - 70° S       | -0.022   | ± 0.006 | -0.62   | ± 0.18 |
| Northern Hemisphere | -0.014   | ± 0.003 | -0.40   | ± 0.09 |
| Southern Hemisphere | -0.026   | ± 0.006 | -0.75   | ± 0.18 |
| Global              | -0.016   | ± 0.004 | -0.47   | ± 0.10 |
|                     | Evening  |         |         |        |
|                     | ppb/year |         | % /year |        |
| 70° N - 30° N       | -0.013   | ± 0.007 | -0.36   | ± 0.21 |
| 30° N - 0° N        | -0.010   | ± 0.008 | -0.30   | ± 0.22 |
| 0° N - 30° S        | -0.023   | ± 0.005 | -0.65   | ± 0.14 |
| 30° S - 70° S       | -0.015   | ± 0.005 | -0.44   | ± 0.13 |
| Northern Hemisphere | -0.012   | ± 0.007 | -0.33   | ± 0.20 |
| Southern Hemisphere | -0.022   | ± 0.004 | -0.64   | ± 0.11 |
| Global              | -0.015   | ± 0.004 | -0.44   | ± 0.12 |

Table 6.5 Continued

|                     | Mean (Morning & Evening) |              |
|---------------------|--------------------------|--------------|
|                     | ppb/year                 | %/year       |
| 70° N - 30° N       | -0.013 ± 0.001           | -0.38 ± 0.03 |
| 30° N - 0° N        | -0.012 ± 0.002           | -0.35 ± 0.07 |
| 0° N - 30° S        | -0.019 ± 0.005           | -0.54 ± 0.16 |
| 30° S - 70° S       | -0.018 ± 0.004           | -0.53 ± 0.12 |
| Northern Hemisphere | -0.013 ± 0.002           | -0.37 ± 0.05 |
| Southern Hemisphere | -0.024 ± 0.003           | -0.70 ± 0.08 |
| Global              | -0.016 ± 0.001           | -0.46 ± 0.02 |

Changes in the mean VMR in the total chlorine between 48.5km and 53.5km between 2004 and 2009 have also been calculated. These results can be seen in Table 6.6. These calculations show no statistically significant hemispheric dependence on the rate of decrease of chlorine. Globally the total chlorine is decreasing at a rate of  $-0.70 \pm 0.12$  % per year between these altitudes. This value is very close to the rate calculated by Froidevaux et al. (2006b) of  $0.78 \pm 0.08$  % per year. This suggests that there has been no statistically significant change in the rate at which chlorine is decreasing at higher altitudes during this time.

## Global stratospheric chlorine inventories

Table 6.6 The trends in the mean stratospheric total chlorine VMR (ppb) between 2004 and 2009 for different regions and for morning, evening and combined morning and evening occultations. These values correspond to the changes in the total chlorine between the altitudes of 48.5 and 53.5 km. The errors on the morning and evening values are the 1- $\sigma$  fitting error of a linear least squares fit to the data. The errors on the mean values are the standard deviations of the corresponding calculations.

|                     | Mean (Morning) |   |       |         |   |      |
|---------------------|----------------|---|-------|---------|---|------|
|                     | ppb/year       |   |       | % /year |   |      |
| 70°N-30°N           | -0.022         | ± | 0.006 | -0.59   | ± | 0.17 |
| 30°N-0°N            | -0.017         | ± | 0.004 | -0.47   | ± | 0.10 |
| 0°N-30°S            | -0.031         | ± | 0.004 | -0.84   | ± | 0.11 |
| 30°S-70°S           | -0.019         | ± | 0.011 | -0.52   | ± | 0.30 |
| Northern Hemisphere | -0.020         | ± | 0.003 | -0.53   | ± | 0.09 |
| Southern Hemisphere | -0.025         | ± | 0.008 | -0.68   | ± | 0.22 |
| Global              | -0.022         | ± | 0.006 | -0.60   | ± | 0.16 |

|                     | Mean (Evening) |   |       |         |   |      |
|---------------------|----------------|---|-------|---------|---|------|
|                     | ppb/year       |   |       | % /year |   |      |
| 70°N-30°N           | -0.034         | ± | 0.014 | -0.89   | ± | 0.36 |
| 30°N-0°N            | -0.019         | ± | 0.004 | -0.50   | ± | 0.10 |
| 0°N-30°S            | -0.030         | ± | 0.007 | -0.80   | ± | 0.19 |
| 30°S-70°S           | -0.035         | ± | 0.016 | -0.95   | ± | 0.43 |
| Northern Hemisphere | -0.026         | ± | 0.011 | -0.70   | ± | 0.27 |
| Southern Hemisphere | -0.033         | ± | 0.004 | -0.88   | ± | 0.10 |
| Global              | -0.029         | ± | 0.008 | -0.79   | ± | 0.20 |

Table 6.6 Continued

|                     | Mean (Morning & Evening) |   |       |         |   |      |
|---------------------|--------------------------|---|-------|---------|---|------|
|                     | ppb/year                 |   |       | % /year |   |      |
| 70°N-30°N           | -0.028                   | ± | 0.008 | -0.74   | ± | 0.21 |
| 30°N-0°N            | -0.018                   | ± | 0.001 | -0.49   | ± | 0.02 |
| 0°N-30°S            | -0.030                   | ± | 0.001 | -0.82   | ± | 0.02 |
| 30°S-70°S           | -0.027                   | ± | 0.011 | -0.73   | ± | 0.30 |
| Northern Hemisphere | -0.023                   | ± | 0.007 | -0.61   | ± | 0.18 |
| Southern Hemisphere | -0.029                   | ± | 0.002 | -0.78   | ± | 0.06 |
| Global              | -0.026                   | ± | 0.004 | -0.70   | ± | 0.12 |

### 6.3.5 Radiative Efficiency- and Global Warming Potential-weighted fluorine budget trends

Many of the species used in this work are potent greenhouse gases; any changes in the VMR of these species will therefore have an effect on climate. Different species have different REs and GWPs leading to different radiative forcing effects. Once more a useful measure of the effects of changes in the VMR of chlorine-containing species can be gained by calculating the RE- and GWP-weighted trend of total chlorine during this time. The methods employed here are outlined fully in Chapter 5. For the RE-weighting each species was weighted by its RE before the species were summed and a least squares linear fit was calculated for the data. GWP-weighted trends were calculated by weighting each species by its relative molecular mass, GWP (on a 20-year timeframe) and the atmospheric pressure. The time series of these means can be seen in Figs. 6.7 and 6.8. It should be noted that since data above the tropopause was not used the overall RE- and GWP-weighted trends do not exhibit diurnal dependence.

## Global stratospheric chlorine inventories

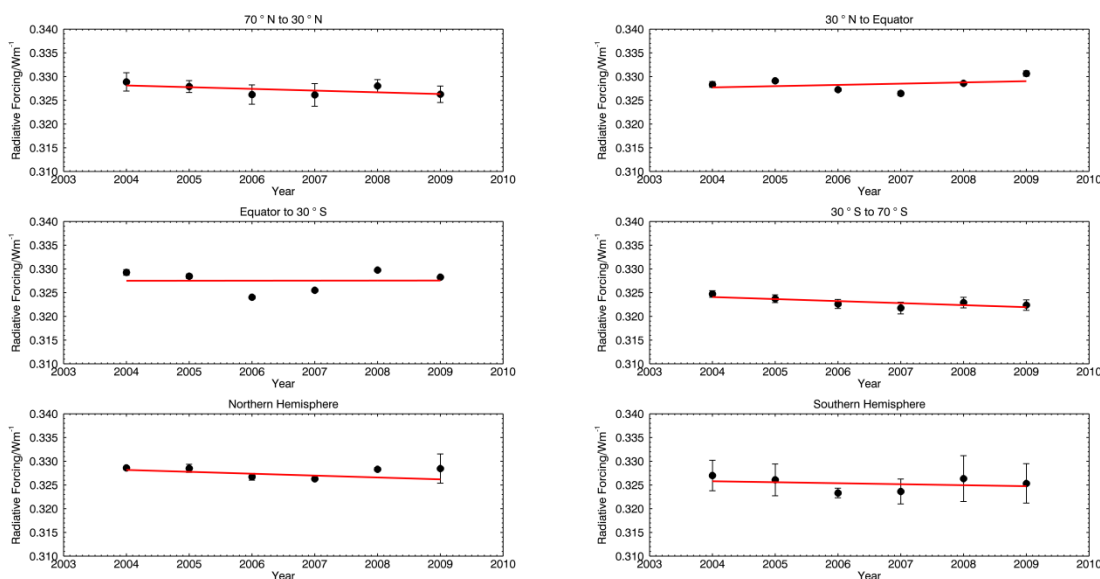


Figure 6.7: The trends in the radiative efficiency-weighted total chlorine mean between 2004 and 2009. The red line represents the line of best fit for the radiative efficiency-weighted mean volume mixing ratio (the black circles). The error bars shown in the plots are calculated from the standard deviation of the data used to calculate the means. These errors are extremely small since by and large these values do not change significantly in the troposphere.

The results of this analysis can be seen in Table 6.7. RE-weighted chlorine exhibit small decreases in the extra-tropics:  $-0.11 \pm 0.08$  %/year in the northern hemisphere and  $-0.13 \pm 0.06$  %/year in the southern hemisphere. There is no statistically significant trend in either the northern hemisphere tropics:  $0.08 \pm 0.11$  %/year, or the southern hemisphere tropics,  $0.00 \pm 0.18$  %/year. It appears that the decrease in CFCs and halons has been offset (in terms of radiative efficiency) by the increase in HCFCs during this time (Brown et al., 2011; Montzka et al., 2011a). This is evidenced if the HCFCs are not included in the calculation. In this case all the latitudes display very similar trends which are within error of each other. This value appears to be around 0.60 %/year (c.f Table 6.7).

## Global stratospheric chlorine inventories

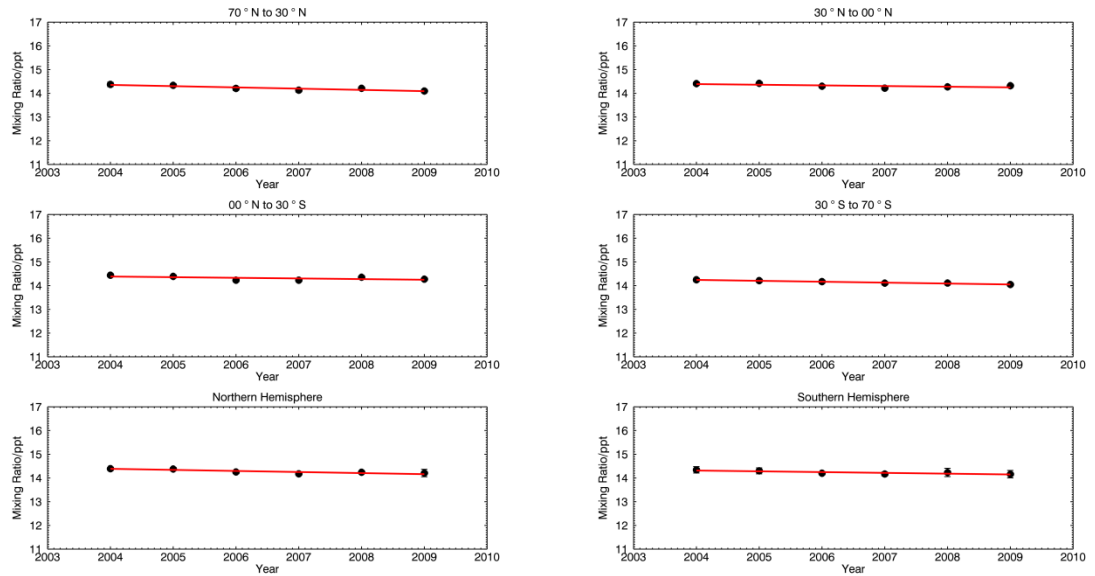


Figure 6.8: The trends in the GWP-weighted total chlorine between 2004 and 2009. The red line represents the line of best fit for the GWP weighted mean VMR (the black circles). The error bars shown in the plots are calculated from the weighted standard deviation of the data used to calculate the means. These errors are extremely small since by and large these values do not change significantly in the troposphere.

GWP-weighted total chlorine is decreasing globally, with the most rapid rate in the extra-tropical region. The rate of decrease is largest in the extra-tropical Northern Hemisphere, where GWP-weighted chlorine is decreasing at a rate of  $-0.37 \pm 0.09\%$  per year. In the Southern Hemisphere extra-tropical latitudes the GWP weighted total chlorine is decreasing at a rate of  $-0.27 \pm 0.13\%$  per year. The tropical latitudes show smaller changes in GWP total chlorine with trends of  $-0.19 \pm 0.11\%$  per year (Northern Hemisphere) and  $-0.19 \pm 0.13\%$  per year (Southern Hemisphere). It seems likely that the difference between the rates of decrease of the extra-tropical and tropical latitudes is down to the increase of HCFCs during this time.

If HCFCs are not included in the calculations the rate of decrease becomes significantly higher as can be seen in Table 6.7. HCFCs reach the stratosphere

## Global stratospheric chlorine inventories

through strong upwelling in the tropics leading to higher VMR of HCFCs in the upper troposphere lower stratosphere region in tropical latitudes than in extra-tropical latitudes. This would have the effect of reducing the rate of decrease of and RE- GWP-weighted chlorine in these areas. When considered together these results suggest that in the short term there has been very little, if any, change in climatologically effective chlorine. However, in the long term the reduction in the emissions of long lived CFCs and halons will produce a reduction in the climatological effect of chlorine containing species.

Table 6.7: The RE- and GWP-weighted trends in the total chlorine VMR between 2004 and 2009. The errors quoted here are the 1- $\sigma$  fitting error of a linear least squares fit to the data. The weighted total chlorine budgets were also calculated without including HCFCs so that the impact of the replacement of CFCs by HCFCs, under the Montreal Protocol, on global warming potential-weighted chlorine could be quantified.

RE-weighted total chlorine

| Latitude band       | Weighted total chlorine trend (%/year) | Weighted total chlorine trend without HCFCs (%/year) |
|---------------------|--|--|
| 70° N - 30° N       | -0.11 ± 0.08 %/year                    | -0.68 ± 0.08 %/year                                  |
| 30° N - 0° N        | 0.08 ± 0.11 %/year                     | -0.55 ± 0.13 %/year                                  |
| 0° N - 30° S        | 0.00 ± 0.18 %/year                     | -0.54 ± 0.15 %/year                                  |
| 30° S - 70° S       | -0.13 ± 0.06 %/year                    | -0.62 ± 0.03 %/year                                  |
| Northern Hemisphere | -0.11 ± 0.04 %/year                    | -0.62 ± 0.07 %/year                                  |
| Southern Hemisphere | -0.06 ± 0.12 %/year                    | -0.58 ± 0.08 %/year                                  |

Table 6.7 continued

| Latitude band       | GWP-weighted total chlorine |        | Weighted total chlorine trend without HCFCs |        |
|---------------------|-----------------------------|--------|---|--------|
|                     | trend (%/year)              |        | trend (%/year)                              |        |
| 70° N - 30° N       | -0.37                       | ± 0.09 | -0.72                                       | ± 0.06 |
| 30° N - 0° N        | -0.19                       | ± 0.11 | -0.58                                       | ± 0.12 |
| 0° N - 30° S        | -0.19                       | ± 0.13 | -0.51                                       | ± 0.11 |
| 30° S - 70° S       | -0.27                       | ± 0.12 | -0.57                                       | ± 0.03 |
| Northern Hemisphere | -0.31                       | ± 0.08 | -0.68                                       | ± 0.02 |
| Southern Hemisphere | -0.23                       | ± 0.08 | -0.56                                       | ± 0.11 |

### 6.3.6 Ozone Depleting Potential-weighted chlorine budget trends

The primary aim of the Montreal Protocol is to reduce the emission of ozone-destroying substances. The calculation of the trend in total atmospheric chlorine is valuable to see how effective the Montreal Protocol has been. The calculation of a trend, weighted by the ODP of the individual species, offers a more specific view of the impact of this reduction on ozone destruction. Like the GWP, ODP is a comparative value: the ozone depleting potential of 1 kg of substance as compared to 1 kg of CFC-11. The ODP-weighted total chlorine is calculated in a similar manner to the GWP-weighted total fluorine. Each source species was weighted by its ODP, relative molecular mass and pressure. The results of this analysis can be seen in Table 6.8 and Fig. 6.9. As expected the ODP-weighted total chlorine is decreasing in all latitude bands. The weighted total chlorine is decreasing at the fastest rate in the extra-tropics, where ODP-weighted total chlorine is decreasing at a rate of  $-1.00 \pm 0.19\%$  per year in the Southern Hemisphere and  $-0.82 \pm 0.09\%$  per year in the Northern Hemisphere. The tropics exhibit a strong, but slower, rate of decrease of  $-0.66$

## Global stratospheric chlorine inventories

$\pm 0.08\%$  (Northern Hemisphere) and  $-0.49 \pm 0.08\%$  (Southern Hemisphere) per year. ODP weighted total chlorine is decreasing at an equal rate in the Northern Hemisphere ( $-0.74 \pm 0.05\%$  per year) and in the Southern Hemisphere ( $-0.73 \pm 0.13\%$  per year). These results show that the Montreal Protocol has had great success in reducing the emissions of ODS.

Table 6.8: The ozone depletion potential-weighted trends in the total chlorine VMR between 2004 and 2009. The error on the trends is the 1- $\sigma$  error on the least squares fit.

| Latitude band       | Weighted total chlorine trend (%/year) |       |      |
|---------------------|--|-------|------|
| 70° N - 30° N       | -0.82                                  | $\pm$ | 0.09 |
| 30° N - 0° N        | -0.66                                  | $\pm$ | 0.08 |
| 0° N - 30° S        | -0.49                                  | $\pm$ | 0.08 |
| 30° S - 70° S       | -1.00                                  | $\pm$ | 0.19 |
| Northern Hemisphere | -0.74                                  | $\pm$ | 0.05 |
| Southern Hemisphere | -0.73                                  | $\pm$ | 0.13 |

## Global stratospheric chlorine inventories

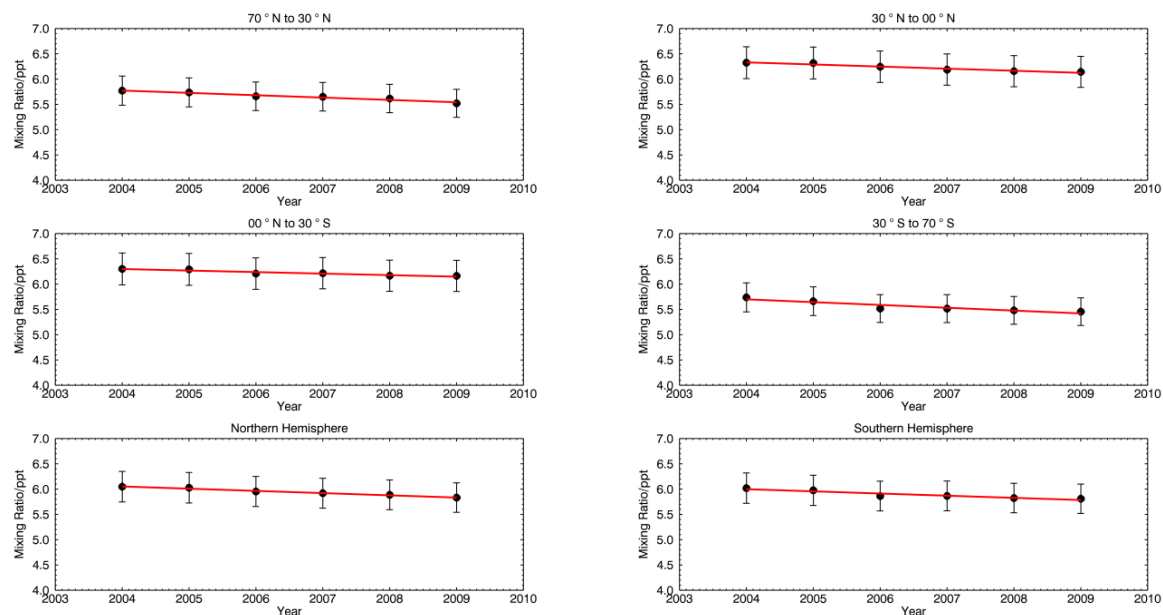


Figure 6.9: The trends in the ODP weighted total chlorine between 2004 and 2009. The red line represents the line of best fit for the ODP weighted mean VMR (the black circles). The error bars shown in the plots are calculated from the weighted standard deviation of the data used to calculate the means.

## 6.4 Conclusion

This chapter presented chlorine budgets calculated between 2004 and 2009 for the latitude bands of 70° N - 30° N, 30° N - 0° N, 0° N - 30° S, and 30° S - 70° S which represent the extra-tropical and tropical latitudes in the stratosphere. The chlorine budgets were calculated using ACE-FTS version 3.0 retrievals of nine chlorine-containing species: CCl<sub>4</sub>, CFC-12, CFC-11, COCl<sub>2</sub>, COClF, HCFC-22, CH<sub>3</sub>Cl, HCl and ClONO<sub>2</sub>. This data was supplemented with data for the following species from the SLIMCAT 3D chemical transport model: CFC-113, CFC-114, CFC-115, H-1211, H-1301, HCFC-141b, HCFC-142b, ClO and HOCl. Since HOCl, ClO and ClONO<sub>2</sub> exhibit diurnal variation, it is necessary to separate the data into morning and evening occultations. This allows both morning and evening total chlorine budgets to be calculated.

## Global stratospheric chlorine inventories

The total chlorine profiles are dominated by CFCs at lower altitudes, where CFCs and halons account for 58% of the total chlorine. This remains the case until around 24 km in the tropics and 19 km in the extra-tropics when HCl rapidly dominates the chlorine budget. At its peak, at around 53 km, HCl accounts for around 95% of the total stratospheric chlorine. All total chlorine profiles exhibit a positive slope with altitude. A positive slope to the total chlorine profile suggests that the atmospheric VMR of chlorine is decreasing with time. This is supported by the time series of the mean stratospheric total chlorine budgets. This data shows mean decreases in total stratospheric chlorine of  $-0.38 \pm 0.03$  % per year in the northern hemisphere extra-tropics,  $-0.35 \pm 0.07$  % per year in the northern hemisphere tropical stratosphere,  $-0.54 \pm 0.16$  % per year in the southern hemisphere tropics and  $-0.53 \pm 0.12$  % per year in the southern hemisphere extra-tropical stratosphere. As expected, these values suggest a very similar decrease in total stratospheric chlorine globally. Globally stratospheric chlorine is decreasing by  $-0.46 \pm 0.02$  % per year.

As with the fluorine budget it is possible to compare the results of this work with the results of previous budgets. Between 1985 and 1997 the total fluorine VMR increased from  $2.58 \pm 0.1$  ppb (Zander et al., 1992) to  $3.7 \pm 0.2$  ppb (Sen et al., 1999). Subsequently, Nassar et al. (2006a) found that in 2004 the total chlorine had reduced to  $3.65 \pm 0.13$  ppb. This work shows a continued downwards trend in total chlorine VMR with the VMR declining from  $3.55 \pm 0.18$  ppb in 2004 to  $3.50 \pm 0.13$  ppb.

Trends in weighted total chlorine have also been calculated using the ODP, RE and GWP of individual species for weighting. These values allow the impact of the Montreal Protocol on radiative forcing and ozone depletion to be further analysed. RE-weighted chlorine decreased slightly in the extra-tropics and remained constant in the tropics, whilst GWP-weighted chlorine decreased in all latitude bands. However, decreases in the tropics are not significant and

## Global stratospheric chlorine inventories

appear to be suppressed by the increase in HCFCs during this time. These results suggest that whilst in the short term the decrease in chlorine containing species will have little effect on the climate, in the longer term (a 20-year horizon) decreases in CFCs and halons will reduce the climatological effects of these species. ODP-weighted chlorine is also decreasing in all bands with the fastest rate in the southern hemisphere extra-tropical latitude band. This work suggests that the Montreal Protocol has been successful in reducing the VMR of chlorine-containing gases in the atmosphere. It has also been inadvertently successful in reducing the VMR of GWP-weighted chlorine during this time.

# 7

## **Stratospheric lifetimes of CFC-12, CCl<sub>4</sub>, CH<sub>4</sub>, CH<sub>3</sub>Cl and N<sub>2</sub>O**

### ***7.1 Introduction***

Catalytic stratospheric ozone destruction occurs through the formation of halogen, nitrogen and hydrogen radicals. The halogen and nitrogen source gases also play a role in global radiative transfer blocking outgoing infrared radiation. In the case of halogen source gases, the long tropospheric lifetimes of many halogen-containing species allow them to reach the stratosphere through the upwelling tropical circulation. Once in the stratosphere they undergo photolysis and the halogen atoms which they contain are released into the surrounding atmosphere. Chlorine and bromine atoms released into the

stratosphere catalyse ozone destruction. Fluorine atoms react rapidly to form stable HF.

A full analysis of ozone destruction must also take into account species such as  $\text{N}_2\text{O}$ , which is the major source of stratospheric NO and  $\text{NO}_2$ , and  $\text{CH}_4$ , which acts as a sink for atmospheric OH. The long-term impact of these species on the environment is determined by their atmospheric lifetimes. Accurate estimates of atmospheric lifetimes of species which are directly and indirectly involved in stratospheric ozone loss are therefore vital. In particular, atmospheric lifetimes are used to set environmental policies on the emissions of ozone depleting substances and greenhouse gases. Nitrous oxide and methane are also greenhouse gases; furthermore methane contributes to stratospheric water vapour that can affect surface temperatures (Solomon, 2010).

The 2010 scientific assessment of ozone depletion report from the World Meteorology Organisation (WMO) (Montzka et al., 2011a) highlighted problems with the current lifetimes of some halogen-containing species such as carbon tetrachloride ( $\text{CCl}_4$ ). Atmospheric concentrations of  $\text{CCl}_4$  are declining more slowly than expected which could be caused by an unreliable atmospheric lifetime (Montzka et al., 2011a). This has led to the formation of the Stratospheric-Troposphere Processes And their Role in Climate (SPARC) lifetimes reassessment project. The aim of the re-evaluation is to estimate the numerical values of the lifetimes and the associated errors, assess the influence of different lifetime definitions and assess the effect of changing climate on lifetimes. The SPARC science report was published in spring 2014 and will form the basis for the 2014 WMO Ozone Assessment (<http://www.sparc-climate.org/activities/lifetime-halogen-gases/>).

There are a number of methods for calculating the stratospheric lifetimes of long lived gases using satellite measurements. Stratospheric lifetimes can be calculated using a combination of satellite measurements and an atmospheric

model. Satellite measurements are used to calculate the total amount of a species in the atmospheric. If the chemistry of the species is well known model data can be used to calculate the loss rates for the species from photolysis and chemical reaction. The instantaneous lifetime of a species is simply the global atmospheric burden divided by the sum of all the loss rates (Johnston et al., 1979; Minschwaner et al., 1998). In situ measurements made using balloon and aircraft borne instruments can be used to calculate the stratospheric lifetimes of a number of long lived species using correlations with CFC-11 (Volk et al., 1997; Bujok et al., 2001; Laube et al., 2013). This method relies on accurate knowledge of the lifetime of CFC-11. Recent calculations of the lifetime of CFC-11, carried out using model data, have produced values between 56 and 64 years (Douglass et al., 2008), whilst older estimates suggest a lifetime of 45 years (Prinn et al., 1999). This uncertainty in the lifetime of CFC-11 has a significant effect on the stratospheric lifetime estimates of a number of other halogen-containing species. If satellite data is to be used to carry out this analysis it should have sufficiently high vertical resolution to be able to extrapolate the slope of the correlation to the tropopause. Limb-sounding satellite-borne instruments, such as the ACE-FTS and MIPAS, have sufficiently high vertical resolution to be used for this method of lifetime calculation.

This chapter presents new stratospheric lifetime estimates for CFC-12, CCl<sub>4</sub>, CH<sub>4</sub>, CH<sub>3</sub>Cl and N<sub>2</sub>O calculated from correlations with CFC-11 using data from the ACE-FTS. For CFC-12, CCl<sub>4</sub> and N<sub>2</sub>O, which have no chemical sink in the troposphere, these lifetimes correspond to the global lifetime with respect to atmospheric removal.

## 7.2 Calculating stratospheric lifetimes using correlations with CFC-11

The lifetime calculations presented in this chapter were calculated following the well-established method laid out by Volk et al. (1997). This work was based on the theoretical work of Plumb and Ko (1992) and Plumb (1996). An outline of this method is given in this section.

The stratospheric lifetimes ( $\tau_a$ ,  $\tau_b$ ) of two long lived species, a and b, which have the same stratospheric sinks are related by the ratio of their average atmospheric VMR,  $\bar{\sigma}$ , and the steady-state slope of the correlation at the extratropical tropopause ( $d\sigma_a/d\sigma_b$ ). This method requires that there be very little transport across the tropopause so that the correlation of the species at the tropopause is a function of lifetime and not atmospheric transport. In the tropics the correlation of species at the tropopause would be highly dependent on the transport of individual species through the tropopause as described in Chapter 2. Transport across the tropopause does occur in the extra-tropics, it is the reason for the curve of the slope of the tracer-tracer correlations which can be seen in Fig. 7.1. This transport is extremely slow and thus data from the extratropics are therefore used for this calculation. In addition to tropical data, data inside the polar vortex is generally not used for these calculations. Since air inside the vortex subsides there exists a discontinuity in lines of constant VMR at the edge of the vortex. Thus correlations in this region cannot be used for lifetimes calculations. This chapter follows the convention of Volk et al. (1997), where  $\chi$  refers to the transient mixing ratios and  $\sigma$  represents the mixing ratios corresponding to a steady state situation with the same tropopause mixing ratio.

$$\frac{\tau_a}{\tau_b} = \frac{\frac{\bar{\sigma}_a}{\bar{\sigma}_b}}{\left. \frac{d\sigma_a}{d\sigma_b} \right|_{tropopause}} \quad \text{Eqn. 7.1}$$

## Global stratospheric chlorine inventories

This method can be used to calculate the relative lifetime of a long-lived species, a, assuming that the lifetime of a second long-lived species, b, is known. Conventionally lifetimes derived in this manner are calculated relative to CFC-11. This convention derives from the calculation of ODP using Eqn. 2.11. It should not be forgotten that this equation is a measure of the ODP of a molecule compared to that of CFC-11 and is dependent on the lifetime of both CFC-11 and the molecule. Calculating lifetime relative to CFC-11 reduces the error in ODP resulting from uncertainties in the lifetime of CFC-11.

Calculations of lifetimes using correlations is complicated by the fact that the observed VMRs ( $\chi$ ) of the species used in this study are changing independently of one another. Since age-of-air increases with altitude the VMR of a species at a particular altitude is not only dependent on the sinks at that altitude but also on the VMR of the species when it was released. Thus if the emissions of a species are changing over time the correlation is dependent on both the changes in VMR. An additional problem arises from the fact that there are not discrete ages-of-air at each altitude, since the air is mixed (this is explained in more detail a little later in this section). Eqn. 7.1 requires steady-state quantities ( $\sigma$ ), thus some correction is required. Any correction must include the tropospheric growth rate, the width of the stratospheric age-of-air spectrum, and the slope of a tracer's VMR with respect to mean age-of-air must be accounted for.

$$\left. \frac{d\sigma_a}{d\sigma_b} \right|_{tropopause} = \left. \frac{d\chi_a}{d\chi_b} \right|_{tropopause} \frac{C_a}{C_b} \quad \text{Eqn. 7.2}$$

$$C = \frac{\left. \frac{d\sigma}{d\Gamma} \right|_{tropopause}}{\left. \frac{d\chi}{d\Gamma} \right|_{tropopause}} \quad \text{Eqn. 7.3}$$

$$\left. \frac{d\sigma}{d\Gamma} \right|_{\Gamma=0} = \frac{\left( \left. \frac{d\chi}{d\Gamma} \right|_{\Gamma=0} + \gamma_0 \sigma_0 \right)}{(1 - 2\gamma_0 \Lambda)} \quad \text{Eqn. 7.4}$$

$$\chi_0(t') = \chi_0(t)[1 + b(t' - t) + c(t' - t)^2] \quad \text{Eqn. 7.5}$$

$$\gamma_0 = b - 2\Lambda c \quad \text{Eqn. 7.6}$$

Volk et al., (1997) calculated the steady-state correlation using Eq. 7.2 which is the observed correlation ( $d\chi_a/d\chi_b$ ) multiplied by a correction factor for each species. The correction factor (C – Eqn. 7.3) which was calculated using the correlation between the VMR of a species and the age-of-air at the tropopause ( $d\chi/d\Gamma$ ). The correction of  $d\chi/d\Gamma$  to account for growth in the VMR of a species ( $do/d\Gamma$  - Eqn. 7.4) is complicated by a number of factors. The atmospheric growth rates of individual species are not necessarily linear. This necessitates the calculation of the effective linear growth rate ( $\gamma_0$ ), and knowledge of the VMR of a species at the tropopause ( $\sigma_0$ ). In order that  $\gamma_0$  may be calculated, a long-term tropospheric data set for each species is required. A polynomial curve (Eqn. 7.5) is fitted to this time series over a five year interval prior to a specific reference time when the measurements were made (for example if the ACE-FTS measurement was made in 2009,  $t = 2009$ ,  $t' =$  year in which the individual ground based measurement in the time series was made). The fit coefficients,  $b$  and  $c$  (Eqn. 7.5), can be used to calculate the  $\gamma_0$  from Eqn. 7.6.

The second factor which complicates the process comes from the stratospheric age of air spectrum. The atmosphere can be thought to be constructed from a series of air packets stacked on top of one another. These packets will gradually travel upwards through the troposphere through convection. Once in the stratosphere they are mixed by braking planetary waves. Vertical transport of these packets is not instant; parcels at higher altitudes therefore contain gases which were emitted into the atmosphere a longer time ago than packets which are at lower altitudes. The gases in each of these packets were not emitted at the same time, there will be a spread of ages of air within each packet. The  $\Lambda$  factor in Eqns. 7.4 and 7.6 is the ratio of the squared width of the age spectrum to the mean age and accounts for the effects of the finite width of the age of air spectrum (Volk et al., 1997). In the past a range of

values between, 0.7, 1.25 and 1.75 have been used for this variable. Following the convention of Volk et al. (1997) and Laube et al. (2013) a value of 1.25 years for  $\Lambda$  has been used in this work. The uncertainty in this value however is reflected in the final errors on the lifetime. Lifetimes were calculated using values of 0.7 and 1.75 and were factored into the final error calculations.

It was found that if the age-of-air correlations included 0 in their error range then the error on the correction factor increased to the point that the correction factors were essentially unconstrained. In previous work the age-of-air correlations were well constrained, thus this problem did not arise and thus went undetected. However, the age-of-air data used in this study produced unconstrained correlations (this is discussed below). This finding led to a re-evaluation of the equations used to calculate the steady state correlations. Rather than evaluating Eqn. 7.2 for each species combination, as was done in Volk et al. (1997), Eqn. 7.4 it was combined for two tracers a and b and  $d\chi_a/d\Gamma$  has been substituted for  $d\chi_a/d\chi_b \cdot d\chi_b/d\Gamma$ , so that only the gradient with respect to mean age of tracer species b is required (the derivation of this equation can be found in Appendix E). This results in the following relationship between the steady-state tracer-tracer correlation slope ( $d\sigma_a/d\sigma_b$ ) required in Eqn. 7.1 and the observed transient slope ( $d\chi_a/d\chi_b$ ):

$$\frac{d\sigma_a}{d\sigma_b}\Big|_{tropopause} = \frac{\frac{d\chi_a}{d\chi_b}\Big|_{tropopause} \cdot \frac{d\chi_b}{d\Gamma}\Big|_{\Gamma=0} + \gamma_{0_a}\sigma_{0_a}}{\frac{d\chi_b}{d\Gamma}\Big|_{\Gamma=0} + \gamma_{0_b}\sigma_{0_b}} \cdot \frac{1 - 2\gamma_{0_b}\Lambda}{1 - 2\gamma_{0_a}\Lambda} \quad \text{Eqn. 7.7}$$

This method is more desirable as it minimises the errors that could otherwise propagate throughout the calculations if age-of-air correlations were required. The overall error in the steady state correlation is relatively insensitive to errors in the age-of-air correlation, it is far more sensitive to errors in the tracer-tracer correlations. The slope of the correlation of mean age against

## Global stratospheric chlorine inventories

CFC-11 at the tropopause required in Eqn.7.7 was calculated by Laube et al. (2013) based on laboratory analysis of CFC-11 and SF<sub>6</sub> in whole air samples taken on board the Geophysica aircraft in October 2009 and January 2010. These calculations produced a value of  $-20.6 \pm 4.6$  ppt/year for early 2010 for the slope at the tropopause. For other years this value has been scaled using the effective linear growth rate ( $\gamma_0$ ) of CFC-11 during this time (the values for which can be seen in Table 7.2). The resulting values for the age of air slopes can be seen in Table 7.1. The use of the Laube et al. (2013) CFC-11 versus age-of-air slopes facilitated the comparisons of lifetimes calculated from ACE with those derived from the Geophysica samples by Laube et al. (2013). However, the primary reason for using these values was that the model age-of-air data (discussed later) produced unconstrained age-of-air correlations, thus new data was required.

Table 7.1: The slope of the age of air against the VMR of CFC-11 at the tropopause

|      | Age of Air ppt/year |   |     |
|------|---------------------|---|-----|
| 2005 | -21.3               | ± | 4.6 |
| 2006 | -21.1               | ± | 4.6 |
| 2007 | -20.9               | ± | 4.6 |
| 2008 | -20.7               | ± | 4.6 |
| 2009 | -20.6               | ± | 4.6 |
| 2010 | -20.5               | ± | 4.6 |

Global stratospheric chlorine inventories

Table 7.2: The effective linear growth rates ( $\gamma_0$ ) in % Year<sup>-1</sup> of CFC-11, CFC-12, CCl<sub>4</sub>, CH<sub>4</sub>, CH<sub>3</sub>Cl and N<sub>2</sub>O

|      | CFC-11 |   |       | CFC-12 |   |       | CH <sub>3</sub> Cl |   |       |
|------|--------|---|-------|--------|---|-------|--------------------|---|-------|
| 2005 | -0.853 | ± | 0.019 | -0.181 | ± | 0.01  | 1.661              | ± | 0.556 |
| 2006 | -0.92  | ± | 0.022 | -0.286 | ± | 0.012 | -0.428             | ± | 0.712 |
| 2007 | -0.905 | ± | 0.023 | -0.383 | ± | 0.011 | 0.665              | ± | 0.469 |
| 2008 | -0.831 | ± | 0.026 | -0.452 | ± | 0.013 | 0.862              | ± | 0.326 |
| 2009 | -0.727 | ± | 0.019 | -0.486 | ± | 0.012 | -0.144             | ± | 0.291 |
| 2010 | -0.718 | ± | 0.018 | -0.478 | ± | 0.009 | -0.384             | ± | 0.245 |

|      | CCl <sub>4</sub> |   |       | N <sub>2</sub> O |   |       | CH <sub>4</sub> |   |       |
|------|------------------|---|-------|------------------|---|-------|-----------------|---|-------|
| 2005 | -0.933           | ± | 0.024 | 0.205            | ± | 0.007 | 0.003           | ± | 0.043 |
| 2006 | -0.944           | ± | 0.026 | 0.212            | ± | 0.008 | -0.034          | ± | 0.039 |
| 2007 | -1.133           | ± | 0.032 | 0.217            | ± | 0.011 | 0.17            | ± | 0.059 |
| 2008 | -1.305           | ± | 0.028 | 0.262            | ± | 0.008 | 0.477           | ± | 0.045 |
| 2009 | -1.451           | ± | 0.023 | 0.257            | ± | 0.009 | 0.444           | ± | 0.046 |
| 2010 | -1.479           | ± | 0.027 | 0.262            | ± | 0.009 | 0.328           | ± | 0.047 |

Initially we tested whether a correlation between model age data and ACE-FTS CFC-11 could contain the slopes but it was found that this was not the case. The model data used to test this was from NASA's Modern-Era Retrospective analysis for Research and Application (MERRA) project which was supplied by Dr M. R. Schoeberl from the science and technology corporation. Due to computational limitations monthly age of air data was supplied on a 2 km (altitude) by 2° (latitude) grid. This grid required significant interpolation so that each ACE-FTS occultation had an age of air profile. This interpolation introduced errors into the ACE-FTS age of air profiles which when plotted against CFC-11 produced correlations with errors which were greater than 100 %. Since the model data could not constrain the age of air against CFC-11 correlations these values were not used. An

additional consideration was whether model data should be used in this study. Slight errors in the atmospheric transport used by the model would introduce errors into the age of air data which in turn would propagate into the lifetimes. For this reason, and those mentioned previously, the Laube et al. (2013) CFC-11 versus age of air slopes were used in this work.

## **7.3 Results and Discussion**

### **7.3.1 Treatment of data**

ACE-FTS occultations were divided into 24 separate data bins dependent on their stratospheric season and year. The data was first divided into four bins which corresponded with Northern Hemisphere stratospheric Winter (NHW), Northern Hemisphere stratospheric Summer (NHS), Southern Hemisphere stratospheric Winter (SHW) and Southern Hemisphere stratospheric Summer (SHS). These four bins were defined by the month in which the occultations were made in the following manner:

#### **Northern Hemisphere Stratospheric Winter**

November – December – January – February – March – April

#### **Northern Hemisphere Stratospheric Summer**

May\* - June – July – August – September – October\*

#### **Southern Hemisphere Stratospheric Winter**

May - June – July – August – September – October

#### **Southern Hemisphere Stratospheric Summer**

November\* – December – January – February – March – April\*

## Global stratospheric chlorine inventories

The months marked with asterisks are not truly stratospheric summer months; they were selected to increase the sample size used in this study. The NHW bin for 2005 would include data from November and December 2004 and from January, February, March and April 2005. Likewise, SHS 2005 included November and December 2004 and January, February, March and April 2005. The decision to use six month periods of analysis was made to increase the sample size used in this work. If seasonality has a significant effect on the calculated lifetime, dividing the data into two periods would be sufficient to see this difference.

In the tropics, there is large scale upwelling through the tropopause to higher altitudes in relative isolation from mid-latitudes, resulting in tropical correlation curves different from those in the extra-tropical surf zone (e.g. Volk et al., 1996). Tropical correlations thus reflect local rather than global sources and sinks and are therefore not suited to derive global stratospheric lifetimes (Plumb, 1996; Neu and Plumb, 1999). In the higher latitudes, the polar vortex causes stratospheric air to subside in isolation from mid-latitudes and correlation curves within the vortex develop separately from those at mid-latitudes over the course of the winter (Plumb, 2007), thus making occultations within the polar vortex unsuitable for the derivation of stratospheric lifetimes. Tropical and polar latitudes thus act as the lower and upper limits for the latitudes from which data can be used in this study. The latitudes used in this study run from 30° North/South, to 70° North/South. Measurements made within the polar vortex appeared as outliers to the overall data and were removed as they fell outside of the boundaries set by the MAD filter. In this way both the tropical and the polar-regions are avoided. The division of the data into northern and southern hemisphere was designed to test whether there is any hemispheric dependence in the calculated lifetimes. By dividing the data seasonally the sensitivity of the calculated lifetimes to seasonal variation was also to be explored. Since the background VMR of these species varies annually the data was divided into additional bins inside the four

mentioned previously. These bins were separated by the year in which the occultations were made before the data was filtered using the MAD (see Chapter 4.2). As has been mentioned previously, data within the polar vortex was outside these parameters and was therefore discarded during this stage of filtering. A final round of filtering removed data below the tropopause using tropopause altitudes from the ACE DMPs. Each ACE occultation has a unique DMP which presents the altitude of the tropopause at the latitude, longitude and local time of the occultation.

### 7.3.2 CFC-11 Correlations

Mean correlation curves were produced for the correlations of each species versus CFC-11. The mean correlation curves were calculated using the mean of the data in non-overlapping windows which were 2 ppt of CFC-11 wide. The error on the mean of this data in both x and y (where x is CFC-11 and y is the correlating species) is the standard error of the mean. These windows ran the entire range of the CFC-11 data beginning at the minimum concentration and moving along every 2 ppt until the maximum concentration value had been passed. Once a mean correlation curve had been produced the slope of the data within a moving window of 80 ppt of CFC-11 was calculated using a linear least squares fit which took both the error in the CFC-11 and the correlating species' mean into account. After measuring the slope of the data the window would be moved forwards by 5 ppt and the slope of the data would be calculated again. The procedure started 80 ppt of CFC-11 below the minimum CFC-11 VMR, providing a blank first reading. This procedure continued until the window was 80 ppt larger than the maximum CFC-11 VMR. At both ends of the data the windows contain areas with no data in them. In this case the middle of the data range was not the centre of the window. Instead, the centre of the window was amended to reflect the centre of the data. The same effect occurs at the tropopause. This produced a series of windows which became

## Global stratospheric chlorine inventories

smaller and smaller, the closer they got to the tropopause and the lower limit of the data.

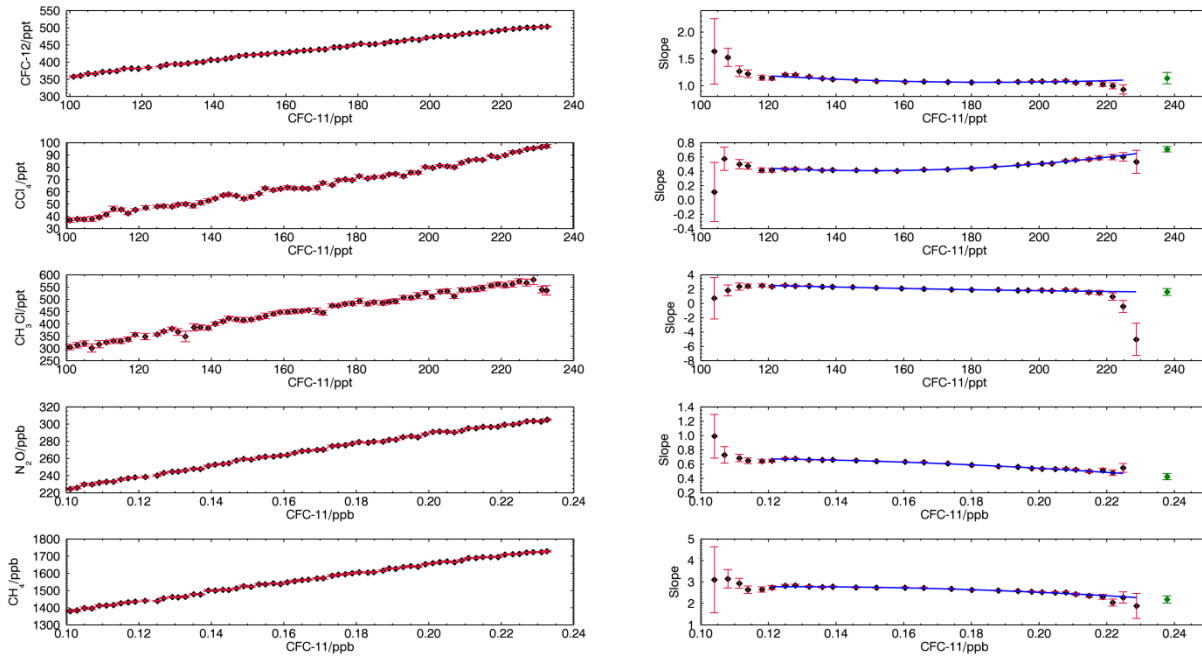


Figure 7.1: Correlations between the VMRs of CFC-12,  $\text{CCl}_4$ ,  $\text{CH}_4$ ,  $\text{CH}_3\text{Cl}$  and  $\text{N}_2\text{O}$  and CFC-11 for the data from the northern hemisphere during the stratospheric winter of 2008. Left panels: The mean correlation curves. Each point represents the mean of the data within a window of 2 ppt of CFC-11 wide. The errors on this data are the standard deviations of the data within this window. Right panels: The black points are the slopes of the data within a moving 5 ppt window. The errors on this data are the fitting errors of this slope. The blue line is a second order polynomial least squares fit to this data. The green point is the extrapolated slope at the tropopause.

Once this procedure had been carried out, data from windows corresponding to a CFC-11 VMR of less than 120 ppt were discarded and a second degree polynomial was fitted to the remaining data. The data was weighted using the square of the inverse fitting errors on each point from the previous step. The aim of these calculations was to extrapolate the slope of the correlation to the tropopause. Above around 120 ppt it was found that the linear correlations

would begin to break down. Thus, removing data below 120 ppt of CFC-11 ensured that the polynomial fit would not be biased towards the higher altitudes. On the other hand, the range of the fit (120 to ~220 ppt) ensured that the extrapolated slope at the tropopause would not be unduly affected from points directly at the tropopause where complex mixing from the troposphere can cause the observed correlation to break down. Examples of the correlation plots and slope calculations can be seen in Figure 7.1, the remaining plots can be found in Appendix B (Fig. 1 to 21).

Fluxes of chemical species into the stratosphere from the tropopause are not constant and are prone to change as long as the species are not in steady state. This produces a curving effect in the correlations around the tropopause that can be clearly seen in Fig. 7.1. The method employed in this paper requires the knowledge of the slope of the stratospheric tracer-tracer correlation at the tropopause. The slope of the correlation at the tropopause was calculated using the equation derived from the polynomial fit along with the mean CFC-11 VMR at the tropopause. Following the work of Volk et al. (1997) statistical errors on the fit were calculated using a bootstrap method (Efron et al., 1979) and scaled using the number of independent points used in the extrapolation fit.

Global stratospheric chlorine inventories

Table 7.3: The slopes of the correlations of CFC-12, CH<sub>3</sub>Cl, CCl<sub>4</sub>, N<sub>2</sub>O and CH<sub>4</sub> with CFC-11, extrapolated to the tropopause. NHS = Northern Hemisphere Summer, NHW = Northern Hemisphere Winter, SHS = Southern Hemisphere Summer, SHW = Southern Hemisphere Winter. Data with errors greater than the correlations have been removed.

|      | Bin | CFC-12           | CH <sub>3</sub> Cl | CCl <sub>4</sub> | N <sub>2</sub> O |
|------|-----|------------------|--------------------|------------------|------------------|
| 2005 | NHW | 0.96 ± 0.08      | 1.21 ± 0.37        | 0.6 ± 0.07       | -                |
|      | SHW | 1.19 ± 0.29      | 3.16 ± 2.24        | 0.31 ± 0.22      | 716.81 ± 75.47   |
|      | NHS | 0.82 ± 0.06      | -                  | 0.41 ± 0.13      | 386.3 ± 47.25    |
| 2006 | NHW | 1.14 ± 0.17      | 1.91 ± 0.37        | 0.89 ± 0.1       | -                |
|      | SHS | 1.25 ± 0.10      | 2.68 ± 0.43        | 0.47 ± 0.09      | 441.96 ± 89.48   |
|      | SHW | 0.75 ± 0.12      | 0.68 ± 0.39        | 0.44 ± 0.03      | 764.16 ± 66.93   |
|      | NHS | 0.73 ± 0.08      | -                  | 0.91 ± 0.07      | -                |
| 2007 | NHW | 0.72 ± 0.07      | -                  | 0.48 ± 0.08      | 384.17 ± 158.75  |
|      | SHS | 1.10 ± 0.16      | 1.71 ± 0.93        | 0.42 ± 0.18      | 568.32 ± 76.45   |
|      | SHW | 1.04 ± 0.08      | 1.38 ± 0.52        | 0.57 ± 0.05      | 668.52 ± 63.26   |
|      | NHS | 1.02 ± 0.06      | 1.08 ± 0.38        | 0.67 ± 0.05      | -                |
| 2008 | NHW | 1.14 ± 0.11      | 1.60 ± 0.47        | 0.71 ± 0.04      | 425.58 ± 43.92   |
|      | SHS | 0.79 ± 0.09      | 1.29 ± 0.36        | 0.61 ± 0.06      | 405.89 ± 48.77   |
|      | SHW | 0.78 ± 0.17      | 1.43 ± 0.61        | 0.48 ± 0.03      | 599.92 ± 61.47   |
|      | NHS | 0.92 ± 0.11      | -                  | 1.24 ± 0.26      | 342.99 ± 122.16  |
| 2009 | NHW | -                | -                  | -                | -                |
|      | SHS | 1.17 ± 0.34      | -                  | 0.72 ± 0.18      | 992.12 ± 144.53  |
|      | SHW | 0.87 ± 0.05      | 2.72 ± 0.75        | 0.54 ± 0.12      | 710.83 ± 43.07   |
|      | NHS | 0.61 ± 0.04      | -                  | 0.71 ± 0.08      | 386.97 ± 74.89   |
| 2010 | NHW | 0.76 ± 0.11      | 1.95 ± 0.76        | 0.72 ± 0.04      | 716.72 ± 98.31   |
|      | SHS | 1.01 ± 0.12      | 1.34 ± 0.87        | 0.47 ± 0.11      | 572.71 ± 81.13   |
|      | SHW | 1.14 ± 0.17      | 1.77 ± 0.92        | 0.18 ± 0.1       | 680.5 ± 55.37    |
|      | Bin | CH <sub>4</sub>  |                    |                  |                  |
| 2005 | NHW | -                |                    |                  |                  |
|      | SHW | 4403.1 ± 1080.64 |                    |                  |                  |
|      | NHS | 1609.02 ± 257.51 |                    |                  |                  |
| 2006 | NHW | 1794.21 ± 599.76 |                    |                  |                  |
|      | SHS | 1130.28 ± 348.86 |                    |                  |                  |
|      | SHW | 2240.74 ± 193.1  |                    |                  |                  |
|      | NHS | 1631.25 ± 154.93 |                    |                  |                  |
| 2007 | NHW | 1768.92 ± 385.62 |                    |                  |                  |
|      | SHS | 1694.7 ± 255.45  |                    |                  |                  |
|      | SHW | 2775.14 ± 288.66 |                    |                  |                  |

Table 7.5 Continued

|      | Bin | CH <sub>4</sub>   |
|------|-----|-------------------|
| 2008 | NHS | -                 |
|      | NHW | 2180.86 ± 171.34  |
|      | SHS | -                 |
|      | SHW | 2049.66 ± 145.78  |
| 2009 | NHS | 2139.97 ± 351.11  |
|      | NHW | -                 |
|      | SHS | 4408.87 ± 1253.71 |
|      | SHW | 1997.24 ± 111.75  |
| 2010 | NHS | 2566.37 ± 387.05  |
|      | NHW | 3244.25 ± 157.55  |
|      | SHS | 1485.76 ± 396.57  |
|      | SHW | 2003.68 ± 256.47  |

The slopes at the tropopause are shown in Table 7.3. There are three bins with no correlation data, NHS 2005, SHS 2005 and NHW 2009. In these bins problems with the retrieval program, used to retrieve VMR from ACE-FTS spectra, caused a failure in the retrieval of CFC-11. Work is on-going at this time to rectify this problem. Correlations between CFC-12 and CFC-11 produce slopes that range between  $0.61 \pm 0.04$  and  $1.25 \pm 0.1$ . With a median (of all 24 bins) of 0.99 and a standard deviation of 0.19 these data exhibit good self-consistency. The slopes of the CH<sub>3</sub>Cl correlation show a significant spread with a maximum of  $3.16 \pm 2.24$  and a minimum of  $0.68 \pm 0.39$ . The slopes have a median of 1.60 and a standard deviation of 0.65. CCl<sub>4</sub> has a large spread of slopes with a median of 0.59 and a standard deviation of 0.23. The maxima and minima of this data are  $1.24 \pm 0.26$  and  $0.18 \pm 0.1$ . Both CH<sub>4</sub> and N<sub>2</sub>O show relatively wide spreads of values with medians of 2026 and 577 and standard deviations of 914 and 178 respectively. One source of variation for CH<sub>3</sub>Cl and CH<sub>4</sub> could be the flux of species across the tropopause, for example, due to seasonal or inter-annual variations in tropospheric growth, leading to changes to the correlation slopes in the lowest part of the stratosphere.

The effective linear growth rate ( $\gamma_0$  – equation 7.4) was calculated using monthly global means from the AGAGE network (Prinn et al., 2000, 2001) for

## Global stratospheric chlorine inventories

CFC-11 (Cunnold et al., 2002), CFC-12 (Cunnold et al., 1997), CCl<sub>4</sub> (Simmonds et al., 1998), CH<sub>4</sub> (Cunnold et al., 2002; Rigby et al., 2008), CH<sub>3</sub>Cl (Simmonds et al., 2004; Cox et al., 2003) and N<sub>2</sub>O (Prinn et al., 1990), following the method laid out in Volk et al. (1997) using equations 7.3 and 7.4. For this study a quadratic function was fitted to 5 years of AGAGE data prior to each year between 2005 and 2010. For CH<sub>3</sub>Cl AGAGE data from between 2004 and 2010 was used. Strong seasonality was removed from the data using a sinusoidal term.

Table 7.4: The mean VMR at the tropopause ( $\sigma_0$ ).

|      | CFC-11 |        | CFC-12 |        | CH <sub>3</sub> Cl |         |
|------|--------|--------|--------|--------|--------------------|---------|
| 2005 | 245.24 | ± 3.14 | 515.63 | ± 4.88 | 575.60             | ± 9.86  |
| 2006 | 240.90 | ± 3.00 | 512.54 | ± 7.82 | 586.40             | ± 27.78 |
| 2007 | 238.23 | ± 1.72 | 510.97 | ± 4.19 | 612.36             | ± 25.76 |
| 2008 | 237.84 | ± 3.03 | 509.52 | ± 5.94 | 571.52             | ± 39.13 |
| 2009 | 235.54 | ± 4.54 | 510.17 | ± 7.25 | 596.21             | ± 11.75 |
| 2010 | 232.00 | ± 2.72 | 503.36 | ± 6.83 | 572.45             | ± 23.35 |

|      | CCl <sub>4</sub> |        | N <sub>2</sub> O |       | CH <sub>4</sub> |        |
|------|------------------|--------|------------------|-------|-----------------|--------|
| 2005 | 106.33           | ± 3.14 | 315.3            | ± 2.0 | 1747.5          | ± 33.4 |
| 2006 | 106.83           | ± 7.34 | 315.7            | ± 2.5 | 1755.8          | ± 36.2 |
| 2007 | 106.59           | ± 7.80 | 316.5            | ± 0.7 | 1762.6          | ± 34.9 |
| 2008 | 104.51           | ± 6.89 | 317.4            | ± 2.0 | 1765.5          | ± 36.1 |
| 2009 | 105.45           | ± 9.15 | 317.7            | ± 2.2 | 1770.0          | ± 26.2 |
| 2010 | 101.29           | ± 7.47 | 317.3            | ± 4.4 | 1770.5          | ± 38.2 |

The VMRs at the tropopause ( $\sigma_0$ ) were calculated by removing any data below 3 km below the tropopause and any data which lay above the tropopause. The remaining data was used to calculate an annual mean VMR which represented  $\sigma_0$ ; these values can be seen in Table 7.4. The corrected correlations, calculated using Eqn 7.5, can be found in Table 7.5.

Global stratospheric chlorine inventories

Table 7.5: The corrected slopes of the correlations of CFC-12, CCl<sub>4</sub>, CH<sub>4</sub>, CH<sub>3</sub>Cl and N<sub>2</sub>O with CFC-11, extrapolated to the tropopause. NHS = Northern Hemisphere Summer, NHW = Northern Hemisphere Winter, SHS = Southern Hemisphere Summer, SHW = Southern Hemisphere Winter

| Bin  |     | CFC-12 |      |      |          | CH <sub>3</sub> Cl |      |      |          |
|------|-----|--------|------|------|----------|--------------------|------|------|----------|
| 2005 | NHW | 0.93   | +(-) | 0.08 | ( 0.08 ) | 0.74               | +(-) | 0.4  | ( 0.41 ) |
|      | SHW | 1.15   | +(-) | 0.27 | ( 0.27 ) | 2.63               | +(-) | 2.18 | ( 2.19 ) |
|      | NHS | 0.82   | +(-) | 0.06 | ( 0.06 ) |                    |      | -    |          |
| 2006 | NHW | 1.11   | +(-) | 0.16 | ( 0.16 ) | 1.86               | +(-) | 0.37 | ( 0.37 ) |
|      | SHS | 1.21   | +(-) | 0.09 | ( 0.09 ) | 2.56               | +(-) | 0.42 | ( 0.42 ) |
|      | SHW | 0.75   | +(-) | 0.11 | ( 0.11 ) | 0.73               | +(-) | 0.4  | ( 0.4 )  |
| 2007 | NHS | 0.76   | +(-) | 0.08 | ( 0.08 ) |                    |      | -    |          |
|      | NHW | 0.75   | +(-) | 0.07 | ( 0.07 ) |                    |      | -    |          |
|      | SHS | 1.1    | +(-) | 0.14 | ( 0.14 ) | 1.43               | +(-) | 0.88 | ( 0.88 ) |
|      | SHW | 1.04   | +(-) | 0.08 | ( 0.08 ) | 1.11               | +(-) | 0.51 | ( 0.52 ) |
| 2008 | NHS | 1.04   | +(-) | 0.05 | ( 0.05 ) | 0.81               | +(-) | 0.37 | ( 0.38 ) |
|      | NHW | 1.15   | +(-) | 0.1  | ( 0.1 )  | 1.3                | +(-) | 0.45 | ( 0.46 ) |
|      | SHS | 0.83   | +(-) | 0.09 | ( 0.09 ) | 1                  | +(-) | 0.35 | ( 0.36 ) |
|      | SHW | 0.82   | +(-) | 0.16 | ( 0.16 ) | 1.13               | +(-) | 0.59 | ( 0.59 ) |
| 2009 | NHS | 0.97   | +(-) | 0.1  | ( 0.1 )  |                    |      | -    |          |
|      | NHW |        |      | -    |          |                    |      | -    |          |
|      | SHS | 1.2    | +(-) | 0.31 | ( 0.31 ) |                    |      | -    |          |
|      | SHW | 0.92   | +(-) | 0.04 | ( 0.05 ) | 2.58               | +(-) | 0.71 | ( 0.71 ) |
| 2010 | NHS | 0.67   | +(-) | 0.04 | ( 0.04 ) |                    |      | -    |          |
|      | NHW | 0.82   | +(-) | 0.11 | ( 0.11 ) | 1.92               | +(-) | 0.71 | ( 0.71 ) |
|      | SHS | 1.05   | +(-) | 0.11 | ( 0.11 ) | 1.35               | +(-) | 0.82 | ( 0.82 ) |
|      | SHW | 1.17   | +(-) | 0.16 | ( 0.16 ) | 1.75               | +(-) | 0.86 | ( 0.86 ) |

Global stratospheric chlorine inventories

Table 7.5 Continued

| Bin  |     | CCl <sub>4</sub> |      |               | N <sub>2</sub> O |                 |  |
|------|-----|------------------|------|---------------|------------------|-----------------|--|
| 2005 | NHW | 0.59             | +(-) | 0.06 ( 0.06 ) |                  | -               |  |
|      | SHW | 0.32             | +(-) | 0.2 ( 0.2 )   | 641.7 +(-)       | 72.5 ( 74.6 )   |  |
|      | NHS | 0.41             | +(-) | 0.12 ( 0.12 ) | 330 +(-)         | 45.5 ( 47.2 )   |  |
| 2006 | NHW | 0.85             | +(-) | 0.09 ( 0.09 ) |                  | -               |  |
|      | SHS | 0.47             | +(-) | 0.08 ( 0.08 ) | 381.8 +(-)       | 84.3 ( 85.3 )   |  |
|      | SHW | 0.44             | +(-) | 0.03 ( 0.03 ) | 681.7 +(-)       | 65.1 ( 67.9 )   |  |
| 2007 | NHS | 0.87             | +(-) | 0.07 ( 0.07 ) |                  | -               |  |
|      | NHW | 0.48             | +(-) | 0.08 ( 0.08 ) | 327.5 +(-)       | 148.5 ( 149 )   |  |
|      | SHS | 0.43             | +(-) | 0.16 ( 0.16 ) | 499.2 +(-)       | 72.9 ( 74.6 )   |  |
|      | SHW | 0.57             | +(-) | 0.05 ( 0.05 ) | 592.6 +(-)       | 61.4 ( 63.9 )   |  |
| 2008 | NHS | 0.67             | +(-) | 0.04 ( 0.04 ) |                  | -               |  |
|      | NHW | 0.7              | +(-) | 0.03 ( 0.03 ) | 361.7 +(-)       | 43.3 ( 45.7 )   |  |
|      | SHS | 0.61             | +(-) | 0.06 ( 0.06 ) | 343.2 +(-)       | 47.6 ( 49.6 )   |  |
|      | SHW | 0.49             | +(-) | 0.02 ( 0.02 ) | 525.2 +(-)       | 60 ( 62.5 )     |  |
| 2009 | NHS | 1.19             | +(-) | 0.23 ( 0.23 ) | 287 +(-)         | 116.1 ( 116.8 ) |  |
|      | NHW |                  |      | -             |                  | -               |  |
|      | SHS | 0.72             | +(-) | 0.17 ( 0.17 ) | 901.2 +(-)       | 138.5 ( 140.3 ) |  |
|      | SHW | 0.56             | +(-) | 0.11 ( 0.11 ) | 635 +(-)         | 44.2 ( 47.9 )   |  |
| 2010 | NHS | 0.71             | +(-) | 0.07 ( 0.07 ) | 328.1 +(-)       | 72 ( 73.3 )     |  |
|      | NHW | 0.72             | +(-) | 0.04 ( 0.04 ) | 640.6 +(-)       | 94.8 ( 96.6 )   |  |
|      | SHS | 0.5              | +(-) | 0.1 ( 0.1 )   | 504.1 +(-)       | 78.3 ( 80.1 )   |  |
|      | SHW | 0.23             | +(-) | 0.1 ( 0.1 )   | 606.3 +(-)       | 55.1 ( 58 )     |  |

Table 7.5 Continued

|      |  | Bin |             | CH <sub>4</sub> |            |
|------|--|-----|-------------|-----------------|------------|
| 2005 |  | NHW |             | -               |            |
|      |  | SHW | 4093 +(-)   | 1008.3          | ( 1011.1 ) |
|      |  | NHS | 1514.5 +(-) | 241.2           | ( 242.5 )  |
| 2006 |  | NHW | 1685.8 +(-) | 556.3           | ( 556.9 )  |
|      |  | SHS | 1071.7 +(-) | 324.4           | ( 324.8 )  |
|      |  | SHW | 2098.9 +(-) | 184.5           | ( 187.9 )  |
|      |  | NHS | 1385.4 +(-) | 159.1           | ( 168.1 )  |
| 2007 |  | NHW | 1513.6 +(-) | 365.6           | ( 369.9 )  |
|      |  | SHS | 1444.5 +(-) | 247.3           | ( 253.5 )  |
|      |  | SHW | 2450.4 +(-) | 281.3           | ( 291.2 )  |
|      |  | NHS |             | -               |            |
| 2008 |  | NHW | 1674.3 +(-) | 193.2           | ( 222.5 )  |
|      |  | SHS |             | -               |            |
|      |  | SHW | 1550.5 +(-) | 172.3           | ( 203.4 )  |
|      |  | NHS | 1671.6 +(-) | 348.4           | ( 363.6 )  |
| 2009 |  | NHW |             | -               |            |
|      |  | SHS | 3828.4 +(-) | 1199.3          | ( 1207.5 ) |
|      |  | SHW | 1535.9 +(-) | 144.3           | ( 176.8 )  |
|      |  | NHS | 2166.2 +(-) | 378.5           | ( 389.8 )  |
| 2010 |  | NHW | 2809.5 +(-) | 180.4           | ( 208.2 )  |
|      |  | SHS | 1140.6 +(-) | 384.2           | ( 391.7 )  |
|      |  | SHW | 1632.1 +(-) | 257.4           | ( 270.9 )  |

### 7.3.3 Lifetime Calculations

The annual global mean atmospheric VMR ( $\bar{\sigma}$ ) of each species was calculated using ACE-FTS profiles of the VMR ( $\sigma$ ) weighted by atmospheric pressure (P). In this case pressure is being used as a proxy for density. Whilst using pressure will weight the lower stratosphere less than it deserves, thus giving a slightly higher bias in the atmospheric means, this effect will not be larger than the errors on the means. Mean VMR profiles were calculated for each species in 15° latitude bins. Profiles were extended from their lowest point to the ground by assuming a constant VMR. Each VMR value was weighted by the corresponding pressure; this allowed a weighted mean to be calculated using Eqn. 7.7. The global mean atmospheric VMRs were then calculated by

weighting the pressure weighted means from the latitude bins using the cosine of the latitude. This was done since the majority of the mass of the global atmosphere is contained in the tropical troposphere. The results of this analysis can be seen in Table 7.6.

$$\bar{\sigma} = \frac{\sum P_i \sigma_i}{\sum P_i} \quad \text{Eqn. 7.7}$$

Table 7.6: Mean atmospheric VMR ( $\bar{\sigma}$ ).

|      | CFC-11 |        | CFC-12 |         | CH <sub>3</sub> Cl |         |
|------|--------|--------|--------|---------|--------------------|---------|
| 2005 | 230.31 | ± 5.74 | 508.14 | ± 13.75 | 463.23             | ± 12.83 |
| 2006 | 230.27 | ± 6.22 | 505.64 | ± 13.67 | 458.31             | ± 13.64 |
| 2007 | 227.95 | ± 6.20 | 502.60 | ± 13.63 | 468.97             | ± 13.08 |
| 2008 | 225.61 | ± 6.07 | 500.15 | ± 13.51 | 470.97             | ± 13.15 |
| 2009 | 222.60 | ± 6.04 | 497.68 | ± 13.48 | 456.11             | ± 12.73 |
| 2010 | 221.03 | ± 6.00 | 495.96 | ± 13.39 | 462.15             | ± 12.77 |

|      | CCl <sub>4</sub> |        | N <sub>2</sub> O |       | CH <sub>4</sub> |        |
|------|------------------|--------|------------------|-------|-----------------|--------|
| 2005 | 103.28           | ± 2.67 | 299.0            | ± 8.0 | 1689.0          | ± 44.9 |
| 2006 | 103.56           | ± 2.87 | 298.1            | ± 8.0 | 1689.6          | ± 44.9 |
| 2007 | 100.25           | ± 2.77 | 297.9            | ± 7.9 | 1690.7          | ± 44.8 |
| 2008 | 99.20            | ± 2.72 | 296.9            | ± 7.9 | 1695.8          | ± 45.0 |
| 2009 | 98.48            | ± 2.73 | 295.5            | ± 7.9 | 1683.4          | ± 44.7 |
| 2010 | 97.52            | ± 2.67 | 298.1            | ± 7.9 | 1694.4          | ± 44.8 |

Calculations were carried out using a CFC-11 lifetime of 45 years for ease of comparison with previous studies. These lifetimes are presented in Table 7.7 (a plot of these slopes for comparison can be found in Appendix C). The final error on the calculated lifetimes is a combination of the errors from each step of the calculation. It should be noted that the errors on the lifetime (and the corrected correlations) are not symmetrical. This is because these errors represent the maximum and minimum lifetimes (corrected correlations). These were calculated by increasing and decreasing the variables by their error in order to maximise or minimise the lifetime (corrected correlation). For example the value of 1.25 was used for the width of the age-of-air spectrum in the

## Global stratospheric chlorine inventories

calculation of the corrected correlation. In literature this value varies between 0.7 and 1.75. Thus when the maxima and the minima were calculated the width of the age-of-air spectrum was varied between 0.7 and 1.75. The difference between these new values and the old value was then the maximum and minimum error related to the width of the age-of-air spectrum. This was carried out for each variable before the maximum lifetimes were combined to produce the '+' error. The '-' error came from the combination of the minimum values.

Table 7.7: The calculated lifetimes of CFC-12, CCl<sub>4</sub>, CH<sub>4</sub>, CH<sub>3</sub>Cl and N<sub>2</sub>O using a CFC-11 lifetime of 45 years. NHS = Northern Hemisphere Summer, NHW = Northern Hemisphere Winter, SHS = Southern Hemisphere Summer, SHW = Southern Hemisphere Winter

|      | Bin | CFC-12 |      |           | CH <sub>3</sub> Cl |      |            |
|------|-----|--------|------|-----------|--------------------|------|------------|
| 2005 | NHW | 107    | +(-) | 11 ( 9 )  | 123                | +(-) | 156 ( 43 ) |
|      | SHW | 87     | +(-) | 27 ( 17 ) | 34                 | +(-) | 170 ( 16 ) |
|      | NHS | 121    | +(-) | 11 ( 9 )  |                    |      | -          |
| 2006 | NHW | 89     | +(-) | 15 ( 12 ) | 48                 | +(-) | 12 ( 8 )   |
|      | SHS | 82     | +(-) | 7 ( 6 )   | 35                 | +(-) | 7 ( 5 )    |
|      | SHW | 132    | +(-) | 23 ( 18 ) | 123                | +(-) | 149 ( 44 ) |
|      | NHS | 131    | +(-) | 16 ( 13 ) |                    |      | -          |
| 2007 | NHW | 132    | +(-) | 14 ( 12 ) |                    |      | -          |
|      | SHS | 90     | +(-) | 14 ( 11 ) | 65                 | +(-) | 105 ( 25 ) |
|      | SHW | 95     | +(-) | 8 ( 7 )   | 83                 | +(-) | 72 ( 26 )  |
|      | NHS | 96     | +(-) | 6 ( 6 )   | 116                | +(-) | 103 ( 37 ) |
| 2008 | NHW | 87     | +(-) | 9 ( 8 )   | 72                 | +(-) | 40 ( 19 )  |
|      | SHS | 121    | +(-) | 15 ( 12 ) | 94                 | +(-) | 53 ( 25 )  |
|      | SHW | 121    | +(-) | 30 ( 20 ) | 83                 | +(-) | 91 ( 29 )  |
|      | NHS | 104    | +(-) | 13 ( 11 ) |                    |      | -          |
| 2009 | NHW |        |      | -         |                    |      | -          |
|      | SHS | 84     | +(-) | 29 ( 18 ) |                    |      | -          |
|      | SHW | 109    | +(-) | 7 ( 7 )   | 36                 | +(-) | 14 ( 8 )   |
|      | NHS | 150    | +(-) | 11 ( 10 ) |                    |      | -          |
| 2010 | NHW | 123    | +(-) | 19 ( 15 ) | 49                 | +(-) | 29 ( 13 )  |
|      | SHS | 96     | +(-) | 12 ( 10 ) | 70                 | +(-) | 108 ( 27 ) |
|      | SHW | 87     | +(-) | 14 ( 11 ) | 54                 | +(-) | 51 ( 18 )  |

Global stratospheric chlorine inventories

Table 7.7 Continued

| Bin  |     | CCl <sub>4</sub> |      |            | N <sub>2</sub> O |      |            |
|------|-----|------------------|------|------------|------------------|------|------------|
| 2005 | NHW | 34               | +(-) | 4 ( 3 )    |                  |      | -          |
|      | SHW | 62               | +(-) | 107 ( 24 ) | 91               | +(-) | 12 ( 10 )  |
|      | NHS | 49               | +(-) | 20 ( 11 )  | 177              | +(-) | 30 ( 22 )  |
| 2006 | NHW | 24               | +(-) | 3 ( 2 )    |                  |      | -          |
|      | SHS | 43               | +(-) | 9 ( 7 )    | 153              | +(-) | 44 ( 28 )  |
|      | SHW | 46               | +(-) | 4 ( 4 )    | 85               | +(-) | 10 ( 8 )   |
|      | NHS | 23               | +(-) | 2 ( 2 )    |                  |      | -          |
| 2007 | NHW | 41               | +(-) | 8 ( 6 )    | 180              | +(-) | 150 ( 56 ) |
|      | SHS | 46               | +(-) | 27 ( 13 )  | 118              | +(-) | 21 ( 16 )  |
|      | SHW | 35               | +(-) | 3 ( 3 )    | 99               | +(-) | 13 ( 10 )  |
|      | NHS | 30               | +(-) | 2 ( 2 )    |                  |      | -          |
| 2008 | NHW | 28               | +(-) | 2 ( 2 )    | 164              | +(-) | 24 ( 19 )  |
|      | SHS | 32               | +(-) | 4 ( 3 )    | 173              | +(-) | 30 ( 22 )  |
|      | SHW | 40               | +(-) | 3 ( 2 )    | 113              | +(-) | 16 ( 12 )  |
|      | NHS | 17               | +(-) | 4 ( 3 )    | 208              | +(-) | 143 ( 60 ) |
| 2009 | NHW |                  |      | -          |                  |      | -          |
|      | SHS | 28               | +(-) | 8 ( 5 )    | 66               | +(-) | 12 ( 9 )   |
|      | SHW | 36               | +(-) | 9 ( 6 )    | 94               | +(-) | 8 ( 7 )    |
|      | NHS | 28               | +(-) | 3 ( 3 )    | 185              | +(-) | 54 ( 34 )  |
| 2010 | NHW | 28               | +(-) | 2 ( 2 )    | 95               | +(-) | 17 ( 13 )  |
|      | SHS | 40               | +(-) | 10 ( 7 )   | 120              | +(-) | 23 ( 17 )  |
|      | SHW | 85               | +(-) | 59 ( 25 )  | 100              | +(-) | 11 ( 9 )   |

Table 7.7 Continued

| Bin  |     | CH <sub>4</sub> |      |            |
|------|-----|-----------------|------|------------|
| 2005 | NHW |                 |      | -          |
|      | SHW | 81              | +(-) | 27 ( 16 )  |
|      | NHS | 218             | +(-) | 42 ( 31 )  |
| 2006 | NHW | 196             | +(-) | 97 ( 49 )  |
|      | SHS | 308             | +(-) | 135 ( 73 ) |
|      | SHW | 157             | +(-) | 17 ( 14 )  |
|      | NHS | 241             | +(-) | 35 ( 26 )  |
| 2007 | NHW | 221             | +(-) | 72 ( 44 )  |
|      | SHS | 231             | +(-) | 50 ( 35 )  |
|      | SHW | 136             | +(-) | 19 ( 15 )  |
|      | NHS |                 |      | -          |
| 2008 | NHW | 202             | +(-) | 32 ( 22 )  |
|      | SHS |                 |      | -          |
|      | SHW | 218             | +(-) | 34 ( 23 )  |

Table 7.7 Continued

|      |     | Bin |      | CH <sub>4</sub> |        |
|------|-----|-----|------|-----------------|--------|
| 2009 | NHS | 204 | +(-) | 57              | ( 36 ) |
|      | NHW |     |      | -               |        |
|      | SHS | 89  | +(-) | 41              | ( 21 ) |
|      | SHW | 222 | +(-) | 30              | ( 21 ) |
| 2010 | NHS | 159 | +(-) | 35              | ( 24 ) |
|      | NHW | 123 | +(-) | 11              | ( 9 )  |
|      | SHS | 302 | +(-) | 159             | ( 77 ) |
|      | SHW | 211 | +(-) | 43              | ( 30 ) |

Weighted mean lifetimes were calculated for each seasonal and hemispheric combination. The means were weighted using the inverse square of the largest error on each calculated lifetime. As a measure for uncertainty, these weighted means were assigned the weighed standard deviation of the individual lifetimes. The various means and their uncertainties are shown in Table 7.8. It should be noted that, due to problems caused within the fitting program, it was only possible to produce one calculated lifetime for CH<sub>3</sub>Cl for the northern hemisphere summer. The mean lifetime reported here is therefore this calculated lifetime and associated error. As has been noted previously the errors quoted here are the statistical uncertainties of the calculated results. Whilst the mean lifetimes calculated from the northern hemisphere (NH in Table 7.8) are longer than those calculated from the southern hemisphere (SH in Table 7.8) for CFC-12, CH<sub>3</sub>Cl and N<sub>2</sub>O, they are shorter for CCl<sub>4</sub> and CH<sub>4</sub> and so it is hard to draw any solid conclusions from this fact. None of the variations between the hemispherically calculated lifetimes are larger than the combined errors on the lifetimes. Lifetimes calculated using summer data are smaller than those calculated using winter data. Once more however this is not always the case; the calculated lifetimes using winter data of both N<sub>2</sub>O and CH<sub>4</sub> are smaller than those calculated using summer data. Variation between the seasonally calculated lifetimes is in fact always smaller than the error. Horizontal mixing in the stratosphere occurs due to breaking Rossby waves found during the winter in the extra-tropical surf zone (Plumb, 2002). The

implication of this is that mixing occurs at a greater rate in the winter stratosphere than in the summer stratosphere. The mean lifetimes calculated here suggest that this phenomenon has not significantly affected our stratospheric lifetime calculations. Thus systematic hemispheric and seasonal differences are not apparent in the variations in lifetime between the individual bins, the data is thus consistent with the universality of the tracer correlations found by Volk et al. (1997) over an interval of one year.

Table 7.8: The mean lifetimes of CFC-12, CH<sub>3</sub>Cl, CCl<sub>4</sub>, N<sub>2</sub>O and CH<sub>4</sub> using a CFC-11 lifetime of 45 years. NHS = Northern Hemisphere Summer, NHW = Northern Hemisphere Winter, SHS = Southern Hemisphere Summer, SHW = Southern Hemisphere Winter, NH = Northern Hemisphere, SH = Southern Hemisphere

|          | CFC-12           |      |    |        | CH <sub>3</sub> Cl |      |     |        |
|----------|------------------|------|----|--------|--------------------|------|-----|--------|
| NHS      | 123              | +(-) | 31 | ( 21 ) | 116                | +(-) | 102 | ( 37 ) |
| NHW      | 111              | +(-) | 25 | ( 17 ) | 66                 | +(-) | 45  | ( 19 ) |
| SHS      | 97               | +(-) | 21 | ( 15 ) | 58                 | +(-) | 68  | ( 20 ) |
| SHW      | 106              | +(-) | 15 | ( 12 ) | 75                 | +(-) | 86  | ( 26 ) |
| NH       | 119              | +(-) | 29 | ( 19 ) | 74                 | +(-) | 62  | ( 23 ) |
| SH       | 103              | +(-) | 18 | ( 13 ) | 66                 | +(-) | 72  | ( 23 ) |
| Summer   | 116              | +(-) | 32 | ( 21 ) | 69                 | +(-) | 103 | ( 26 ) |
| Winter   | 108              | +(-) | 19 | ( 14 ) | 70                 | +(-) | 55  | ( 21 ) |
| All data | 113              | +(-) | 26 | ( 18 ) | 69                 | +(-) | 65  | ( 23 ) |
|          | CCl <sub>4</sub> |      |    |        | N <sub>2</sub> O   |      |     |        |
| NHS      | 28               | +(-) | 8  | ( 5 )  | 182                | +(-) | 12  | ( 10 ) |
| NHW      | 30               | +(-) | 5  | ( 4 )  | 146                | +(-) | 65  | ( 34 ) |
| SHS      | 36               | +(-) | 7  | ( 5 )  | 136                | +(-) | 68  | ( 34 ) |
| SHW      | 42               | +(-) | 8  | ( 6 )  | 97                 | +(-) | 9   | ( 8 )  |
| NH       | 29               | +(-) | 6  | ( 4 )  | 163                | +(-) | 53  | ( 32 ) |
| SH       | 41               | +(-) | 9  | ( 6 )  | 109                | +(-) | 34  | ( 21 ) |
| Summer   | 31               | +(-) | 9  | ( 6 )  | 153                | +(-) | 69  | ( 36 ) |
| Winter   | 36               | +(-) | 11 | ( 7 )  | 108                | +(-) | 31  | ( 20 ) |
| All data | 35               | +(-) | 11 | ( 7 )  | 123                | +(-) | 53  | ( 28 ) |

Table 7.8 continued

|          | CH <sub>4</sub> |      |     |        |
|----------|-----------------|------|-----|--------|
| NHS      | 218             | +(-) | 43  | ( 31 ) |
| NHW      | 161             | +(-) | 69  | ( 37 ) |
| SHS      | 253             | +(-) | 139 | ( 66 ) |
| SHW      | 189             | +(-) | 62  | ( 37 ) |
| NH       | 188             | +(-) | 76  | ( 42 ) |
| SH       | 200             | +(-) | 78  | ( 44 ) |
| Summer   | 229             | +(-) | 67  | ( 42 ) |
| Winter   | 179             | +(-) | 65  | ( 38 ) |
| All data | 195             | +(-) | 75  | ( 42 ) |

The calculated best estimates for lifetimes of CFC-12, CCl<sub>4</sub> and N<sub>2</sub>O - 113 + (-) 26 (18), 35 + (-) 11 (7) and 123 + (-) 53 (28) years respectively – are within the margin of error of the lifetimes quoted by the WMO/IPCC – 100 (Montzka et al., 2011a), 35 (Montzka et al., 2011a) and 114 (Solomon, 2007) years. The lifetime calculated for methane, of 195 + (-) 75 (42) years, is significantly larger than that calculated by (Volk et al., 1997) of  $93 \pm 18$  years. However, that latter value was derived from in situ data taken within one month and the quoted uncertainty may be an underestimate, as it does not account for the potential effect on the correlation slope of seasonal and inter-annual variations of tropospheric CH<sub>4</sub>. The stratospheric lifetime of CH<sub>3</sub>Cl of 69 + (-) 65 (23) years, reported here, represents the first calculations of the stratospheric lifetime of CH<sub>3</sub>Cl using data from a space based instrument.

An analysis of the altitude dependent systematic errors in ACE-FTS retrievals has not been carried out at this time. However, ACE-FTS occultations have been compared to data from other instruments such as the MK-IV and FIRS-2 balloon borne spectrometers (e.g. Mahieu et al., 2008). Previous validation papers for N<sub>2</sub>O, CH<sub>4</sub>, CFC-11 and CFC-12 have not shown significant altitude dependent errors for the altitude range used in this study (Mahieu et al. 2008; Velasco et al. 2011). In addition to these comparisons, the profiles of CFC-11 and CFC-12 were compared to those from the SLIMCAT 3-D Chemical

Transform Model (Brown et al., 2011). The profiles used in this work showed that, whilst there were differences in the VMR from ACE-FTS and from SLIMCAT, the overall shapes of the profiles were extremely similar. The differences between VMRs from ACE-FTS and other instruments (mentioned previously) can be used as a proxy for the systematic error, due to the fact that the full systematic errors associated with ACE-FTS retrievals are not known at this time. The methods described in this chapter have been repeated using ACE-FTS VMRs which have been modified by the differences calculated in previous validation work. The values used to modify the VMRs were + 10% for CFC-11 & CFC-12 from the validation work of Mahieu et al. (2008). Work by Velazco et al. (2011) also showed differences of + 10% for CH<sub>4</sub> and N<sub>2</sub>O. The results of the re-analysis using these errors were combined with the statistical error. The final mean lifetimes were 113 +(-) 32 (20) for CFC-12, 123 +(-) 83 (35) for N<sub>2</sub>O and 195 +(-) 139 (57) for CH<sub>4</sub>.

The remaining species, CH<sub>3</sub>Cl and CCl<sub>4</sub>, are more problematic than the other species. Previous validations of these species have shown large differences between ACE-FTS retrievals and the retrievals from other species. For example comparisons between ACE-FTS and the MK-IV instrument (Velazco et al., 2011) found differences of 30% in the VMR retrievals of CH<sub>3</sub>Cl. The errors on ACE-FTS retrievals of CCl<sub>4</sub> are estimated to be between 20 and 30% (Allen et al., 2009). The estimation of systematic errors for the CCl<sub>4</sub> retrieval is complicated by the position of the spectral feature used to retrieve CCl<sub>4</sub> VMR. There is an interfering Q-branch of CO<sub>2</sub>, the line mixing of which is not properly accounted for in the forward model. Similarly the Q-branch of CH<sub>3</sub>Cl suffers from line mixing which is not properly included in the forward model. The effects of line mixing on both of these retrievals are most serious in the troposphere, where the density of the atmosphere is at its greatest. In the stratosphere, where the density of the atmosphere is lower, line mixing becomes less of a problem within the retrieval. Quantifying the effects of line mixing on the retrieved VMR is a research project in and of itself. In this work

we have approximated the systematic errors to be - 30% for CH<sub>3</sub>Cl (Velazco et al., 2011) and + 20% for CCl<sub>4</sub> (Allen et al., 2009). Once more lifetimes were calculated using VMR which had been modified by the corresponding systematic error. The final mean lifetimes for these species were 35 +(-) 14 (8) for CCl<sub>4</sub> and 69 +(-) 2119 (34) for CH<sub>3</sub>Cl. These errors represent the best attempt to quantify the effect of systematic errors on the lifetimes of CCl<sub>4</sub> and CH<sub>3</sub>Cl. However, due to the reasons outlined previously, these errors may be different from those quoted here.

Recent model simulations have suggested CFC-11 lifetimes of between 56 and 64 years (Douglass et al., 2008), and the older value of 45 years which was used in the 2010 WMO report (Montzka et al., 2011a). Changes to the lifetime of CFC-11 would naturally have an effect on the stratospheric lifetime of atmospheric species calculated using correlations with CFC-11. For example using the range of CFC-11 lifetimes noted above produces a lifetime for CFC-12 which lies between 140 and 163 years. The ratio of the lifetime of CFC-12, CCl<sub>4</sub>, CH<sub>4</sub>, CH<sub>3</sub>Cl and N<sub>2</sub>O to CFC-11 are shown in Table 7.9. These values can be multiplied by the lifetime of CFC-11 to calculate the stratospheric lifetime of the species of interest. If the lifetime of CFC-11 is constrained further these ratios can be used to calculate new stratospheric lifetimes.

Table 7.9 The ratio of  $\tau_x/\tau_{CFC-11}$  for CFC-12, CCl<sub>4</sub>, CH<sub>4</sub>, CH<sub>3</sub>Cl and N<sub>2</sub>O

| Trace Gas          | Lifetime ratio to CFC-11 |       |      |          |
|--------------------|--------------------------|-------|------|----------|
| CFC-12             | 2.5                      | + (-) | 0.57 | ( 0.39 ) |
| CH <sub>3</sub> Cl | 1.54                     | + (-) | 1.44 | ( 0.5 )  |
| CCl <sub>4</sub>   | 0.77                     | + (-) | 0.25 | ( 0.15 ) |
| N <sub>2</sub> O   | 2.74                     | + (-) | 1.18 | ( 0.63 ) |
| CH <sub>4</sub>    | 4.33                     | + (-) | 1.66 | ( 0.94 ) |

## **7.4 Conclusion**

This chapter presents calculations for the stratospheric lifetimes of CFC-12, CCl<sub>4</sub>, CH<sub>4</sub>, CH<sub>3</sub>Cl and N<sub>2</sub>O. The calculations were carried out using measurements made by the ACE-FTS. The aim of this project was not only to calculate the stratospheric lifetimes of the species in question but also to test the assumptions which are intrinsic to these calculations. These assumptions are that there should be negligible hemispheric or seasonal dependence in the calculated lifetimes. To do this the data was divided into 24 bins representing stratospheric summer and winter in the northern and southern hemisphere for years between 2005 and 2010.

Stratospheric lifetimes were calculated using the slope of the correlation with CFC-11 at the tropopause which had to be corrected for changing atmospheric concentrations of each species. Stratospheric lifetimes were calculated using a lifetime of 45 years for CFC-11. CFC-12 and N<sub>2</sub>O are chemically inert in the troposphere and so their stratospheric lifetimes represent their atmospheric lifetimes. Calculated lifetimes showed no significant hemispheric or seasonal dependency. This suggested that for relative lifetime calculations the hemispheres are identical throughout the year. Individual lifetimes calculated for CH<sub>3</sub>Cl, N<sub>2</sub>O and CH<sub>4</sub> displayed a large spread of values (about 48 %, 30 %, and 28 % respectively), presumably in part caused by variability of their tropospheric sources affecting the flux into the stratosphere.

Weighted means were calculated by weighting the individual lifetimes by the reciprocal of the square of their error. These calculations produced values of 113 + (-) 26 (18) years (CFC-12), 35 + (-) 11 (7) years (CCl<sub>4</sub>), 195 + (-) 75 (42) years (CH<sub>4</sub>), 69 + (-) 65 (23) years (CH<sub>3</sub>Cl) and 123 + (-) 53 (28) years (N<sub>2</sub>O). The calculated lifetimes of CFC-12, CCl<sub>4</sub> and N<sub>2</sub>O are within the error margins of the lifetimes quoted by the WMO/IPCC – 100 (Montzka et al., 2011a), 35 (Montzka et al., 2011a) and 114 (Solomon, 2007) years. The lifetime calculated

## Global stratospheric chlorine inventories

for methane, of  $195 + (-) 75$  (42) years, is significantly larger than that calculated by (Volk et al., 1997) of  $93 \pm 18$  years. The altitude dependent systematic errors in ACE-FTS retrievals are not currently known at this time. An attempt has been made to estimate the effect of systematic errors on the calculated lifetimes. Lifetimes were recalculated using VMRs which had been modified to reflect differences between ACE-FTS retrieved VMRs and those from other instruments. The mean lifetimes were unaffected by these calculations, which affected the error ranges of these calculations. The results of these calculations were as follows:  $113 +(-) 32$  (20) for CFC-12,  $123 +(-) 83$  (35) for N<sub>2</sub>O,  $195 +(-) 139$  (57) for CH<sub>4</sub>,  $35 +(-) 14$  (8) for CCl<sub>4</sub> and  $69 +(-) 2119$  (34) for CH<sub>3</sub>Cl.

The lifetimes calculated in this work are relative to the lifetime of CFC-11 (45 years); thus if the lifetime of CFC-11 changes so will the lifetime of these species. The ratios between the lifetime of CFC-12, CCl<sub>4</sub>, CH<sub>4</sub>, CH<sub>3</sub>Cl and N<sub>2</sub>O and CFC-11 were also calculated allowing the results reported here to be used once the lifetime of CFC-11 has been reassessed.

# 8

## Conclusion

Climate change due to global warming, and the destruction of the ozone layer, are arguably two of the largest effects mankind has had on Earth's atmosphere. Observations of ozone loss above Antarctica forced the world's governments into action, culminating in the enacting of the Montreal Protocol. The Montreal Protocol has been extremely successful in reducing the emissions of ozone-depleting substances (ODS) [WMO, 2010]. Although, due to the long stratospheric lifetimes of ODS, ozone destruction continues, by midway through the current century (between 2040 and 2080) the mean level of global stratospheric ozone should have returned to its pre-1960 level [WMO, 2010]. In stark contrast to its reaction to ozone loss, the global reaction to climate change has been subdued. Whilst scientists around the globe continue to monitor the VMR of greenhouse gases in the atmosphere, international agreement on how to react to this phenomenon seems some way off. Understanding these challenges requires the constant monitoring of the VMR of atmospheric constituents. The work presented in this thesis represents one small part of this global monitoring program.

## Conclusion

The thesis focuses on observations of chlorine- and fluorine-containing species retrieved from atmospheric spectra taken by the ACE-FTS. ACE-FTS is the main instrument on-board the Canadian satellite SCISAT-I, which was designed to observe ozone and ozone depleting substances in the polar stratosphere. Currently 16 fluorine- and chlorine-containing species are regularly retrieved from ACE-FTS spectra. Retrievals of the atmospheric VMR of these species have been used to calculate the trends in these chlorine- and fluorine-containing species between 2004 and 2009, the total chlorine and fluorine in the stratosphere and the stratospheric lifetime of CFC-12, CCl<sub>4</sub>, CH<sub>3</sub>Cl, N<sub>2</sub>O and CH<sub>4</sub>. In this final chapter each of these projects is discussed individually, following the structure of the chapters in this thesis.

### ***8.1 Trends in atmospheric halogen containing gases since 2004***

The trends of 16 halogen-containing species: CCl<sub>4</sub>, CF<sub>4</sub>, CFC-11, CFC-12, CFC-113, CH<sub>3</sub>Cl, ClONO<sub>2</sub>, COF<sub>2</sub>, COCl<sub>2</sub>, COClF, HCFC-22, HCFC-141b, HCFC-142b, HCl, HF and SF<sub>6</sub> were calculated from retrievals made from ACE-FTS spectra. Since the majority of the transport through the tropopause occurs in the tropics, tropical data was used to analyse trends in VMR in the upper troposphere and lower stratosphere between 2004 and 2010. The results of these trends were compared to those from the SLIMCAT 3D CTM and AGAGE surface measurements.

There is generally good agreement between trends calculated from ACE-FTS data and those from ground-based instruments. The agreement between ACE-FTS and SLIMCAT is less good however, five species have differences larger than 35% (CH<sub>3</sub>Cl, COClF, HCFC-141b, HCFC-142b and HCl). The ODS banned under the Montreal Protocol (CFC-11, CFC-12, CFC-113 and CCl<sub>4</sub>)

## Conclusion

analysed in this study have decreased between 2004 and 2010. The HCFCs (which have replaced these species) have increased over this time, and appear to be increasing at a greater rate than the decrease in CFCs. These changes in VMR have led to an increase in HF (which is produced by the decomposition of fluorine-containing species) and a decrease in HCl (which is produced by the decomposition of chlorine-containing species). These results illustrate the success of the Montreal Protocol in reducing ozone depleting substances. Chlorine-containing species continue to be phased out and replaced by fluorine-containing molecules; it is unlikely that total atmospheric fluorine will decrease in the near future.

This work revealed a problem in the retrieved profiles of CFC-113, HCFC-22, HCFC-141b and HCFC-142b. These atmospheric profiles exhibit an unphysical increasing VMR with increasing altitude in the troposphere. These species are not formed at higher altitudes and so these profiles cannot be correct. In subsequent work the ACE-FTS retrievals of CFC-113, HCFC-141b and HCFC-142b were no longer used due to these unphysical features. A new research retrieval was produced for HCFC-22 following this work which did not produce these unphysical profiles. Since the effects of this retrieval problem are systematic and are not related to the year in which the occultations were made it is still possible to compare the trends calculated from these data.

The calculated trends for chlorine nitrate seem to exhibit some diurnal dependency. Morning occultations show an increasing trend in VMR whilst evening occultations show a decreasing VMR. The reason for this difference is not currently understood. However, subsequent work by Mahieu et al. (2013) has shown an increasing trend in partial column measurements of HCl after 2008. An increasing trend in the VMR of chlorine reservoir species observed by two separate investigations is of importance since the source species appear to have decreased during this time. Work is currently on going to explain these observations.

## ***8.2 Global stratospheric fluorine inventories for 2004 to 2009***

The total VMR of stratospheric fluorine have been calculated for the years between 2004 and 2009 in the following latitudes bands: 70° N - 30° N, 30° N - 00° N, 00° N - 30° S, and 30° S - 70° S. These latitude bands were chosen to represent the extra-tropical and tropical latitudes in the Northern and Southern hemisphere stratosphere. ACE-FTS data, supplemented with output from the SLIMCAT 3D chemical transport model, were used to calculate the total fluorine budgets. The results presented in this thesis, represent the most comprehensive fluorine budget to date. In total 18 fluorine-containing species were used in this study: CF<sub>4</sub>, CFC-12, CFC-11, COF<sub>2</sub>, COClF, HCFC-22, HF and SF<sub>6</sub> from ACE-FTS, CFC-113, CFC-114, CFC-115, H-1211, H-1301, HCFC-141b, HCFC-142b, HFC-23, HFC-134a and HFC-152a from SLIMCAT. The majority of the major fluorine-containing species currently in the atmosphere are included. At lower altitudes these budgets are dominated by CFC-12; despite the reduction in the VMR of CFC-12 during the time period studied by this work. As altitude increases, HF overtakes CFC-12 as the most dominant species in the total fluorine budget.

The long-term changes in the VMR of total fluorine in the stratosphere have been demonstrated using two separate methods. The first used the slope of the total fluorine profile. All budgets exhibit a negative slope with altitude which is produced by a decreasing total fluorine VMR with altitude. The second method used a least-squares fit to the mean stratospheric total fluorine VMR for each year in the study. Whilst the first method simply indicated whether stratospheric fluorine was increasing or decreasing with time, the second produced a numerical value for this trend. These complementary methods have both indicated that whilst stratospheric fluorine is increasing in all latitude bands, the largest increases are seen in the tropical stratosphere. In addition to this trend, the changes in the total tropospheric fluorine, weighted

## Conclusion

by the GWPs and the RE of the individual species used in this study, have been produced. These values are of particular importance since each species used in this study has a unique GWP and RE. The trend allows the climatological implication of the increase in fluorine between 2004 and 2009 and into the future to be quantified. There was an increase in the RE-weighted fluorine during this time; however over the longer term GWP-weighted fluorine does not change significantly. This is caused by the replacement of CFCs and halons, which have long lifetimes, with HFCs and HCFCs which have significantly shorter lifetimes. This reduces the long term effect of fluorine containing species. The decrease in species prohibited by the Montreal Protocol also appears to be limiting the climatological effects of the general increase in the VMR of total fluorine-containing species during this time. Trends calculated without CFCs and Halons included show a strong increase in GWP- and RE-weighted fluorine during this time. However, when CFCs and Halons are included these trends decrease significantly. These results suggest that the Montreal Protocol has had a positive impact on reducing the effects of greenhouse gases.

### ***8.3 Global stratospheric chlorine inventories for 2004 to 2009***

This work was a companion piece to the stratospheric fluorine inventories. In this work chlorine budgets were calculated between 2004 and 2009 for the latitude bands used in the fluorine budget (70°N-30°N, 30°N-00°N, 00°N-30°S, and 30°S-70°S). Chlorine budget calculations were carried out using ACE-FTS version 3.0 retrievals of 9 chlorine-containing species: CCl<sub>4</sub>, CFC-12, CFC-11, COCl<sub>2</sub>, COClF, HCFC-22, CH<sub>3</sub>Cl, HCl and ClONO<sub>2</sub>. These species were supplemented with data for the following species from the SLIMCAT 3D chemical transport model: CFC-113, CFC-114, CFC-115, H-1211, H-1301,

## Conclusion

HCFC-141b, HCFC-142b, ClO and HOCl. At lower altitudes the total chlorine profiles are dominated by CFCs; as altitude increases, HCl rapidly dominates the chlorine budget.

In a similar manner to the fluorine budget, the trends in the VMR of total stratospheric chlorine were calculated using both the slope of the profiles and the mean total stratospheric chlorine VMR. All total chlorine profiles exhibit a positive slope with altitude suggests that the stratospheric VMR of chlorine has decreased during this time. The time series of the mean stratospheric total chlorine budgets supports this conclusion. All latitudes exhibit decreasing VMRs of total stratospheric chlorine during this time. This is in line with decreases in individual chlorine-containing species due to their prohibition under the Montreal Protocol.

The ODP, RE and GWP weighted trends in VMR of the total tropospheric chlorine were calculated. These values were weighted using the individual ODP, RE or GWP of each species used in this study. These values have allowed the impact of the Montreal Protocol on the climate and ozone depletion during this time to be quantified. Whilst RE-weighted chlorine, which represents changes in radiative effect between 2004 and 2009, showed very little change, GWP-weighted chlorine is decreasing in all latitude bands. . In the short term the decrease in chlorine containing species has had little effect on the climate, but on a 20-year horizon, decreases in CFCs and halons will reduce the climatological effects of chlorine containing species. The success of the Montreal Protocol in decreasing the emissions of chlorine-containing species has been widely discussed, and this work offers further evidence of this success. ODP-weighted chlorine is decreasing in all bands with the fastest rate in the Southern Hemisphere extra-tropical latitude band. The Montreal Protocol has not only been successful in reducing the VMR of total stratospheric chlorine, it has also been inadvertently successful in reducing the

## Conclusion

VMR of GWP-weighted chlorine. These results offer further evidence for the success of the Montreal Protocol in reducing the effects of climate change.

### ***8.4 Stratospheric lifetimes of CFC-12, CCl<sub>4</sub>, CH<sub>4</sub>, CH<sub>3</sub>Cl and N<sub>2</sub>O***

New stratospheric lifetimes of CFC-12, CCl<sub>4</sub>, CH<sub>4</sub>, CH<sub>3</sub>Cl and N<sub>2</sub>O have been calculated using measurements made by the ACE-FTS. These values were calculated using the slopes of the correlations of these species with CFC-11 at the tropopause. This work has helped test the assumptions which are intrinsic to these calculations: (1) there should be no hemispheric dependence in the calculated lifetimes. (2) there should be no seasonal dependence in the calculated lifetimes.

For ease of comparison with other studies, stratospheric lifetimes were calculated using a lifetime of 45 years for CFC-11. There were no significant seasonal or hemispheric dependencies shown by the calculated lifetimes, proving the assumptions given above are correct. The calculated lifetimes for CH<sub>3</sub>Cl and CH<sub>4</sub> exhibited a large spread of values, unlike the lifetimes of the other species. The method used to calculate the stratospheric lifetimes described in this paper relies on both correlating species having the same main stratospheric sink. In this case it is likely that the reactions of these species with OH are a more important sink for the species than photolysis.

The calculated lifetimes of CFC-12, CCl<sub>4</sub> and N<sub>2</sub>O are within error of the lifetimes quoted by the WMO (Montzka et al., 2011a) and IPCC (Solomon, 2007) reports. However, the lifetime calculated for methane is significantly larger than that calculated by Volk et al. (1997). Since these lifetimes were calculated relative to the lifetime of CFC-11 (45 years), any change to the accepted lifetime of CFC-11 will, in turn, change the lifetime of these species.

## Conclusion

The ratios between the lifetime of CFC-12, CCl<sub>4</sub>, CH<sub>4</sub>, CH<sub>3</sub>Cl and N<sub>2</sub>O and CFC-11 were also calculated. This will allow the results calculated by this work to be used once the lifetime of CFC-11 has been reassessed.

## ***8.5 Future Work***

The most important areas for future work identified by the research presented in this thesis. The first is specific to the systematic errors in the ACE-FTS retrieval process and the second is an issue for the larger atmospheric science community,

As has been discussed in Section 3.2.4, systematic errors are altitude dependent. Accurately correcting profiles for these errors therefore requires that the full systematic error budget is known. This work highlights the need for a comprehensive systematic error budget for each species retrieved from ACE-FTS spectra. It is a common criticism of ACE-FTS data by reviewers and more importantly it would allow full error budgets which included both statistical and systematic errors to be calculated. This would better constrain the lifetimes calculated using the tracer-tracer correlations from ACE-FTS data.

Chapter 7 highlights the need for the atmospheric community to better establish the lifetime of CFC-11 allowing it to become a better reference for calculated lifetimes. Accurate simulations of the ozone recovery require that the lifetime of CFC-11 and the other ODS be accurately known. Whilst large uncertainties surround these values it is very difficult to accurately predict when ozone recovery will occur.

Each chapter of this work offers significant potential for future work. The future work leading from each chapter will now be discussed individually.

### **8.5.1 Trends in atmospheric halogen containing gases since 2004**

Chapter 4 is merely a preliminary report on more extensive analyses of individual species in the future. Whilst ACE-FTS continues to function, it will be possible to calculate the longer-term trend in these species. Long-term trends from a single instrument are important since they do not require normalisation against another as calculating a trend from two separate instruments would. Further chlorine- and fluorine-containing species are being routinely retrieved from ACE-FTS spectra allowing future projects to analyse the trends in a larger number of these species. This will allow the effectiveness of the Montreal Protocol in reducing the emissions of chlorine to be more fully analysed. It will also be possible to analyse the effects of the decrease in the emissions of these species on the emissions of the replacement species such as HFCs and HCFCs. More generally, within the next decade HCFCs will have been phased out in most developed nations. Thus, trends in the atmospheric VMR of HCFCs (from both space- and ground-based instruments) will have an added importance in assessing the effects of the Montreal Protocol.

### **8.5.2 Global stratospheric fluorine inventories**

Currently, many additional fluorine-containing species are being added to the stable of molecules which are retrieved from ACE-FTS spectra, including HFCs. Additionally, work is on-going to improve the retrieval of many species such as HCFC-141b, HCFC-142b and HFC-23. Due to problems with the retrieval, ACE-FTS measurements of these species were not used in the fluorine budget presented in this thesis, instead output from SLIMCAT was required. These developments will allow future fluorine budgets to be calculated using a wider range of measurements. This will reduce the need for model output, which may be susceptible to slight errors in both the transport and chemistry of the stratosphere. Finally, there were known problems with

## Conclusion

the retrieved VMR of all species after September 2010. Version 4, which will be released shortly, of the ACE-FTS data rectifies this problem. This will allow the changes in total fluorine to be calculated over a significantly longer time period.

### **8.5.3 Global stratospheric chlorine inventories**

As with the other work presented in this thesis, the addition of further chlorine-containing species (such as ClO) will further enhance future chlorine budgets. In particular an ACE-FTS retrieval of ClO would significantly reduce the problems encountered when adapting SLIMCAT output for ACE-FTS measurement times. Work is currently on-going on improved CH<sub>3</sub>Cl, HCFC-141b, HCFC-142b retrievals which will reduce the dependency of this work on model output. In a similar manner to the fluorine budget, the longer ACE-FTS is operational, the longer the time period over which trends in total stratospheric chlorine can be observed.

### **8.5.4 Stratospheric lifetimes of CFC-12, CCl<sub>4</sub>, CH<sub>4</sub>, CH<sub>3</sub>Cl and N<sub>2</sub>O**

Improvements in the ACE-FTS retrievals of HCFC-22, HCFC-141b & HCFC-142b will allow the relative stratospheric lifetimes of these species to be calculated. ACE-FTS data is ideally placed to carry out this work as it has a large number of widely distributed data, ensuring that it is not susceptible to small-scale metrological events which may increase the transport of species across the tropopause. Additionally ACE-FTS data has sufficiently high vertical resolution to allow the calculation of the slope of the correlation at the tropopause. Thus in future ACE-FTS retrievals will continue to be invaluable to stratospheric lifetime calculations.

It would be extremely useful for future analysis if profiles which were affected by clouds, dust and aerosols could be flagged in the retrieval phase. This would

## Conclusion

allow these points to be removed from the profiles without the need for MAD filtering; once more this would allow more accurate error budgets to be calculated as the standard deviation would truly represent the standard deviation of all of the data.

## ***8.6 Final Thoughts***

The work presented in this thesis has focused on gases, the atmospheric VMR of which have been directly affected by the Montreal Protocol. Every four years the international community, in the guise of the World Meteorological Organisation, reports on the latest observations of the ozone layer and ODS. These reports assess the success of the Montreal Protocol in reducing both ozone loss and the atmospheric VMR of ODS. The next report is due in 2014 and the bulk of the work reported in this thesis is to be included in the report. The work on the stratospheric lifetimes of CFC-12, CCl<sub>4</sub>, CH<sub>4</sub>, CH<sub>3</sub>Cl and N<sub>2</sub>O has been included in chapter 4 of the SPARC science report on the lifetime of halogen source gases. The work presented here will feed back into the global monitoring of these species and will influence future studies and legislation within this field.

# Appendix A

## *Fluorine Budgets*

Table A1: The percentage contribution of HF, CF<sub>4</sub>, CFC-12, CFC-11, COF<sub>2</sub>, COClF, HCFC-22, SF<sub>6</sub> & CFC-113 to the total fluorine budget in the latitude bands between 70° N and 30° N

| Altitude | HF   | CF <sub>4</sub> | CFC-12 | CFC-11 | COF <sub>2</sub> | COClF | HCFC-22 | SF <sub>6</sub> | CFC-113 |
|----------|------|-----------------|--------|--------|------------------|-------|---------|-----------------|---------|
| 10.5     | 1.2  | 11.3            | 38.9   | 8.9    | 0.7              | 0.2   | 14.4    | 1.3             | 8.5     |
| 11.5     | 2.2  | 11.3            | 38.5   | 8.6    | 1.3              | 0.4   | 14.2    | 1.3             | 8.2     |
| 12.5     | 3.1  | 11.4            | 38.1   | 8.3    | 1.8              | 0.5   | 14.1    | 1.3             | 7.9     |
| 13.5     | 3.9  | 11.4            | 37.5   | 8.1    | 2.1              | 0.6   | 14.3    | 1.3             | 7.7     |
| 14.5     | 4.9  | 11.4            | 36.9   | 7.8    | 2.4              | 0.6   | 14.3    | 1.3             | 7.4     |
| 15.5     | 6.2  | 11.4            | 36.1   | 7.3    | 3.1              | 0.7   | 14.1    | 1.3             | 7.2     |
| 16.5     | 8.3  | 11.5            | 34.9   | 6.6    | 4.1              | 0.9   | 13.4    | 1.3             | 6.8     |
| 17.5     | 11.1 | 11.6            | 33.0   | 5.8    | 5.6              | 1.1   | 12.5    | 1.3             | 6.3     |
| 18.5     | 14.5 | 11.7            | 30.8   | 4.8    | 7.3              | 1.4   | 11.8    | 1.3             | 5.6     |
| 19.5     | 18.0 | 11.7            | 28.3   | 3.7    | 9.0              | 1.6   | 11.3    | 1.3             | 5.0     |
| 20.5     | 21.6 | 11.8            | 25.8   | 2.6    | 10.6             | 1.7   | 10.7    | 1.2             | 4.4     |
| 21.5     | 24.9 | 11.7            | 23.2   | 1.7    | 12.3             | 1.8   | 10.2    | 1.2             | 3.9     |
| 22.5     | 27.9 | 11.7            | 20.7   | 1.1    | 13.7             | 1.7   | 9.8     | 1.2             | 3.4     |
| 23.5     | 30.8 | 11.6            | 18.4   | 0.7    | 15.1             | 1.5   | 9.5     | 1.2             | 2.9     |
| 24.5     | 33.6 | 11.6            | 16.0   | 0.4    | 16.3             | 1.3   | 9.1     | 1.2             | 2.4     |
| 25.5     | 36.6 | 11.5            | 13.7   | 0.2    | 17.2             | 1.0   | 8.8     | 1.2             | 2.0     |
| 26.5     | 39.6 | 11.5            | 11.4   | 0.1    | 18.0             | 0.8   | 8.4     | 1.2             | 1.6     |
| 27.5     | 42.8 | 11.5            | 9.2    | 0.1    | 18.4             | 0.6   | 8.0     | 1.2             | 1.2     |
| 28.5     | 45.9 | 11.4            | 7.2    | 0.0    | 18.5             | 0.4   | 7.7     | 1.2             | 0.9     |

## Appendix A – Contributions of species to the fluorine budgets

Table A1 Continued

| Altitude | HF   | CF <sub>4</sub> | CFC-<br>12 | CFC-<br>11 | COF <sub>2</sub> | COCIF | HCFC-<br>22 | SF <sub>6</sub> | CFC-<br>113 |
|----------|------|-----------------|------------|------------|------------------|-------|-------------|-----------------|-------------|
| 29.5     | 49.0 | 11.4            | 5.7        | 0.0        | 18.1             | 0.3   | 7.3         | 1.2             | 0.7         |
| 30.5     | 52.0 | 11.4            | 4.3        | 0.0        | 17.5             | 0.2   | 6.9         | 1.2             | 0.5         |
| 31.5     | 54.7 | 11.5            | 3.2        | 0.0        | 16.5             | 0.1   | 6.6         | 1.2             | 0.3         |
| 32.5     | 57.1 | 11.5            | 2.4        | 0.0        | 15.7             | 0.1   | 6.3         | 1.2             | 0.2         |
| 33.5     | 59.2 | 11.5            | 1.7        | 0.0        | 14.8             | 0.0   | 6.0         | 1.2             | 0.1         |
| 34.5     | 60.8 | 11.5            | 1.2        | 0.0        | 14.1             | 0.0   | 5.7         | 1.2             | 0.1         |
| 35.5     | 62.3 | 11.5            | 0.9        | 0.0        | 13.3             | 0.0   | 5.5         | 1.2             | 0.1         |
| 36.5     | 63.6 | 11.5            | 0.6        | 0.0        | 12.6             | 0.0   | 5.3         | 1.2             | 0.0         |
| 37.5     | 64.7 | 11.5            | 0.4        | 0.0        | 11.9             | 0.0   | 5.2         | 1.2             | 0.0         |
| 38.5     | 65.8 | 11.5            | 0.3        | 0.0        | 11.2             | 0.0   | 5.0         | 1.2             | 0.0         |
| 39.5     | 66.8 | 11.5            | 0.2        | 0.0        | 10.6             | 0.0   | 4.8         | 1.2             | 0.0         |
| 40.5     | 67.7 | 11.5            | 0.2        | 0.0        | 10.0             | 0.0   | 4.7         | 1.2             | 0.0         |
| 41.5     | 68.6 | 11.6            | 0.1        | 0.0        | 9.3              | 0.0   | 4.5         | 1.2             | 0.0         |
| 42.5     | 69.4 | 11.6            | 0.1        | 0.0        | 8.7              | 0.0   | 4.3         | 1.2             | 0.0         |
| 43.5     | 70.3 | 11.7            | 0.1        | 0.0        | 8.1              | 0.0   | 4.2         | 1.2             | 0.0         |
| 44.5     | 71.3 | 11.7            | 0.0        | 0.0        | 7.4              | 0.0   | 4.0         | 1.2             | 0.0         |
| 45.5     | 72.2 | 11.7            | 0.0        | 0.0        | 6.7              | 0.0   | 3.8         | 1.2             | 0.0         |
| 46.5     | 73.2 | 11.6            | 0.0        | 0.0        | 6.1              | 0.0   | 3.7         | 1.2             | 0.0         |
| 47.5     | 74.1 | 11.6            | 0.0        | 0.0        | 5.5              | 0.0   | 3.5         | 1.2             | 0.0         |
| 48.5     | 75.0 | 11.5            | 0.0        | 0.0        | 5.0              | 0.0   | 3.4         | 1.2             | 0.0         |
| 49.5     | 75.8 | 11.5            | 0.0        | 0.0        | 4.4              | 0.0   | 3.2         | 1.2             | 0.0         |
| 50.5     | 76.3 | 11.5            | 0.0        | 0.0        | 4.0              | 0.0   | 3.1         | 1.2             | 0.0         |
| 51.5     | 76.7 | 11.5            | 0.0        | 0.0        | 3.7              | 0.0   | 3.1         | 1.2             | 0.0         |
| 52.5     | 77.0 | 11.6            | 0.0        | 0.0        | 3.5              | 0.0   | 3.0         | 1.2             | 0.0         |
| 53.5     | 77.3 | 11.6            | 0.0        | 0.0        | 3.3              | 0.0   | 2.9         | 1.2             | 0.0         |

Appendix A – Contributions of species to the fluorine budgets

Table A2: The percentage contribution of CFC-114, CFC-115, HCFC-142b, HCFC-141b, HFC-23, HFC-134a, HFC-152a, H-1211 & H-1301 to the total fluorine budget in the latitude bands between 70° N and 30° N

| Altitude | CFC-114 | CFC-115 | HCFC-142b | HCFC-141b | HFC-23 | HFC-134a | HFC-152a | H-1211 | H-1301 |
|----------|---------|---------|-----------|-----------|--------|----------|----------|--------|--------|
| 10.5     | 2.5     | 1.7     | 1.2       | 0.7       | 2.1    | 5.4      | 0.3      | 0.3    | 0.4    |
| 11.5     | 2.4     | 1.7     | 1.1       | 0.6       | 2.1    | 5.1      | 0.3      | 0.3    | 0.4    |
| 12.5     | 2.4     | 1.7     | 1.1       | 0.6       | 2.1    | 4.9      | 0.3      | 0.2    | 0.4    |
| 13.5     | 2.3     | 1.7     | 1.1       | 0.6       | 2.0    | 4.8      | 0.2      | 0.2    | 0.4    |
| 14.5     | 2.3     | 1.7     | 1.0       | 0.6       | 2.0    | 4.6      | 0.2      | 0.2    | 0.3    |
| 15.5     | 2.2     | 1.7     | 1.0       | 0.5       | 2.0    | 4.5      | 0.2      | 0.2    | 0.3    |
| 16.5     | 2.2     | 1.6     | 1.0       | 0.5       | 2.0    | 4.3      | 0.2      | 0.2    | 0.3    |
| 17.5     | 2.1     | 1.6     | 0.9       | 0.4       | 1.9    | 4.0      | 0.2      | 0.1    | 0.3    |
| 18.5     | 2.0     | 1.6     | 0.9       | 0.4       | 1.9    | 3.6      | 0.2      | 0.1    | 0.2    |
| 19.5     | 1.8     | 1.6     | 0.8       | 0.3       | 1.9    | 3.3      | 0.1      | 0.1    | 0.2    |
| 20.5     | 1.7     | 1.5     | 0.8       | 0.3       | 1.8    | 3.1      | 0.1      | 0.0    | 0.2    |
| 21.5     | 1.6     | 1.5     | 0.7       | 0.2       | 1.8    | 2.9      | 0.1      | 0.0    | 0.1    |
| 22.5     | 1.5     | 1.5     | 0.7       | 0.2       | 1.8    | 2.8      | 0.1      | 0.0    | 0.1    |
| 23.5     | 1.5     | 1.4     | 0.7       | 0.2       | 1.8    | 2.7      | 0.1      | 0.0    | 0.1    |
| 24.5     | 1.4     | 1.4     | 0.6       | 0.1       | 1.7    | 2.6      | 0.1      | 0.0    | 0.1    |
| 25.5     | 1.3     | 1.4     | 0.6       | 0.1       | 1.7    | 2.5      | 0.1      | 0.0    | 0.0    |
| 26.5     | 1.2     | 1.4     | 0.6       | 0.1       | 1.7    | 2.4      | 0.1      | 0.0    | 0.0    |
| 27.5     | 1.1     | 1.3     | 0.5       | 0.1       | 1.7    | 2.3      | 0.0      | 0.0    | 0.0    |
| 28.5     | 1.0     | 1.3     | 0.5       | 0.0       | 1.7    | 2.2      | 0.0      | 0.0    | 0.0    |
| 29.5     | 0.9     | 1.3     | 0.4       | 0.0       | 1.6    | 2.1      | 0.0      | 0.0    | 0.0    |
| 30.5     | 0.8     | 1.3     | 0.4       | 0.0       | 1.6    | 2.0      | 0.0      | 0.0    | 0.0    |
| 31.5     | 0.7     | 1.2     | 0.4       | 0.0       | 1.6    | 1.9      | 0.0      | 0.0    | 0.0    |
| 32.5     | 0.7     | 1.2     | 0.4       | 0.0       | 1.6    | 1.8      | 0.0      | 0.0    | 0.0    |
| 33.5     | 0.6     | 1.2     | 0.3       | 0.0       | 1.6    | 1.8      | 0.0      | 0.0    | 0.0    |

Appendix A – Contributions of species to the fluorine budgets

Table A2 Continued

| Altitude | CFC-114 | CFC-115 | HCFC-142b | HCFC-141b | HFC-23 | HFC-134a | HFC-152a | H-1211 | H-1301 |
|----------|---------|---------|-----------|-----------|--------|----------|----------|--------|--------|
| 34.5     | 0.6     | 1.2     | 0.3       | 0.0       | 1.6    | 1.7      | 0.0      | 0.0    | 0.0    |
| 35.5     | 0.5     | 1.2     | 0.3       | 0.0       | 1.6    | 1.6      | 0.0      | 0.0    | 0.0    |
| 36.5     | 0.5     | 1.2     | 0.3       | 0.0       | 1.6    | 1.6      | 0.0      | 0.0    | 0.0    |
| 37.5     | 0.5     | 1.2     | 0.3       | 0.0       | 1.6    | 1.6      | 0.0      | 0.0    | 0.0    |
| 38.5     | 0.4     | 1.1     | 0.3       | 0.0       | 1.6    | 1.5      | 0.0      | 0.0    | 0.0    |
| 39.5     | 0.4     | 1.1     | 0.2       | 0.0       | 1.6    | 1.5      | 0.0      | 0.0    | 0.0    |
| 40.5     | 0.4     | 1.1     | 0.2       | 0.0       | 1.6    | 1.4      | 0.0      | 0.0    | 0.0    |
| 41.5     | 0.4     | 1.1     | 0.2       | 0.0       | 1.6    | 1.4      | 0.0      | 0.0    | 0.0    |
| 42.5     | 0.3     | 1.1     | 0.2       | 0.0       | 1.6    | 1.4      | 0.0      | 0.0    | 0.0    |
| 43.5     | 0.3     | 1.1     | 0.2       | 0.0       | 1.6    | 1.3      | 0.0      | 0.0    | 0.0    |
| 44.5     | 0.3     | 1.1     | 0.2       | 0.0       | 1.6    | 1.3      | 0.0      | 0.0    | 0.0    |
| 45.5     | 0.3     | 1.1     | 0.2       | 0.0       | 1.6    | 1.3      | 0.0      | 0.0    | 0.0    |
| 46.5     | 0.2     | 1.1     | 0.2       | 0.0       | 1.6    | 1.2      | 0.0      | 0.0    | 0.0    |
| 47.5     | 0.2     | 1.0     | 0.1       | 0.0       | 1.6    | 1.2      | 0.0      | 0.0    | 0.0    |
| 48.5     | 0.2     | 1.0     | 0.1       | 0.0       | 1.5    | 1.1      | 0.0      | 0.0    | 0.0    |
| 49.5     | 0.2     | 1.0     | 0.1       | 0.0       | 1.5    | 1.1      | 0.0      | 0.0    | 0.0    |
| 50.5     | 0.1     | 1.0     | 0.1       | 0.0       | 1.5    | 1.1      | 0.0      | 0.0    | 0.0    |
| 51.5     | 0.1     | 1.0     | 0.1       | 0.0       | 1.5    | 1.1      | 0.0      | 0.0    | 0.0    |
| 52.5     | 0.1     | 1.0     | 0.1       | 0.0       | 1.5    | 1.0      | 0.0      | 0.0    | 0.0    |
| 53.5     | 0.1     | 1.0     | 0.1       | 0.0       | 1.5    | 1.0      | 0.0      | 0.0    | 0.0    |

Appendix A – Contributions of species to the fluorine budgets

Table A3: The percentage contribution of HF, CF<sub>4</sub>, CFC-12, CFC-11, COF<sub>2</sub>, COClF, HCFC-22, SF<sub>6</sub> & CFC-113 to the total fluorine budget in the latitude bands between 30° N and 0° N

| Altitude | HF    | CF <sub>4</sub> | CFC-12 | CFC-11 | COF <sub>2</sub> | COClF | HCFC-22 | SF <sub>6</sub> | CFC-113 |
|----------|-------|-----------------|--------|--------|------------------|-------|---------|-----------------|---------|
| 10.5     | 0.00  | 11.10           | 39.18  | 9.40   | 0.02             | 0.02  | 15.31   | 1.35            | 8.67    |
| 11.5     | 0.00  | 11.10           | 39.19  | 9.40   | 0.03             | 0.02  | 15.31   | 1.35            | 8.67    |
| 12.5     | 0.00  | 11.11           | 39.21  | 9.40   | 0.04             | 0.02  | 15.32   | 1.36            | 8.64    |
| 13.5     | 0.00  | 11.12           | 39.25  | 9.41   | 0.07             | 0.04  | 15.34   | 1.36            | 8.61    |
| 14.5     | 0.05  | 11.13           | 39.28  | 9.42   | 0.09             | 0.05  | 15.35   | 1.36            | 8.57    |
| 15.5     | 0.17  | 11.16           | 39.26  | 9.45   | 0.13             | 0.07  | 15.29   | 1.35            | 8.53    |
| 16.5     | 0.34  | 11.24           | 39.45  | 9.34   | 0.19             | 0.10  | 15.06   | 1.36            | 8.46    |
| 17.5     | 0.79  | 11.29           | 39.37  | 9.16   | 0.47             | 0.19  | 14.92   | 1.37            | 8.30    |
| 18.5     | 1.84  | 11.31           | 38.59  | 8.64   | 1.06             | 0.38  | 15.23   | 1.35            | 7.97    |
| 19.5     | 3.37  | 11.38           | 37.56  | 8.01   | 1.98             | 0.75  | 15.08   | 1.32            | 7.54    |
| 20.5     | 5.45  | 11.57           | 36.56  | 7.27   | 3.20             | 1.20  | 13.66   | 1.31            | 7.20    |
| 21.5     | 7.51  | 11.64           | 35.30  | 6.36   | 4.40             | 1.63  | 12.82   | 1.30            | 6.87    |
| 22.5     | 9.25  | 11.67           | 34.07  | 5.37   | 5.75             | 2.08  | 12.15   | 1.30            | 6.54    |
| 23.5     | 10.85 | 11.72           | 32.69  | 4.35   | 7.12             | 2.49  | 11.75   | 1.30            | 6.21    |
| 24.5     | 12.20 | 11.83           | 31.34  | 3.29   | 8.67             | 2.79  | 11.35   | 1.31            | 5.89    |
| 25.5     | 14.14 | 11.85           | 29.50  | 2.38   | 10.22            | 3.01  | 11.06   | 1.31            | 5.47    |
| 26.5     | 15.96 | 11.85           | 27.68  | 1.62   | 11.99            | 3.04  | 10.85   | 1.31            | 4.95    |
| 27.5     | 17.57 | 11.93           | 25.86  | 1.00   | 14.16            | 2.73  | 10.64   | 1.32            | 4.32    |
| 28.5     | 19.63 | 11.92           | 23.76  | 0.51   | 16.55            | 2.21  | 10.34   | 1.31            | 3.68    |
| 29.5     | 22.16 | 11.84           | 21.49  | 0.30   | 18.54            | 1.63  | 9.96    | 1.30            | 3.06    |
| 30.5     | 25.10 | 11.85           | 18.83  | 0.11   | 20.12            | 1.13  | 9.70    | 1.30            | 2.48    |
| 31.5     | 28.34 | 11.92           | 15.85  | 0.03   | 21.51            | 0.34  | 9.50    | 1.31            | 2.01    |
| 32.5     | 31.41 | 11.91           | 12.81  | 0.02   | 22.65            | 0.23  | 9.20    | 1.32            | 1.56    |
| 33.5     | 34.39 | 11.93           | 9.87   | 0.01   | 23.66            | 0.12  | 8.93    | 1.32            | 1.13    |

Appendix A – Contributions of species to the fluorine budgets

Table A3 Continued

| Altitude | HF    | CF <sub>4</sub> | CFC-<br>12 | CFC-<br>11 | COF <sub>2</sub> | COCIF | HCFC-<br>22 | SF <sub>6</sub> | CFC-<br>113 |
|----------|-------|-----------------|------------|------------|------------------|-------|-------------|-----------------|-------------|
| 34.5     | 37.00 | 11.87           | 7.65       | 0.01       | 24.39            | 0.08  | 8.55        | 1.32            | 0.83        |
| 35.5     | 39.68 | 11.90           | 5.51       | 0.00       | 24.75            | 0.04  | 8.21        | 1.32            | 0.56        |
| 36.5     | 42.27 | 11.94           | 3.88       | 0.00       | 24.77            | 0.02  | 7.77        | 1.32            | 0.36        |
| 37.5     | 45.17 | 11.91           | 2.72       | 0.00       | 24.04            | 0.01  | 7.28        | 1.32            | 0.24        |
| 38.5     | 48.30 | 11.87           | 1.66       | 0.00       | 22.92            | 0.01  | 6.83        | 1.32            | 0.13        |
| 39.5     | 50.70 | 11.87           | 1.20       | 0.00       | 21.62            | 0.00  | 6.48        | 1.32            | 0.09        |
| 40.5     | 53.16 | 11.82           | 0.81       | 0.00       | 20.24            | 0.00  | 6.13        | 1.32            | 0.06        |
| 41.5     | 55.56 | 11.86           | 0.51       | 0.00       | 18.62            | 0.00  | 5.83        | 1.33            | 0.03        |
| 42.5     | 57.47 | 11.90           | 0.38       | 0.00       | 17.25            | 0.00  | 5.57        | 1.34            | 0.02        |
| 43.5     | 59.32 | 12.01           | 0.25       | 0.00       | 15.86            | 0.00  | 5.31        | 1.34            | 0.01        |
| 44.5     | 61.28 | 12.12           | 0.17       | 0.00       | 14.34            | 0.00  | 5.03        | 1.35            | 0.01        |
| 45.5     | 63.27 | 12.18           | 0.11       | 0.00       | 12.84            | 0.00  | 4.74        | 1.35            | 0.01        |
| 46.5     | 65.37 | 12.17           | 0.06       | 0.00       | 11.31            | 0.00  | 4.44        | 1.35            | 0.00        |
| 47.5     | 67.23 | 12.12           | 0.03       | 0.00       | 10.01            | 0.00  | 4.17        | 1.34            | 0.00        |
| 48.5     | 69.01 | 12.00           | 0.02       | 0.00       | 8.85             | 0.00  | 3.91        | 1.33            | 0.00        |
| 49.5     | 70.78 | 11.87           | 0.02       | 0.00       | 7.72             | 0.00  | 3.64        | 1.32            | 0.00        |
| 50.5     | 72.17 | 11.85           | 0.01       | 0.00       | 6.73             | 0.00  | 3.43        | 1.31            | 0.00        |
| 51.5     | 73.09 | 11.81           | 0.01       | 0.00       | 6.10             | 0.00  | 3.28        | 1.31            | 0.00        |
| 52.5     | 73.77 | 11.81           | 0.00       | 0.00       | 5.62             | 0.00  | 3.17        | 1.31            | 0.00        |
| 53.5     | 74.48 | 11.79           | 0.00       | 0.00       | 5.14             | 0.00  | 3.06        | 1.31            | 0.00        |

Appendix A – Contributions of species to the fluorine budgets

Table A4: The percentage contribution of CFC-114, CFC-115, HCFC-142b, HCFC-141b, HFC-23, HFC-134a, HFC-152a, H-1211 & H-1301 to the total fluorine budget in the latitude bands between 30° N and 0° N

| Altitude | CFC-114 | CFC-115 | HCFC-142b | HCFC-141b | HFC-23 | HFC-134a | HFC-152a | H-1211 | H-1301 |
|----------|---------|---------|-----------|-----------|--------|----------|----------|--------|--------|
| 10.5     | 2.51    | 1.70    | 1.17      | 0.69      | 2.14   | 5.68     | 0.33     | 0.32   | 0.42   |
| 11.5     | 2.51    | 1.70    | 1.17      | 0.69      | 2.14   | 5.67     | 0.33     | 0.31   | 0.42   |
| 12.5     | 2.50    | 1.70    | 1.17      | 0.69      | 2.14   | 5.63     | 0.33     | 0.31   | 0.41   |
| 13.5     | 2.50    | 1.70    | 1.17      | 0.69      | 2.13   | 5.58     | 0.33     | 0.31   | 0.41   |
| 14.5     | 2.49    | 1.70    | 1.16      | 0.68      | 2.12   | 5.53     | 0.32     | 0.30   | 0.41   |
| 15.5     | 2.48    | 1.70    | 1.15      | 0.67      | 2.11   | 5.46     | 0.31     | 0.30   | 0.41   |
| 16.5     | 2.47    | 1.70    | 1.15      | 0.66      | 2.11   | 5.37     | 0.30     | 0.29   | 0.40   |
| 17.5     | 2.44    | 1.70    | 1.13      | 0.64      | 2.09   | 5.21     | 0.29     | 0.27   | 0.39   |
| 18.5     | 2.38    | 1.68    | 1.09      | 0.61      | 2.05   | 4.95     | 0.26     | 0.24   | 0.37   |
| 19.5     | 2.30    | 1.66    | 1.05      | 0.56      | 2.01   | 4.65     | 0.24     | 0.20   | 0.35   |
| 20.5     | 2.25    | 1.66    | 1.02      | 0.52      | 2.00   | 4.43     | 0.22     | 0.15   | 0.32   |
| 21.5     | 2.21    | 1.65    | 1.00      | 0.49      | 1.98   | 4.25     | 0.20     | 0.11   | 0.30   |
| 22.5     | 2.17    | 1.64    | 0.97      | 0.45      | 1.96   | 4.09     | 0.18     | 0.07   | 0.28   |
| 23.5     | 2.13    | 1.64    | 0.96      | 0.42      | 1.95   | 3.98     | 0.17     | 0.04   | 0.25   |
| 24.5     | 2.11    | 1.64    | 0.95      | 0.38      | 1.95   | 3.90     | 0.16     | 0.02   | 0.23   |
| 25.5     | 2.08    | 1.64    | 0.93      | 0.34      | 1.94   | 3.81     | 0.15     | 0.01   | 0.19   |
| 26.5     | 2.03    | 1.62    | 0.91      | 0.29      | 1.92   | 3.70     | 0.14     | 0.00   | 0.16   |
| 27.5     | 1.97    | 1.62    | 0.88      | 0.24      | 1.91   | 3.61     | 0.13     | 0.00   | 0.12   |
| 28.5     | 1.89    | 1.60    | 0.85      | 0.18      | 1.89   | 3.49     | 0.12     | 0.00   | 0.09   |
| 29.5     | 1.79    | 1.56    | 0.81      | 0.14      | 1.86   | 3.36     | 0.11     | 0.00   | 0.06   |
| 30.5     | 1.71    | 1.55    | 0.78      | 0.10      | 1.85   | 3.26     | 0.10     | 0.00   | 0.04   |
| 31.5     | 1.65    | 1.55    | 0.76      | 0.07      | 1.85   | 3.20     | 0.09     | 0.00   | 0.02   |
| 32.5     | 1.56    | 1.53    | 0.73      | 0.05      | 1.84   | 3.10     | 0.08     | 0.00   | 0.01   |
| 33.5     | 1.47    | 1.52    | 0.69      | 0.03      | 1.84   | 3.01     | 0.07     | 0.00   | 0.01   |

Appendix A – Contributions of species to the fluorine budgets

| Table A4 Continued |         |         |           |           |        |          |          |        |        |
|--------------------|---------|---------|-----------|-----------|--------|----------|----------|--------|--------|
| Altitude           | CFC-114 | CFC-115 | HCFC-142b | HCFC-141b | HFC-23 | HFC-134a | HFC-152a | H-1211 | H-1301 |
| 34.5               | 1.37    | 1.49    | 0.66      | 0.02      | 1.82   | 2.89     | 0.06     | 0.00   | 0.00   |
| 35.5               | 1.28    | 1.47    | 0.62      | 0.01      | 1.81   | 2.78     | 0.05     | 0.00   | 0.00   |
| 36.5               | 1.17    | 1.45    | 0.58      | 0.01      | 1.79   | 2.65     | 0.04     | 0.00   | 0.00   |
| 37.5               | 1.06    | 1.41    | 0.53      | 0.00      | 1.77   | 2.50     | 0.03     | 0.00   | 0.00   |
| 38.5               | 0.95    | 1.38    | 0.48      | 0.00      | 1.75   | 2.36     | 0.02     | 0.00   | 0.00   |
| 39.5               | 0.87    | 1.36    | 0.45      | 0.00      | 1.75   | 2.26     | 0.02     | 0.00   | 0.00   |
| 40.5               | 0.79    | 1.34    | 0.41      | 0.00      | 1.74   | 2.15     | 0.02     | 0.00   | 0.00   |
| 41.5               | 0.72    | 1.33    | 0.39      | 0.00      | 1.73   | 2.07     | 0.01     | 0.00   | 0.00   |
| 42.5               | 0.67    | 1.31    | 0.36      | 0.00      | 1.73   | 1.99     | 0.01     | 0.00   | 0.00   |
| 43.5               | 0.61    | 1.29    | 0.34      | 0.00      | 1.72   | 1.92     | 0.01     | 0.00   | 0.00   |
| 44.5               | 0.56    | 1.27    | 0.31      | 0.00      | 1.72   | 1.83     | 0.01     | 0.00   | 0.00   |
| 45.5               | 0.50    | 1.25    | 0.29      | 0.00      | 1.71   | 1.75     | 0.01     | 0.00   | 0.00   |
| 46.5               | 0.44    | 1.23    | 0.26      | 0.00      | 1.70   | 1.66     | 0.00     | 0.00   | 0.00   |
| 47.5               | 0.39    | 1.20    | 0.24      | 0.00      | 1.68   | 1.58     | 0.00     | 0.00   | 0.00   |
| 48.5               | 0.35    | 1.16    | 0.22      | 0.00      | 1.65   | 1.49     | 0.00     | 0.00   | 0.00   |
| 49.5               | 0.30    | 1.13    | 0.20      | 0.00      | 1.62   | 1.41     | 0.00     | 0.00   | 0.00   |
| 50.5               | 0.26    | 1.11    | 0.18      | 0.00      | 1.61   | 1.35     | 0.00     | 0.00   | 0.00   |
| 51.5               | 0.24    | 1.09    | 0.17      | 0.00      | 1.60   | 1.30     | 0.00     | 0.00   | 0.00   |
| 52.5               | 0.22    | 1.08    | 0.16      | 0.00      | 1.59   | 1.27     | 0.00     | 0.00   | 0.00   |
| 53.5               | 0.20    | 1.06    | 0.15      | 0.00      | 1.58   | 1.23     | 0.00     | 0.00   | 0.00   |

Appendix A – Contributions of species to the fluorine budgets

Table A5: The percentage contribution of HF, CF<sub>4</sub>, CFC-12, CFC-11, COF<sub>2</sub>, COClF, HCFC-22, SF<sub>6</sub> & CFC-113 to the total fluorine budget in the latitude bands between 0° N and 30° S

| Altitude | HF    | CF <sub>4</sub> | CFC-12 | CFC-11 | COF <sub>2</sub> | COClF | HCFC-22 | SF <sub>6</sub> | CFC-113 |
|----------|-------|-----------------|--------|--------|------------------|-------|---------|-----------------|---------|
| 10.5     | 0.02  | 11.08           | 39.31  | 9.42   | 0.03             | 0.02  | 15.08   | 1.36            | 8.69    |
| 11.5     | 0.04  | 11.08           | 39.31  | 9.42   | 0.03             | 0.02  | 15.08   | 1.36            | 8.69    |
| 12.5     | 0.08  | 11.08           | 39.31  | 9.43   | 0.04             | 0.02  | 15.08   | 1.35            | 8.67    |
| 13.5     | 0.14  | 11.08           | 39.31  | 9.43   | 0.06             | 0.03  | 15.08   | 1.35            | 8.64    |
| 14.5     | 0.21  | 11.08           | 39.31  | 9.43   | 0.08             | 0.03  | 15.08   | 1.35            | 8.61    |
| 15.5     | 0.39  | 11.11           | 39.26  | 9.46   | 0.13             | 0.05  | 15.01   | 1.35            | 8.56    |
| 16.5     | 0.75  | 11.17           | 39.27  | 9.32   | 0.22             | 0.09  | 14.90   | 1.35            | 8.45    |
| 17.5     | 1.32  | 11.22           | 39.14  | 9.14   | 0.52             | 0.18  | 14.80   | 1.36            | 8.23    |
| 18.5     | 2.35  | 11.29           | 38.43  | 8.64   | 1.26             | 0.41  | 15.00   | 1.34            | 7.82    |
| 19.5     | 3.95  | 11.40           | 37.38  | 7.95   | 2.25             | 0.80  | 14.78   | 1.32            | 7.35    |
| 20.5     | 6.10  | 11.57           | 36.26  | 7.20   | 3.57             | 1.20  | 13.43   | 1.30            | 7.01    |
| 21.5     | 7.84  | 11.67           | 34.91  | 6.30   | 4.84             | 1.69  | 12.68   | 1.28            | 6.74    |
| 22.5     | 9.77  | 11.66           | 33.63  | 5.31   | 6.16             | 2.04  | 12.03   | 1.27            | 6.43    |
| 23.5     | 11.59 | 11.70           | 32.07  | 4.30   | 7.49             | 2.39  | 11.70   | 1.27            | 6.10    |
| 24.5     | 13.51 | 11.81           | 30.46  | 3.19   | 9.19             | 2.61  | 11.09   | 1.28            | 5.70    |
| 25.5     | 15.91 | 11.83           | 27.99  | 2.25   | 11.20            | 2.74  | 10.78   | 1.28            | 5.18    |
| 26.5     | 18.30 | 11.87           | 25.72  | 1.47   | 13.04            | 2.70  | 10.53   | 1.28            | 4.60    |
| 27.5     | 20.27 | 11.84           | 23.42  | 0.92   | 15.40            | 2.36  | 10.30   | 1.28            | 4.01    |
| 28.5     | 22.27 | 11.85           | 21.28  | 0.49   | 17.46            | 1.92  | 10.09   | 1.27            | 3.45    |
| 29.5     | 24.33 | 11.83           | 18.94  | 0.30   | 19.49            | 1.50  | 9.83    | 1.27            | 2.92    |
| 30.5     | 26.93 | 11.94           | 16.29  | 0.11   | 20.94            | 1.01  | 9.68    | 1.28            | 2.42    |
| 31.5     | 29.50 | 12.10           | 13.67  | 0.04   | 22.15            | 0.58  | 9.49    | 1.29            | 1.97    |
| 32.5     | 32.08 | 12.20           | 10.98  | 0.02   | 23.31            | 0.39  | 9.23    | 1.30            | 1.52    |
| 33.5     | 34.87 | 12.31           | 8.34   | 0.01   | 24.22            | 0.21  | 8.94    | 1.32            | 1.09    |

Appendix A – Contributions of species to the fluorine budgets

Table A5 Continued

| Altitude | HF    | CF <sub>4</sub> | CFC-<br>12 | CFC-<br>11 | COF <sub>2</sub> | COClF | HCFC-<br>22 | SF <sub>6</sub> | CFC-<br>113 |
|----------|-------|-----------------|------------|------------|------------------|-------|-------------|-----------------|-------------|
| 34.5     | 37.17 | 12.27           | 6.52       | 0.00       | 24.79            | 0.14  | 8.58        | 1.31            | 0.82        |
| 35.5     | 39.92 | 12.17           | 4.74       | 0.00       | 25.07            | 0.08  | 8.14        | 1.30            | 0.56        |
| 36.5     | 42.97 | 12.02           | 3.41       | 0.00       | 24.59            | 0.04  | 7.67        | 1.29            | 0.38        |
| 37.5     | 45.81 | 11.94           | 2.50       | 0.00       | 23.60            | 0.03  | 7.26        | 1.28            | 0.27        |
| 38.5     | 48.39 | 11.96           | 1.69       | 0.00       | 22.51            | 0.01  | 6.92        | 1.29            | 0.17        |
| 39.5     | 51.08 | 11.91           | 1.23       | 0.00       | 21.11            | 0.01  | 6.50        | 1.29            | 0.12        |
| 40.5     | 53.67 | 11.97           | 0.80       | 0.00       | 19.58            | 0.01  | 6.12        | 1.30            | 0.07        |
| 41.5     | 56.50 | 11.98           | 0.50       | 0.00       | 17.76            | 0.00  | 5.71        | 1.30            | 0.04        |
| 42.5     | 59.12 | 12.09           | 0.34       | 0.00       | 15.83            | 0.00  | 5.35        | 1.31            | 0.03        |
| 43.5     | 61.61 | 12.27           | 0.19       | 0.00       | 13.92            | 0.00  | 4.99        | 1.32            | 0.01        |
| 44.5     | 63.44 | 12.45           | 0.12       | 0.00       | 12.42            | 0.00  | 4.72        | 1.33            | 0.01        |
| 45.5     | 65.61 | 12.39           | 0.08       | 0.00       | 10.90            | 0.00  | 4.41        | 1.32            | 0.00        |
| 46.5     | 67.50 | 12.42           | 0.04       | 0.00       | 9.50             | 0.00  | 4.13        | 1.33            | 0.00        |
| 47.5     | 69.14 | 12.36           | 0.02       | 0.00       | 8.36             | 0.00  | 3.89        | 1.32            | 0.00        |
| 48.5     | 70.41 | 12.22           | 0.02       | 0.00       | 7.59             | 0.00  | 3.71        | 1.31            | 0.00        |
| 49.5     | 71.66 | 12.07           | 0.01       | 0.00       | 6.84             | 0.00  | 3.53        | 1.29            | 0.00        |
| 50.5     | 72.78 | 11.95           | 0.01       | 0.00       | 6.15             | 0.00  | 3.37        | 1.28            | 0.00        |
| 51.5     | 73.61 | 11.82           | 0.00       | 0.00       | 5.70             | 0.00  | 3.25        | 1.26            | 0.00        |
| 52.5     | 74.01 | 11.82           | 0.00       | 0.00       | 5.40             | 0.00  | 3.19        | 1.26            | 0.00        |
| 53.5     | 74.52 | 11.77           | 0.00       | 0.00       | 5.08             | 0.00  | 3.11        | 1.26            | 0.00        |

Appendix A – Contributions of species to the fluorine budgets

Table A6: The percentage contribution of CFC-114, CFC-115, HCFC-142b, HCFC-141b, HFC-23, HFC-134a, HFC-152a, H-1211 & H-1301 to the total fluorine budget in the latitude bands between 0° N and 30° S

| Altitude | CFC-114 | CFC-115 | HCFC-142b | HCFC-141b | HFC-23 | HFC-134a | HFC-152a | H-1211 | H-1301 |
|----------|---------|---------|-----------|-----------|--------|----------|----------|--------|--------|
| 10.5     | 2.51    | 1.70    | 1.18      | 0.70      | 2.15   | 5.69     | 0.34     | 0.32   | 0.42   |
| 11.5     | 2.51    | 1.70    | 1.18      | 0.70      | 2.14   | 5.68     | 0.34     | 0.32   | 0.42   |
| 12.5     | 2.51    | 1.70    | 1.17      | 0.69      | 2.14   | 5.66     | 0.33     | 0.31   | 0.42   |
| 13.5     | 2.50    | 1.70    | 1.17      | 0.69      | 2.14   | 5.63     | 0.33     | 0.31   | 0.41   |
| 14.5     | 2.50    | 1.70    | 1.17      | 0.69      | 2.13   | 5.59     | 0.33     | 0.31   | 0.41   |
| 15.5     | 2.48    | 1.70    | 1.16      | 0.68      | 2.12   | 5.52     | 0.32     | 0.30   | 0.41   |
| 16.5     | 2.46    | 1.70    | 1.15      | 0.66      | 2.11   | 5.40     | 0.31     | 0.29   | 0.40   |
| 17.5     | 2.42    | 1.69    | 1.12      | 0.64      | 2.08   | 5.20     | 0.29     | 0.27   | 0.39   |
| 18.5     | 2.33    | 1.66    | 1.07      | 0.60      | 2.04   | 4.89     | 0.26     | 0.23   | 0.37   |
| 19.5     | 2.24    | 1.64    | 1.02      | 0.55      | 2.01   | 4.58     | 0.24     | 0.19   | 0.34   |
| 20.5     | 2.19    | 1.64    | 0.99      | 0.51      | 1.99   | 4.36     | 0.22     | 0.15   | 0.31   |
| 21.5     | 2.15    | 1.64    | 0.97      | 0.48      | 1.98   | 4.21     | 0.20     | 0.11   | 0.30   |
| 22.5     | 2.12    | 1.63    | 0.95      | 0.45      | 1.95   | 4.07     | 0.19     | 0.07   | 0.27   |
| 23.5     | 2.08    | 1.62    | 0.94      | 0.41      | 1.94   | 3.95     | 0.17     | 0.04   | 0.25   |
| 24.5     | 2.05    | 1.63    | 0.92      | 0.37      | 1.94   | 3.85     | 0.16     | 0.02   | 0.22   |
| 25.5     | 2.00    | 1.61    | 0.90      | 0.32      | 1.92   | 3.73     | 0.15     | 0.01   | 0.18   |
| 26.5     | 1.94    | 1.60    | 0.87      | 0.27      | 1.91   | 3.61     | 0.14     | 0.00   | 0.15   |
| 27.5     | 1.88    | 1.59    | 0.85      | 0.22      | 1.89   | 3.52     | 0.13     | 0.00   | 0.11   |
| 28.5     | 1.82    | 1.58    | 0.83      | 0.17      | 1.88   | 3.43     | 0.12     | 0.00   | 0.08   |
| 29.5     | 1.75    | 1.56    | 0.80      | 0.14      | 1.86   | 3.33     | 0.11     | 0.00   | 0.06   |
| 30.5     | 1.70    | 1.56    | 0.78      | 0.10      | 1.86   | 3.27     | 0.10     | 0.00   | 0.04   |
| 31.5     | 1.63    | 1.56    | 0.76      | 0.07      | 1.87   | 3.21     | 0.09     | 0.00   | 0.02   |
| 32.5     | 1.55    | 1.55    | 0.73      | 0.05      | 1.88   | 3.11     | 0.08     | 0.00   | 0.01   |
| 33.5     | 1.46    | 1.55    | 0.69      | 0.03      | 1.88   | 3.01     | 0.07     | 0.00   | 0.01   |

Appendix A – Contributions of species to the fluorine budgets

| Table A6 Continued |         |         |           |           |        |          |          |        |        |
|--------------------|---------|---------|-----------|-----------|--------|----------|----------|--------|--------|
| Altitude           | CFC-114 | CFC-115 | HCFC-142b | HCFC-141b | HFC-23 | HFC-134a | HFC-152a | H-1211 | H-1301 |
| 34.5               | 1.37    | 1.52    | 0.65      | 0.02      | 1.86   | 2.90     | 0.06     | 0.00   | 0.00   |
| 35.5               | 1.26    | 1.49    | 0.61      | 0.01      | 1.83   | 2.76     | 0.05     | 0.00   | 0.00   |
| 36.5               | 1.15    | 1.45    | 0.57      | 0.01      | 1.80   | 2.62     | 0.04     | 0.00   | 0.00   |
| 37.5               | 1.05    | 1.42    | 0.53      | 0.00      | 1.78   | 2.49     | 0.03     | 0.00   | 0.00   |
| 38.5               | 0.97    | 1.40    | 0.49      | 0.00      | 1.77   | 2.39     | 0.03     | 0.00   | 0.00   |
| 39.5               | 0.88    | 1.37    | 0.45      | 0.00      | 1.76   | 2.27     | 0.02     | 0.00   | 0.00   |
| 40.5               | 0.79    | 1.35    | 0.41      | 0.00      | 1.76   | 2.16     | 0.02     | 0.00   | 0.00   |
| 41.5               | 0.70    | 1.32    | 0.37      | 0.00      | 1.74   | 2.04     | 0.01     | 0.00   | 0.00   |
| 42.5               | 0.62    | 1.30    | 0.34      | 0.00      | 1.73   | 1.93     | 0.01     | 0.00   | 0.00   |
| 43.5               | 0.55    | 1.28    | 0.31      | 0.00      | 1.73   | 1.82     | 0.01     | 0.00   | 0.00   |
| 44.5               | 0.49    | 1.26    | 0.28      | 0.00      | 1.73   | 1.74     | 0.01     | 0.00   | 0.00   |
| 45.5               | 0.43    | 1.23    | 0.26      | 0.00      | 1.71   | 1.65     | 0.00     | 0.00   | 0.00   |
| 46.5               | 0.38    | 1.21    | 0.23      | 0.00      | 1.70   | 1.56     | 0.00     | 0.00   | 0.00   |
| 47.5               | 0.33    | 1.18    | 0.21      | 0.00      | 1.68   | 1.49     | 0.00     | 0.00   | 0.00   |
| 48.5               | 0.30    | 1.15    | 0.20      | 0.00      | 1.66   | 1.43     | 0.00     | 0.00   | 0.00   |
| 49.5               | 0.27    | 1.13    | 0.18      | 0.00      | 1.63   | 1.38     | 0.00     | 0.00   | 0.00   |
| 50.5               | 0.25    | 1.10    | 0.17      | 0.00      | 1.61   | 1.33     | 0.00     | 0.00   | 0.00   |
| 51.5               | 0.23    | 1.08    | 0.16      | 0.00      | 1.59   | 1.29     | 0.00     | 0.00   | 0.00   |
| 52.5               | 0.22    | 1.08    | 0.16      | 0.00      | 1.59   | 1.27     | 0.00     | 0.00   | 0.00   |
| 53.5               | 0.20    | 1.06    | 0.15      | 0.00      | 1.58   | 1.25     | 0.00     | 0.00   | 0.00   |

Appendix A – Contributions of species to the fluorine budgets

Table A7: The percentage contribution of each species to the total fluorine budget in the latitude bands between 30° S and 70° S

| Altitude | HF    | CF <sub>4</sub> | CFC-<br>12 | CFC-<br>11 | COF <sub>2</sub> | COCIF | HCFC-<br>22 | SF <sub>6</sub> | CFC-<br>113 |
|----------|-------|-----------------|------------|------------|------------------|-------|-------------|-----------------|-------------|
| 10.5     | 1.42  | 11.41           | 38.49      | 8.94       | 0.87             | 0.25  | 14.01       | 1.33            | 8.55        |
| 11.5     | 2.56  | 11.41           | 37.85      | 8.71       | 1.52             | 0.42  | 13.98       | 1.33            | 8.13        |
| 12.5     | 3.82  | 11.39           | 37.18      | 8.46       | 2.21             | 0.60  | 13.96       | 1.33            | 7.66        |
| 13.5     | 5.20  | 11.37           | 36.29      | 8.17       | 2.86             | 0.71  | 13.90       | 1.32            | 7.30        |
| 14.5     | 7.06  | 11.33           | 34.96      | 7.71       | 3.70             | 0.82  | 13.72       | 1.31            | 6.95        |
| 15.5     | 9.50  | 11.34           | 33.28      | 7.02       | 4.85             | 0.95  | 13.21       | 1.30            | 6.59        |
| 16.5     | 12.41 | 11.45           | 31.39      | 6.14       | 6.31             | 1.12  | 12.24       | 1.28            | 6.19        |
| 17.5     | 15.88 | 11.58           | 29.11      | 5.13       | 7.97             | 1.30  | 11.25       | 1.26            | 5.68        |
| 18.5     | 19.69 | 11.62           | 26.45      | 4.00       | 9.94             | 1.46  | 10.53       | 1.24            | 5.03        |
| 19.5     | 23.10 | 11.64           | 23.95      | 2.91       | 11.82            | 1.57  | 10.04       | 1.21            | 4.41        |
| 20.5     | 26.29 | 11.68           | 21.57      | 1.90       | 13.36            | 1.62  | 9.67        | 1.19            | 3.90        |
| 21.5     | 29.06 | 11.65           | 19.22      | 1.16       | 14.92            | 1.54  | 9.38        | 1.18            | 3.47        |
| 22.5     | 31.47 | 11.60           | 16.93      | 0.78       | 16.52            | 1.32  | 9.09        | 1.17            | 3.03        |
| 23.5     | 33.88 | 11.59           | 14.80      | 0.52       | 17.71            | 1.07  | 8.85        | 1.17            | 2.59        |
| 24.5     | 36.17 | 11.58           | 12.78      | 0.31       | 18.73            | 0.89  | 8.63        | 1.16            | 2.15        |
| 25.5     | 38.28 | 11.55           | 10.91      | 0.16       | 19.67            | 0.72  | 8.42        | 1.16            | 1.75        |
| 26.5     | 40.38 | 11.48           | 9.20       | 0.08       | 20.35            | 0.58  | 8.19        | 1.15            | 1.40        |
| 27.5     | 42.62 | 11.47           | 7.55       | 0.04       | 20.67            | 0.44  | 7.95        | 1.15            | 1.11        |
| 28.5     | 44.89 | 11.49           | 6.07       | 0.02       | 20.72            | 0.32  | 7.70        | 1.15            | 0.85        |
| 29.5     | 47.13 | 11.53           | 4.89       | 0.01       | 20.34            | 0.23  | 7.45        | 1.15            | 0.66        |
| 30.5     | 49.47 | 11.60           | 3.82       | 0.00       | 19.69            | 0.15  | 7.18        | 1.15            | 0.48        |
| 31.5     | 51.71 | 11.68           | 2.89       | 0.00       | 18.95            | 0.08  | 6.91        | 1.16            | 0.34        |
| 32.5     | 53.81 | 11.69           | 2.19       | 0.00       | 18.18            | 0.05  | 6.61        | 1.16            | 0.24        |
| 33.5     | 55.97 | 11.65           | 1.57       | 0.00       | 17.33            | 0.03  | 6.29        | 1.15            | 0.16        |
| 34.5     | 57.99 | 11.62           | 1.13       | 0.00       | 16.32            | 0.01  | 6.01        | 1.15            | 0.10        |

Appendix A – Contributions of species to the fluorine budgets

Table A7 Continued

| Altitude | HF    | CF <sub>4</sub> | CFC-<br>12 | CFC-<br>11 | COF <sub>2</sub> | COCIF | HCFC-<br>22 | SF <sub>6</sub> | CFC-<br>113 |
|----------|-------|-----------------|------------|------------|------------------|-------|-------------|-----------------|-------------|
| 35.5     | 59.87 | 11.60           | 0.81       | 0.00       | 15.21            | 0.01  | 5.76        | 1.14            | 0.07        |
| 36.5     | 61.64 | 11.57           | 0.57       | 0.00       | 14.15            | 0.01  | 5.51        | 1.14            | 0.05        |
| 37.5     | 63.26 | 11.54           | 0.42       | 0.00       | 13.13            | 0.00  | 5.26        | 1.14            | 0.03        |
| 38.5     | 64.73 | 11.53           | 0.29       | 0.00       | 12.17            | 0.00  | 5.03        | 1.14            | 0.02        |
| 39.5     | 66.07 | 11.55           | 0.20       | 0.00       | 11.25            | 0.00  | 4.81        | 1.14            | 0.01        |
| 40.5     | 67.28 | 11.59           | 0.15       | 0.00       | 10.38            | 0.00  | 4.60        | 1.15            | 0.01        |
| 41.5     | 68.44 | 11.64           | 0.10       | 0.00       | 9.52             | 0.00  | 4.40        | 1.16            | 0.01        |
| 42.5     | 69.44 | 11.69           | 0.06       | 0.00       | 8.76             | 0.00  | 4.22        | 1.16            | 0.00        |
| 43.5     | 70.51 | 11.75           | 0.04       | 0.00       | 7.97             | 0.00  | 4.03        | 1.16            | 0.00        |
| 44.5     | 71.53 | 11.79           | 0.03       | 0.00       | 7.20             | 0.00  | 3.85        | 1.17            | 0.00        |
| 45.5     | 72.48 | 11.77           | 0.02       | 0.00       | 6.55             | 0.00  | 3.69        | 1.16            | 0.00        |
| 46.5     | 73.48 | 11.72           | 0.01       | 0.00       | 5.89             | 0.00  | 3.52        | 1.16            | 0.00        |
| 47.5     | 74.41 | 11.65           | 0.01       | 0.00       | 5.30             | 0.00  | 3.37        | 1.15            | 0.00        |
| 48.5     | 75.02 | 11.57           | 0.00       | 0.00       | 4.94             | 0.00  | 3.28        | 1.14            | 0.00        |
| 49.5     | 75.59 | 11.49           | 0.00       | 0.00       | 4.60             | 0.00  | 3.20        | 1.13            | 0.00        |
| 50.5     | 75.92 | 11.52           | 0.00       | 0.00       | 4.32             | 0.00  | 3.15        | 1.14            | 0.00        |
| 51.5     | 76.17 | 11.54           | 0.00       | 0.00       | 4.11             | 0.00  | 3.11        | 1.14            | 0.00        |
| 52.5     | 76.38 | 11.55           | 0.00       | 0.00       | 3.94             | 0.00  | 3.08        | 1.14            | 0.00        |
| 53.5     | 76.63 | 11.55           | 0.00       | 0.00       | 3.76             | 0.00  | 3.04        | 1.14            | 0.00        |

Appendix A – Contributions of species to the fluorine budgets

Table A8: The percentage contribution of CFC-114, CFC-115, HCFC-142b, HCFC-141b, HFC-23, HFC-134a, HFC-152a, H-1211 & H-1301 to the total fluorine budget in the latitude bands between 30° S and 70° S

| Altitude | CFC-114 | CFC-115 | HCFC-142b | HCFC-141b | HFC-23 | HFC-134a | HFC-152a | H-1211 | H-1301 |
|----------|---------|---------|-----------|-----------|--------|----------|----------|--------|--------|
| 10.5     | 2.50    | 1.74    | 1.16      | 0.67      | 2.16   | 5.49     | 0.31     | 0.30   | 0.41   |
| 11.5     | 2.41    | 1.71    | 1.11      | 0.63      | 2.11   | 5.17     | 0.29     | 0.27   | 0.38   |
| 12.5     | 2.31    | 1.67    | 1.06      | 0.59      | 2.06   | 4.84     | 0.26     | 0.24   | 0.36   |
| 13.5     | 2.22    | 1.65    | 1.02      | 0.55      | 2.02   | 4.61     | 0.24     | 0.22   | 0.34   |
| 14.5     | 2.14    | 1.62    | 0.98      | 0.52      | 1.98   | 4.41     | 0.23     | 0.20   | 0.32   |
| 15.5     | 2.07    | 1.60    | 0.94      | 0.49      | 1.95   | 4.21     | 0.21     | 0.18   | 0.30   |
| 16.5     | 1.98    | 1.58    | 0.90      | 0.46      | 1.93   | 3.98     | 0.19     | 0.16   | 0.28   |
| 17.5     | 1.88    | 1.56    | 0.85      | 0.41      | 1.90   | 3.69     | 0.17     | 0.13   | 0.25   |
| 18.5     | 1.74    | 1.52    | 0.79      | 0.35      | 1.85   | 3.34     | 0.14     | 0.10   | 0.22   |
| 19.5     | 1.62    | 1.49    | 0.73      | 0.30      | 1.80   | 3.04     | 0.12     | 0.06   | 0.18   |
| 20.5     | 1.52    | 1.46    | 0.68      | 0.25      | 1.78   | 2.82     | 0.10     | 0.04   | 0.15   |
| 21.5     | 1.45    | 1.44    | 0.65      | 0.22      | 1.75   | 2.68     | 0.09     | 0.02   | 0.13   |
| 22.5     | 1.38    | 1.42    | 0.62      | 0.18      | 1.73   | 2.57     | 0.08     | 0.01   | 0.11   |
| 23.5     | 1.32    | 1.40    | 0.60      | 0.15      | 1.72   | 2.48     | 0.07     | 0.00   | 0.08   |
| 24.5     | 1.26    | 1.39    | 0.58      | 0.11      | 1.71   | 2.42     | 0.06     | 0.00   | 0.06   |
| 25.5     | 1.20    | 1.38    | 0.56      | 0.08      | 1.70   | 2.37     | 0.06     | 0.00   | 0.04   |
| 26.5     | 1.15    | 1.36    | 0.54      | 0.06      | 1.69   | 2.32     | 0.05     | 0.00   | 0.03   |
| 27.5     | 1.08    | 1.34    | 0.51      | 0.04      | 1.68   | 2.26     | 0.04     | 0.00   | 0.02   |
| 28.5     | 1.02    | 1.33    | 0.49      | 0.03      | 1.67   | 2.21     | 0.04     | 0.00   | 0.01   |
| 29.5     | 0.96    | 1.32    | 0.47      | 0.02      | 1.67   | 2.15     | 0.03     | 0.00   | 0.01   |
| 30.5     | 0.89    | 1.31    | 0.44      | 0.01      | 1.67   | 2.09     | 0.03     | 0.00   | 0.00   |
| 31.5     | 0.83    | 1.29    | 0.42      | 0.01      | 1.67   | 2.03     | 0.02     | 0.00   | 0.00   |
| 32.5     | 0.76    | 1.27    | 0.39      | 0.01      | 1.66   | 1.96     | 0.02     | 0.00   | 0.00   |
| 33.5     | 0.70    | 1.25    | 0.37      | 0.00      | 1.64   | 1.88     | 0.02     | 0.00   | 0.00   |

Appendix A – Contributions of species to the fluorine budgets

Table A8 Continued

| Altitude | CFC-<br>114 | CFC-<br>115 | HCFC-<br>142b | HCFC-<br>141b | HFC-<br>23 | HFC-<br>134a | HFC-<br>152a | H-<br>1211 | H-<br>1301 |
|----------|-------------|-------------|---------------|---------------|------------|--------------|--------------|------------|------------|
| 34.5     | 0.64        | 1.23        | 0.34          | 0.00          | 1.63       | 1.81         | 0.01         | 0.00       | 0.00       |
| 35.5     | 0.59        | 1.21        | 0.32          | 0.00          | 1.62       | 1.76         | 0.01         | 0.00       | 0.00       |
| 36.5     | 0.55        | 1.19        | 0.30          | 0.00          | 1.61       | 1.70         | 0.01         | 0.00       | 0.00       |
| 37.5     | 0.51        | 1.18        | 0.28          | 0.00          | 1.60       | 1.64         | 0.01         | 0.00       | 0.00       |
| 38.5     | 0.47        | 1.16        | 0.27          | 0.00          | 1.60       | 1.59         | 0.01         | 0.00       | 0.00       |
| 39.5     | 0.43        | 1.15        | 0.25          | 0.00          | 1.60       | 1.53         | 0.01         | 0.00       | 0.00       |
| 40.5     | 0.39        | 1.14        | 0.23          | 0.00          | 1.60       | 1.48         | 0.00         | 0.00       | 0.00       |
| 41.5     | 0.36        | 1.13        | 0.22          | 0.00          | 1.60       | 1.44         | 0.00         | 0.00       | 0.00       |
| 42.5     | 0.33        | 1.12        | 0.20          | 0.00          | 1.60       | 1.39         | 0.00         | 0.00       | 0.00       |
| 43.5     | 0.30        | 1.11        | 0.19          | 0.00          | 1.60       | 1.34         | 0.00         | 0.00       | 0.00       |
| 44.5     | 0.27        | 1.09        | 0.18          | 0.00          | 1.59       | 1.30         | 0.00         | 0.00       | 0.00       |
| 45.5     | 0.25        | 1.08        | 0.17          | 0.00          | 1.58       | 1.26         | 0.00         | 0.00       | 0.00       |
| 46.5     | 0.22        | 1.06        | 0.15          | 0.00          | 1.57       | 1.21         | 0.00         | 0.00       | 0.00       |
| 47.5     | 0.20        | 1.04        | 0.14          | 0.00          | 1.55       | 1.17         | 0.00         | 0.00       | 0.00       |
| 48.5     | 0.19        | 1.03        | 0.14          | 0.00          | 1.54       | 1.15         | 0.00         | 0.00       | 0.00       |
| 49.5     | 0.17        | 1.01        | 0.13          | 0.00          | 1.53       | 1.13         | 0.00         | 0.00       | 0.00       |
| 50.5     | 0.16        | 1.01        | 0.13          | 0.00          | 1.53       | 1.12         | 0.00         | 0.00       | 0.00       |
| 51.5     | 0.15        | 1.01        | 0.13          | 0.00          | 1.53       | 1.11         | 0.00         | 0.00       | 0.00       |
| 52.5     | 0.15        | 1.00        | 0.12          | 0.00          | 1.53       | 1.10         | 0.00         | 0.00       | 0.00       |
| 53.5     | 0.14        | 1.00        | 0.12          | 0.00          | 1.53       | 1.09         | 0.00         | 0.00       | 0.00       |

# Appendix B

## Chlorine Budgets

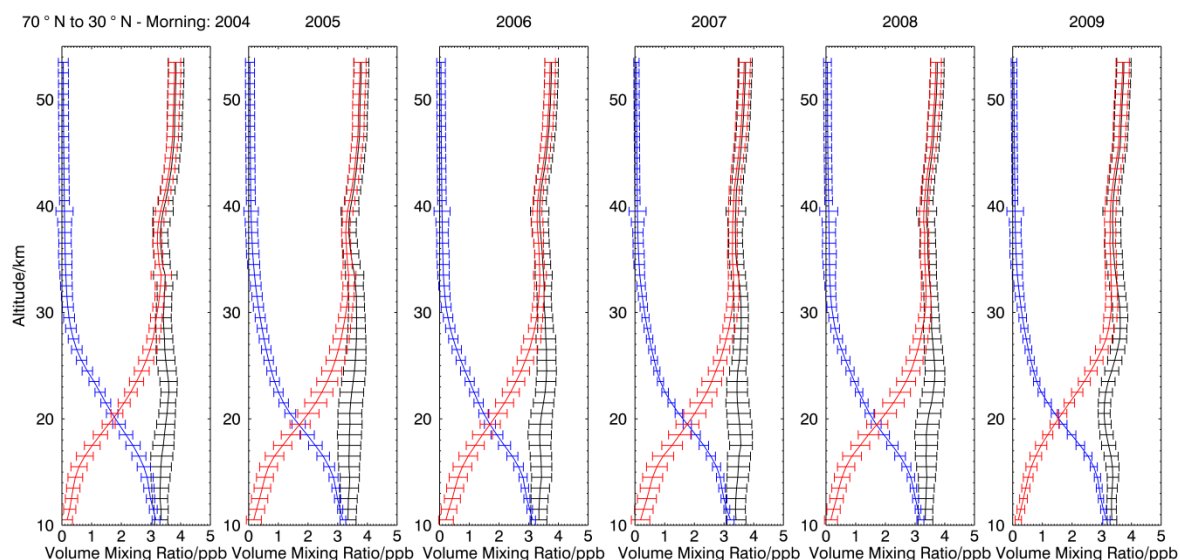


Figure B1: The total chlorine (black), inorganic chlorine (blue) and organic chlorine (red) profiles between 70° and 30° in the northern hemisphere. The error bars on the profiles are a linear combination of the standard deviations of the data which was used to calculate these profiles. These profiles were calculated using morning profiles of ClO, ClONO<sub>2</sub> and HOCl.

## Appendix B – Contributions of species to the chlorine budgets

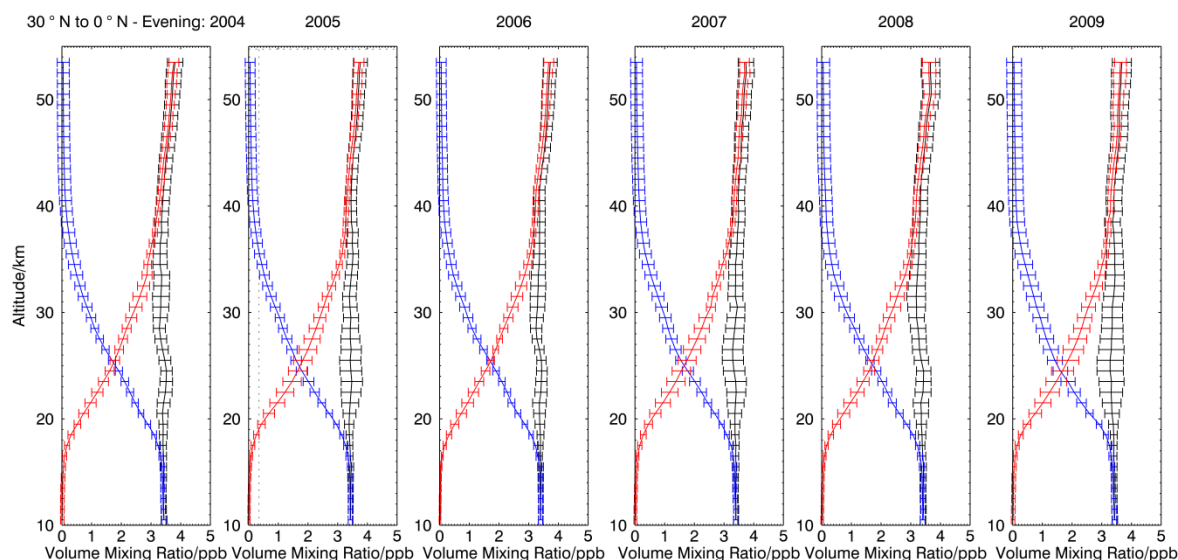


Figure B2: The total chlorine (black), inorganic chlorine (blue) and organic chlorine (red) profiles between 30° and the equator in the northern hemisphere. The error bars on the profiles are a linear combination of the standard deviations of the data which was used to calculate these profiles. These profiles were calculated using evening profiles of ClO, ClONO<sub>2</sub> and HOCl.

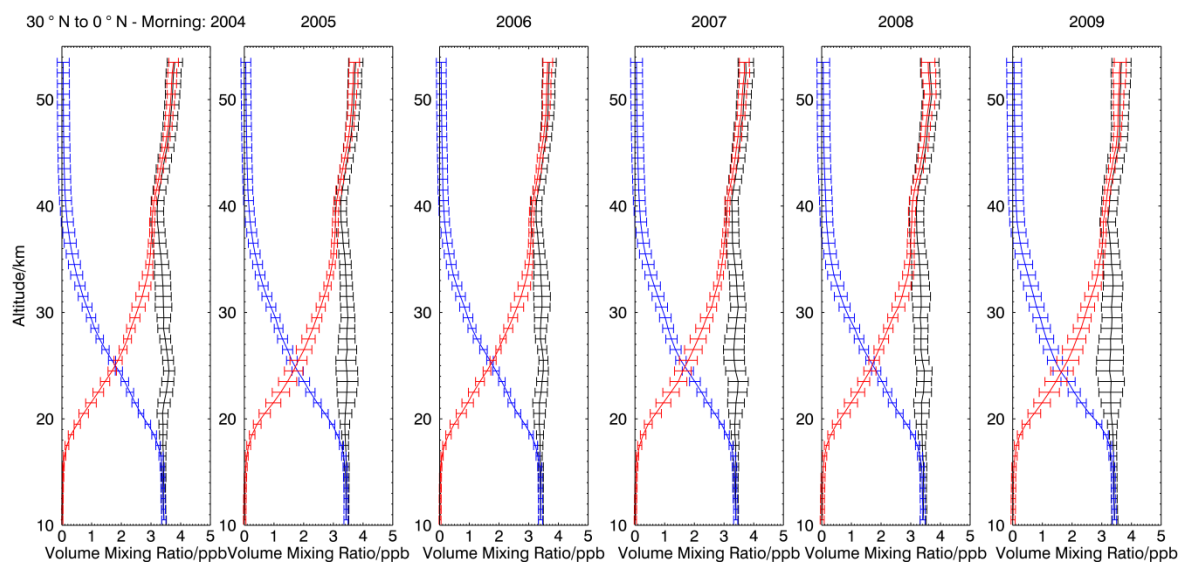


Figure B3: As Figure B2 but calculated using morning profiles of ClO, ClONO<sub>2</sub> and HOCl.

## Appendix B – Contributions of species to the chlorine budgets

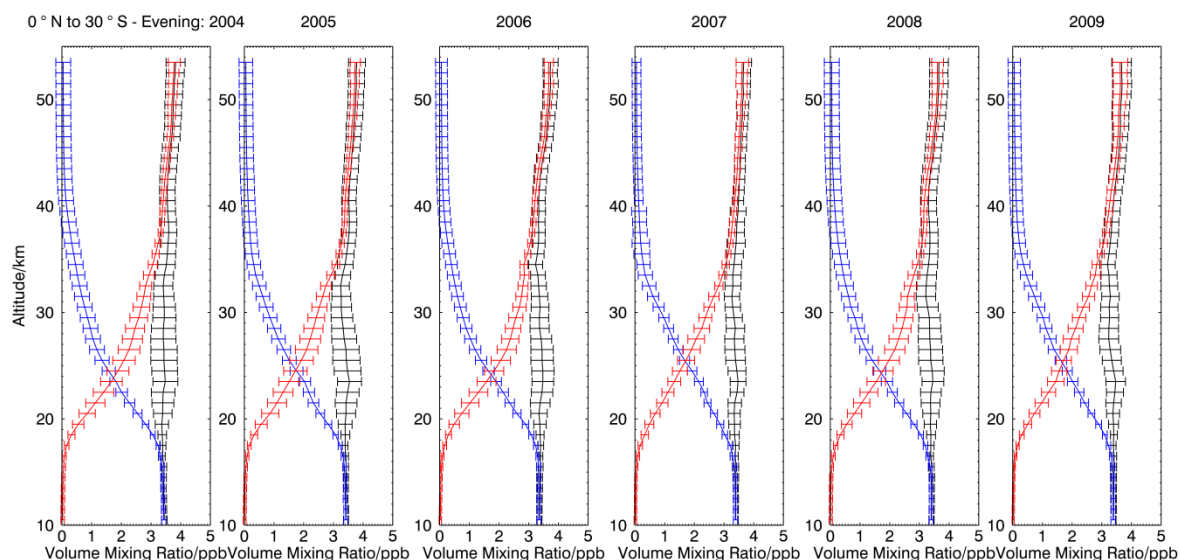


Figure B4: The total chlorine (black), inorganic chlorine (blue) and organic chlorine (red) profiles between the equator and 30° in the southern hemisphere. The error bars on the profiles are a linear combination of the standard deviations of the data which was used to calculate these profiles. These profiles were calculated using evening profiles of ClO, ClONO<sub>2</sub> and HOCl.

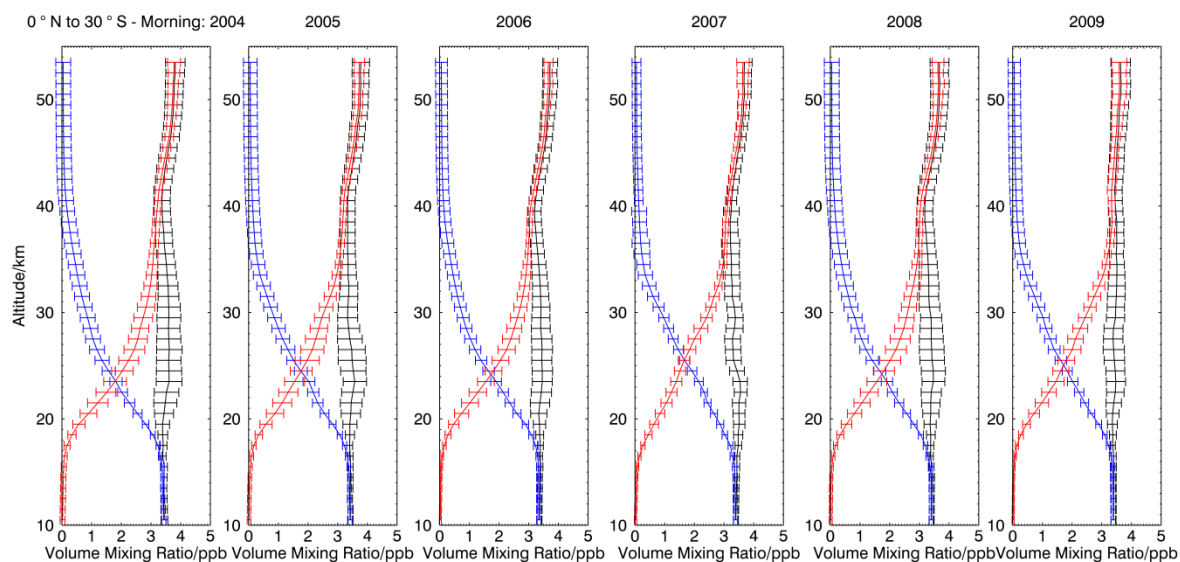


Figure B5: As Figure B4 but calculated using morning profiles of ClO, ClONO<sub>2</sub> and HOCl.

## Appendix B – Contributions of species to the chlorine budgets

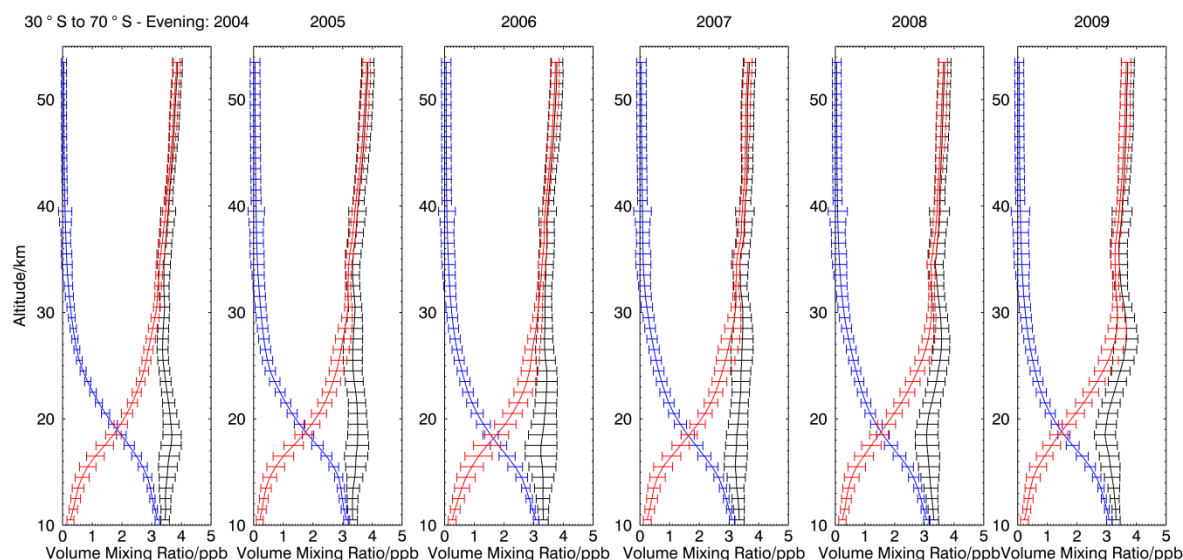


Figure B6: The total chlorine (black), inorganic chlorine (blue) and organic chlorine (red) profiles between 30° and 70° in the southern hemisphere. The error bars on the profiles are a linear combination of the standard deviations of the data which was used to calculate these profiles. These profiles were calculated using evening profiles of ClO, ClONO<sub>2</sub> and HOCl.

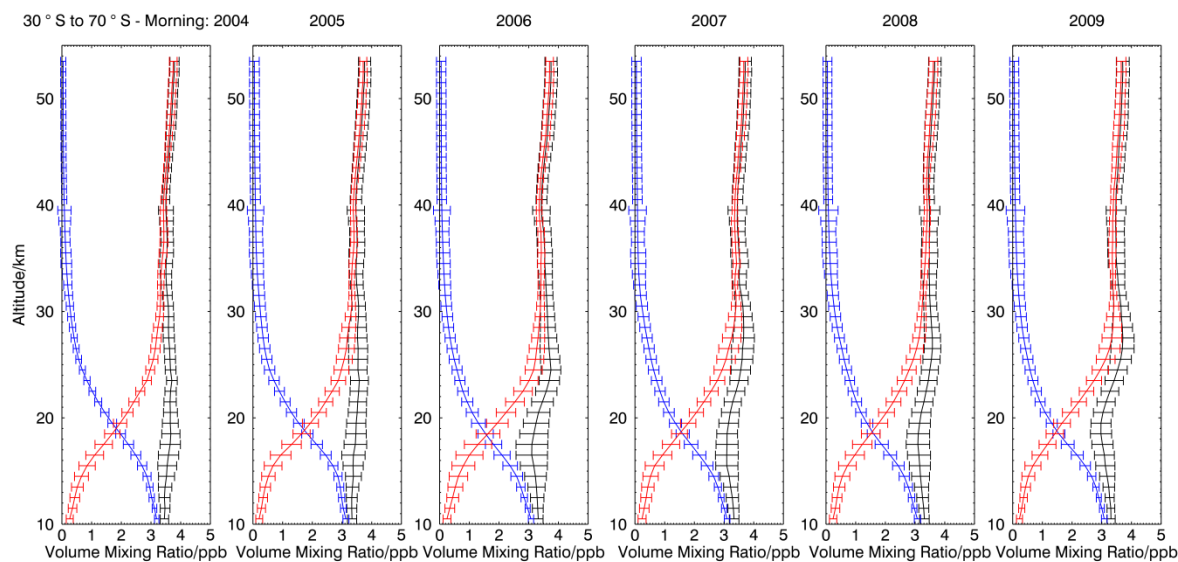


Figure B7: As Figure B6 but calculated using morning profiles of ClO, ClONO<sub>2</sub> and HOCl.

## Appendix B – Contributions of species to the chlorine budgets

Table B1: The percentage contribution of HCl, CCl<sub>4</sub>, CFC-12, CFC-11, COClF, COCl<sub>2</sub>, HCFC-22, CH<sub>3</sub>Cl & CFC-113 to the total chlorine budget in the latitude bands between 70° N and 30° N (evening occultations)

| Altitude | HCl   | CCl <sub>4</sub> | CFC-12 | CFC-11 | COClF | COCl <sub>2</sub> | HCFC-22 | CH <sub>3</sub> Cl | CFC-113 |
|----------|-------|------------------|--------|--------|-------|-------------------|---------|--------------------|---------|
| 10.5     | 3.96  | 12.08            | 30.09  | 20.65  | 1.07  | 0.18              | 5.55    | 16.72              | 6.56    |
| 11.5     | 6.29  | 11.20            | 29.62  | 19.94  | 1.14  | 0.29              | 5.48    | 16.27              | 6.29    |
| 12.5     | 8.52  | 10.38            | 29.15  | 19.16  | 1.19  | 0.39              | 5.40    | 15.79              | 6.02    |
| 13.5     | 10.53 | 9.79             | 28.46  | 18.38  | 1.21  | 0.44              | 5.41    | 15.58              | 5.81    |
| 14.5     | 12.63 | 9.19             | 27.77  | 17.51  | 1.21  | 0.49              | 5.40    | 15.37              | 5.58    |
| 15.5     | 15.65 | 8.53             | 26.95  | 16.28  | 1.22  | 0.56              | 5.26    | 14.44              | 5.35    |
| 16.5     | 19.80 | 7.71             | 25.74  | 14.66  | 1.24  | 0.67              | 4.94    | 12.91              | 5.01    |
| 17.5     | 24.88 | 6.65             | 24.15  | 12.72  | 1.27  | 0.83              | 4.58    | 11.20              | 4.59    |
| 18.5     | 30.33 | 5.58             | 22.42  | 10.50  | 1.31  | 0.99              | 4.31    | 9.60               | 4.11    |
| 19.5     | 35.41 | 4.50             | 20.56  | 8.07   | 1.30  | 1.14              | 4.10    | 8.13               | 3.63    |
| 20.5     | 39.88 | 3.56             | 18.72  | 5.65   | 1.20  | 1.24              | 3.90    | 6.88               | 3.20    |
| 21.5     | 43.49 | 2.77             | 16.91  | 3.82   | 1.04  | 1.28              | 3.73    | 5.78               | 2.81    |
| 22.5     | 46.66 | 1.83             | 15.15  | 2.49   | 0.86  | 1.22              | 3.59    | 4.90               | 2.46    |
| 23.5     | 49.34 | 1.18             | 13.46  | 1.51   | 0.70  | 1.10              | 3.47    | 4.07               | 2.11    |
| 24.5     | 51.89 | 0.62             | 11.72  | 0.92   | 0.63  | 0.94              | 3.34    | 3.25               | 1.78    |
| 25.5     | 54.42 | 0.28             | 10.00  | 0.52   | 0.50  | 0.77              | 3.22    | 2.50               | 1.46    |
| 26.5     | 56.97 | 0.10             | 8.32   | 0.26   | 0.38  | 0.61              | 3.09    | 1.83               | 1.16    |
| 27.5     | 59.44 | 0.05             | 6.77   | 0.14   | 0.28  | 0.45              | 2.96    | 1.31               | 0.90    |
| 28.5     | 62.05 | 0.01             | 5.36   | 0.05   | 0.20  | 0.32              | 2.83    | 0.92               | 0.68    |
| 29.5     | 64.61 | 0.01             | 4.22   | 0.03   | 0.14  | 0.22              | 2.72    | 0.62               | 0.52    |
| 30.5     | 67.07 | 0.00             | 3.20   | 0.01   | 0.08  | 0.13              | 2.58    | 0.46               | 0.37    |
| 31.5     | 69.28 | 0.00             | 2.42   | 0.00   | 0.05  | 0.08              | 2.46    | 0.38               | 0.26    |
| 32.5     | 71.42 | 0.00             | 1.81   | 0.00   | 0.03  | 0.05              | 2.36    | 0.30               | 0.18    |
| 33.5     | 73.26 | 0.00             | 1.26   | 0.00   | 0.01  | 0.02              | 2.26    | 0.23               | 0.11    |
| 34.5     | 75.59 | 0.00             | 0.94   | 0.00   | 0.01  | 0.01              | 2.20    | 0.19               | 0.08    |
| 35.5     | 77.00 | 0.00             | 0.66   | 0.00   | 0.01  | 0.01              | 2.12    | 0.14               | 0.05    |
| 36.5     | 77.72 | 0.00             | 0.47   | 0.00   | 0.00  | 0.00              | 2.04    | 0.11               | 0.03    |

Appendix B – Contributions of species to the chlorine budgets

Table B1 Continued

| Altitude | HCl   | CCl <sub>4</sub> | CFC-<br>12 | CFC-<br>11 | COClF | COCl <sub>2</sub> | HCFC-<br>22 | CH <sub>3</sub> Cl | CFC-<br>113 |
|----------|-------|------------------|------------|------------|-------|-------------------|-------------|--------------------|-------------|
| 37.5     | 77.60 | 0.00             | 0.33       | 0.00       | 0.00  | 0.00              | 1.95        | 0.09               | 0.02        |
| 38.5     | 77.56 | 0.00             | 0.23       | 0.00       | 0.00  | 0.00              | 1.86        | 0.06               | 0.01        |
| 39.5     | 77.78 | 0.00             | 0.17       | 0.00       | 0.00  | 0.00              | 1.77        | 0.05               | 0.01        |
| 40.5     | 78.07 | 0.00             | 0.12       | 0.00       | 0.00  | 0.00              | 1.69        | 0.04               | 0.01        |
| 41.5     | 78.68 | 0.00             | 0.08       | 0.00       | 0.00  | 0.00              | 1.60        | 0.03               | 0.00        |
| 42.5     | 79.49 | 0.00             | 0.06       | 0.00       | 0.00  | 0.00              | 1.52        | 0.02               | 0.00        |
| 43.5     | 80.60 | 0.00             | 0.04       | 0.00       | 0.00  | 0.00              | 1.45        | 0.02               | 0.00        |
| 44.5     | 81.98 | 0.00             | 0.03       | 0.00       | 0.00  | 0.00              | 1.37        | 0.01               | 0.00        |
| 45.5     | 83.53 | 0.00             | 0.02       | 0.00       | 0.00  | 0.00              | 1.31        | 0.01               | 0.00        |
| 46.5     | 85.10 | 0.00             | 0.01       | 0.00       | 0.00  | 0.00              | 1.25        | 0.01               | 0.00        |
| 47.5     | 86.78 | 0.00             | 0.01       | 0.00       | 0.00  | 0.00              | 1.20        | 0.01               | 0.00        |
| 48.5     | 88.32 | 0.00             | 0.01       | 0.00       | 0.00  | 0.00              | 1.15        | 0.00               | 0.00        |
| 49.5     | 89.71 | 0.00             | 0.00       | 0.00       | 0.00  | 0.00              | 1.10        | 0.00               | 0.00        |
| 50.5     | 90.95 | 0.00             | 0.00       | 0.00       | 0.00  | 0.00              | 1.06        | 0.00               | 0.00        |
| 51.5     | 91.95 | 0.00             | 0.00       | 0.00       | 0.00  | 0.00              | 1.03        | 0.00               | 0.00        |
| 52.5     | 92.82 | 0.00             | 0.00       | 0.00       | 0.00  | 0.00              | 1.00        | 0.00               | 0.00        |
| 53.5     | 93.61 | 0.00             | 0.00       | 0.00       | 0.00  | 0.00              | 0.98        | 0.00               | 0.00        |

Appendix B – Contributions of species to the chlorine budgets

Table B2: The percentage contribution of CFC-114, CFC-115, HCFC-142b, HCFC-141b, ClONO<sub>2</sub>, ClO, HOCl & H-1211 to the total chlorine budget in the latitude bands between 70° N and 30° N (evening occultations)

| Altitude | CFC-114 | CFC-115 | HCFC-142b | HCFC-141b | ClONO <sub>2</sub> | ClO   | HOCl | H-1211 |
|----------|---------|---------|-----------|-----------|--------------------|-------|------|--------|
| 10.5     | 0.96    | 0.27    | 0.45      | 1.03      | 0.30               | 0.01  | 0.04 | 0.11   |
| 11.5     | 0.93    | 0.26    | 0.43      | 0.97      | 0.75               | 0.01  | 0.03 | 0.10   |
| 12.5     | 0.91    | 0.26    | 0.42      | 0.91      | 1.37               | 0.01  | 0.03 | 0.09   |
| 13.5     | 0.88    | 0.25    | 0.40      | 0.88      | 1.85               | 0.01  | 0.03 | 0.09   |
| 14.5     | 0.86    | 0.25    | 0.39      | 0.84      | 2.41               | 0.01  | 0.03 | 0.08   |
| 15.5     | 0.83    | 0.25    | 0.38      | 0.79      | 3.39               | 0.02  | 0.03 | 0.07   |
| 16.5     | 0.80    | 0.24    | 0.36      | 0.73      | 5.08               | 0.02  | 0.03 | 0.06   |
| 17.5     | 0.76    | 0.24    | 0.34      | 0.66      | 7.03               | 0.03  | 0.04 | 0.05   |
| 18.5     | 0.71    | 0.23    | 0.32      | 0.57      | 8.86               | 0.05  | 0.06 | 0.04   |
| 19.5     | 0.66    | 0.23    | 0.30      | 0.48      | 11.34              | 0.08  | 0.07 | 0.03   |
| 20.5     | 0.63    | 0.22    | 0.28      | 0.41      | 14.02              | 0.12  | 0.09 | 0.02   |
| 21.5     | 0.59    | 0.22    | 0.27      | 0.34      | 16.67              | 0.15  | 0.11 | 0.01   |
| 22.5     | 0.57    | 0.22    | 0.25      | 0.29      | 19.20              | 0.18  | 0.14 | 0.00   |
| 23.5     | 0.54    | 0.21    | 0.24      | 0.23      | 21.45              | 0.22  | 0.16 | 0.00   |
| 24.5     | 0.50    | 0.21    | 0.23      | 0.19      | 23.30              | 0.28  | 0.19 | 0.00   |
| 25.5     | 0.47    | 0.20    | 0.22      | 0.14      | 24.70              | 0.39  | 0.21 | 0.00   |
| 26.5     | 0.43    | 0.20    | 0.20      | 0.11      | 25.50              | 0.57  | 0.25 | 0.00   |
| 27.5     | 0.40    | 0.20    | 0.19      | 0.08      | 25.71              | 0.82  | 0.31 | 0.00   |
| 28.5     | 0.36    | 0.19    | 0.18      | 0.05      | 25.37              | 1.07  | 0.37 | 0.00   |
| 29.5     | 0.33    | 0.19    | 0.16      | 0.04      | 24.36              | 1.39  | 0.45 | 0.00   |
| 30.5     | 0.30    | 0.19    | 0.15      | 0.02      | 22.79              | 2.05  | 0.59 | 0.00   |
| 31.5     | 0.27    | 0.19    | 0.14      | 0.01      | 20.58              | 3.06  | 0.80 | 0.00   |
| 32.5     | 0.25    | 0.18    | 0.13      | 0.01      | 17.87              | 4.34  | 1.04 | 0.00   |
| 33.5     | 0.23    | 0.18    | 0.12      | 0.00      | 14.91              | 6.05  | 1.33 | 0.00   |
| 34.5     | 0.22    | 0.18    | 0.12      | 0.00      | 10.78              | 8.01  | 1.67 | 0.00   |
| 35.5     | 0.20    | 0.18    | 0.11      | 0.00      | 7.63               | 9.99  | 1.88 | 0.00   |
| 36.5     | 0.19    | 0.18    | 0.11      | 0.00      | 4.75               | 12.40 | 2.00 | 0.00   |
| 37.5     | 0.17    | 0.17    | 0.10      | 0.00      | 2.92               | 14.61 | 2.03 | 0.00   |
| 38.5     | 0.16    | 0.17    | 0.09      | 0.00      | 1.83               | 16.06 | 1.95 | 0.00   |
| 39.5     | 0.15    | 0.17    | 0.09      | 0.00      | 1.02               | 16.97 | 1.81 | 0.00   |
| 40.5     | 0.14    | 0.16    | 0.08      | 0.00      | 0.56               | 17.48 | 1.65 | 0.00   |
| 41.5     | 0.13    | 0.16    | 0.08      | 0.00      | 0.31               | 17.47 | 1.46 | 0.00   |
| 42.5     | 0.12    | 0.16    | 0.07      | 0.00      | 0.16               | 17.15 | 1.25 | 0.00   |
| 43.5     | 0.11    | 0.15    | 0.07      | 0.00      | 0.07               | 16.44 | 1.05 | 0.00   |
| 44.5     | 0.10    | 0.15    | 0.06      | 0.00      | 0.04               | 15.39 | 0.87 | 0.00   |

Appendix B – Contributions of species to the chlorine budgets

Table B2 Continued

| Altitude | CFC-114 | CFC-115 | HCFC-142b | HCFC-141b | ClONO <sub>2</sub> | ClO   | HOCl | H-1211 |
|----------|---------|---------|-----------|-----------|--------------------|-------|------|--------|
| 45.5     | 0.09    | 0.15    | 0.06      | 0.00      | 0.02               | 14.12 | 0.70 | 0.00   |
| 46.5     | 0.08    | 0.14    | 0.05      | 0.00      | 0.01               | 12.78 | 0.56 | 0.00   |
| 47.5     | 0.07    | 0.14    | 0.05      | 0.00      | 0.00               | 11.29 | 0.44 | 0.00   |
| 48.5     | 0.06    | 0.14    | 0.05      | 0.00      | 0.00               | 9.92  | 0.34 | 0.00   |
| 49.5     | 0.06    | 0.14    | 0.04      | 0.00      | 0.00               | 8.68  | 0.26 | 0.00   |
| 50.5     | 0.05    | 0.14    | 0.04      | 0.00      | 0.00               | 7.55  | 0.21 | 0.00   |
| 51.5     | 0.05    | 0.13    | 0.04      | 0.00      | 0.00               | 6.63  | 0.17 | 0.00   |
| 52.5     | 0.04    | 0.13    | 0.04      | 0.00      | 0.00               | 5.82  | 0.13 | 0.00   |
| 53.5     | 0.04    | 0.13    | 0.04      | 0.00      | 0.00               | 5.09  | 0.11 | 0.00   |

Appendix B – Contributions of species to the chlorine budgets

Table B3: The percentage contribution of HCl, CCl<sub>4</sub>, CFC-12, CFC-11, COClF, COCl<sub>2</sub>, HCFC-22, CH<sub>3</sub>Cl & CFC-113 to the total chlorine budget in the latitude bands between 70° N and 30° N (morning occultations)

| Altitude | HCl   | CCl <sub>4</sub> | CFC-12 | CFC-11 | COClF | COCl <sub>2</sub> | HCFC-22 | CH <sub>3</sub> Cl | CFC-113 |
|----------|-------|------------------|--------|--------|-------|-------------------|---------|--------------------|---------|
| 10.5     | 3.96  | 12.09            | 30.11  | 20.66  | 1.07  | 0.18              | 5.56    | 16.73              | 6.57    |
| 11.5     | 6.31  | 11.23            | 29.69  | 19.99  | 1.15  | 0.29              | 5.49    | 16.31              | 6.30    |
| 12.5     | 8.56  | 10.43            | 29.28  | 19.25  | 1.20  | 0.39              | 5.43    | 15.87              | 6.04    |
| 13.5     | 10.60 | 9.85             | 28.65  | 18.50  | 1.22  | 0.44              | 5.44    | 15.68              | 5.85    |
| 14.5     | 12.74 | 9.27             | 28.00  | 17.65  | 1.22  | 0.49              | 5.44    | 15.50              | 5.63    |
| 15.5     | 15.84 | 8.64             | 27.27  | 16.47  | 1.23  | 0.56              | 5.32    | 14.62              | 5.41    |
| 16.5     | 20.14 | 7.84             | 26.18  | 14.91  | 1.26  | 0.69              | 5.02    | 13.13              | 5.10    |
| 17.5     | 25.28 | 6.75             | 24.54  | 12.93  | 1.29  | 0.84              | 4.65    | 11.38              | 4.66    |
| 18.5     | 30.78 | 5.67             | 22.75  | 10.65  | 1.33  | 1.01              | 4.38    | 9.74               | 4.17    |
| 19.5     | 35.84 | 4.55             | 20.81  | 8.17   | 1.31  | 1.15              | 4.15    | 8.23               | 3.67    |
| 20.5     | 40.12 | 3.58             | 18.83  | 5.68   | 1.21  | 1.25              | 3.92    | 6.92               | 3.22    |
| 21.5     | 43.40 | 2.77             | 16.87  | 3.81   | 1.03  | 1.27              | 3.72    | 5.77               | 2.81    |
| 22.5     | 46.15 | 1.81             | 14.99  | 2.46   | 0.85  | 1.21              | 3.55    | 4.85               | 2.43    |
| 23.5     | 48.52 | 1.16             | 13.24  | 1.49   | 0.69  | 1.08              | 3.41    | 4.01               | 2.08    |
| 24.5     | 50.86 | 0.61             | 11.49  | 0.90   | 0.62  | 0.93              | 3.28    | 3.19               | 1.74    |
| 25.5     | 53.24 | 0.27             | 9.78   | 0.51   | 0.49  | 0.75              | 3.15    | 2.44               | 1.43    |
| 26.5     | 55.70 | 0.10             | 8.13   | 0.26   | 0.37  | 0.60              | 3.03    | 1.79               | 1.13    |
| 27.5     | 58.08 | 0.04             | 6.62   | 0.13   | 0.28  | 0.44              | 2.89    | 1.28               | 0.88    |
| 28.5     | 60.57 | 0.01             | 5.23   | 0.05   | 0.19  | 0.31              | 2.77    | 0.90               | 0.66    |
| 29.5     | 62.95 | 0.01             | 4.12   | 0.03   | 0.14  | 0.22              | 2.65    | 0.60               | 0.51    |
| 30.5     | 65.15 | 0.00             | 3.11   | 0.01   | 0.08  | 0.13              | 2.51    | 0.45               | 0.36    |
| 31.5     | 67.22 | 0.00             | 2.35   | 0.00   | 0.05  | 0.08              | 2.39    | 0.36               | 0.25    |
| 32.5     | 69.22 | 0.00             | 1.75   | 0.00   | 0.03  | 0.05              | 2.29    | 0.29               | 0.18    |
| 33.5     | 71.28 | 0.00             | 1.23   | 0.00   | 0.01  | 0.02              | 2.20    | 0.22               | 0.11    |
| 34.5     | 73.70 | 0.00             | 0.92   | 0.00   | 0.01  | 0.01              | 2.15    | 0.18               | 0.08    |
| 35.5     | 75.57 | 0.00             | 0.64   | 0.00   | 0.01  | 0.01              | 2.08    | 0.14               | 0.05    |
| 36.5     | 77.16 | 0.00             | 0.46   | 0.00   | 0.00  | 0.00              | 2.03    | 0.11               | 0.03    |
| 37.5     | 78.29 | 0.00             | 0.33   | 0.00   | 0.00  | 0.00              | 1.97    | 0.09               | 0.02    |
| 38.5     | 79.43 | 0.00             | 0.23   | 0.00   | 0.00  | 0.00              | 1.90    | 0.07               | 0.01    |
| 39.5     | 79.95 | 0.00             | 0.17   | 0.00   | 0.00  | 0.00              | 1.82    | 0.05               | 0.01    |
| 40.5     | 80.36 | 0.00             | 0.12   | 0.00   | 0.00  | 0.00              | 1.74    | 0.04               | 0.01    |
| 41.5     | 80.79 | 0.00             | 0.09   | 0.00   | 0.00  | 0.00              | 1.64    | 0.03               | 0.00    |
| 42.5     | 81.32 | 0.00             | 0.06   | 0.00   | 0.00  | 0.00              | 1.56    | 0.02               | 0.00    |
| 43.5     | 82.06 | 0.00             | 0.04   | 0.00   | 0.00  | 0.00              | 1.47    | 0.02               | 0.00    |
| 44.5     | 83.12 | 0.00             | 0.03   | 0.00   | 0.00  | 0.00              | 1.39    | 0.01               | 0.00    |

Appendix B – Contributions of species to the chlorine budgets

Table B3 Continued

| Altitude | HCl   | CCl <sub>4</sub> | CFC-<br>12 | CFC-<br>11 | COClF | COCl <sub>2</sub> | HCFC-<br>22 | CH <sub>3</sub> Cl | CFC-<br>113 |
|----------|-------|------------------|------------|------------|-------|-------------------|-------------|--------------------|-------------|
| 45.5     | 84.29 | 0.00             | 0.02       | 0.00       | 0.00  | 0.00              | 1.33        | 0.01               | 0.00        |
| 46.5     | 85.55 | 0.00             | 0.01       | 0.00       | 0.00  | 0.00              | 1.26        | 0.01               | 0.00        |
| 47.5     | 86.99 | 0.00             | 0.01       | 0.00       | 0.00  | 0.00              | 1.21        | 0.01               | 0.00        |
| 48.5     | 88.52 | 0.00             | 0.01       | 0.00       | 0.00  | 0.00              | 1.16        | 0.00               | 0.00        |
| 49.5     | 89.89 | 0.00             | 0.00       | 0.00       | 0.00  | 0.00              | 1.11        | 0.00               | 0.00        |
| 50.5     | 91.11 | 0.00             | 0.00       | 0.00       | 0.00  | 0.00              | 1.06        | 0.00               | 0.00        |
| 51.5     | 92.17 | 0.00             | 0.00       | 0.00       | 0.00  | 0.00              | 1.03        | 0.00               | 0.00        |
| 52.5     | 93.13 | 0.00             | 0.00       | 0.00       | 0.00  | 0.00              | 1.01        | 0.00               | 0.00        |
| 53.5     | 93.97 | 0.00             | 0.00       | 0.00       | 0.00  | 0.00              | 0.99        | 0.00               | 0.00        |

Appendix B – Contributions of species to the chlorine budgets

Table B4: The percentage contribution of CFC-114, CFC-115, HCFC-142b, HCFC-141b, ClONO<sub>2</sub>, ClO, HOCl & H-1211 to the total chlorine budget in the latitude bands between 70° N and 30° N (morning occultations)

| Altitude | CFC-114 | CFC-115 | HCFC-142b | HCFC-141b | ClONO <sub>2</sub> | ClO   | HOCl | H-1211 |
|----------|---------|---------|-----------|-----------|--------------------|-------|------|--------|
| 10.5     | 0.96    | 0.27    | 0.45      | 1.03      | 0.19               | 0.01  | 0.05 | 0.11   |
| 11.5     | 0.94    | 0.26    | 0.43      | 0.97      | 0.48               | 0.01  | 0.04 | 0.10   |
| 12.5     | 0.91    | 0.26    | 0.42      | 0.92      | 0.88               | 0.02  | 0.04 | 0.09   |
| 13.5     | 0.89    | 0.26    | 0.41      | 0.88      | 1.20               | 0.03  | 0.03 | 0.09   |
| 14.5     | 0.86    | 0.25    | 0.39      | 0.84      | 1.56               | 0.04  | 0.02 | 0.08   |
| 15.5     | 0.84    | 0.25    | 0.38      | 0.80      | 2.21               | 0.05  | 0.03 | 0.08   |
| 16.5     | 0.81    | 0.25    | 0.37      | 0.75      | 3.40               | 0.08  | 0.03 | 0.07   |
| 17.5     | 0.77    | 0.24    | 0.35      | 0.67      | 5.48               | 0.11  | 0.03 | 0.05   |
| 18.5     | 0.72    | 0.24    | 0.32      | 0.58      | 7.41               | 0.17  | 0.04 | 0.04   |
| 19.5     | 0.67    | 0.23    | 0.30      | 0.49      | 10.12              | 0.23  | 0.06 | 0.03   |
| 20.5     | 0.63    | 0.22    | 0.28      | 0.41      | 13.29              | 0.33  | 0.08 | 0.02   |
| 21.5     | 0.59    | 0.22    | 0.27      | 0.34      | 16.52              | 0.48  | 0.11 | 0.01   |
| 22.5     | 0.56    | 0.21    | 0.25      | 0.28      | 19.66              | 0.61  | 0.13 | 0.00   |
| 23.5     | 0.53    | 0.21    | 0.24      | 0.23      | 22.16              | 0.79  | 0.17 | 0.00   |
| 24.5     | 0.49    | 0.20    | 0.23      | 0.18      | 24.12              | 0.95  | 0.21 | 0.00   |
| 25.5     | 0.46    | 0.20    | 0.21      | 0.14      | 25.57              | 1.09  | 0.25 | 0.00   |
| 26.5     | 0.42    | 0.20    | 0.20      | 0.10      | 26.44              | 1.23  | 0.29 | 0.00   |
| 27.5     | 0.39    | 0.19    | 0.18      | 0.07      | 26.77              | 1.40  | 0.34 | 0.00   |
| 28.5     | 0.35    | 0.19    | 0.17      | 0.05      | 26.61              | 1.55  | 0.39 | 0.00   |
| 29.5     | 0.32    | 0.19    | 0.16      | 0.04      | 25.89              | 1.75  | 0.45 | 0.00   |
| 30.5     | 0.29    | 0.18    | 0.15      | 0.02      | 24.96              | 2.03  | 0.56 | 0.00   |
| 31.5     | 0.27    | 0.18    | 0.14      | 0.01      | 23.52              | 2.45  | 0.71 | 0.00   |
| 32.5     | 0.24    | 0.18    | 0.13      | 0.01      | 21.77              | 2.99  | 0.86 | 0.00   |
| 33.5     | 0.22    | 0.18    | 0.12      | 0.00      | 19.69              | 3.67  | 1.03 | 0.00   |
| 34.5     | 0.21    | 0.18    | 0.12      | 0.00      | 16.61              | 4.62  | 1.21 | 0.00   |
| 35.5     | 0.20    | 0.18    | 0.11      | 0.00      | 13.87              | 5.78  | 1.36 | 0.00   |
| 36.5     | 0.19    | 0.18    | 0.10      | 0.00      | 11.06              | 7.23  | 1.45 | 0.00   |
| 37.5     | 0.18    | 0.18    | 0.10      | 0.00      | 8.45               | 8.89  | 1.49 | 0.00   |
| 38.5     | 0.16    | 0.17    | 0.10      | 0.00      | 5.77               | 10.65 | 1.49 | 0.00   |
| 39.5     | 0.15    | 0.17    | 0.09      | 0.00      | 3.71               | 12.43 | 1.44 | 0.00   |
| 40.5     | 0.14    | 0.17    | 0.08      | 0.00      | 2.04               | 13.92 | 1.37 | 0.00   |
| 41.5     | 0.13    | 0.16    | 0.08      | 0.00      | 1.12               | 14.70 | 1.26 | 0.00   |
| 42.5     | 0.12    | 0.16    | 0.07      | 0.00      | 0.56               | 15.00 | 1.12 | 0.00   |
| 43.5     | 0.11    | 0.16    | 0.07      | 0.00      | 0.27               | 14.84 | 0.96 | 0.00   |
| 44.5     | 0.10    | 0.15    | 0.06      | 0.00      | 0.13               | 14.20 | 0.79 | 0.00   |

Appendix B – Contributions of species to the chlorine budgets

| Table B4 Continued |         |         |           |           |                    |       |      |        |
|--------------------|---------|---------|-----------|-----------|--------------------|-------|------|--------|
| Altitude           | CFC-114 | CFC-115 | HCFC-142b | HCFC-141b | ClONO <sub>2</sub> | ClO   | HOCl | H-1211 |
| 45.5               | 0.09    | 0.15    | 0.06      | 0.00      | 0.06               | 13.35 | 0.65 | 0.00   |
| 46.5               | 0.08    | 0.14    | 0.05      | 0.00      | 0.03               | 12.33 | 0.53 | 0.00   |
| 47.5               | 0.07    | 0.14    | 0.05      | 0.00      | 0.01               | 11.08 | 0.43 | 0.00   |
| 48.5               | 0.06    | 0.14    | 0.05      | 0.00      | 0.01               | 9.71  | 0.34 | 0.00   |
| 49.5               | 0.06    | 0.14    | 0.04      | 0.00      | 0.00               | 8.48  | 0.26 | 0.00   |
| 50.5               | 0.05    | 0.14    | 0.04      | 0.00      | 0.00               | 7.38  | 0.21 | 0.00   |
| 51.5               | 0.05    | 0.13    | 0.04      | 0.00      | 0.00               | 6.39  | 0.17 | 0.00   |
| 52.5               | 0.04    | 0.13    | 0.04      | 0.00      | 0.00               | 5.51  | 0.14 | 0.00   |
| 53.5               | 0.04    | 0.13    | 0.04      | 0.00      | 0.00               | 4.73  | 0.11 | 0.00   |

## Appendix B – Contributions of species to the chlorine budgets

Table B5: The percentage contribution of HCl, CCl<sub>4</sub>, CFC-12, CFC-11, COClF, COCl<sub>2</sub>, HCFC-22, CH<sub>3</sub>Cl & CFC-113 to the total chlorine budget in the latitude bands between 30° N and 0° N (evening occultations)

| Altitude | HCl   | CCl <sub>4</sub> | CFC-12 | CFC-11 | COClF | COCl <sub>2</sub> | HCFC-22 | CH <sub>3</sub> Cl | CFC-113 |
|----------|-------|------------------|--------|--------|-------|-------------------|---------|--------------------|---------|
| 10.5     | 0.11  | 13.07            | 30.56  | 21.98  | 0.13  | 0.01              | 5.97    | 18.43              | 6.77    |
| 11.5     | 0.20  | 12.96            | 30.54  | 21.97  | 0.15  | 0.01              | 5.97    | 18.42              | 6.75    |
| 12.5     | 0.17  | 12.73            | 30.60  | 22.01  | 0.22  | 0.02              | 5.98    | 18.46              | 6.75    |
| 13.5     | 0.22  | 12.55            | 30.60  | 22.01  | 0.32  | 0.03              | 5.98    | 18.46              | 6.71    |
| 14.5     | 0.22  | 12.54            | 30.55  | 21.99  | 0.43  | 0.04              | 5.97    | 18.43              | 6.66    |
| 15.5     | 0.46  | 12.25            | 30.42  | 21.98  | 0.59  | 0.05              | 5.92    | 18.41              | 6.61    |
| 16.5     | 1.03  | 12.01            | 30.51  | 21.66  | 0.80  | 0.08              | 5.82    | 18.10              | 6.54    |
| 17.5     | 2.64  | 11.49            | 30.36  | 21.19  | 0.97  | 0.14              | 5.75    | 17.38              | 6.40    |
| 18.5     | 5.83  | 10.75            | 29.78  | 20.00  | 1.10  | 0.29              | 5.88    | 16.31              | 6.15    |
| 19.5     | 10.67 | 9.57             | 28.91  | 18.49  | 1.30  | 0.58              | 5.80    | 14.72              | 5.80    |
| 20.5     | 16.08 | 8.28             | 27.78  | 16.56  | 1.54  | 0.91              | 5.19    | 13.03              | 5.47    |
| 21.5     | 20.68 | 6.85             | 26.59  | 14.38  | 1.75  | 1.23              | 4.83    | 11.41              | 5.17    |
| 22.5     | 24.04 | 5.47             | 25.33  | 11.97  | 1.88  | 1.55              | 4.52    | 10.76              | 4.86    |
| 23.5     | 26.55 | 4.19             | 24.10  | 9.61   | 1.93  | 1.83              | 4.33    | 10.21              | 4.58    |
| 24.5     | 29.28 | 3.15             | 23.01  | 7.25   | 1.98  | 2.05              | 4.17    | 9.10               | 4.32    |
| 25.5     | 31.77 | 1.93             | 21.87  | 5.28   | 1.87  | 2.23              | 4.10    | 8.18               | 4.05    |
| 26.5     | 34.51 | 0.97             | 20.66  | 3.62   | 1.66  | 2.27              | 4.05    | 7.37               | 3.69    |
| 27.5     | 37.90 | 0.51             | 19.37  | 2.24   | 1.32  | 2.04              | 3.98    | 6.33               | 3.24    |
| 28.5     | 41.74 | 0.17             | 17.90  | 1.15   | 1.09  | 1.67              | 3.89    | 5.72               | 2.77    |
| 29.5     | 46.28 | 0.10             | 16.31  | 0.69   | 0.87  | 1.24              | 3.78    | 4.74               | 2.32    |
| 30.5     | 52.19 | 0.03             | 14.24  | 0.25   | 0.65  | 0.85              | 3.67    | 3.83               | 1.87    |
| 31.5     | 57.87 | 0.00             | 11.91  | 0.08   | 0.48  | 0.26              | 3.57    | 3.20               | 1.51    |
| 32.5     | 62.59 | 0.01             | 9.55   | 0.05   | 0.32  | 0.17              | 3.43    | 2.64               | 1.16    |
| 33.5     | 67.18 | 0.01             | 7.30   | 0.03   | 0.17  | 0.09              | 3.30    | 2.07               | 0.83    |
| 34.5     | 71.02 | 0.01             | 5.67   | 0.02   | 0.11  | 0.06              | 3.17    | 1.70               | 0.62    |
| 35.5     | 74.22 | 0.00             | 4.05   | 0.01   | 0.05  | 0.03              | 3.02    | 1.35               | 0.41    |
| 36.5     | 77.06 | 0.00             | 2.86   | 0.01   | 0.03  | 0.01              | 2.86    | 1.05               | 0.27    |
| 37.5     | 78.99 | 0.00             | 1.99   | 0.01   | 0.02  | 0.01              | 2.67    | 0.79               | 0.18    |
| 38.5     | 80.71 | 0.00             | 1.22   | 0.01   | 0.01  | 0.00              | 2.51    | 0.56               | 0.10    |
| 39.5     | 81.84 | 0.00             | 0.88   | 0.01   | 0.01  | 0.00              | 2.37    | 0.43               | 0.07    |
| 40.5     | 83.23 | 0.00             | 0.59   | 0.00   | 0.00  | 0.00              | 2.23    | 0.31               | 0.04    |
| 41.5     | 84.56 | 0.00             | 0.37   | 0.00   | 0.00  | 0.00              | 2.10    | 0.22               | 0.02    |
| 42.5     | 85.83 | 0.00             | 0.27   | 0.00   | 0.00  | 0.00              | 1.99    | 0.18               | 0.02    |
| 43.5     | 87.17 | 0.00             | 0.17   | 0.00   | 0.00  | 0.00              | 1.87    | 0.13               | 0.01    |
| 44.5     | 88.43 | 0.00             | 0.11   | 0.00   | 0.00  | 0.00              | 1.75    | 0.09               | 0.01    |
| 45.5     | 89.52 | 0.00             | 0.08   | 0.00   | 0.00  | 0.00              | 1.63    | 0.07               | 0.00    |

Appendix B – Contributions of species to the chlorine budgets

Table B5 Continued

| Altitude | HCl   | CCl <sub>4</sub> | CFC-12 | CFC-11 | COClF | COCl <sub>2</sub> | HCFC-22 | CH <sub>3</sub> Cl | CFC-113 |
|----------|-------|------------------|--------|--------|-------|-------------------|---------|--------------------|---------|
| 46.5     | 90.61 | 0.00             | 0.04   | 0.00   | 0.00  | 0.00              | 1.51    | 0.05               | 0.00    |
| 47.5     | 91.50 | 0.00             | 0.02   | 0.00   | 0.00  | 0.00              | 1.41    | 0.03               | 0.00    |
| 48.5     | 92.38 | 0.00             | 0.02   | 0.00   | 0.00  | 0.00              | 1.33    | 0.02               | 0.00    |
| 49.5     | 93.02 | 0.00             | 0.01   | 0.00   | 0.00  | 0.00              | 1.24    | 0.02               | 0.00    |
| 50.5     | 93.50 | 0.00             | 0.01   | 0.00   | 0.00  | 0.00              | 1.16    | 0.01               | 0.00    |
| 51.5     | 93.94 | 0.00             | 0.00   | 0.00   | 0.00  | 0.00              | 1.11    | 0.01               | 0.00    |
| 52.5     | 94.36 | 0.00             | 0.00   | 0.00   | 0.00  | 0.00              | 1.07    | 0.01               | 0.00    |
| 53.5     | 94.69 | 0.00             | 0.00   | 0.00   | 0.00  | 0.00              | 1.03    | 0.01               | 0.00    |

Appendix B – Contributions of species to the chlorine budgets

Table B6: The percentage contribution of CFC-114, CFC-115, HCFC-142b, HCFC-141b, ClONO<sub>2</sub>, ClO, HOCl & H-1211 to the total chlorine budget in the latitude bands between 30° N and 0° N (evening occultations)

| Altitude | CFC-114 | CFC-115 | HCFC-142b | HCFC-141b | ClONO <sub>2</sub> | ClO   | HOCl | H-1211 |
|----------|---------|---------|-----------|-----------|--------------------|-------|------|--------|
| 10.5     | 0.98    | 0.27    | 0.46      | 1.08      | 0.03               | 0.00  | 0.03 | 0.12   |
| 11.5     | 0.98    | 0.27    | 0.46      | 1.08      | 0.08               | 0.00  | 0.03 | 0.12   |
| 12.5     | 0.98    | 0.27    | 0.46      | 1.08      | 0.15               | 0.00  | 0.03 | 0.12   |
| 13.5     | 0.97    | 0.26    | 0.45      | 1.07      | 0.20               | 0.01  | 0.03 | 0.12   |
| 14.5     | 0.97    | 0.26    | 0.45      | 1.06      | 0.26               | 0.02  | 0.05 | 0.12   |
| 15.5     | 0.96    | 0.26    | 0.45      | 1.04      | 0.37               | 0.04  | 0.07 | 0.12   |
| 16.5     | 0.96    | 0.26    | 0.44      | 1.03      | 0.57               | 0.02  | 0.05 | 0.11   |
| 17.5     | 0.94    | 0.26    | 0.43      | 0.99      | 0.92               | 0.01  | 0.01 | 0.10   |
| 18.5     | 0.92    | 0.26    | 0.42      | 0.94      | 1.27               | 0.00  | 0.01 | 0.09   |
| 19.5     | 0.89    | 0.26    | 0.40      | 0.87      | 1.65               | 0.01  | 0.01 | 0.08   |
| 20.5     | 0.86    | 0.25    | 0.39      | 0.80      | 2.76               | 0.01  | 0.02 | 0.06   |
| 21.5     | 0.83    | 0.25    | 0.38      | 0.74      | 4.78               | 0.04  | 0.06 | 0.04   |
| 22.5     | 0.80    | 0.24    | 0.36      | 0.67      | 7.33               | 0.08  | 0.11 | 0.03   |
| 23.5     | 0.79    | 0.24    | 0.35      | 0.61      | 10.30              | 0.15  | 0.19 | 0.02   |
| 24.5     | 0.78    | 0.24    | 0.35      | 0.56      | 13.17              | 0.27  | 0.31 | 0.01   |
| 25.5     | 0.77    | 0.24    | 0.34      | 0.50      | 15.98              | 0.40  | 0.48 | 0.00   |
| 26.5     | 0.76    | 0.24    | 0.34      | 0.43      | 18.18              | 0.56  | 0.69 | 0.00   |
| 27.5     | 0.74    | 0.24    | 0.33      | 0.35      | 19.86              | 0.70  | 0.86 | 0.00   |
| 28.5     | 0.71    | 0.24    | 0.32      | 0.28      | 20.56              | 0.83  | 0.97 | 0.00   |
| 29.5     | 0.68    | 0.24    | 0.31      | 0.22      | 20.17              | 0.99  | 1.08 | 0.00   |
| 30.5     | 0.65    | 0.23    | 0.30      | 0.15      | 18.63              | 1.27  | 1.20 | 0.00   |
| 31.5     | 0.62    | 0.23    | 0.29      | 0.11      | 16.84              | 1.69  | 1.34 | 0.00   |
| 32.5     | 0.58    | 0.23    | 0.27      | 0.08      | 14.84              | 2.62  | 1.46 | 0.00   |
| 33.5     | 0.54    | 0.22    | 0.26      | 0.04      | 12.61              | 3.80  | 1.54 | 0.00   |
| 34.5     | 0.51    | 0.22    | 0.24      | 0.03      | 10.28              | 4.72  | 1.62 | 0.00   |
| 35.5     | 0.47    | 0.22    | 0.23      | 0.01      | 8.22               | 6.04  | 1.66 | 0.00   |
| 36.5     | 0.43    | 0.21    | 0.21      | 0.01      | 6.37               | 6.96  | 1.67 | 0.00   |
| 37.5     | 0.39    | 0.21    | 0.19      | 0.00      | 4.84               | 8.05  | 1.66 | 0.00   |
| 38.5     | 0.35    | 0.20    | 0.18      | 0.00      | 3.35               | 9.28  | 1.52 | 0.00   |
| 39.5     | 0.32    | 0.20    | 0.16      | 0.00      | 2.10               | 10.25 | 1.37 | 0.00   |
| 40.5     | 0.29    | 0.20    | 0.15      | 0.00      | 1.17               | 10.57 | 1.21 | 0.00   |
| 41.5     | 0.26    | 0.19    | 0.14      | 0.00      | 0.65               | 10.44 | 1.03 | 0.00   |
| 42.5     | 0.24    | 0.19    | 0.13      | 0.00      | 0.33               | 9.98  | 0.85 | 0.00   |
| 43.5     | 0.22    | 0.18    | 0.12      | 0.00      | 0.16               | 9.27  | 0.69 | 0.00   |
| 44.5     | 0.19    | 0.18    | 0.11      | 0.00      | 0.08               | 8.49  | 0.56 | 0.00   |

Appendix B – Contributions of species to the chlorine budgets

| Table B6 Continued |         |         |           |           |                    |      |      |        |
|--------------------|---------|---------|-----------|-----------|--------------------|------|------|--------|
| Altitude           | CFC-114 | CFC-115 | HCFC-142b | HCFC-141b | ClONO <sub>2</sub> | ClO  | HOCl | H-1211 |
| 45.5               | 0.17    | 0.17    | 0.10      | 0.00      | 0.04               | 7.80 | 0.43 | 0.00   |
| 46.5               | 0.15    | 0.17    | 0.09      | 0.00      | 0.02               | 7.03 | 0.34 | 0.00   |
| 47.5               | 0.13    | 0.16    | 0.08      | 0.00      | 0.01               | 6.36 | 0.28 | 0.00   |
| 48.5               | 0.12    | 0.16    | 0.07      | 0.00      | 0.00               | 5.68 | 0.22 | 0.00   |
| 49.5               | 0.10    | 0.15    | 0.07      | 0.00      | 0.00               | 5.20 | 0.18 | 0.00   |
| 50.5               | 0.09    | 0.15    | 0.06      | 0.00      | 0.00               | 4.86 | 0.15 | 0.00   |
| 51.5               | 0.08    | 0.15    | 0.06      | 0.00      | 0.00               | 4.52 | 0.12 | 0.00   |
| 52.5               | 0.07    | 0.15    | 0.05      | 0.00      | 0.00               | 4.19 | 0.10 | 0.00   |
| 53.5               | 0.07    | 0.14    | 0.05      | 0.00      | 0.00               | 3.94 | 0.08 | 0.00   |

Appendix B – Contributions of species to the chlorine budgets

Table B7: The percentage contribution of HCl, CCl<sub>4</sub>, CFC-12, CFC-11, COClF, COCl<sub>2</sub>, HCFC-22, CH<sub>3</sub>Cl & CFC-113 to the total chlorine budget in the latitude bands between 30° N and 0° N (morning occultations)

| Altitude | HCl   | CCl <sub>4</sub> | CFC-12 | CFC-11 | COClF | COCl <sub>2</sub> | HCFC-22 | CH <sub>3</sub> Cl | CFC-113 |
|----------|-------|------------------|--------|--------|-------|-------------------|---------|--------------------|---------|
| 10.5     | 0.11  | 13.07            | 30.55  | 21.98  | 0.13  | 0.01              | 5.97    | 18.43              | 6.76    |
| 11.5     | 0.20  | 12.96            | 30.54  | 21.97  | 0.15  | 0.01              | 5.97    | 18.42              | 6.75    |
| 12.5     | 0.17  | 12.73            | 30.60  | 22.02  | 0.22  | 0.02              | 5.98    | 18.46              | 6.75    |
| 13.5     | 0.22  | 12.56            | 30.61  | 22.02  | 0.32  | 0.03              | 5.98    | 18.46              | 6.71    |
| 14.5     | 0.22  | 12.55            | 30.57  | 22.00  | 0.43  | 0.04              | 5.97    | 18.44              | 6.67    |
| 15.5     | 0.46  | 12.27            | 30.46  | 22.01  | 0.59  | 0.05              | 5.93    | 18.44              | 6.62    |
| 16.5     | 1.03  | 12.02            | 30.55  | 21.69  | 0.80  | 0.08              | 5.83    | 18.13              | 6.55    |
| 17.5     | 2.64  | 11.51            | 30.41  | 21.22  | 0.97  | 0.14              | 5.76    | 17.41              | 6.41    |
| 18.5     | 5.84  | 10.77            | 29.85  | 20.05  | 1.10  | 0.29              | 5.89    | 16.35              | 6.17    |
| 19.5     | 10.70 | 9.60             | 28.99  | 18.54  | 1.31  | 0.58              | 5.82    | 14.77              | 5.82    |
| 20.5     | 16.07 | 8.28             | 27.77  | 16.56  | 1.54  | 0.91              | 5.19    | 13.02              | 5.47    |
| 21.5     | 20.64 | 6.84             | 26.54  | 14.36  | 1.74  | 1.23              | 4.82    | 11.39              | 5.16    |
| 22.5     | 23.93 | 5.44             | 25.22  | 11.91  | 1.87  | 1.54              | 4.50    | 10.71              | 4.84    |
| 23.5     | 26.32 | 4.16             | 23.90  | 9.53   | 1.92  | 1.82              | 4.30    | 10.12              | 4.54    |
| 24.5     | 28.98 | 3.12             | 22.78  | 7.17   | 1.96  | 2.03              | 4.12    | 9.00               | 4.28    |
| 25.5     | 31.38 | 1.90             | 21.59  | 5.22   | 1.85  | 2.20              | 4.05    | 8.07               | 4.00    |
| 26.5     | 33.94 | 0.96             | 20.32  | 3.56   | 1.63  | 2.23              | 3.98    | 7.25               | 3.63    |
| 27.5     | 37.18 | 0.50             | 19.00  | 2.19   | 1.29  | 2.00              | 3.91    | 6.21               | 3.18    |
| 28.5     | 40.76 | 0.17             | 17.48  | 1.12   | 1.06  | 1.63              | 3.80    | 5.59               | 2.71    |
| 29.5     | 45.14 | 0.09             | 15.91  | 0.68   | 0.85  | 1.21              | 3.69    | 4.62               | 2.27    |
| 30.5     | 50.91 | 0.03             | 13.89  | 0.25   | 0.64  | 0.83              | 3.58    | 3.73               | 1.83    |
| 31.5     | 56.43 | 0.00             | 11.62  | 0.08   | 0.47  | 0.25              | 3.48    | 3.12               | 1.48    |
| 32.5     | 61.55 | 0.01             | 9.40   | 0.05   | 0.31  | 0.17              | 3.38    | 2.59               | 1.14    |
| 33.5     | 66.73 | 0.01             | 7.25   | 0.03   | 0.17  | 0.09              | 3.28    | 2.06               | 0.83    |
| 34.5     | 71.12 | 0.01             | 5.68   | 0.02   | 0.11  | 0.06              | 3.17    | 1.70               | 0.62    |
| 35.5     | 75.33 | 0.00             | 4.12   | 0.01   | 0.05  | 0.03              | 3.07    | 1.37               | 0.41    |
| 36.5     | 79.00 | 0.00             | 2.93   | 0.01   | 0.03  | 0.01              | 2.93    | 1.07               | 0.27    |
| 37.5     | 81.88 | 0.00             | 2.07   | 0.01   | 0.02  | 0.01              | 2.77    | 0.82               | 0.18    |
| 38.5     | 84.38 | 0.00             | 1.28   | 0.01   | 0.01  | 0.00              | 2.62    | 0.59               | 0.10    |
| 39.5     | 85.90 | 0.00             | 0.92   | 0.01   | 0.01  | 0.00              | 2.48    | 0.45               | 0.07    |
| 40.5     | 87.07 | 0.00             | 0.62   | 0.00   | 0.00  | 0.00              | 2.33    | 0.33               | 0.04    |
| 41.5     | 87.55 | 0.00             | 0.38   | 0.00   | 0.00  | 0.00              | 2.18    | 0.23               | 0.02    |
| 42.5     | 87.99 | 0.00             | 0.28   | 0.00   | 0.00  | 0.00              | 2.04    | 0.18               | 0.02    |
| 43.5     | 88.67 | 0.00             | 0.18   | 0.00   | 0.00  | 0.00              | 1.90    | 0.13               | 0.01    |
| 44.5     | 89.46 | 0.00             | 0.12   | 0.00   | 0.00  | 0.00              | 1.77    | 0.10               | 0.01    |

Appendix B – Contributions of species to the chlorine budgets

Table B7 Continued

| Altitude | HCl   | CCl <sub>4</sub> | CFC-<br>12 | CFC-<br>11 | COClF | COCl <sub>2</sub> | HCFC-<br>22 | CH <sub>3</sub> Cl | CFC-<br>113 |
|----------|-------|------------------|------------|------------|-------|-------------------|-------------|--------------------|-------------|
| 45.5     | 90.09 | 0.00             | 0.08       | 0.00       | 0.00  | 0.00              | 1.64        | 0.07               | 0.00        |
| 46.5     | 90.77 | 0.00             | 0.04       | 0.00       | 0.00  | 0.00              | 1.51        | 0.05               | 0.00        |
| 47.5     | 91.56 | 0.00             | 0.02       | 0.00       | 0.00  | 0.00              | 1.42        | 0.03               | 0.00        |
| 48.5     | 92.29 | 0.00             | 0.02       | 0.00       | 0.00  | 0.00              | 1.33        | 0.02               | 0.00        |
| 49.5     | 92.91 | 0.00             | 0.01       | 0.00       | 0.00  | 0.00              | 1.24        | 0.02               | 0.00        |
| 50.5     | 93.54 | 0.00             | 0.01       | 0.00       | 0.00  | 0.00              | 1.16        | 0.01               | 0.00        |
| 51.5     | 94.12 | 0.00             | 0.00       | 0.00       | 0.00  | 0.00              | 1.12        | 0.01               | 0.00        |
| 52.5     | 94.73 | 0.00             | 0.00       | 0.00       | 0.00  | 0.00              | 1.08        | 0.01               | 0.00        |
| 53.5     | 95.20 | 0.00             | 0.00       | 0.00       | 0.00  | 0.00              | 1.04        | 0.01               | 0.00        |

Appendix B – Contributions of species to the chlorine budgets

Table B8: The percentage contribution of CFC-114, CFC-115, HCFC-142b, HCFC-141b, ClONO<sub>2</sub>, ClO, HOCl & H-1211 to the total chlorine budget in the latitude bands between 30° N and 0° N (morning occultations)

| Altitude | CFC-114 | CFC-115 | HCFC-142b | HCFC-141b | ClONO <sub>2</sub> | ClO  | HOCl | H-1211 |
|----------|---------|---------|-----------|-----------|--------------------|------|------|--------|
| 10.5     | 0.98    | 0.27    | 0.46      | 1.08      | 0.03               | 0.01 | 0.04 | 0.12   |
| 11.5     | 0.98    | 0.27    | 0.46      | 1.08      | 0.06               | 0.01 | 0.04 | 0.12   |
| 12.5     | 0.98    | 0.27    | 0.46      | 1.08      | 0.12               | 0.01 | 0.04 | 0.12   |
| 13.5     | 0.97    | 0.26    | 0.45      | 1.07      | 0.16               | 0.01 | 0.04 | 0.12   |
| 14.5     | 0.97    | 0.26    | 0.45      | 1.06      | 0.21               | 0.02 | 0.04 | 0.12   |
| 15.5     | 0.96    | 0.26    | 0.45      | 1.04      | 0.30               | 0.02 | 0.03 | 0.12   |
| 16.5     | 0.96    | 0.26    | 0.44      | 1.03      | 0.46               | 0.04 | 0.02 | 0.11   |
| 17.5     | 0.94    | 0.26    | 0.44      | 0.99      | 0.74               | 0.03 | 0.01 | 0.10   |
| 18.5     | 0.92    | 0.26    | 0.42      | 0.94      | 1.02               | 0.03 | 0.01 | 0.09   |
| 19.5     | 0.89    | 0.26    | 0.41      | 0.87      | 1.33               | 0.03 | 0.01 | 0.08   |
| 20.5     | 0.86    | 0.25    | 0.39      | 0.80      | 2.73               | 0.08 | 0.03 | 0.06   |
| 21.5     | 0.83    | 0.25    | 0.37      | 0.73      | 4.85               | 0.15 | 0.05 | 0.04   |
| 22.5     | 0.80    | 0.24    | 0.36      | 0.67      | 7.57               | 0.27 | 0.09 | 0.03   |
| 23.5     | 0.78    | 0.24    | 0.35      | 0.61      | 10.81              | 0.44 | 0.16 | 0.02   |
| 24.5     | 0.77    | 0.24    | 0.34      | 0.55      | 13.75              | 0.62 | 0.28 | 0.01   |
| 25.5     | 0.76    | 0.24    | 0.34      | 0.49      | 16.63              | 0.85 | 0.42 | 0.00   |
| 26.5     | 0.74    | 0.24    | 0.33      | 0.42      | 19.07              | 1.09 | 0.58 | 0.00   |
| 27.5     | 0.72    | 0.24    | 0.32      | 0.35      | 20.91              | 1.29 | 0.72 | 0.00   |
| 28.5     | 0.69    | 0.23    | 0.31      | 0.27      | 21.90              | 1.46 | 0.81 | 0.00   |
| 29.5     | 0.66    | 0.23    | 0.30      | 0.21      | 21.68              | 1.57 | 0.89 | 0.00   |
| 30.5     | 0.63    | 0.23    | 0.29      | 0.15      | 20.32              | 1.72 | 0.98 | 0.00   |
| 31.5     | 0.60    | 0.23    | 0.28      | 0.11      | 18.98              | 1.81 | 1.07 | 0.00   |
| 32.5     | 0.57    | 0.22    | 0.27      | 0.08      | 17.14              | 1.97 | 1.16 | 0.00   |
| 33.5     | 0.54    | 0.22    | 0.25      | 0.04      | 15.16              | 2.13 | 1.21 | 0.00   |
| 34.5     | 0.51    | 0.22    | 0.24      | 0.03      | 13.03              | 2.22 | 1.26 | 0.00   |
| 35.5     | 0.48    | 0.22    | 0.23      | 0.02      | 10.80              | 2.58 | 1.29 | 0.00   |
| 36.5     | 0.44    | 0.22    | 0.22      | 0.01      | 8.46               | 3.11 | 1.29 | 0.00   |
| 37.5     | 0.40    | 0.22    | 0.20      | 0.00      | 6.50               | 3.66 | 1.26 | 0.00   |
| 38.5     | 0.37    | 0.21    | 0.19      | 0.00      | 4.53               | 4.52 | 1.19 | 0.00   |
| 39.5     | 0.33    | 0.21    | 0.17      | 0.00      | 2.86               | 5.46 | 1.12 | 0.00   |
| 40.5     | 0.30    | 0.20    | 0.16      | 0.00      | 1.58               | 6.35 | 1.00 | 0.00   |
| 41.5     | 0.27    | 0.20    | 0.14      | 0.00      | 0.87               | 7.28 | 0.87 | 0.00   |
| 42.5     | 0.24    | 0.19    | 0.13      | 0.00      | 0.43               | 7.75 | 0.74 | 0.00   |
| 43.5     | 0.22    | 0.19    | 0.12      | 0.00      | 0.21               | 7.74 | 0.63 | 0.00   |
| 44.5     | 0.20    | 0.18    | 0.11      | 0.00      | 0.10               | 7.43 | 0.53 | 0.00   |

Appendix B – Contributions of species to the chlorine budgets

Table B8 Continued

| Altitude | CFC-114 | CFC-115 | HCFC-142b | HCFC-141b | ClONO <sub>2</sub> | ClO  | HOCl | H-1211 |
|----------|---------|---------|-----------|-----------|--------------------|------|------|--------|
| 45.5     | 0.17    | 0.17    | 0.10      | 0.00      | 0.05               | 7.21 | 0.42 | 0.00   |
| 46.5     | 0.15    | 0.17    | 0.09      | 0.00      | 0.02               | 6.85 | 0.34 | 0.00   |
| 47.5     | 0.13    | 0.16    | 0.08      | 0.00      | 0.01               | 6.30 | 0.29 | 0.00   |
| 48.5     | 0.12    | 0.16    | 0.07      | 0.00      | 0.01               | 5.75 | 0.23 | 0.00   |
| 49.5     | 0.10    | 0.15    | 0.07      | 0.00      | 0.00               | 5.30 | 0.19 | 0.00   |
| 50.5     | 0.09    | 0.15    | 0.06      | 0.00      | 0.00               | 4.82 | 0.15 | 0.00   |
| 51.5     | 0.08    | 0.15    | 0.06      | 0.00      | 0.00               | 4.34 | 0.13 | 0.00   |
| 52.5     | 0.08    | 0.15    | 0.05      | 0.00      | 0.00               | 3.81 | 0.10 | 0.00   |
| 53.5     | 0.07    | 0.14    | 0.05      | 0.00      | 0.00               | 3.41 | 0.08 | 0.00   |

Appendix B – Contributions of species to the chlorine budgets

Table B9: The percentage contribution of HCl, CCl<sub>4</sub>, CFC-12, CFC-11, COClF, COCl<sub>2</sub>, HCFC-22, CH<sub>3</sub>Cl & CFC-113 to the total chlorine budget in the latitude bands between 0° N and 30° S (evening occultations)

| Altitude | HCl   | CCl <sub>4</sub> | CFC-12 | CFC-11 | COClF | COCl <sub>2</sub> | HCFC-22 | CH <sub>3</sub> Cl | CFC-113 |
|----------|-------|------------------|--------|--------|-------|-------------------|---------|--------------------|---------|
| 10.5     | 0.11  | 12.70            | 30.75  | 22.12  | 0.21  | 0.01              | 5.90    | 18.42              | 6.80    |
| 11.5     | 0.20  | 12.61            | 30.72  | 22.10  | 0.24  | 0.01              | 5.89    | 18.40              | 6.79    |
| 12.5     | 0.18  | 12.47            | 30.74  | 22.11  | 0.29  | 0.02              | 5.90    | 18.41              | 6.78    |
| 13.5     | 0.21  | 12.37            | 30.72  | 22.10  | 0.38  | 0.02              | 5.89    | 18.40              | 6.76    |
| 14.5     | 0.24  | 12.32            | 30.68  | 22.07  | 0.50  | 0.03              | 5.88    | 18.38              | 6.72    |
| 15.5     | 0.48  | 12.11            | 30.54  | 22.07  | 0.63  | 0.04              | 5.84    | 18.36              | 6.65    |
| 16.5     | 1.14  | 11.90            | 30.54  | 21.75  | 0.87  | 0.07              | 5.80    | 17.89              | 6.57    |
| 17.5     | 2.79  | 11.45            | 30.34  | 21.24  | 0.99  | 0.14              | 5.73    | 17.16              | 6.38    |
| 18.5     | 6.57  | 10.56            | 29.67  | 20.01  | 1.10  | 0.32              | 5.79    | 15.91              | 6.04    |
| 19.5     | 11.77 | 9.34             | 28.65  | 18.29  | 1.26  | 0.62              | 5.67    | 14.45              | 5.64    |
| 20.5     | 17.58 | 8.00             | 27.37  | 16.30  | 1.52  | 0.90              | 5.07    | 12.54              | 5.29    |
| 21.5     | 22.01 | 6.65             | 26.03  | 14.08  | 1.74  | 1.26              | 4.73    | 10.84              | 5.02    |
| 22.5     | 25.18 | 5.09             | 24.78  | 11.74  | 1.85  | 1.51              | 4.43    | 10.15              | 4.74    |
| 23.5     | 27.95 | 3.87             | 23.22  | 9.33   | 1.84  | 1.73              | 4.24    | 9.57               | 4.41    |
| 24.5     | 30.83 | 2.78             | 22.08  | 6.95   | 1.81  | 1.90              | 4.02    | 8.45               | 4.13    |
| 25.5     | 33.92 | 1.62             | 20.49  | 4.95   | 1.65  | 2.01              | 3.95    | 7.25               | 3.80    |
| 26.5     | 37.13 | 0.81             | 18.88  | 3.24   | 1.45  | 1.98              | 3.86    | 6.32               | 3.38    |
| 27.5     | 40.32 | 0.43             | 17.45  | 2.06   | 0.99  | 1.76              | 3.84    | 5.59               | 2.99    |
| 28.5     | 44.06 | 0.16             | 15.92  | 1.11   | 0.84  | 1.44              | 3.77    | 5.01               | 2.58    |
| 29.5     | 48.40 | 0.09             | 14.26  | 0.67   | 0.68  | 1.13              | 3.70    | 4.41               | 2.20    |
| 30.5     | 53.83 | 0.02             | 12.24  | 0.25   | 0.53  | 0.76              | 3.64    | 3.58               | 1.82    |
| 31.5     | 58.91 | 0.01             | 10.19  | 0.09   | 0.38  | 0.44              | 3.54    | 2.92               | 1.47    |
| 32.5     | 64.07 | 0.01             | 8.13   | 0.05   | 0.25  | 0.29              | 3.42    | 2.40               | 1.13    |
| 33.5     | 68.16 | 0.01             | 6.09   | 0.01   | 0.13  | 0.16              | 3.26    | 1.93               | 0.80    |
| 34.5     | 71.58 | 0.01             | 4.74   | 0.01   | 0.09  | 0.10              | 3.12    | 1.59               | 0.60    |
| 35.5     | 73.85 | 0.00             | 3.43   | 0.01   | 0.05  | 0.06              | 2.95    | 1.26               | 0.41    |
| 36.5     | 75.82 | 0.00             | 2.47   | 0.00   | 0.02  | 0.03              | 2.78    | 0.99               | 0.28    |
| 37.5     | 77.48 | 0.00             | 1.81   | 0.00   | 0.02  | 0.02              | 2.63    | 0.78               | 0.19    |
| 38.5     | 79.07 | 0.00             | 1.22   | 0.00   | 0.01  | 0.01              | 2.49    | 0.59               | 0.12    |
| 39.5     | 80.49 | 0.00             | 0.88   | 0.00   | 0.00  | 0.01              | 2.34    | 0.45               | 0.08    |
| 40.5     | 81.88 | 0.00             | 0.57   | 0.00   | 0.00  | 0.00              | 2.18    | 0.32               | 0.05    |
| 41.5     | 83.14 | 0.00             | 0.35   | 0.00   | 0.00  | 0.00              | 2.02    | 0.22               | 0.03    |
| 42.5     | 84.47 | 0.00             | 0.24   | 0.00   | 0.00  | 0.00              | 1.87    | 0.16               | 0.02    |
| 43.5     | 85.83 | 0.00             | 0.13   | 0.00   | 0.00  | 0.00              | 1.72    | 0.10               | 0.01    |
| 44.5     | 87.16 | 0.00             | 0.08   | 0.00   | 0.00  | 0.00              | 1.59    | 0.07               | 0.01    |

Appendix B – Contributions of species to the chlorine budgets

Table B9 Continued

| Altitude | HCl   | CCl <sub>4</sub> | CFC-12 | CFC-11 | COClF | COCl <sub>2</sub> | HCFC-22 | CH <sub>3</sub> Cl | CFC-113 |
|----------|-------|------------------|--------|--------|-------|-------------------|---------|--------------------|---------|
| 45.5     | 88.31 | 0.00             | 0.05   | 0.00   | 0.00  | 0.00              | 1.48    | 0.05               | 0.00    |
| 46.5     | 89.39 | 0.00             | 0.03   | 0.00   | 0.00  | 0.00              | 1.37    | 0.03               | 0.00    |
| 47.5     | 90.45 | 0.00             | 0.01   | 0.00   | 0.00  | 0.00              | 1.29    | 0.02               | 0.00    |
| 48.5     | 91.37 | 0.00             | 0.01   | 0.00   | 0.00  | 0.00              | 1.24    | 0.02               | 0.00    |
| 49.5     | 92.26 | 0.00             | 0.01   | 0.00   | 0.00  | 0.00              | 1.18    | 0.01               | 0.00    |
| 50.5     | 92.95 | 0.00             | 0.00   | 0.00   | 0.00  | 0.00              | 1.13    | 0.01               | 0.00    |
| 51.5     | 93.55 | 0.00             | 0.00   | 0.00   | 0.00  | 0.00              | 1.10    | 0.01               | 0.00    |
| 52.5     | 94.19 | 0.00             | 0.00   | 0.00   | 0.00  | 0.00              | 1.08    | 0.01               | 0.00    |
| 53.5     | 94.66 | 0.00             | 0.00   | 0.00   | 0.00  | 0.00              | 1.06    | 0.00               | 0.00    |

Appendix B – Contributions of species to the chlorine budgets

Table B10: The percentage contribution of CFC-114, CFC-115, HCFC-142b, HCFC-141b, ClONO<sub>2</sub>, ClO, HOCl & H-1211 to the total chlorine budget in the latitude bands between 0° N and 30° S (evening occultations)

| Altitude | CFC-114 | CFC-115 | HCFC-142b | HCFC-141b | ClONO <sub>2</sub> | ClO   | HOCl | H-1211 |
|----------|---------|---------|-----------|-----------|--------------------|-------|------|--------|
| 10.5     | 0.98    | 0.27    | 0.46      | 1.09      | 0.04               | 0.00  | 0.02 | 0.12   |
| 11.5     | 0.98    | 0.27    | 0.46      | 1.09      | 0.09               | 0.00  | 0.02 | 0.12   |
| 12.5     | 0.98    | 0.27    | 0.46      | 1.08      | 0.17               | 0.00  | 0.02 | 0.12   |
| 13.5     | 0.98    | 0.27    | 0.46      | 1.08      | 0.23               | 0.00  | 0.02 | 0.12   |
| 14.5     | 0.97    | 0.27    | 0.45      | 1.07      | 0.29               | 0.00  | 0.01 | 0.12   |
| 15.5     | 0.97    | 0.26    | 0.45      | 1.06      | 0.42               | 0.00  | 0.01 | 0.12   |
| 16.5     | 0.96    | 0.26    | 0.45      | 1.03      | 0.64               | 0.00  | 0.01 | 0.11   |
| 17.5     | 0.94    | 0.26    | 0.43      | 0.99      | 1.04               | 0.00  | 0.01 | 0.10   |
| 18.5     | 0.90    | 0.26    | 0.41      | 0.92      | 1.43               | 0.01  | 0.01 | 0.09   |
| 19.5     | 0.86    | 0.25    | 0.39      | 0.85      | 1.86               | 0.01  | 0.01 | 0.07   |
| 20.5     | 0.82    | 0.25    | 0.37      | 0.78      | 3.10               | 0.02  | 0.03 | 0.06   |
| 21.5     | 0.80    | 0.24    | 0.36      | 0.72      | 5.35               | 0.06  | 0.06 | 0.04   |
| 22.5     | 0.78    | 0.24    | 0.35      | 0.66      | 8.23               | 0.12  | 0.12 | 0.03   |
| 23.5     | 0.75    | 0.24    | 0.34      | 0.60      | 11.45              | 0.23  | 0.22 | 0.01   |
| 24.5     | 0.74    | 0.24    | 0.33      | 0.54      | 14.44              | 0.40  | 0.35 | 0.01   |
| 25.5     | 0.73    | 0.24    | 0.33      | 0.47      | 17.47              | 0.62  | 0.51 | 0.00   |
| 26.5     | 0.71    | 0.24    | 0.32      | 0.39      | 19.80              | 0.80  | 0.68 | 0.00   |
| 27.5     | 0.70    | 0.24    | 0.32      | 0.33      | 21.20              | 0.97  | 0.83 | 0.00   |
| 28.5     | 0.68    | 0.24    | 0.31      | 0.26      | 21.56              | 1.16  | 0.89 | 0.00   |
| 29.5     | 0.66    | 0.23    | 0.30      | 0.21      | 20.70              | 1.34  | 1.02 | 0.00   |
| 30.5     | 0.64    | 0.23    | 0.29      | 0.15      | 19.06              | 1.79  | 1.16 | 0.00   |
| 31.5     | 0.61    | 0.23    | 0.28      | 0.11      | 16.94              | 2.58  | 1.30 | 0.00   |
| 32.5     | 0.57    | 0.23    | 0.27      | 0.08      | 14.52              | 3.13  | 1.46 | 0.00   |
| 33.5     | 0.53    | 0.23    | 0.25      | 0.04      | 12.11              | 4.66  | 1.62 | 0.00   |
| 34.5     | 0.50    | 0.22    | 0.24      | 0.03      | 9.12               | 6.26  | 1.80 | 0.00   |
| 35.5     | 0.46    | 0.22    | 0.22      | 0.02      | 7.40               | 7.80  | 1.88 | 0.00   |
| 36.5     | 0.42    | 0.21    | 0.21      | 0.01      | 5.68               | 9.20  | 1.88 | 0.00   |
| 37.5     | 0.38    | 0.21    | 0.19      | 0.01      | 4.31               | 10.12 | 1.85 | 0.00   |
| 38.5     | 0.35    | 0.20    | 0.18      | 0.00      | 2.98               | 11.02 | 1.76 | 0.00   |
| 39.5     | 0.31    | 0.20    | 0.16      | 0.00      | 1.87               | 11.62 | 1.57 | 0.00   |
| 40.5     | 0.28    | 0.19    | 0.15      | 0.00      | 1.04               | 11.92 | 1.40 | 0.00   |
| 41.5     | 0.25    | 0.19    | 0.13      | 0.00      | 0.58               | 11.89 | 1.19 | 0.00   |
| 42.5     | 0.22    | 0.18    | 0.12      | 0.00      | 0.29               | 11.43 | 1.00 | 0.00   |
| 43.5     | 0.19    | 0.18    | 0.11      | 0.00      | 0.14               | 10.78 | 0.82 | 0.00   |
| 44.5     | 0.17    | 0.17    | 0.10      | 0.00      | 0.07               | 9.93  | 0.67 | 0.00   |

Appendix B – Contributions of species to the chlorine budgets

Table B10 Continued

| Altitude | CFC-114 | CFC-115 | HCFC-142b | HCFC-141b | ClONO <sub>2</sub> | ClO  | HOCl | H-1211 |
|----------|---------|---------|-----------|-----------|--------------------|------|------|--------|
| 45.5     | 0.15    | 0.17    | 0.09      | 0.00      | 0.03               | 9.15 | 0.52 | 0.00   |
| 46.5     | 0.13    | 0.16    | 0.08      | 0.00      | 0.01               | 8.39 | 0.41 | 0.00   |
| 47.5     | 0.11    | 0.16    | 0.07      | 0.00      | 0.01               | 7.55 | 0.33 | 0.00   |
| 48.5     | 0.10    | 0.15    | 0.07      | 0.00      | 0.00               | 6.78 | 0.26 | 0.00   |
| 49.5     | 0.09    | 0.15    | 0.06      | 0.00      | 0.00               | 6.03 | 0.20 | 0.00   |
| 50.5     | 0.08    | 0.15    | 0.06      | 0.00      | 0.00               | 5.44 | 0.17 | 0.00   |
| 51.5     | 0.08    | 0.15    | 0.06      | 0.00      | 0.00               | 4.91 | 0.14 | 0.00   |
| 52.5     | 0.07    | 0.15    | 0.05      | 0.00      | 0.00               | 4.35 | 0.10 | 0.00   |
| 53.5     | 0.07    | 0.14    | 0.05      | 0.00      | 0.00               | 3.93 | 0.08 | 0.00   |

Appendix B – Contributions of species to the chlorine budgets

Table B11: The percentage contribution of HCl, CCl<sub>4</sub>, CFC-12, CFC-11, COClF, COCl<sub>2</sub>, HCFC-22, CH<sub>3</sub>Cl & CFC-113 to the total chlorine budget in the latitude bands between 0° N and 30° S (morning occultations)

| Altitude | HCl   | CCl <sub>4</sub> | CFC-12 | CFC-11 | COClF | COCl <sub>2</sub> | HCFC-22 | CH <sub>3</sub> Cl | CFC-113 |
|----------|-------|------------------|--------|--------|-------|-------------------|---------|--------------------|---------|
| 10.5     | 0.11  | 12.70            | 30.74  | 22.11  | 0.21  | 0.01              | 5.89    | 18.41              | 6.80    |
| 11.5     | 0.20  | 12.61            | 30.71  | 22.09  | 0.24  | 0.01              | 5.89    | 18.39              | 6.79    |
| 12.5     | 0.18  | 12.46            | 30.72  | 22.10  | 0.29  | 0.02              | 5.89    | 18.40              | 6.78    |
| 13.5     | 0.21  | 12.36            | 30.70  | 22.08  | 0.38  | 0.02              | 5.89    | 18.39              | 6.75    |
| 14.5     | 0.24  | 12.30            | 30.65  | 22.04  | 0.50  | 0.03              | 5.88    | 18.36              | 6.72    |
| 15.5     | 0.48  | 12.10            | 30.49  | 22.04  | 0.63  | 0.04              | 5.83    | 18.33              | 6.65    |
| 16.5     | 1.14  | 11.88            | 30.47  | 21.70  | 0.87  | 0.07              | 5.78    | 17.86              | 6.56    |
| 17.5     | 2.78  | 11.41            | 30.23  | 21.17  | 0.99  | 0.14              | 5.71    | 17.10              | 6.35    |
| 18.5     | 6.54  | 10.51            | 29.53  | 19.91  | 1.09  | 0.32              | 5.76    | 15.84              | 6.01    |
| 19.5     | 11.69 | 9.28             | 28.47  | 18.17  | 1.25  | 0.61              | 5.63    | 14.36              | 5.60    |
| 20.5     | 17.41 | 7.92             | 27.10  | 16.14  | 1.50  | 0.89              | 5.02    | 12.42              | 5.24    |
| 21.5     | 21.74 | 6.56             | 25.71  | 13.91  | 1.72  | 1.24              | 4.67    | 10.70              | 4.96    |
| 22.5     | 24.86 | 5.03             | 24.46  | 11.59  | 1.83  | 1.49              | 4.38    | 10.02              | 4.68    |
| 23.5     | 27.64 | 3.83             | 22.96  | 9.23   | 1.82  | 1.71              | 4.19    | 9.46               | 4.37    |
| 24.5     | 30.44 | 2.74             | 21.80  | 6.86   | 1.78  | 1.87              | 3.97    | 8.34               | 4.08    |
| 25.5     | 33.49 | 1.60             | 20.24  | 4.88   | 1.63  | 1.98              | 3.90    | 7.16               | 3.75    |
| 26.5     | 36.56 | 0.80             | 18.59  | 3.19   | 1.43  | 1.95              | 3.80    | 6.22               | 3.32    |
| 27.5     | 39.58 | 0.43             | 17.12  | 2.03   | 0.97  | 1.72              | 3.76    | 5.49               | 2.93    |
| 28.5     | 43.13 | 0.16             | 15.58  | 1.08   | 0.82  | 1.41              | 3.69    | 4.91               | 2.53    |
| 29.5     | 47.11 | 0.09             | 13.88  | 0.66   | 0.66  | 1.10              | 3.60    | 4.29               | 2.14    |
| 30.5     | 52.26 | 0.02             | 11.88  | 0.24   | 0.51  | 0.74              | 3.53    | 3.48               | 1.77    |
| 31.5     | 57.16 | 0.00             | 9.89   | 0.08   | 0.37  | 0.42              | 3.44    | 2.84               | 1.42    |
| 32.5     | 61.96 | 0.01             | 7.86   | 0.04   | 0.25  | 0.28              | 3.30    | 2.32               | 1.09    |
| 33.5     | 66.65 | 0.01             | 5.96   | 0.01   | 0.13  | 0.15              | 3.19    | 1.88               | 0.78    |
| 34.5     | 70.57 | 0.01             | 4.67   | 0.01   | 0.09  | 0.10              | 3.07    | 1.57               | 0.59    |
| 35.5     | 74.27 | 0.00             | 3.45   | 0.01   | 0.05  | 0.06              | 2.97    | 1.27               | 0.41    |
| 36.5     | 77.43 | 0.00             | 2.52   | 0.00   | 0.03  | 0.03              | 2.84    | 1.01               | 0.28    |
| 37.5     | 79.89 | 0.00             | 1.87   | 0.00   | 0.02  | 0.02              | 2.71    | 0.81               | 0.20    |
| 38.5     | 81.98 | 0.00             | 1.27   | 0.00   | 0.01  | 0.01              | 2.58    | 0.61               | 0.12    |
| 39.5     | 83.67 | 0.00             | 0.92   | 0.00   | 0.01  | 0.01              | 2.43    | 0.47               | 0.09    |
| 40.5     | 85.04 | 0.00             | 0.59   | 0.00   | 0.00  | 0.00              | 2.26    | 0.33               | 0.05    |
| 41.5     | 86.13 | 0.00             | 0.37   | 0.00   | 0.00  | 0.00              | 2.09    | 0.23               | 0.03    |
| 42.5     | 86.82 | 0.00             | 0.25   | 0.00   | 0.00  | 0.00              | 1.92    | 0.17               | 0.02    |
| 43.5     | 87.67 | 0.00             | 0.13   | 0.00   | 0.00  | 0.00              | 1.75    | 0.11               | 0.01    |
| 44.5     | 88.47 | 0.00             | 0.08   | 0.00   | 0.00  | 0.00              | 1.62    | 0.07               | 0.01    |

Appendix B – Contributions of species to the chlorine budgets

Table B11 Continued

| Altitude | HCl   | CCl <sub>4</sub> | CFC-12 | CFC-11 | COClF | COCl <sub>2</sub> | HCFC-22 | CH <sub>3</sub> Cl | CFC-113 |
|----------|-------|------------------|--------|--------|-------|-------------------|---------|--------------------|---------|
| 45.5     | 89.20 | 0.00             | 0.05   | 0.00   | 0.00  | 0.00              | 1.49    | 0.05               | 0.00    |
| 46.5     | 89.92 | 0.00             | 0.03   | 0.00   | 0.00  | 0.00              | 1.38    | 0.03               | 0.00    |
| 47.5     | 90.69 | 0.00             | 0.01   | 0.00   | 0.00  | 0.00              | 1.29    | 0.02               | 0.00    |
| 48.5     | 91.35 | 0.00             | 0.01   | 0.00   | 0.00  | 0.00              | 1.23    | 0.02               | 0.00    |
| 49.5     | 92.07 | 0.00             | 0.01   | 0.00   | 0.00  | 0.00              | 1.18    | 0.01               | 0.00    |
| 50.5     | 92.81 | 0.00             | 0.00   | 0.00   | 0.00  | 0.00              | 1.13    | 0.01               | 0.00    |
| 51.5     | 93.49 | 0.00             | 0.00   | 0.00   | 0.00  | 0.00              | 1.10    | 0.01               | 0.00    |
| 52.5     | 94.18 | 0.00             | 0.00   | 0.00   | 0.00  | 0.00              | 1.08    | 0.01               | 0.00    |
| 53.5     | 94.77 | 0.00             | 0.00   | 0.00   | 0.00  | 0.00              | 1.06    | 0.00               | 0.00    |

Appendix B – Contributions of species to the chlorine budgets

Table B12: The percentage contribution of CFC-114, CFC-115, HCFC-142b, HCFC-141b, ClONO<sub>2</sub>, ClO, HOCl & H-1211 to the total chlorine budget in the latitude bands between 0° N and 30° S (morning occultations)

| Altitude | CFC-114 | CFC-115 | HCFC-142b | HCFC-141b | ClONO <sub>2</sub> | ClO  | HOCl | H-1211 |
|----------|---------|---------|-----------|-----------|--------------------|------|------|--------|
| 10.5     | 0.98    | 0.27    | 0.46      | 1.09      | 0.05               | 0.01 | 0.04 | 0.12   |
| 11.5     | 0.98    | 0.27    | 0.46      | 1.09      | 0.12               | 0.01 | 0.04 | 0.12   |
| 12.5     | 0.98    | 0.27    | 0.46      | 1.08      | 0.22               | 0.01 | 0.03 | 0.12   |
| 13.5     | 0.98    | 0.27    | 0.46      | 1.08      | 0.30               | 0.01 | 0.03 | 0.12   |
| 14.5     | 0.97    | 0.26    | 0.45      | 1.07      | 0.39               | 0.01 | 0.02 | 0.12   |
| 15.5     | 0.96    | 0.26    | 0.45      | 1.05      | 0.55               | 0.01 | 0.01 | 0.12   |
| 16.5     | 0.96    | 0.26    | 0.44      | 1.03      | 0.85               | 0.01 | 0.01 | 0.11   |
| 17.5     | 0.93    | 0.26    | 0.43      | 0.99      | 1.37               | 0.02 | 0.01 | 0.10   |
| 18.5     | 0.90    | 0.26    | 0.41      | 0.92      | 1.88               | 0.03 | 0.01 | 0.09   |
| 19.5     | 0.85    | 0.25    | 0.39      | 0.84      | 2.45               | 0.05 | 0.01 | 0.07   |
| 20.5     | 0.82    | 0.25    | 0.37      | 0.77      | 3.98               | 0.09 | 0.03 | 0.06   |
| 21.5     | 0.79    | 0.24    | 0.36      | 0.71      | 6.41               | 0.18 | 0.05 | 0.04   |
| 22.5     | 0.77    | 0.24    | 0.35      | 0.65      | 9.26               | 0.28 | 0.09 | 0.03   |
| 23.5     | 0.75    | 0.23    | 0.34      | 0.59      | 12.33              | 0.39 | 0.16 | 0.01   |
| 24.5     | 0.73    | 0.23    | 0.33      | 0.53      | 15.47              | 0.55 | 0.27 | 0.01   |
| 25.5     | 0.72    | 0.23    | 0.32      | 0.47      | 18.41              | 0.80 | 0.41 | 0.00   |
| 26.5     | 0.70    | 0.23    | 0.32      | 0.39      | 20.87              | 1.06 | 0.57 | 0.00   |
| 27.5     | 0.69    | 0.23    | 0.31      | 0.32      | 22.51              | 1.22 | 0.69 | 0.00   |
| 28.5     | 0.67    | 0.23    | 0.30      | 0.26      | 23.11              | 1.37 | 0.76 | 0.00   |
| 29.5     | 0.64    | 0.23    | 0.29      | 0.20      | 22.77              | 1.51 | 0.83 | 0.00   |
| 30.5     | 0.62    | 0.23    | 0.28      | 0.15      | 21.68              | 1.68 | 0.93 | 0.00   |
| 31.5     | 0.59    | 0.23    | 0.27      | 0.11      | 20.28              | 1.83 | 1.06 | 0.00   |
| 32.5     | 0.56    | 0.22    | 0.26      | 0.07      | 18.62              | 1.98 | 1.17 | 0.00   |
| 33.5     | 0.52    | 0.22    | 0.25      | 0.04      | 16.71              | 2.21 | 1.28 | 0.00   |
| 34.5     | 0.49    | 0.22    | 0.23      | 0.03      | 14.51              | 2.46 | 1.39 | 0.00   |
| 35.5     | 0.46    | 0.22    | 0.22      | 0.02      | 12.25              | 2.90 | 1.46 | 0.00   |
| 36.5     | 0.43    | 0.21    | 0.21      | 0.01      | 9.82               | 3.68 | 1.49 | 0.00   |
| 37.5     | 0.39    | 0.21    | 0.20      | 0.01      | 7.75               | 4.46 | 1.47 | 0.00   |
| 38.5     | 0.36    | 0.21    | 0.18      | 0.00      | 5.65               | 5.62 | 1.38 | 0.00   |
| 39.5     | 0.33    | 0.21    | 0.17      | 0.00      | 3.81               | 6.64 | 1.27 | 0.00   |
| 40.5     | 0.29    | 0.20    | 0.15      | 0.00      | 2.39               | 7.54 | 1.13 | 0.00   |
| 41.5     | 0.26    | 0.19    | 0.14      | 0.00      | 1.45               | 8.14 | 0.97 | 0.00   |
| 42.5     | 0.22    | 0.19    | 0.12      | 0.00      | 0.81               | 8.65 | 0.83 | 0.00   |
| 43.5     | 0.19    | 0.18    | 0.11      | 0.00      | 0.41               | 8.72 | 0.70 | 0.00   |
| 44.5     | 0.17    | 0.17    | 0.10      | 0.00      | 0.22               | 8.51 | 0.59 | 0.00   |

Appendix B – Contributions of species to the chlorine budgets

| Table B12 Continued |         |         |           |           |                    |      |      |        |
|---------------------|---------|---------|-----------|-----------|--------------------|------|------|--------|
| Altitude            | CFC-114 | CFC-115 | HCFC-142b | HCFC-141b | ClONO <sub>2</sub> | ClO  | HOCl | H-1211 |
| 45.5                | 0.15    | 0.17    | 0.09      | 0.00      | 0.10               | 8.20 | 0.48 | 0.00   |
| 46.5                | 0.13    | 0.16    | 0.08      | 0.00      | 0.05               | 7.83 | 0.40 | 0.00   |
| 47.5                | 0.11    | 0.16    | 0.07      | 0.00      | 0.03               | 7.28 | 0.33 | 0.00   |
| 48.5                | 0.10    | 0.15    | 0.07      | 0.00      | 0.01               | 6.80 | 0.26 | 0.00   |
| 49.5                | 0.09    | 0.15    | 0.06      | 0.00      | 0.01               | 6.21 | 0.22 | 0.00   |
| 50.5                | 0.08    | 0.15    | 0.06      | 0.00      | 0.00               | 5.57 | 0.18 | 0.00   |
| 51.5                | 0.08    | 0.15    | 0.06      | 0.00      | 0.00               | 4.97 | 0.15 | 0.00   |
| 52.5                | 0.07    | 0.15    | 0.05      | 0.00      | 0.00               | 4.34 | 0.12 | 0.00   |
| 53.5                | 0.07    | 0.14    | 0.05      | 0.00      | 0.00               | 3.81 | 0.09 | 0.00   |

Appendix B – Contributions of species to the chlorine budgets

Table B13: The percentage contribution of HCl, CCl<sub>4</sub>, CFC-12, CFC-11, COClF, COCl<sub>2</sub>, HCFC-22, CH<sub>3</sub>Cl & CFC-113 to the total chlorine budget in the latitude bands between 30° S and 70° S (evening occultations)

| Altitude | HCl   | CCl <sub>4</sub> | CFC-12 | CFC-11 | COClF | COCl <sub>2</sub> | HCFC-22 | CH <sub>3</sub> Cl | CFC-113 |
|----------|-------|------------------|--------|--------|-------|-------------------|---------|--------------------|---------|
| 10.5     | 5.53  | 11.60            | 29.44  | 20.51  | 1.06  | 0.19              | 5.35    | 16.63              | 6.54    |
| 11.5     | 7.51  | 11.07            | 29.01  | 20.02  | 1.13  | 0.32              | 5.35    | 15.93              | 6.23    |
| 12.5     | 9.01  | 10.49            | 28.71  | 19.61  | 1.19  | 0.46              | 5.39    | 15.34              | 5.92    |
| 13.5     | 10.76 | 9.99             | 28.18  | 19.03  | 1.22  | 0.55              | 5.40    | 14.86              | 5.67    |
| 14.5     | 13.35 | 9.36             | 27.26  | 18.04  | 1.23  | 0.64              | 5.35    | 14.15              | 5.42    |
| 15.5     | 17.44 | 8.51             | 26.04  | 16.47  | 1.25  | 0.74              | 5.17    | 12.69              | 5.16    |
| 16.5     | 23.46 | 7.41             | 24.40  | 14.32  | 1.28  | 0.87              | 4.76    | 10.85              | 4.81    |
| 17.5     | 30.15 | 6.14             | 22.34  | 11.81  | 1.28  | 0.99              | 4.32    | 8.95               | 4.36    |
| 18.5     | 36.37 | 4.85             | 20.19  | 9.17   | 1.27  | 1.12              | 4.02    | 7.34               | 3.84    |
| 19.5     | 41.39 | 3.73             | 18.13  | 6.61   | 1.17  | 1.19              | 3.80    | 6.01               | 3.34    |
| 20.5     | 45.38 | 2.82             | 16.17  | 4.27   | 0.97  | 1.21              | 3.61    | 4.96               | 2.93    |
| 21.5     | 48.49 | 2.10             | 14.31  | 2.59   | 0.75  | 1.15              | 3.46    | 4.07               | 2.58    |
| 22.5     | 51.08 | 1.37             | 12.57  | 1.74   | 0.56  | 0.98              | 3.34    | 3.23               | 2.25    |
| 23.5     | 53.52 | 0.79             | 10.95  | 1.15   | 0.42  | 0.79              | 3.23    | 2.53               | 1.91    |
| 24.5     | 55.75 | 0.39             | 9.42   | 0.68   | 0.37  | 0.66              | 3.14    | 1.96               | 1.59    |
| 25.5     | 58.01 | 0.16             | 8.03   | 0.36   | 0.30  | 0.53              | 3.06    | 1.53               | 1.29    |
| 26.5     | 60.30 | 0.07             | 6.79   | 0.18   | 0.24  | 0.43              | 2.98    | 1.20               | 1.03    |
| 27.5     | 62.82 | 0.03             | 5.56   | 0.10   | 0.18  | 0.33              | 2.89    | 0.96               | 0.82    |
| 28.5     | 65.42 | 0.01             | 4.46   | 0.04   | 0.13  | 0.23              | 2.79    | 0.81               | 0.63    |
| 29.5     | 67.93 | 0.00             | 3.59   | 0.02   | 0.09  | 0.17              | 2.69    | 0.65               | 0.48    |
| 30.5     | 70.17 | 0.00             | 2.80   | 0.01   | 0.06  | 0.11              | 2.60    | 0.54               | 0.36    |
| 31.5     | 72.11 | 0.00             | 2.13   | 0.00   | 0.03  | 0.06              | 2.51    | 0.44               | 0.25    |
| 32.5     | 73.59 | 0.00             | 1.63   | 0.00   | 0.02  | 0.04              | 2.42    | 0.36               | 0.18    |
| 33.5     | 74.83 | 0.00             | 1.17   | 0.00   | 0.01  | 0.02              | 2.32    | 0.28               | 0.12    |
| 34.5     | 76.57 | 0.00             | 0.85   | 0.00   | 0.01  | 0.01              | 2.24    | 0.23               | 0.08    |
| 35.5     | 77.41 | 0.00             | 0.61   | 0.00   | 0.00  | 0.01              | 2.14    | 0.18               | 0.06    |
| 36.5     | 77.75 | 0.00             | 0.42   | 0.00   | 0.00  | 0.00              | 2.03    | 0.14               | 0.04    |
| 37.5     | 77.96 | 0.00             | 0.31   | 0.00   | 0.00  | 0.00              | 1.92    | 0.11               | 0.03    |
| 38.5     | 78.47 | 0.00             | 0.21   | 0.00   | 0.00  | 0.00              | 1.83    | 0.09               | 0.02    |
| 39.5     | 78.85 | 0.00             | 0.15   | 0.00   | 0.00  | 0.00              | 1.73    | 0.06               | 0.01    |
| 40.5     | 79.44 | 0.00             | 0.10   | 0.00   | 0.00  | 0.00              | 1.63    | 0.05               | 0.01    |
| 41.5     | 80.26 | 0.00             | 0.07   | 0.00   | 0.00  | 0.00              | 1.54    | 0.03               | 0.00    |
| 42.5     | 81.27 | 0.00             | 0.04   | 0.00   | 0.00  | 0.00              | 1.46    | 0.02               | 0.00    |
| 43.5     | 82.51 | 0.00             | 0.03   | 0.00   | 0.00  | 0.00              | 1.38    | 0.02               | 0.00    |
| 44.5     | 84.01 | 0.00             | 0.02   | 0.00   | 0.00  | 0.00              | 1.31    | 0.01               | 0.00    |

Appendix B – Contributions of species to the chlorine budgets

Table B13 Continued

| Altitude | HCl   | CCl <sub>4</sub> | CFC-12 | CFC-11 | COClF | COCl <sub>2</sub> | HCFC-22 | CH <sub>3</sub> Cl | CFC-113 |
|----------|-------|------------------|--------|--------|-------|-------------------|---------|--------------------|---------|
| 45.5     | 85.58 | 0.00             | 0.01   | 0.00   | 0.00  | 0.00              | 1.25    | 0.01               | 0.00    |
| 46.5     | 87.22 | 0.00             | 0.01   | 0.00   | 0.00  | 0.00              | 1.20    | 0.01               | 0.00    |
| 47.5     | 88.79 | 0.00             | 0.00   | 0.00   | 0.00  | 0.00              | 1.15    | 0.00               | 0.00    |
| 48.5     | 90.20 | 0.00             | 0.00   | 0.00   | 0.00  | 0.00              | 1.12    | 0.00               | 0.00    |
| 49.5     | 91.40 | 0.00             | 0.00   | 0.00   | 0.00  | 0.00              | 1.10    | 0.00               | 0.00    |
| 50.5     | 92.42 | 0.00             | 0.00   | 0.00   | 0.00  | 0.00              | 1.08    | 0.00               | 0.00    |
| 51.5     | 93.23 | 0.00             | 0.00   | 0.00   | 0.00  | 0.00              | 1.06    | 0.00               | 0.00    |
| 52.5     | 93.86 | 0.00             | 0.00   | 0.00   | 0.00  | 0.00              | 1.04    | 0.00               | 0.00    |
| 53.5     | 94.37 | 0.00             | 0.00   | 0.00   | 0.00  | 0.00              | 1.03    | 0.00               | 0.00    |

Appendix B – Contributions of species to the chlorine budgets

Table B14: The percentage contribution of CFC-114, CFC-115, HCFC-142b, HCFC-141b, ClONO<sub>2</sub>, ClO, HOCl & H-1211 to the total chlorine budget in the latitude bands between 30° S and 70° S (evening occultations)

| Altitude | CFC-114 | CFC-115 | HCFC-142b | HCFC-141b | ClONO <sub>2</sub> | ClO   | HOCl | H-1211 |
|----------|---------|---------|-----------|-----------|--------------------|-------|------|--------|
| 10.5     | 0.96    | 0.27    | 0.44      | 1.03      | 0.27               | 0.02  | 0.05 | 0.11   |
| 11.5     | 0.92    | 0.26    | 0.43      | 0.97      | 0.66               | 0.03  | 0.05 | 0.10   |
| 12.5     | 0.89    | 0.26    | 0.41      | 0.91      | 1.22               | 0.04  | 0.06 | 0.09   |
| 13.5     | 0.86    | 0.26    | 0.40      | 0.86      | 1.76               | 0.06  | 0.06 | 0.09   |
| 14.5     | 0.84    | 0.25    | 0.38      | 0.82      | 2.68               | 0.09  | 0.07 | 0.08   |
| 15.5     | 0.81    | 0.25    | 0.37      | 0.77      | 4.03               | 0.13  | 0.09 | 0.07   |
| 16.5     | 0.77    | 0.25    | 0.35      | 0.71      | 5.46               | 0.15  | 0.11 | 0.06   |
| 17.5     | 0.72    | 0.24    | 0.33      | 0.63      | 7.34               | 0.22  | 0.13 | 0.05   |
| 18.5     | 0.67    | 0.23    | 0.30      | 0.54      | 9.58               | 0.32  | 0.16 | 0.04   |
| 19.5     | 0.61    | 0.22    | 0.27      | 0.45      | 12.44              | 0.43  | 0.18 | 0.02   |
| 20.5     | 0.57    | 0.22    | 0.26      | 0.38      | 15.49              | 0.55  | 0.19 | 0.01   |
| 21.5     | 0.54    | 0.21    | 0.24      | 0.32      | 18.36              | 0.60  | 0.22 | 0.01   |
| 22.5     | 0.51    | 0.21    | 0.23      | 0.27      | 20.81              | 0.63  | 0.23 | 0.00   |
| 23.5     | 0.49    | 0.21    | 0.22      | 0.22      | 22.74              | 0.60  | 0.24 | 0.00   |
| 24.5     | 0.46    | 0.20    | 0.21      | 0.17      | 24.09              | 0.69  | 0.23 | 0.00   |
| 25.5     | 0.44    | 0.20    | 0.20      | 0.12      | 24.74              | 0.78  | 0.24 | 0.00   |
| 26.5     | 0.42    | 0.20    | 0.20      | 0.09      | 24.69              | 0.93  | 0.25 | 0.00   |
| 27.5     | 0.40    | 0.20    | 0.19      | 0.07      | 24.07              | 1.13  | 0.28 | 0.00   |
| 28.5     | 0.38    | 0.20    | 0.18      | 0.05      | 22.91              | 1.46  | 0.32 | 0.00   |
| 29.5     | 0.35    | 0.19    | 0.17      | 0.03      | 21.40              | 1.84  | 0.38 | 0.00   |
| 30.5     | 0.33    | 0.19    | 0.16      | 0.02      | 19.70              | 2.47  | 0.50 | 0.00   |
| 31.5     | 0.30    | 0.19    | 0.15      | 0.01      | 17.55              | 3.56  | 0.69 | 0.00   |
| 32.5     | 0.28    | 0.19    | 0.15      | 0.01      | 15.08              | 5.12  | 0.92 | 0.00   |
| 33.5     | 0.26    | 0.19    | 0.14      | 0.00      | 12.37              | 7.12  | 1.16 | 0.00   |
| 34.5     | 0.24    | 0.19    | 0.13      | 0.00      | 9.10               | 8.99  | 1.37 | 0.00   |
| 35.5     | 0.22    | 0.18    | 0.12      | 0.00      | 6.44               | 11.11 | 1.51 | 0.00   |
| 36.5     | 0.20    | 0.18    | 0.11      | 0.00      | 4.27               | 13.23 | 1.62 | 0.00   |
| 37.5     | 0.19    | 0.17    | 0.11      | 0.00      | 2.78               | 14.76 | 1.66 | 0.00   |
| 38.5     | 0.17    | 0.17    | 0.10      | 0.00      | 1.54               | 15.79 | 1.62 | 0.00   |
| 39.5     | 0.16    | 0.17    | 0.09      | 0.00      | 0.89               | 16.38 | 1.51 | 0.00   |
| 40.5     | 0.14    | 0.16    | 0.08      | 0.00      | 0.49               | 16.51 | 1.37 | 0.00   |
| 41.5     | 0.13    | 0.16    | 0.08      | 0.00      | 0.27               | 16.25 | 1.20 | 0.00   |
| 42.5     | 0.12    | 0.16    | 0.07      | 0.00      | 0.14               | 15.69 | 1.02 | 0.00   |
| 43.5     | 0.10    | 0.15    | 0.07      | 0.00      | 0.07               | 14.81 | 0.86 | 0.00   |
| 44.5     | 0.09    | 0.15    | 0.06      | 0.00      | 0.03               | 13.61 | 0.69 | 0.00   |

Appendix B – Contributions of species to the chlorine budgets

Table B14 Continued

| Altitude | CFC-114 | CFC-115 | HCFC-142b | HCFC-141b | ClONO <sub>2</sub> | ClO   | HOCl | H-1211 |
|----------|---------|---------|-----------|-----------|--------------------|-------|------|--------|
| 45.5     | 0.09    | 0.15    | 0.06      | 0.00      | 0.02               | 12.29 | 0.55 | 0.00   |
| 46.5     | 0.08    | 0.15    | 0.05      | 0.00      | 0.01               | 10.85 | 0.43 | 0.00   |
| 47.5     | 0.07    | 0.14    | 0.05      | 0.00      | 0.00               | 9.45  | 0.33 | 0.00   |
| 48.5     | 0.06    | 0.14    | 0.05      | 0.00      | 0.00               | 8.16  | 0.25 | 0.00   |
| 49.5     | 0.06    | 0.14    | 0.05      | 0.00      | 0.00               | 7.07  | 0.18 | 0.00   |
| 50.5     | 0.06    | 0.14    | 0.04      | 0.00      | 0.00               | 6.12  | 0.14 | 0.00   |
| 51.5     | 0.05    | 0.14    | 0.04      | 0.00      | 0.00               | 5.36  | 0.11 | 0.00   |
| 52.5     | 0.05    | 0.14    | 0.04      | 0.00      | 0.00               | 4.78  | 0.09 | 0.00   |
| 53.5     | 0.05    | 0.14    | 0.04      | 0.00      | 0.00               | 4.30  | 0.07 | 0.00   |

Appendix B – Contributions of species to the chlorine budgets

Table B15: The percentage contribution of HCl, CCl<sub>4</sub>, CFC-12, CFC-11, COClF, COCl<sub>2</sub>, HCFC-22, CH<sub>3</sub>Cl & CFC-113 to the total chlorine budget in the latitude bands between 30° S and 70° S (morning occultations)

| Altitude | HCl   | CCl <sub>4</sub> | CFC-12 | CFC-11 | COClF | COCl <sub>2</sub> | HCFC-22 | CH <sub>3</sub> Cl | CFC-113 |
|----------|-------|------------------|--------|--------|-------|-------------------|---------|--------------------|---------|
| 10.5     | 5.54  | 11.61            | 29.46  | 20.53  | 1.06  | 0.19              | 5.36    | 16.64              | 6.54    |
| 11.5     | 7.53  | 11.09            | 29.06  | 20.05  | 1.13  | 0.32              | 5.36    | 15.95              | 6.24    |
| 12.5     | 9.04  | 10.52            | 28.80  | 19.67  | 1.19  | 0.46              | 5.40    | 15.39              | 5.94    |
| 13.5     | 10.82 | 10.04            | 28.31  | 19.12  | 1.23  | 0.55              | 5.42    | 14.93              | 5.69    |
| 14.5     | 13.47 | 9.44             | 27.51  | 18.21  | 1.24  | 0.65              | 5.40    | 14.28              | 5.47    |
| 15.5     | 17.71 | 8.64             | 26.44  | 16.72  | 1.27  | 0.75              | 5.25    | 12.89              | 5.24    |
| 16.5     | 23.86 | 7.53             | 24.81  | 14.57  | 1.30  | 0.89              | 4.84    | 11.03              | 4.89    |
| 17.5     | 30.65 | 6.24             | 22.70  | 12.00  | 1.30  | 1.01              | 4.39    | 9.10               | 4.43    |
| 18.5     | 36.89 | 4.92             | 20.49  | 9.30   | 1.29  | 1.13              | 4.08    | 7.45               | 3.90    |
| 19.5     | 41.88 | 3.77             | 18.35  | 6.69   | 1.18  | 1.20              | 3.85    | 6.08               | 3.38    |
| 20.5     | 45.53 | 2.83             | 16.23  | 4.28   | 0.97  | 1.22              | 3.62    | 4.98               | 2.93    |
| 21.5     | 48.09 | 2.08             | 14.19  | 2.57   | 0.75  | 1.14              | 3.43    | 4.03               | 2.56    |
| 22.5     | 49.83 | 1.33             | 12.26  | 1.70   | 0.54  | 0.96              | 3.26    | 3.15               | 2.19    |
| 23.5     | 51.32 | 0.75             | 10.50  | 1.10   | 0.41  | 0.76              | 3.10    | 2.43               | 1.84    |
| 24.5     | 53.22 | 0.37             | 8.99   | 0.65   | 0.35  | 0.63              | 2.99    | 1.87               | 1.52    |
| 25.5     | 55.21 | 0.15             | 7.64   | 0.34   | 0.29  | 0.50              | 2.91    | 1.45               | 1.22    |
| 26.5     | 57.40 | 0.06             | 6.46   | 0.18   | 0.23  | 0.41              | 2.84    | 1.14               | 0.98    |
| 27.5     | 60.08 | 0.03             | 5.32   | 0.09   | 0.17  | 0.31              | 2.76    | 0.92               | 0.78    |
| 28.5     | 62.89 | 0.01             | 4.29   | 0.04   | 0.12  | 0.22              | 2.68    | 0.78               | 0.60    |
| 29.5     | 65.41 | 0.00             | 3.46   | 0.02   | 0.09  | 0.16              | 2.59    | 0.63               | 0.47    |
| 30.5     | 67.61 | 0.00             | 2.70   | 0.01   | 0.06  | 0.10              | 2.50    | 0.52               | 0.34    |
| 31.5     | 69.45 | 0.00             | 2.05   | 0.00   | 0.03  | 0.06              | 2.42    | 0.42               | 0.24    |
| 32.5     | 71.01 | 0.00             | 1.57   | 0.00   | 0.02  | 0.04              | 2.34    | 0.35               | 0.17    |
| 33.5     | 72.37 | 0.00             | 1.14   | 0.00   | 0.01  | 0.02              | 2.24    | 0.27               | 0.11    |
| 34.5     | 73.77 | 0.00             | 0.82   | 0.00   | 0.01  | 0.01              | 2.16    | 0.22               | 0.08    |
| 35.5     | 75.09 | 0.00             | 0.59   | 0.00   | 0.00  | 0.01              | 2.07    | 0.18               | 0.05    |
| 36.5     | 76.32 | 0.00             | 0.42   | 0.00   | 0.00  | 0.00              | 1.99    | 0.14               | 0.04    |
| 37.5     | 77.58 | 0.00             | 0.31   | 0.00   | 0.00  | 0.00              | 1.91    | 0.11               | 0.02    |
| 38.5     | 78.84 | 0.00             | 0.21   | 0.00   | 0.00  | 0.00              | 1.84    | 0.09               | 0.02    |
| 39.5     | 80.02 | 0.00             | 0.15   | 0.00   | 0.00  | 0.00              | 1.75    | 0.06               | 0.01    |
| 40.5     | 81.11 | 0.00             | 0.11   | 0.00   | 0.00  | 0.00              | 1.67    | 0.05               | 0.01    |
| 41.5     | 82.20 | 0.00             | 0.07   | 0.00   | 0.00  | 0.00              | 1.58    | 0.03               | 0.00    |
| 42.5     | 83.29 | 0.00             | 0.05   | 0.00   | 0.00  | 0.00              | 1.50    | 0.02               | 0.00    |
| 43.5     | 84.47 | 0.00             | 0.03   | 0.00   | 0.00  | 0.00              | 1.42    | 0.02               | 0.00    |
| 44.5     | 85.83 | 0.00             | 0.02   | 0.00   | 0.00  | 0.00              | 1.34    | 0.01               | 0.00    |

Appendix B – Contributions of species to the chlorine budgets

Table B15 Continued

| Altitude | HCl   | CCl <sub>4</sub> | CFC-12 | CFC-11 | COClF | COCl <sub>2</sub> | HCFC-22 | CH <sub>3</sub> Cl | CFC-113 |
|----------|-------|------------------|--------|--------|-------|-------------------|---------|--------------------|---------|
| 45.5     | 87.20 | 0.00             | 0.01   | 0.00   | 0.00  | 0.00              | 1.28    | 0.01               | 0.00    |
| 46.5     | 88.57 | 0.00             | 0.01   | 0.00   | 0.00  | 0.00              | 1.22    | 0.01               | 0.00    |
| 47.5     | 89.89 | 0.00             | 0.00   | 0.00   | 0.00  | 0.00              | 1.16    | 0.00               | 0.00    |
| 48.5     | 91.07 | 0.00             | 0.00   | 0.00   | 0.00  | 0.00              | 1.13    | 0.00               | 0.00    |
| 49.5     | 92.06 | 0.00             | 0.00   | 0.00   | 0.00  | 0.00              | 1.11    | 0.00               | 0.00    |
| 50.5     | 92.93 | 0.00             | 0.00   | 0.00   | 0.00  | 0.00              | 1.08    | 0.00               | 0.00    |
| 51.5     | 93.69 | 0.00             | 0.00   | 0.00   | 0.00  | 0.00              | 1.06    | 0.00               | 0.00    |
| 52.5     | 94.41 | 0.00             | 0.00   | 0.00   | 0.00  | 0.00              | 1.05    | 0.00               | 0.00    |
| 53.5     | 95.03 | 0.00             | 0.00   | 0.00   | 0.00  | 0.00              | 1.03    | 0.00               | 0.00    |

Appendix B – Contributions of species to the chlorine budgets

Table B16: The percentage contribution of CFC-114, CFC-115, HCFC-142b, HCFC-141b, ClONO<sub>2</sub>, ClO, HOCl & H-1211 to the total chlorine budget in the latitude bands between 30° S and 70° S (morning occultations)

| Altitude | CFC-114 | CFC-115 | HCFC-142b | HCFC-141b | ClONO <sub>2</sub> | ClO   | HOCl | H-1211 |
|----------|---------|---------|-----------|-----------|--------------------|-------|------|--------|
| 10.5     | 0.96    | 0.27    | 0.45      | 1.03      | 0.20               | 0.02  | 0.04 | 0.11   |
| 11.5     | 0.93    | 0.26    | 0.43      | 0.97      | 0.50               | 0.04  | 0.04 | 0.10   |
| 12.5     | 0.89    | 0.26    | 0.41      | 0.91      | 0.92               | 0.06  | 0.03 | 0.09   |
| 13.5     | 0.87    | 0.26    | 0.40      | 0.87      | 1.24               | 0.14  | 0.03 | 0.09   |
| 14.5     | 0.84    | 0.26    | 0.39      | 0.83      | 1.65               | 0.25  | 0.04 | 0.08   |
| 15.5     | 0.82    | 0.25    | 0.37      | 0.78      | 2.38               | 0.38  | 0.04 | 0.07   |
| 16.5     | 0.78    | 0.25    | 0.36      | 0.72      | 3.51               | 0.55  | 0.06 | 0.06   |
| 17.5     | 0.73    | 0.24    | 0.33      | 0.64      | 5.32               | 0.78  | 0.07 | 0.05   |
| 18.5     | 0.67    | 0.24    | 0.30      | 0.55      | 7.76               | 0.94  | 0.08 | 0.04   |
| 19.5     | 0.62    | 0.23    | 0.28      | 0.46      | 10.94              | 0.98  | 0.09 | 0.02   |
| 20.5     | 0.57    | 0.22    | 0.26      | 0.38      | 14.69              | 1.17  | 0.12 | 0.01   |
| 21.5     | 0.54    | 0.21    | 0.24      | 0.32      | 18.33              | 1.37  | 0.14 | 0.01   |
| 22.5     | 0.50    | 0.21    | 0.22      | 0.26      | 21.92              | 1.49  | 0.18 | 0.00   |
| 23.5     | 0.47    | 0.20    | 0.21      | 0.21      | 24.88              | 1.64  | 0.20 | 0.00   |
| 24.5     | 0.44    | 0.20    | 0.20      | 0.16      | 26.52              | 1.68  | 0.23 | 0.00   |
| 25.5     | 0.42    | 0.19    | 0.19      | 0.12      | 27.27              | 1.82  | 0.26 | 0.00   |
| 26.5     | 0.40    | 0.19    | 0.19      | 0.09      | 27.36              | 1.78  | 0.28 | 0.00   |
| 27.5     | 0.38    | 0.19    | 0.18      | 0.06      | 26.79              | 1.61  | 0.31 | 0.00   |
| 28.5     | 0.36    | 0.19    | 0.17      | 0.04      | 25.59              | 1.67  | 0.35 | 0.00   |
| 29.5     | 0.34    | 0.19    | 0.17      | 0.03      | 24.19              | 1.87  | 0.40 | 0.00   |
| 30.5     | 0.31    | 0.18    | 0.16      | 0.02      | 22.80              | 2.21  | 0.46 | 0.00   |
| 31.5     | 0.29    | 0.18    | 0.15      | 0.01      | 21.42              | 2.68  | 0.58 | 0.00   |
| 32.5     | 0.27    | 0.18    | 0.14      | 0.01      | 19.75              | 3.41  | 0.72 | 0.00   |
| 33.5     | 0.25    | 0.18    | 0.13      | 0.00      | 17.99              | 4.39  | 0.88 | 0.00   |
| 34.5     | 0.23    | 0.18    | 0.13      | 0.00      | 15.54              | 5.83  | 1.04 | 0.00   |
| 35.5     | 0.22    | 0.18    | 0.12      | 0.00      | 12.81              | 7.52  | 1.16 | 0.00   |
| 36.5     | 0.20    | 0.17    | 0.11      | 0.00      | 10.05              | 9.29  | 1.26 | 0.00   |
| 37.5     | 0.19    | 0.17    | 0.10      | 0.00      | 7.51               | 10.76 | 1.31 | 0.00   |
| 38.5     | 0.17    | 0.17    | 0.10      | 0.00      | 5.13               | 12.13 | 1.30 | 0.00   |
| 39.5     | 0.16    | 0.17    | 0.09      | 0.00      | 3.14               | 13.18 | 1.26 | 0.00   |
| 40.5     | 0.14    | 0.17    | 0.09      | 0.00      | 1.75               | 13.74 | 1.18 | 0.00   |
| 41.5     | 0.13    | 0.16    | 0.08      | 0.00      | 0.97               | 13.72 | 1.05 | 0.00   |
| 42.5     | 0.12    | 0.16    | 0.07      | 0.00      | 0.49               | 13.40 | 0.89 | 0.00   |
| 43.5     | 0.11    | 0.16    | 0.07      | 0.00      | 0.23               | 12.75 | 0.74 | 0.00   |
| 44.5     | 0.10    | 0.15    | 0.06      | 0.00      | 0.12               | 11.76 | 0.60 | 0.00   |

Appendix B – Contributions of species to the chlorine budgets

Table B16 Continued

| Altitude | CFC-114 | CFC-115 | HCFC-142b | HCFC-141b | ClONO <sub>2</sub> | ClO   | HOCl | H-1211 |
|----------|---------|---------|-----------|-----------|--------------------|-------|------|--------|
| 45.5     | 0.09    | 0.15    | 0.06      | 0.00      | 0.05               | 10.66 | 0.48 | 0.00   |
| 46.5     | 0.08    | 0.15    | 0.05      | 0.00      | 0.02               | 9.51  | 0.39 | 0.00   |
| 47.5     | 0.07    | 0.15    | 0.05      | 0.00      | 0.01               | 8.35  | 0.31 | 0.00   |
| 48.5     | 0.07    | 0.14    | 0.05      | 0.00      | 0.01               | 7.29  | 0.24 | 0.00   |
| 49.5     | 0.06    | 0.14    | 0.05      | 0.00      | 0.00               | 6.39  | 0.19 | 0.00   |
| 50.5     | 0.06    | 0.14    | 0.04      | 0.00      | 0.00               | 5.60  | 0.15 | 0.00   |
| 51.5     | 0.05    | 0.14    | 0.04      | 0.00      | 0.00               | 4.90  | 0.11 | 0.00   |
| 52.5     | 0.05    | 0.14    | 0.04      | 0.00      | 0.00               | 4.22  | 0.09 | 0.00   |
| 53.5     | 0.05    | 0.14    | 0.04      | 0.00      | 0.00               | 3.64  | 0.07 | 0.00   |

# Appendix C

## *CFC-11 correlation plots*

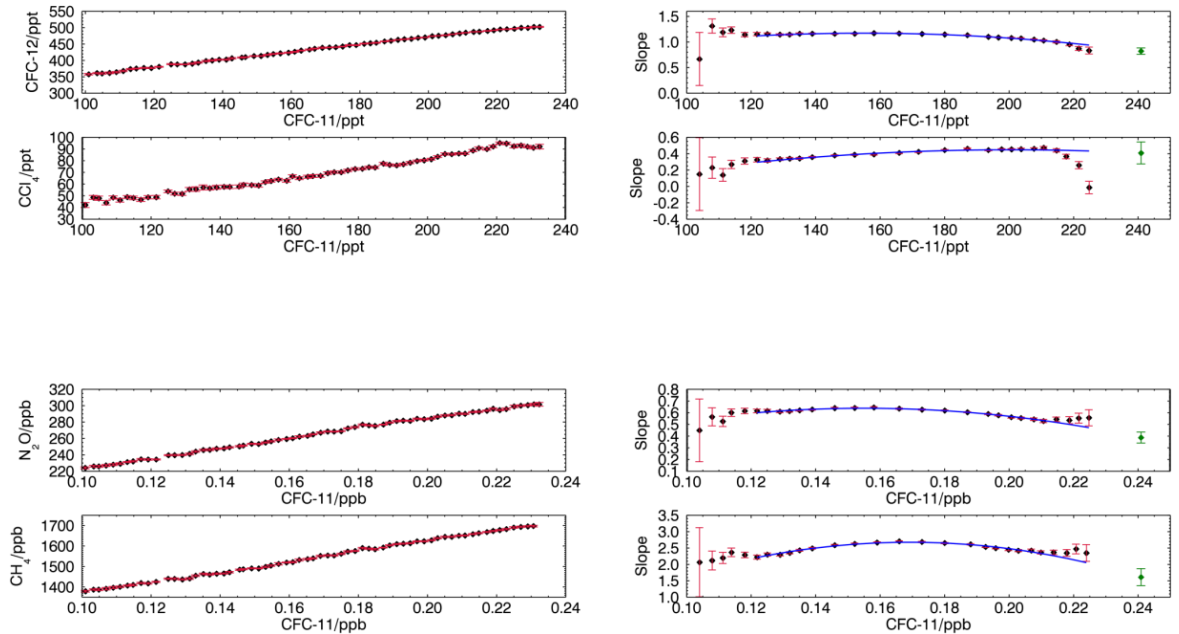


Figure C1: Correlations between the VMRs of CFC-12, CCl<sub>4</sub>, CH<sub>4</sub>, and N<sub>2</sub>O and CFC-11 for the data from the northern hemisphere during the stratospheric summer of 2006. Left panels: The mean correlation profile. Each point represents the mean of the VMR in a window of 2 ppt of CFC-11. The error on these points is the standard deviation of the data within each 2 ppt window. Right panels: The local slope of data in an 80 ppt of CFC-11 window. The error on the points is the fitting error of this fit. The blue line is a second degree polynomial fit to the local slopes. The green point is the extrapolated slope at the tropopause.

## Appendix C – Correlation plots against CFC-11

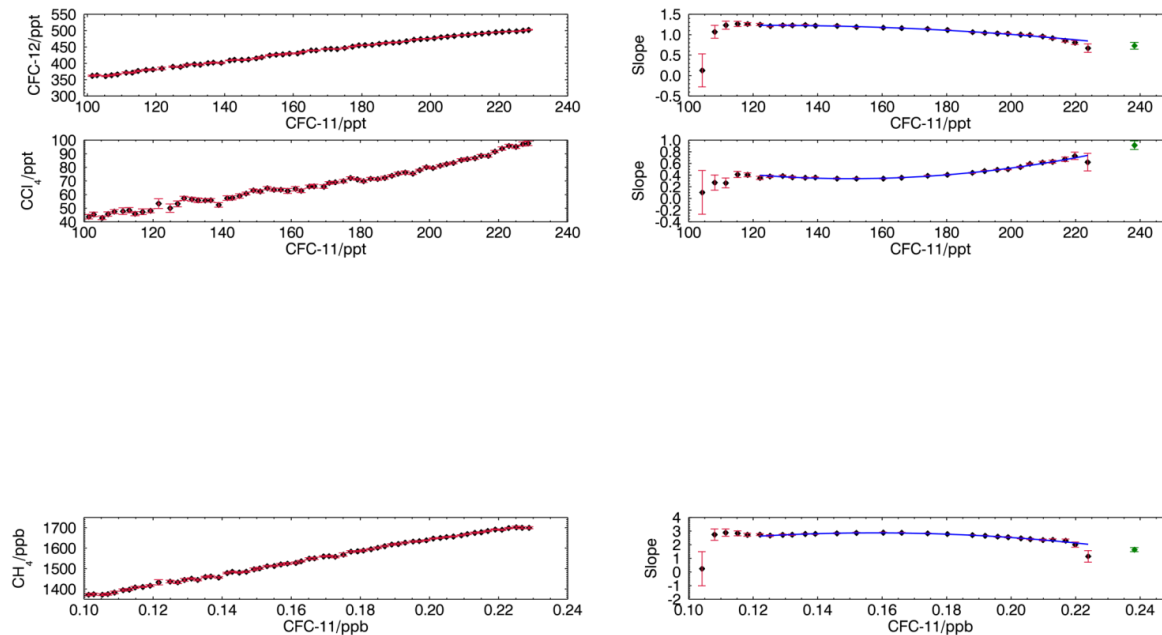


Figure C2: Correlations between the VMRs of CFC-12, CCl<sub>4</sub>, and CH<sub>4</sub> and CFC-11 for the data from the northern hemisphere during the stratospheric summer of 2007. Left panels: The mean correlation profile. Each point represents the mean of the VMR in a window of 2 ppt of CFC-11. The error on these points is the standard deviation of the data within each 2 ppt window. Right panels: The local slope of data in an 80 ppt of CFC-11 window. The error on the points is the fitting error of this fit. The blue line is a second degree polynomial fit to the local slopes. The green point is the extrapolated slope at the tropopause.

## Appendix C – Correlation plots against CFC-11

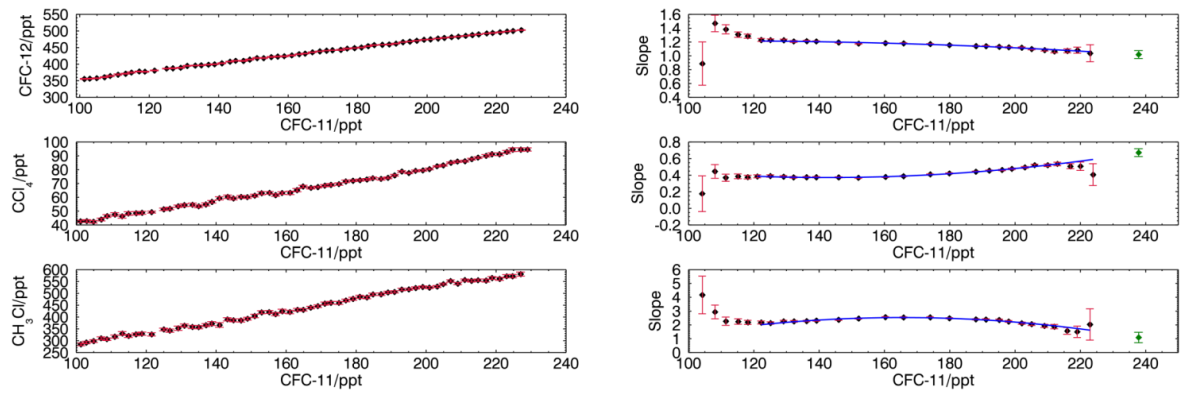


Figure C3: Correlations between the VMRs of CFC-12,  $\text{CCl}_4$ , and  $\text{CH}_3\text{Cl}$  and CFC-11 for the data from the northern hemisphere during the stratospheric summer of 2008. Left panels: The mean correlation profile. Each point represents the mean of the VMR in a window of 2 ppt of CFC-11. The error on these points is the standard deviation of the data within each 2 ppt window. Right panels: The local slope of data in an 80 ppt of CFC-11 window. The error on the points is the fitting error of this fit. The blue line is a second degree polynomial fit to the local slopes. The green point is the extrapolated slope at the tropopause.

## Appendix C – Correlation plots against CFC-11

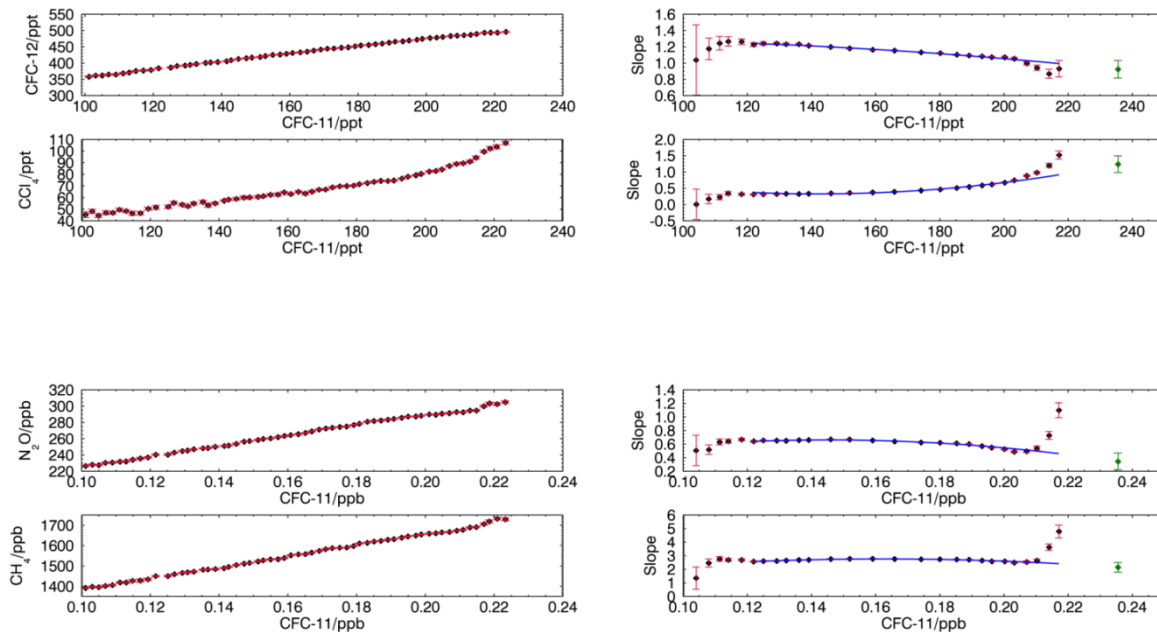


Figure C4: Correlations between the VMRs of CFC-12, CCl<sub>4</sub>, CH<sub>4</sub> and N<sub>2</sub>O and CFC-11 for the data from the northern hemisphere during the stratospheric summer of 2009. Left panels: The mean correlation profile. Each point represents the mean of the VMR in a window of 2 ppt of CFC-11. The error on these points is the standard deviation of the data within each 2 ppt window. Right panels: The local slope of data in an 80 ppt of CFC-11 window. The error on the points is the fitting error of this fit. The blue line is a second degree polynomial fit to the local slopes. The green point is the extrapolated slope at the tropopause.

## Appendix C – Correlation plots against CFC-11

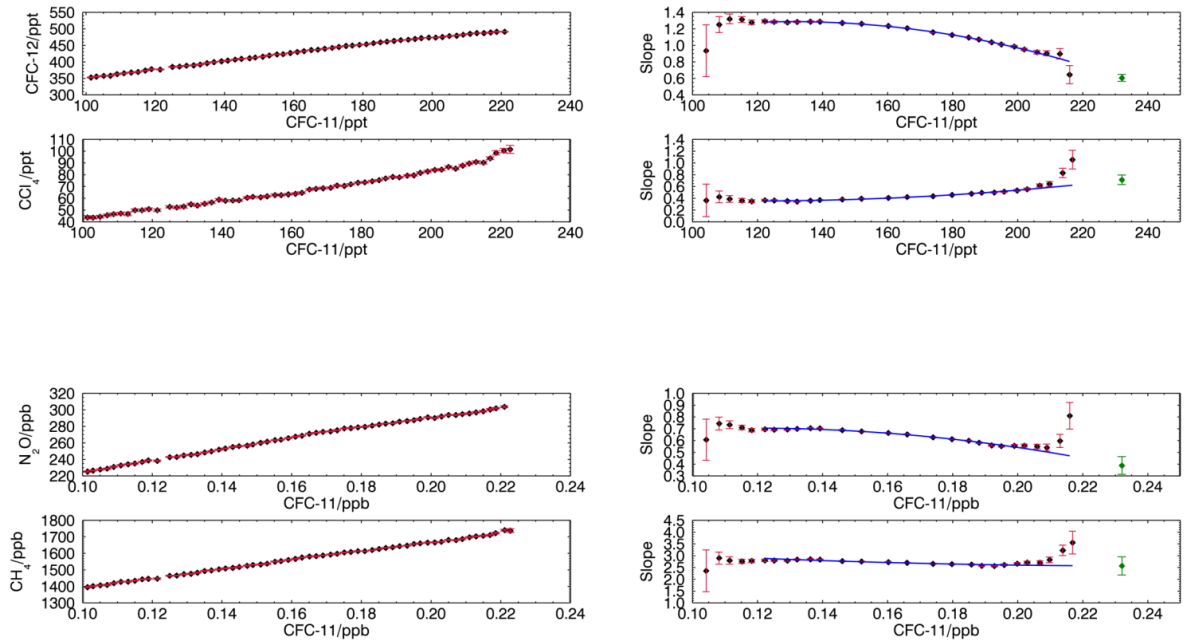


Figure C5: Correlations between the VMRs of CFC-12, CCl<sub>4</sub>, CH<sub>4</sub> and N<sub>2</sub>O and CFC-11 for the data from the northern hemisphere during the stratospheric summer of 2010. Left panels: The mean correlation profile. Each point represents the mean of the VMR in a window of 2 ppt of CFC-11. The error on these points is the standard deviation of the data within each 2 ppt window. Right panels: The local slope of data in an 80 ppt of CFC-11 window. The error on the points is the fitting error of this fit. The blue line is a second degree polynomial fit to the local slopes. The green point is the extrapolated slope at the tropopause.

## Appendix C – Correlation plots against CFC-11

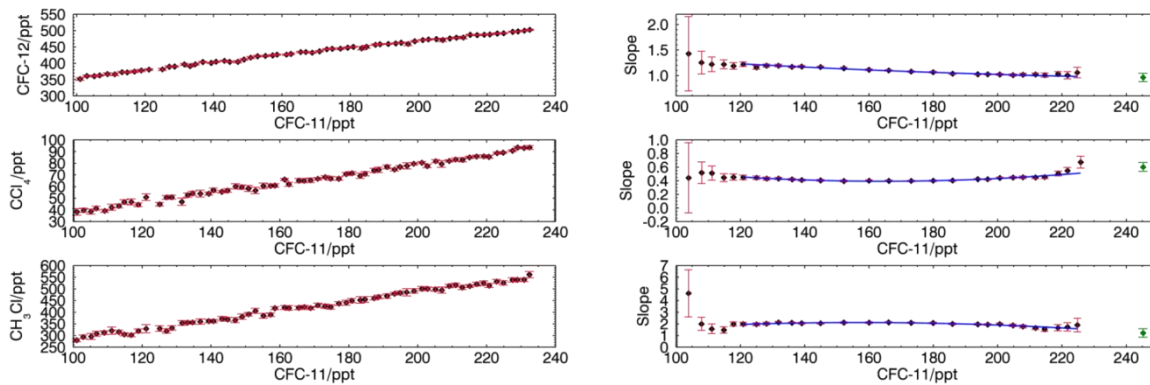


Figure C6: Correlations between the VMRs of CFC-12,  $\text{CCl}_4$  and  $\text{CH}_3\text{Cl}$  and CFC-11 for the data from the northern hemisphere during the stratospheric winter of 2005. Left panels: The mean correlation profile. Each point represents the mean of the VMR in a window of 2 ppt of CFC-11. The error on these points is the standard deviation of the data within each 2 ppt window. Right panels: The local slope of data in an 80 ppt of CFC-11 window. The error on the points is the fitting error of this fit. The blue line is a second degree polynomial fit to the local slopes. The green point is the extrapolated slope at the tropopause.

## Appendix C – Correlation plots against CFC-11

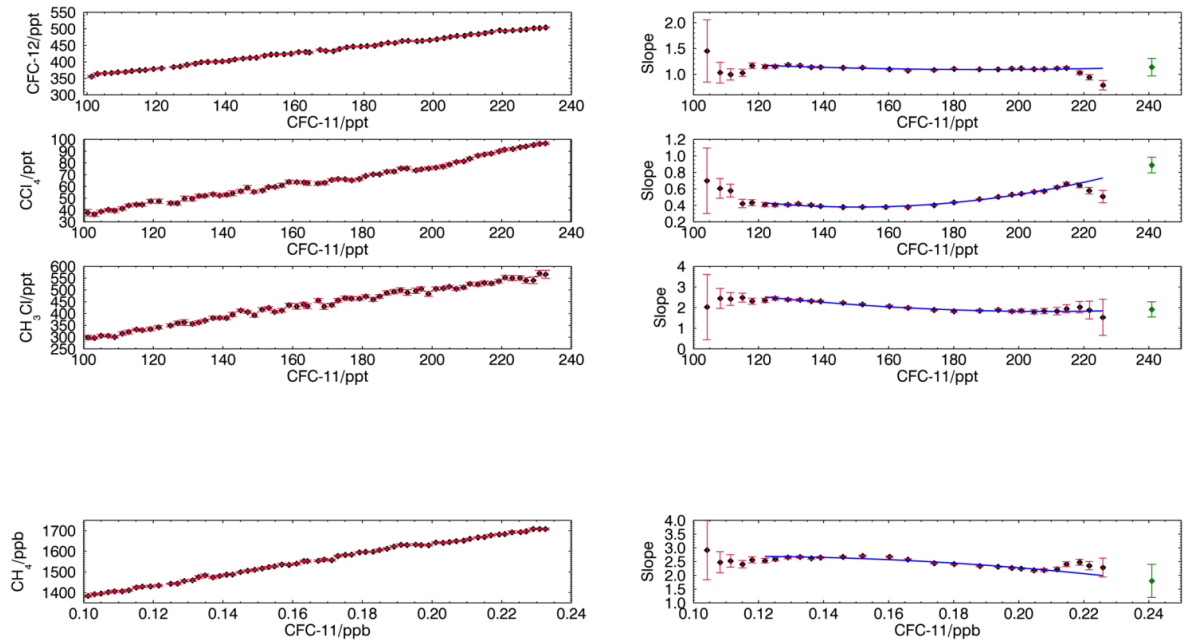


Figure C7: Correlations between the VMRs of CFC-12, CCl<sub>4</sub>, CH<sub>4</sub> and CH<sub>3</sub>Cl and CFC-11 for the data from the northern hemisphere during the stratospheric winter of 2006. Left panels: The mean correlation profile. Each point represents the mean of the VMR in a window of 2 ppt of CFC-11. The error on these points is the standard deviation of the data within each 2 ppt window. Right panels: The local slope of data in an 80 ppt of CFC-11 window. The error on the points is the fitting error of this fit. The blue line is a second degree polynomial fit to the local slopes. The green point is the extrapolated slope at the tropopause.

## Appendix C – Correlation plots against CFC-11

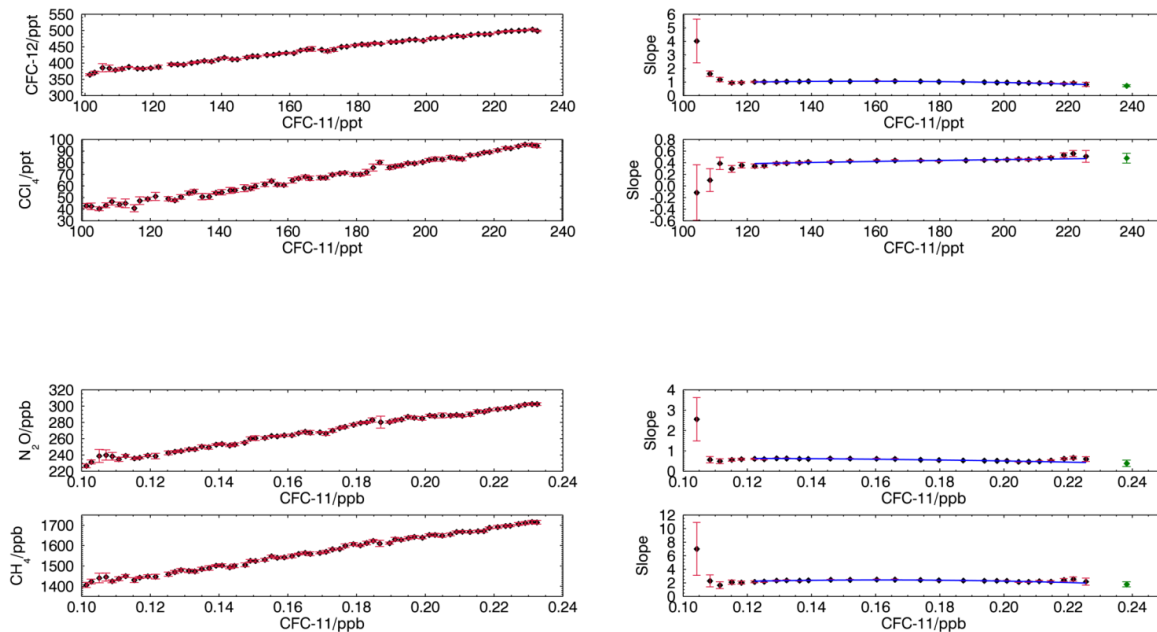


Figure C8: Correlations between the VMRs of CFC-12, CCl<sub>4</sub>, CH<sub>4</sub> and N<sub>2</sub>O and CFC-11 for the data from the northern hemisphere during the stratospheric winter of 2007. Left panels: The mean correlation profile. Each point represents the mean of the VMR in a window of 2 ppt of CFC-11. The error on these points is the standard deviation of the data within each 2 ppt window. Right panels: The local slope of data in an 80 ppt of CFC-11 window. The error on the points is the fitting error of this fit. The blue line is a second degree polynomial fit to the local slopes. The green point is the extrapolated slope at the tropopause.

## Appendix C – Correlation plots against CFC-11

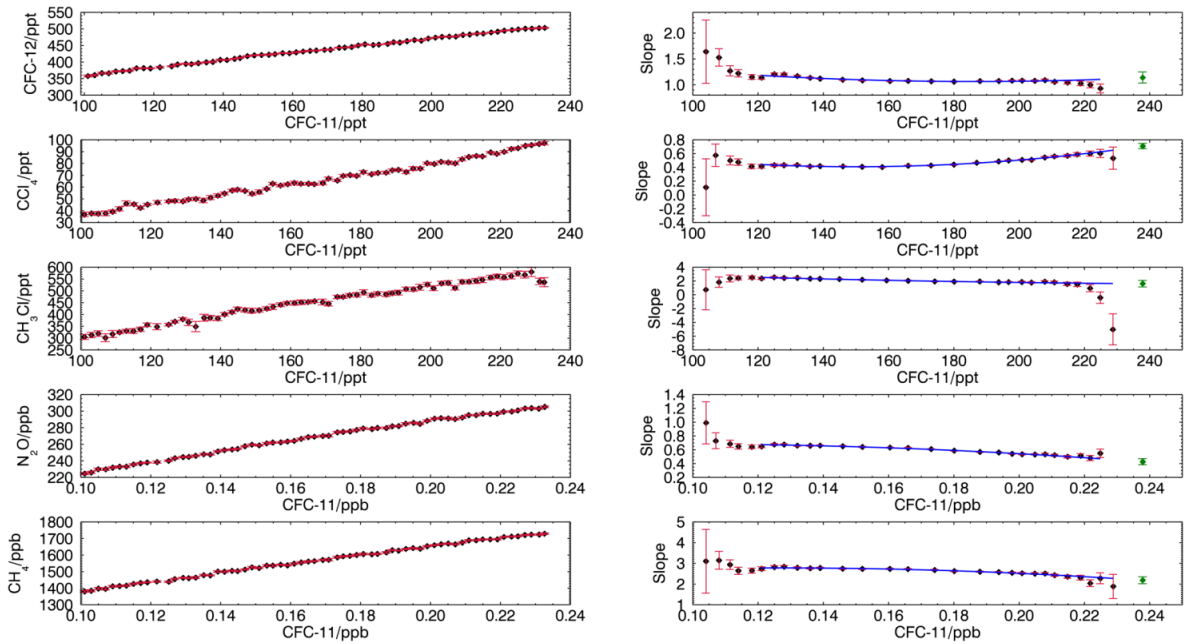


Figure C9: Correlations between the VMRs of CFC-12, CCl<sub>4</sub>, CH<sub>4</sub>, CH<sub>3</sub>Cl and N<sub>2</sub>O and CFC-11 for the data from the northern hemisphere during the stratospheric winter of 2008. Left panels: The mean correlation profile. Each point represents the mean of the VMR in a window of 2 ppt of CFC-11. The error on these points is the standard deviation of the data within each 2 ppt window. Right panels: The local slope of data in an 80 ppt of CFC-11 window. The error on the points is the fitting error of this fit. The blue line is a second degree polynomial fit to the local slopes. The green point is the extrapolated slope at the tropopause.

## Appendix C – Correlation plots against CFC-11

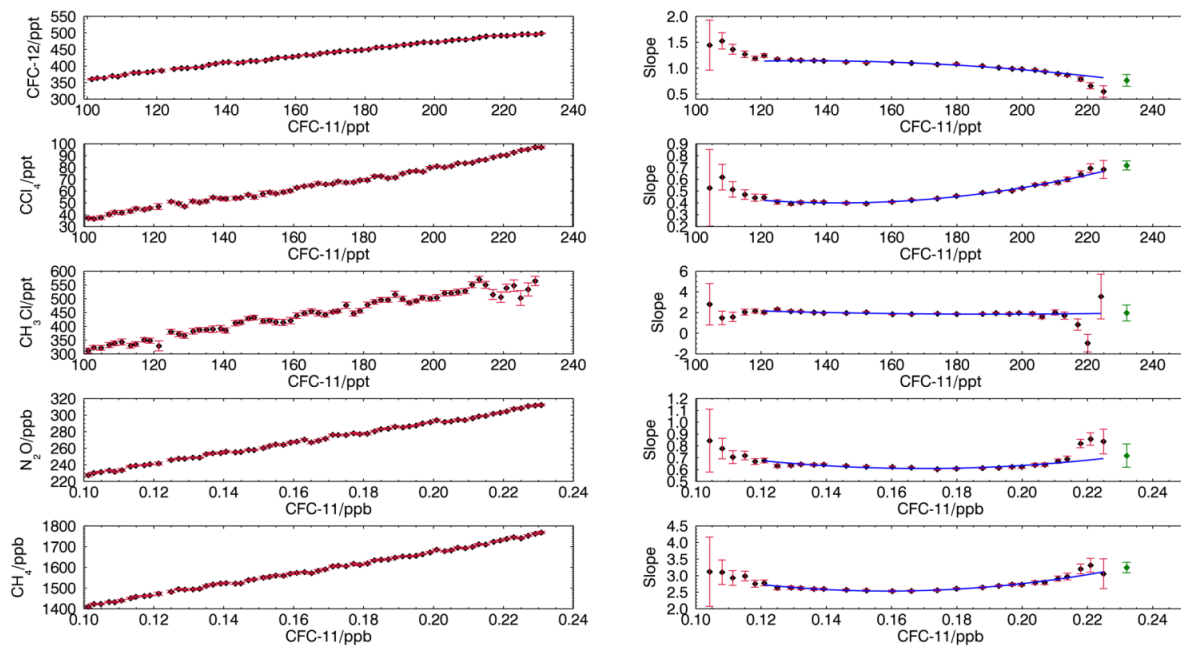


Figure C10: Correlations between the VMRs of CFC-12,  $\text{CCl}_4$ ,  $\text{CH}_4$ ,  $\text{CH}_3\text{Cl}$  and  $\text{N}_2\text{O}$  and CFC-11 for the data from the northern hemisphere during the stratospheric winter of 2010. Left panels: The mean correlation profile. Each point represents the mean of the VMR in a window of 2 ppt of CFC-11. The error on these points is the standard deviation of the data within each 2 ppt window. Right panels: The local slope of data in an 80 ppt of CFC-11 window. The error on the points is the fitting error of this fit. The blue line is a second degree polynomial fit to the local slopes. The green point is the extrapolated slope at the tropopause.

## Appendix C – Correlation plots against CFC-11

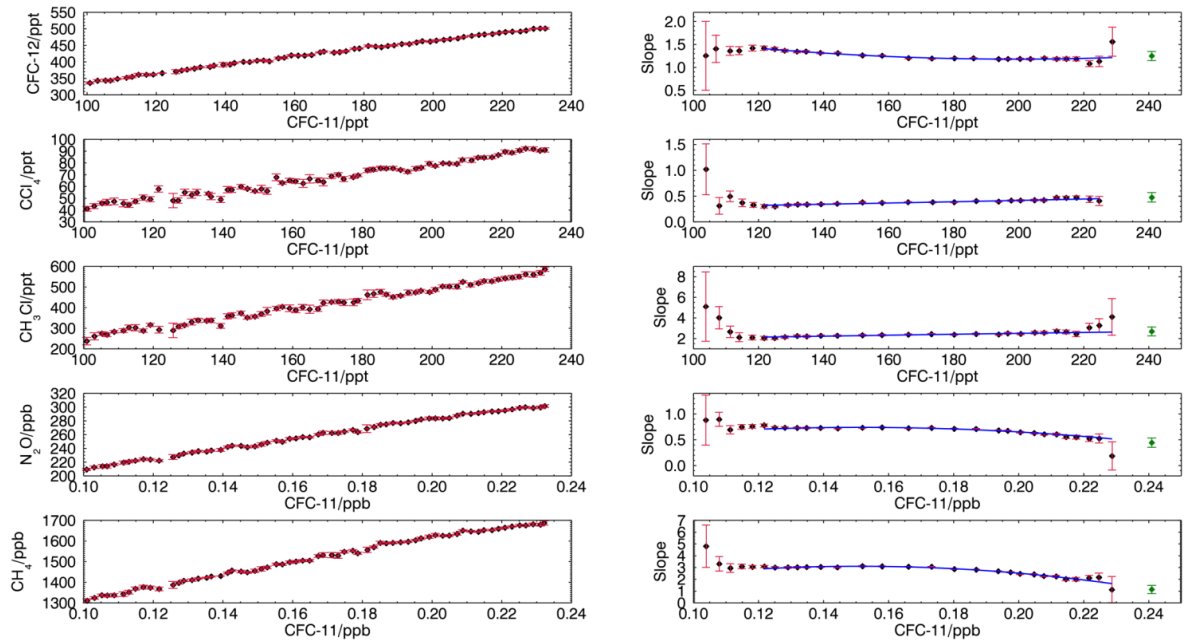


Figure C11: Correlations between the VMRs of CFC-12,  $\text{CCl}_4$ ,  $\text{CH}_4$ ,  $\text{CH}_3\text{Cl}$  and  $\text{N}_2\text{O}$  and CFC-11 for the data from the southern hemisphere during the stratospheric summer of 2006. Left panels: The mean correlation profile. Each point represents the mean of the VMR in a window of 2 ppt of CFC-11. The error on these points is the standard deviation of the data within each 2 ppt window. Right panels: The local slope of data in an 80 ppt of CFC-11 window. The error on the points is the fitting error of this fit. The blue line is a second degree polynomial fit to the local slopes. The green point is the extrapolated slope at the tropopause.

## Appendix C – Correlation plots against CFC-11

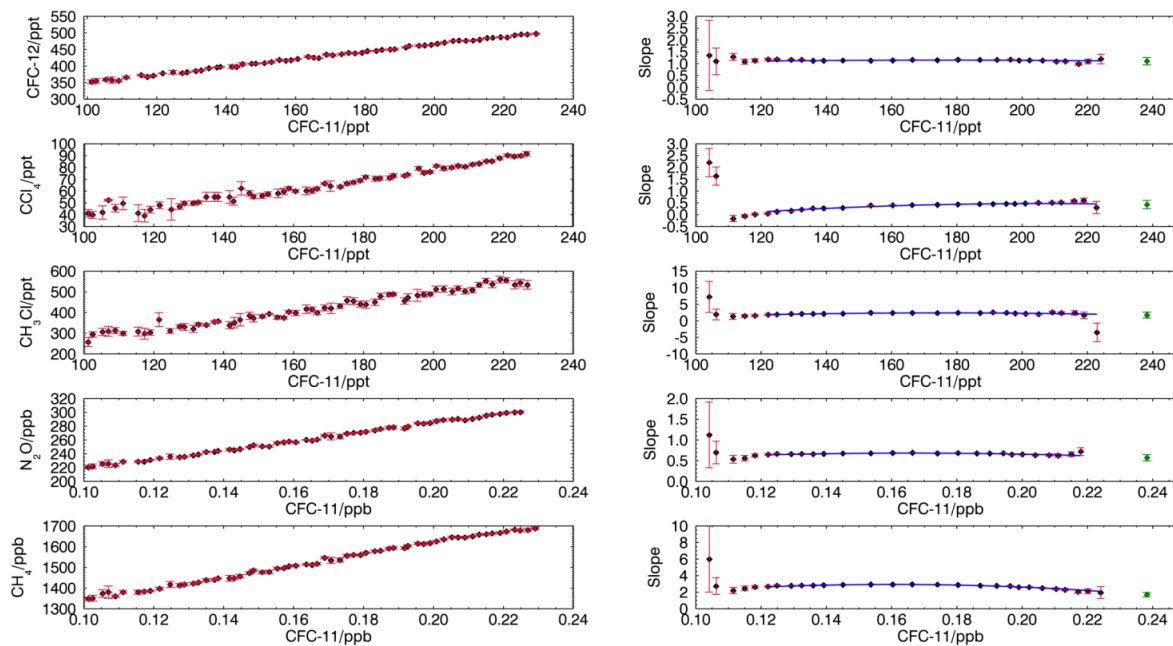


Figure C12: Correlations between the VMRs of CFC-12,  $\text{CCl}_4$ ,  $\text{CH}_4$ ,  $\text{CH}_3\text{Cl}$  and  $\text{N}_2\text{O}$  and CFC-11 for the data from the southern hemisphere during the stratospheric summer of 2007. Left panels: The mean correlation profile. Each point represents the mean of the VMR in a window of 2 ppt of CFC-11. The error on these points is the standard deviation of the data within each 2 ppt window. Right panels: The local slope of data in an 80 ppt of CFC-11 window. The error on the points is the fitting error of this fit. The blue line is a second degree polynomial fit to the local slopes. The green point is the extrapolated slope at the tropopause.

## Appendix C – Correlation plots against CFC-11

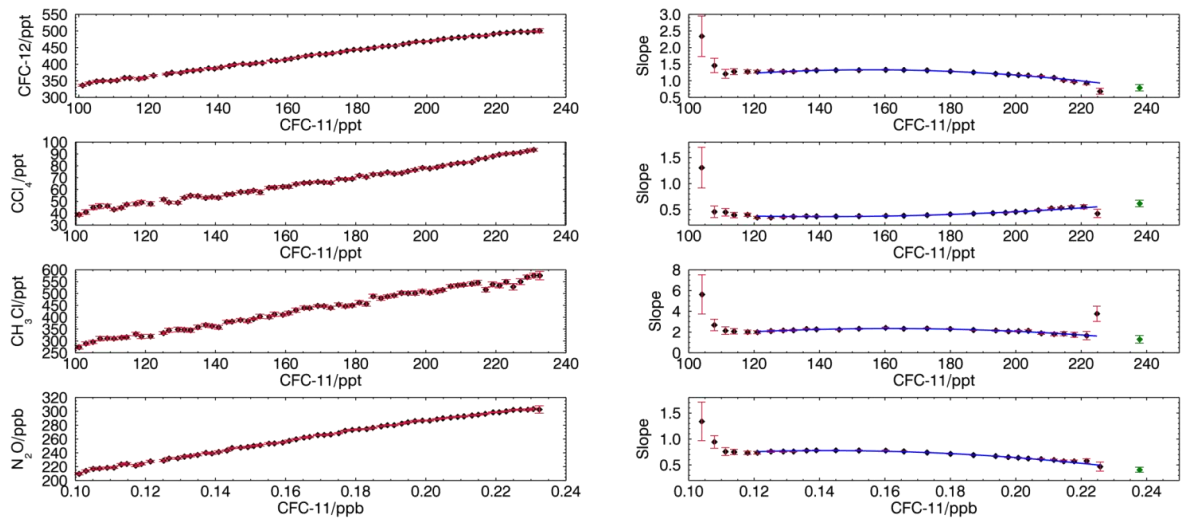


Figure C13: Correlations between the VMRs of CFC-12, CCl<sub>4</sub>, CH<sub>3</sub>Cl and N<sub>2</sub>O and CFC-11 for the data from the southern hemisphere during the stratospheric summer of 2008. Left panels: The mean correlation profile. Each point represents the mean of the VMR in a window of 2 ppt of CFC-11. The error on these points is the standard deviation of the data within each 2 ppt window. Right panels: The local slope of data in an 80 ppt of CFC-11 window. The error on the points is the fitting error of this fit. The blue line is a second degree polynomial fit to the local slopes. The green point is the extrapolated slope at the tropopause.

## Appendix C – Correlation plots against CFC-11

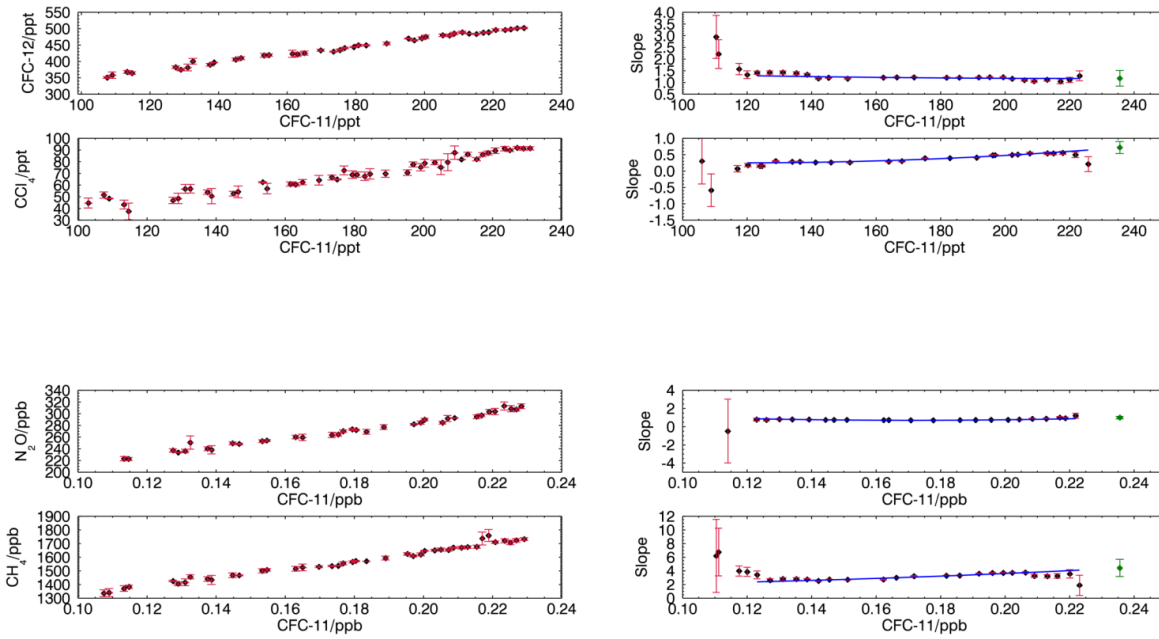


Figure C14: Correlations between the VMRs of CFC-12,  $\text{CCl}_4$ ,  $\text{CH}_4$  and  $\text{N}_2\text{O}$  and CFC-11 for the data from the southern hemisphere during the stratospheric summer of 2009. Left panels: The mean correlation profile. Each point represents the mean of the VMR in a window of 2 ppt of CFC-11. The error on these points is the standard deviation of the data within each 2 ppt window. Right panels: The local slope of data in an 80 ppt of CFC-11 window. The error on the points is the fitting error of this fit. The blue line is a second degree polynomial fit to the local slopes. The green point is the extrapolated slope at the tropopause.

## Appendix C – Correlation plots against CFC-11

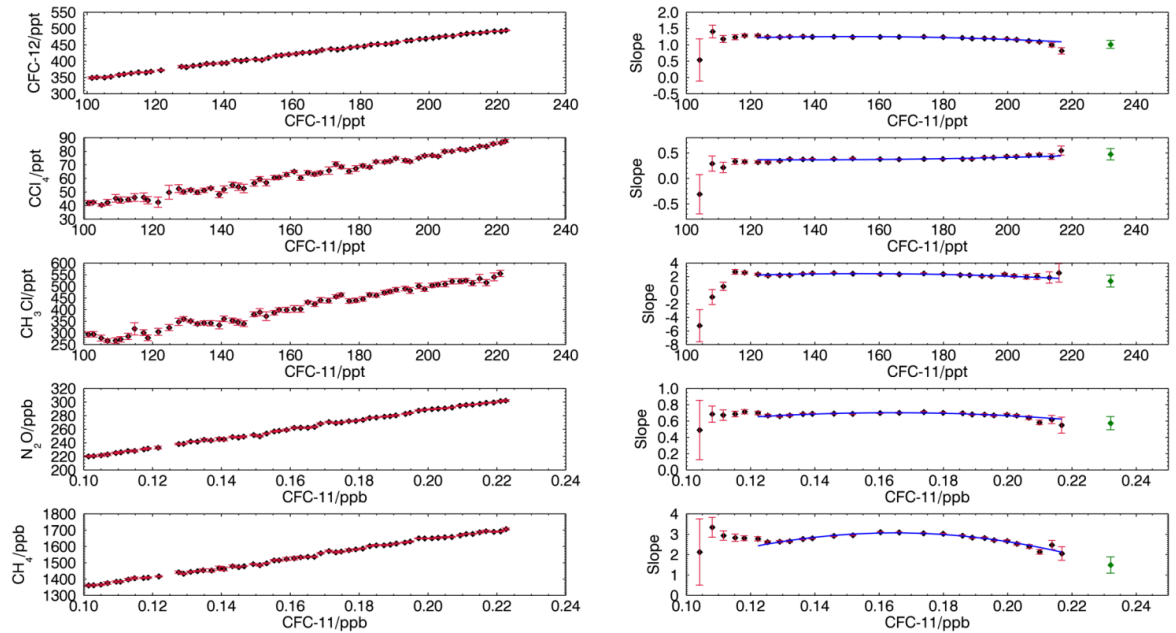


Figure C15: Correlations between the VMRs of CFC-12,  $\text{CCl}_4$ ,  $\text{CH}_4$ ,  $\text{CH}_3\text{Cl}$  and  $\text{N}_2\text{O}$  and CFC-11 for the data from the southern hemisphere during the stratospheric summer of 2010. Left panels: The mean correlation profile. Each point represents the mean of the VMR in a window of 2 ppt of CFC-11. The error on these points is the standard deviation of the data within each 2 ppt window. Right panels: The local slope of data in an 80 ppt of CFC-11 window. The error on the points is the fitting error of this fit. The blue line is a second degree polynomial fit to the local slopes. The green point is the extrapolated slope at the tropopause.

## Appendix C – Correlation plots against CFC-11

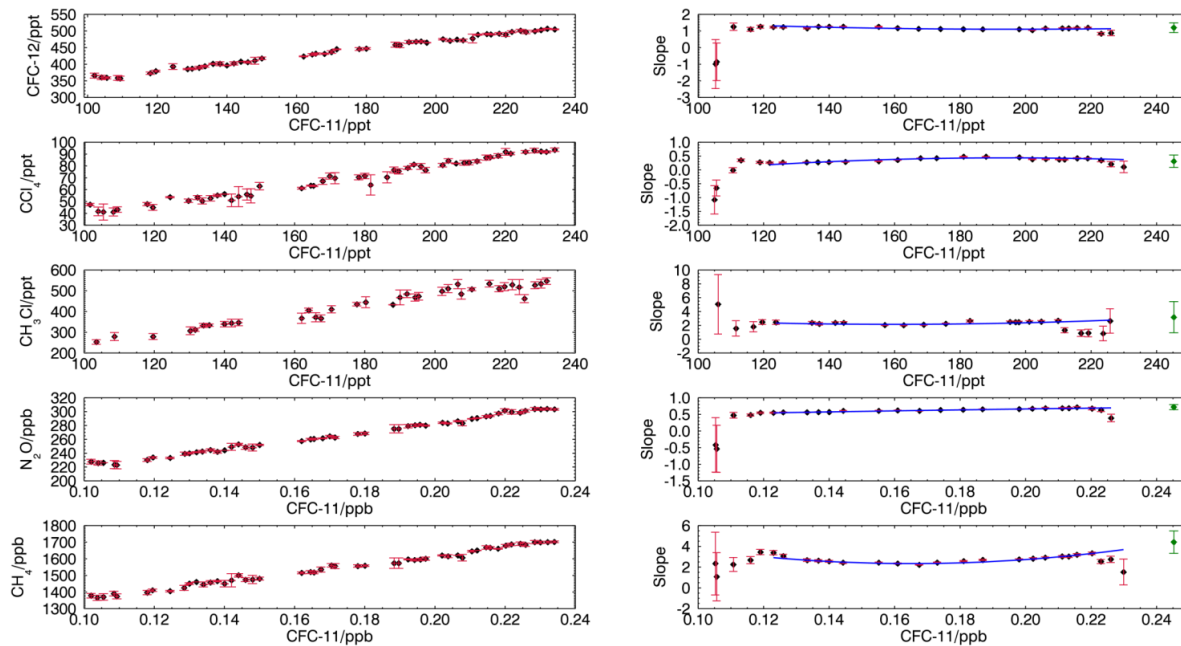


Figure C16: Correlations between the VMRs of CFC-12,  $\text{CCl}_4$ ,  $\text{CH}_4$ ,  $\text{CH}_3\text{Cl}$  and  $\text{N}_2\text{O}$  and CFC-11 for the data from the southern hemisphere during the stratospheric winter of 2005. Left panels: The mean correlation profile. Each point represents the mean of the VMR in a window of 2 ppt of CFC-11. The error on these points is the standard deviation of the data within each 2 ppt window. Right panels: The local slope of data in an 80 ppt of CFC-11 window. The error on the points is the fitting error of this fit. The blue line is a second degree polynomial fit to the local slopes. The green point is the extrapolated slope at the tropopause.

## Appendix C – Correlation plots against CFC-11

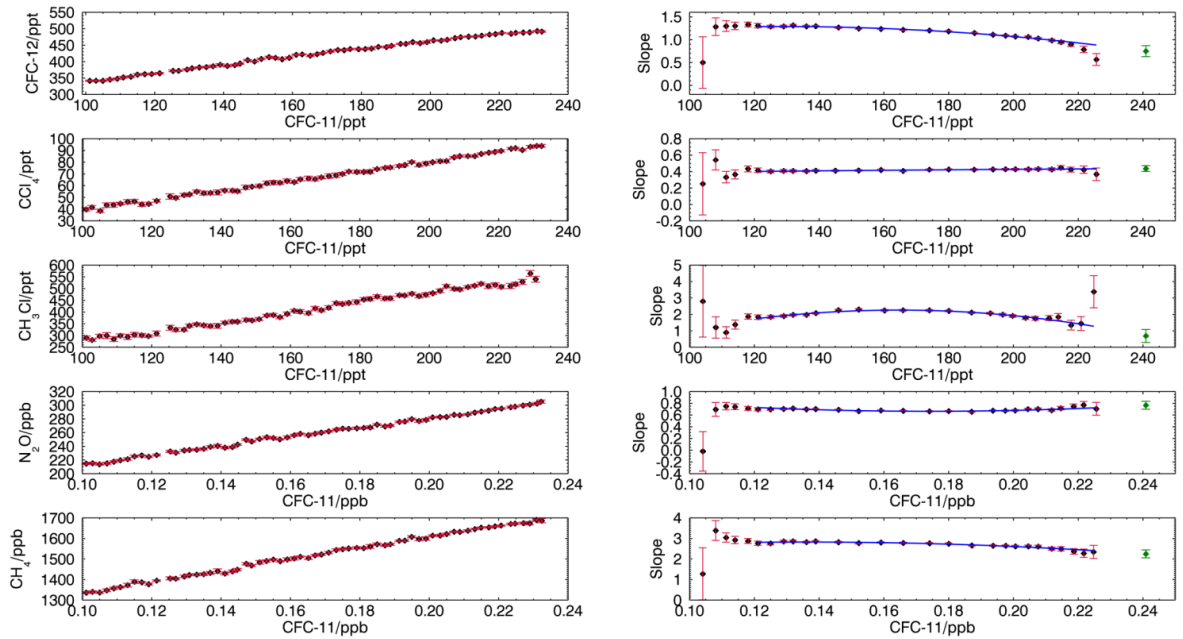


Figure C17: Correlations between the VMRs of CFC-12,  $\text{CCl}_4$ ,  $\text{CH}_4$ ,  $\text{CH}_3\text{Cl}$  and  $\text{N}_2\text{O}$  and CFC-11 for the data from the southern hemisphere during the stratospheric winter of 2006. Left panels: The mean correlation profile. Each point represents the mean of the VMR in a window of 2 ppt of CFC-11. The error on these points is the standard deviation of the data within each 2 ppt window. Right panels: The local slope of data in an 80 ppt of CFC-11 window. The error on the points is the fitting error of this fit. The blue line is a second degree polynomial fit to the local slopes. The green point is the extrapolated slope at the tropopause.

## Appendix C – Correlation plots against CFC-11

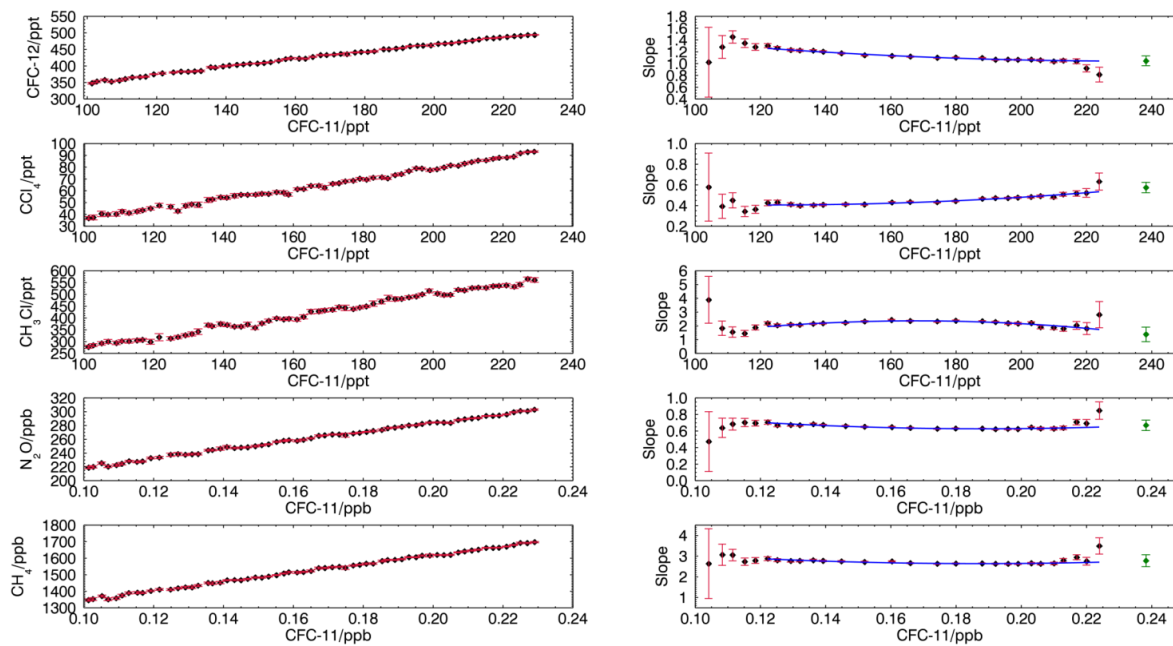


Figure C18: Correlations between the VMRs of CFC-12,  $\text{CCl}_4$ ,  $\text{CH}_4$ ,  $\text{CH}_3\text{Cl}$  and  $\text{N}_2\text{O}$  and CFC-11 for the data from the southern hemisphere during the stratospheric winter of 2007. Left panels: The mean correlation profile. Each point represents the mean of the VMR in a window of 2 ppt of CFC-11. The error on these points is the standard deviation of the data within each 2 ppt window. Right panels: The local slope of data in an 80 ppt of CFC-11 window. The error on the points is the fitting error of this fit. The blue line is a second degree polynomial fit to the local slopes. The green point is the extrapolated slope at the tropopause.

## Appendix C – Correlation plots against CFC-11

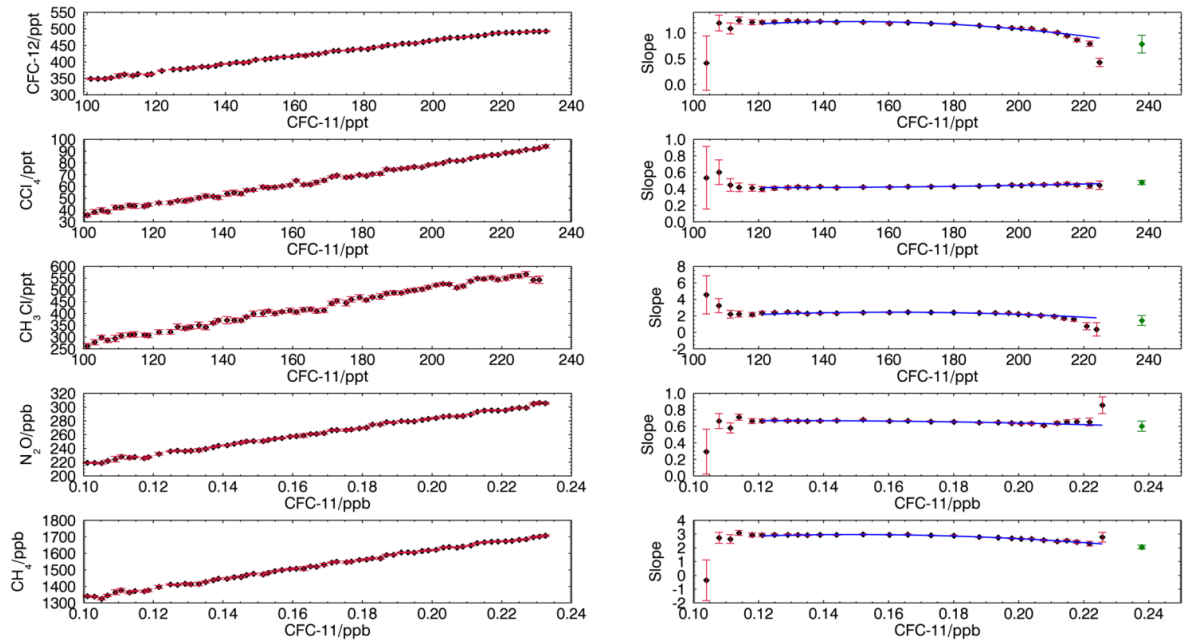


Figure C19: Correlations between the VMRs of CFC-12, CCl<sub>4</sub>, CH<sub>4</sub>, CH<sub>3</sub>Cl and N<sub>2</sub>O and CFC-11 for the data from the southern hemisphere during the stratospheric winter of 2008. Left panels: The mean correlation profile. Each point represents the mean of the VMR in a window of 2 ppt of CFC-11. The error on these points is the standard deviation of the data within each 2 ppt window. Right panels: The local slope of data in an 80 ppt of CFC-11 window. The error on the points is the fitting error of this fit. The blue line is a second degree polynomial fit to the local slopes. The green point is the extrapolated slope at the tropopause.

## Appendix C – Correlation plots against CFC-11

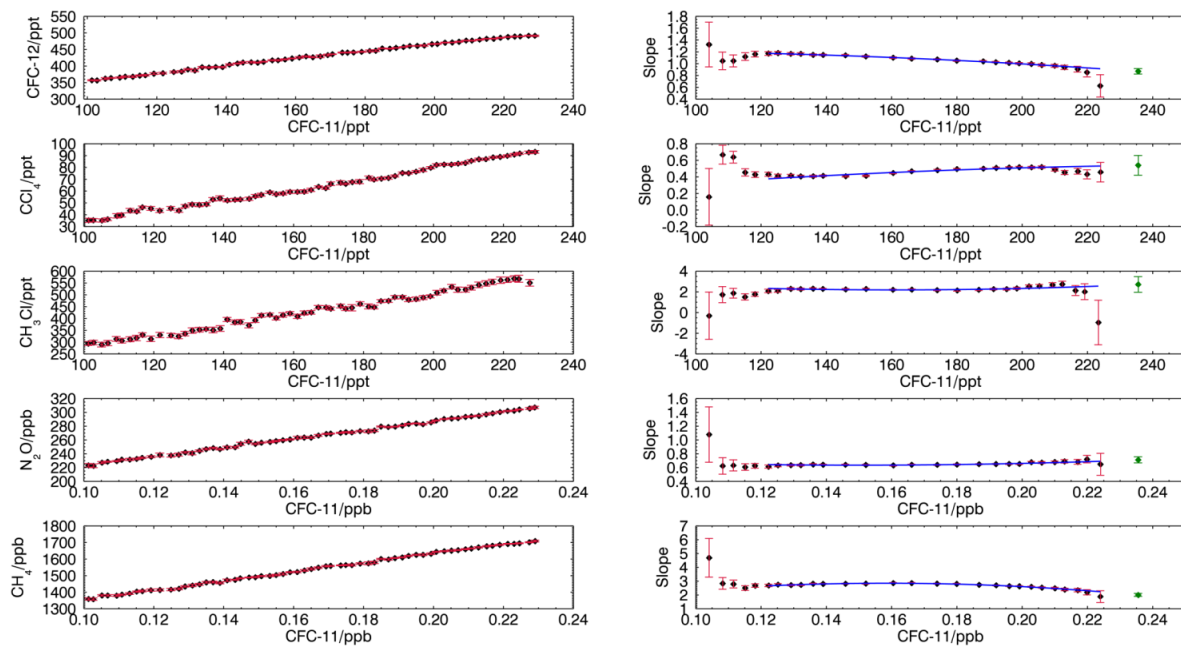


Figure C20: Correlations between the VMRs of CFC-12, CCl<sub>4</sub>, CH<sub>4</sub>, CH<sub>3</sub>Cl and N<sub>2</sub>O and CFC-11 for the data from the southern hemisphere during the stratospheric winter of 2009. Left panels: The mean correlation profile. Each point represents the mean of the VMR in a window of 2 ppt of CFC-11. The error on these points is the standard deviation of the data within each 2 ppt window. Right panels: The local slope of data in an 80 ppt of CFC-11 window. The error on the points is the fitting error of this fit. The blue line is a second degree polynomial fit to the local slopes. The green point is the extrapolated slope at the tropopause.

## Appendix C – Correlation plots against CFC-11

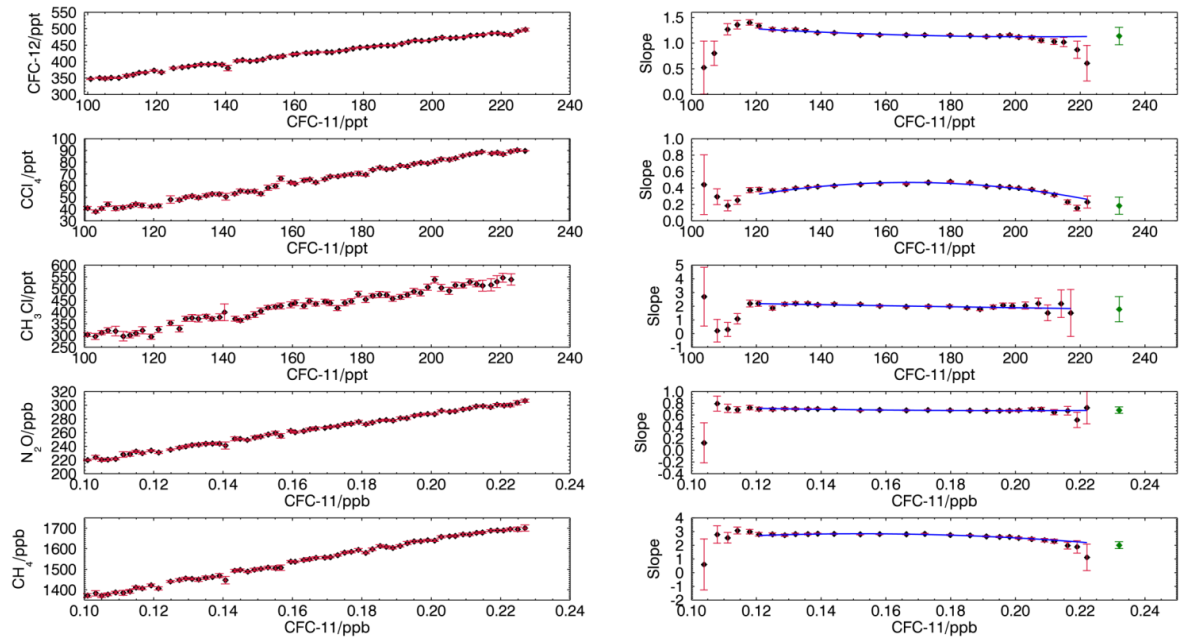


Figure C21: Correlations between the VMRs of CFC-12, CCl<sub>4</sub>, CH<sub>4</sub>, CH<sub>3</sub>Cl and N<sub>2</sub>O and CFC-11 for the data from the southern hemisphere during the stratospheric winter of 2010. Left panels: The mean correlation profile. Each point represents the mean of the VMR in a window of 2 ppt of CFC-11. The error on these points is the standard deviation of the data within each 2 ppt window. Right panels: The local slope of data in an 80 ppt of CFC-11 window. The error on the points is the fitting error of this fit. The blue line is a second degree polynomial fit to the local slopes. The green point is the extrapolated slope at the tropopause.

# Appendix D

## Comparison plots of lifetimes and correlations

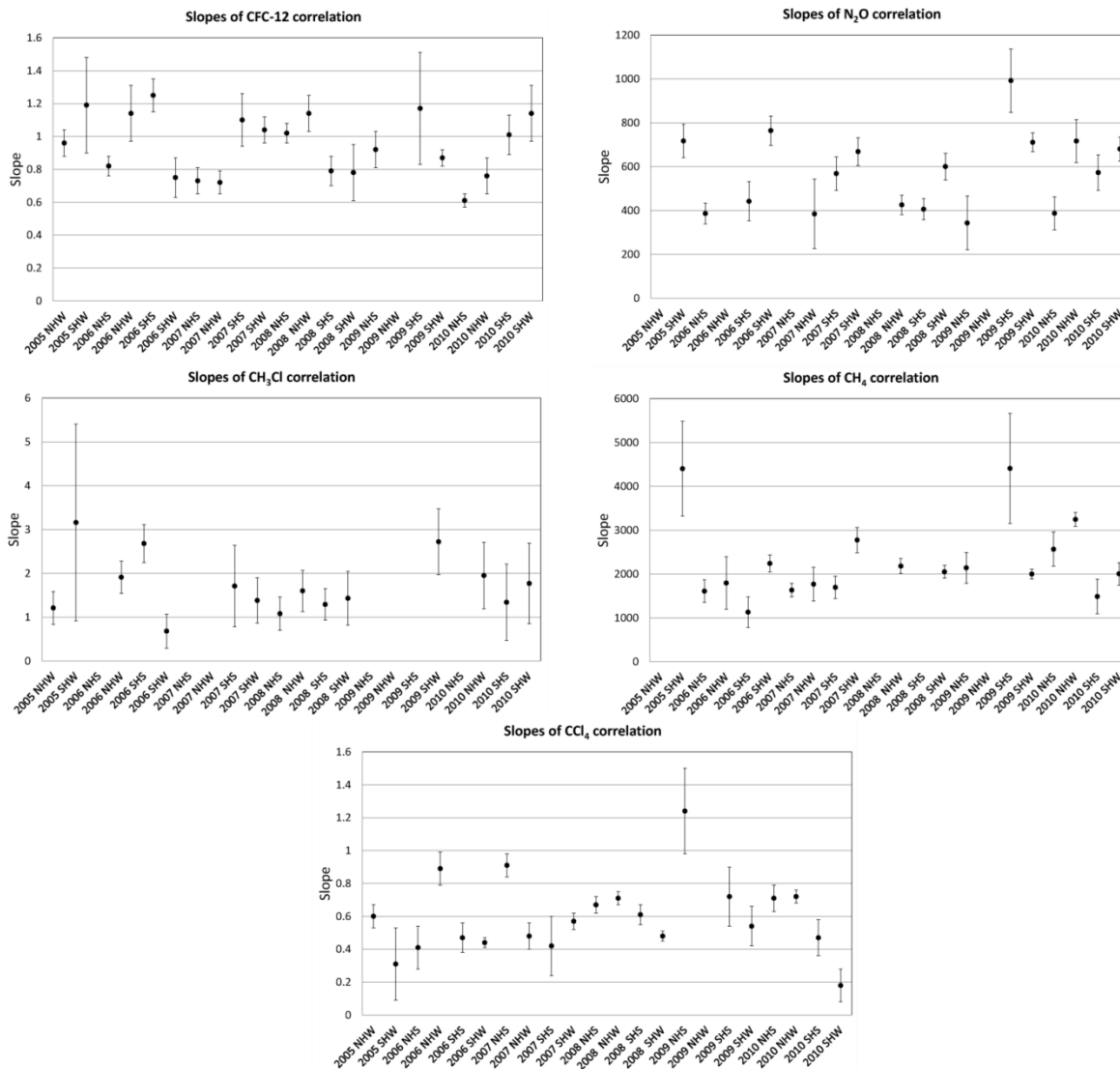


Figure D1: A graphical representation of the slopes of the various correlations with CFC-11.

## Appendix D – Comparison plots of lifetimes and correlations

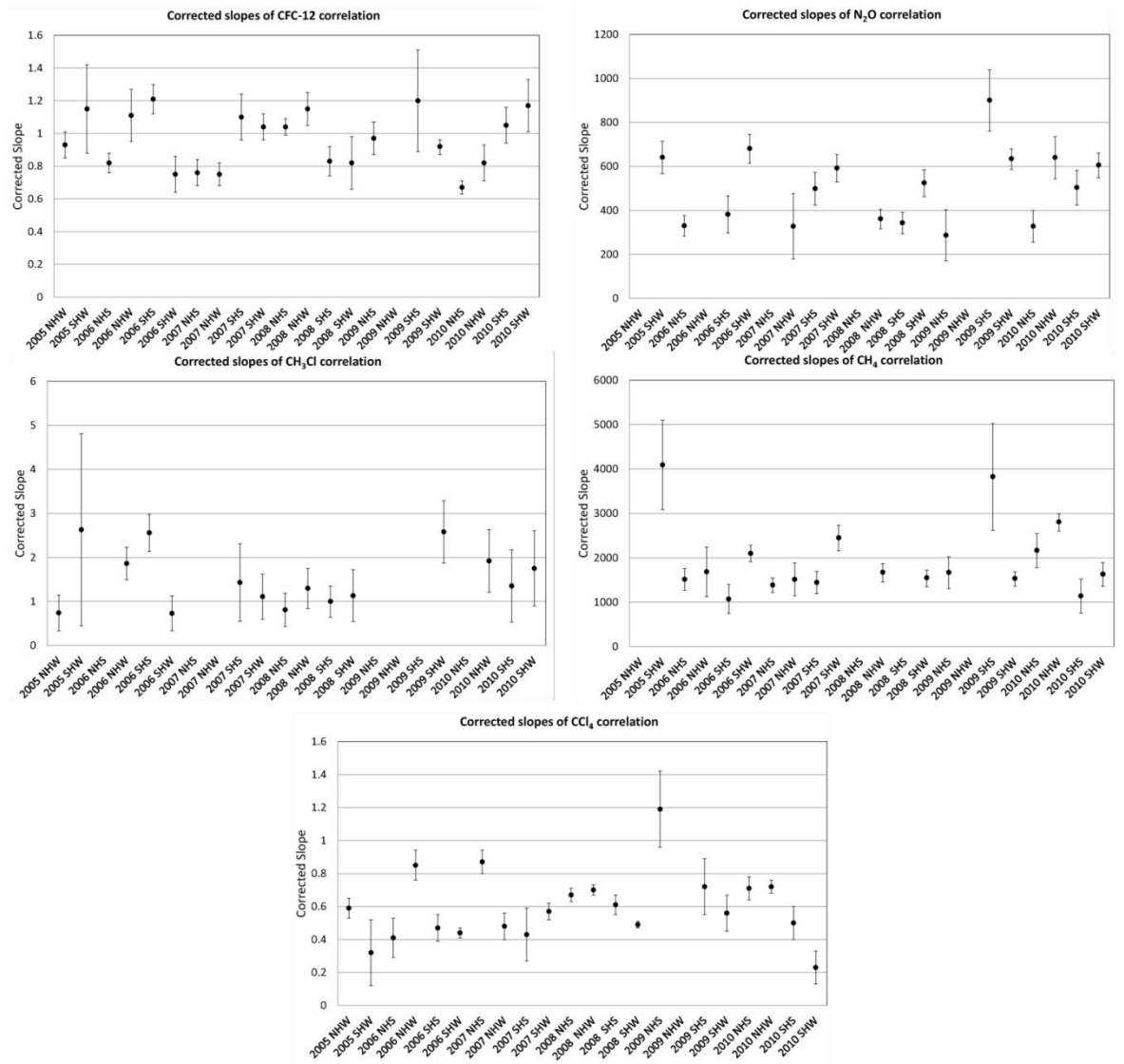


Figure D2: A graphical representation of the corrected slopes of the various correlations with CFC-11.

## Appendix D – Comparison plots of lifetimes and correlations

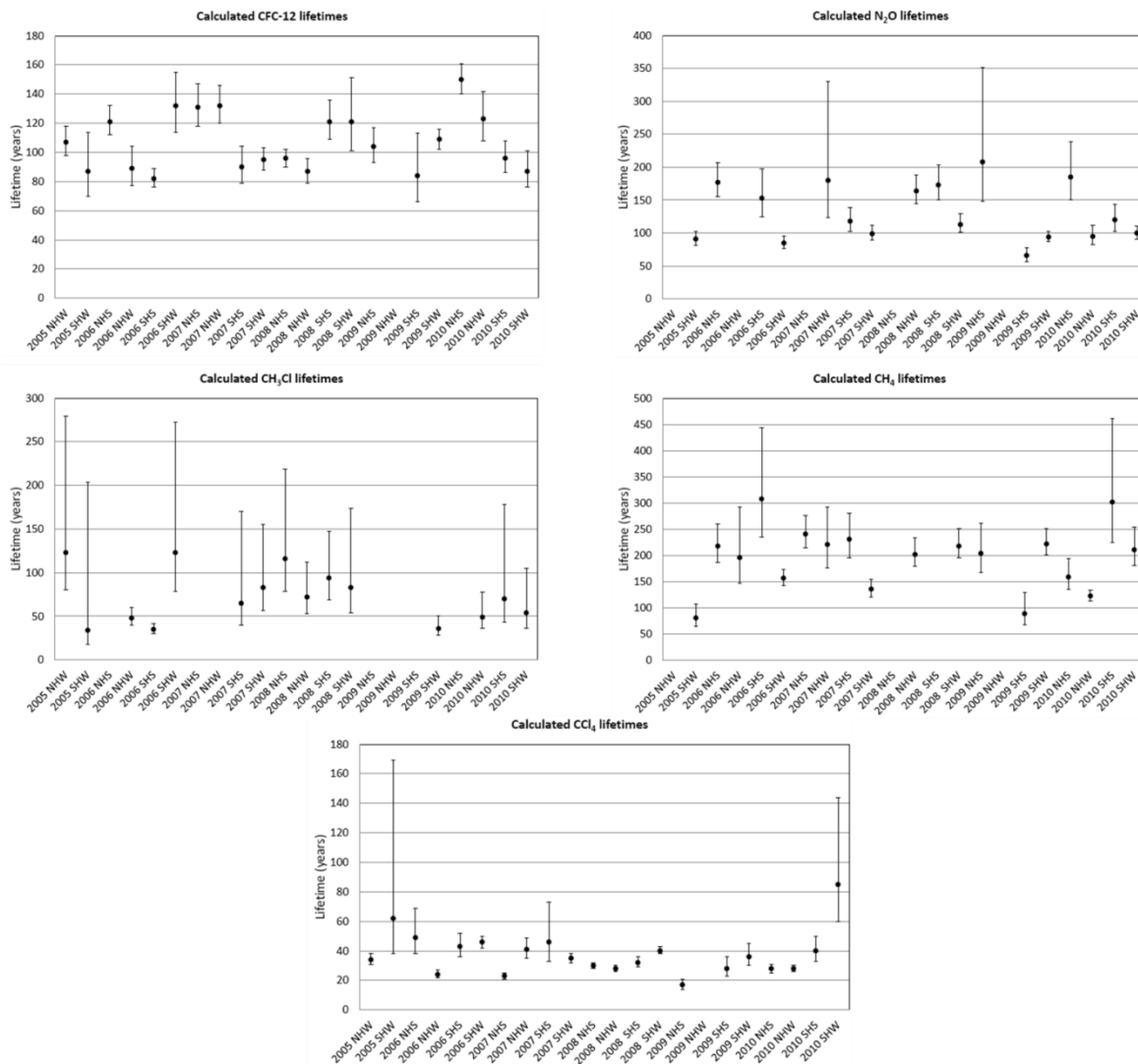


Figure D3: A graphical representation of the lifetimes of CFC-12, CCl<sub>4</sub>, CH<sub>3</sub>Cl, N<sub>2</sub>O and CH<sub>4</sub> calculated using a CFC-11 of 50 years.

# Appendix E

## *The derivation of the new equation for the steady-state correlations for the lifetimes calculations*

This equation was derived by Michael Volk following the preliminary calculations of correction factors (by myself) from MERRA age-of-air and ACE-FTS VMRs. The derivation begins with Eqn. 7.4:

$$\left. \frac{d\sigma}{d\Gamma} \right|_{\Gamma=0} = \frac{\left( \left. \frac{d\chi}{d\Gamma} \right|_{\Gamma=0} + \gamma_0 \sigma_0 \right)}{(1 - 2\gamma_0 \Lambda)} \quad \text{Eqn. 7.4}$$

$$\frac{\left. \frac{d\sigma_a}{d\Gamma} \right|_{\Gamma=0}}{\left. \frac{d\sigma_b}{d\Gamma} \right|_{\Gamma=0}} = \frac{\left( \left. \frac{d\chi_a}{d\Gamma} \right|_{\Gamma=0} + \gamma_{0a} \sigma_{0a} \right) (1 - 2\gamma_{0b} \Lambda)}{\left( \left. \frac{d\chi_b}{d\Gamma} \right|_{\Gamma=0} + \gamma_{0b} \sigma_{0b} \right) (1 - 2\gamma_{0a} \Lambda)} \quad \text{Eqn. E1}$$

The left hand side of Eqn. E1 can be rewritten as follows:

$$\frac{\left. \frac{d\sigma_a}{d\Gamma} \right|_{\Gamma=0}}{\left. \frac{d\sigma_b}{d\Gamma} \right|_{\Gamma=0}} = \frac{d\sigma_a}{d\sigma_b} \Big|_{\text{Tropopause}} \frac{d\Gamma}{d\Gamma} \Big|_{\Gamma=0} = \frac{d\sigma_a}{d\sigma_b} \Big|_{\text{Tropopause}} \quad \text{Eqn. E1a}$$

If the right hand side of Eqn. E1 is multiplied by  $(d\chi_b/d\chi_b)$  it can then be rewritten as follows:

Appendix E – Derivation of new equation for steady state correlations

$$\begin{aligned}
 & \frac{\left(\frac{d\chi_a}{d\Gamma}\Big|_{\Gamma=0} \frac{d\chi_b}{d\chi_b} + \gamma_{0a}\sigma_{0a}\right) (1 - 2\gamma_{0b}\Lambda)}{\left(\frac{d\chi_b}{d\Gamma}\Big|_{\Gamma=0} + \gamma_{0b}\sigma_{0b}\right) (1 - 2\gamma_{0a}\Lambda)} \\
 &= \frac{\frac{d\chi_a}{d\chi_b}\Big|_{tropopause} \cdot \frac{d\chi_b}{d\Gamma}\Big|_{\Gamma=0} + \gamma_{0a}\sigma_{0a}}{\frac{d\chi_b}{d\Gamma}\Big|_{\Gamma=0} + \gamma_{0b}\sigma_{0b}} \cdot \frac{1 - 2\gamma_{0b}\Lambda}{1 - 2\gamma_{0a}\Lambda}
 \end{aligned} \tag{Eqn. E1b}$$

Thus Eqn. E1 can be rewritten as Eqn. 7.7 thus:

$$\frac{d\sigma_a}{d\sigma_b}\Big|_{tropopause} = \frac{\frac{d\chi_a}{d\chi_b}\Big|_{tropopause} \cdot \frac{d\chi_b}{d\Gamma}\Big|_{\Gamma=0} + \gamma_{0a}\sigma_{0a}}{\frac{d\chi_b}{d\Gamma}\Big|_{\Gamma=0} + \gamma_{0b}\sigma_{0b}} \cdot \frac{1 - 2\gamma_{0b}\Lambda}{1 - 2\gamma_{0a}\Lambda} \tag{Eqn. 7.7}$$

# Abbreviations

|         |  |
|---------|--|
| ACE-FTS | Atmospheric Chemistry Experiment-Fourier Transform Spectrometer    |
| AGAGE   | Advanced Global Atmospheric Gases Experiment                       |
| ATMOS   | Atmospheric Trace MOlecule Spectroscopy                            |
| CFC     | Chlorofluorocarbon   |
| CLAES   | Cryogenic Limb Array Etalon Spectrometer                           |
| CRISTA  | CRyogenic Infrared Spectrometers and Telescopes for the Atmosphere |
| CTM     | Chemical Transport Model   |
| DMP     | Derived Meteriological Products                                    |
| ECMWF   | European Center for Median-range Weather Forecasting               |
| ET      | Extra-Tropical   |
| FTIR    | Fourier Transform Infrared Spectrometer                            |
| GC-MS   | Gas Chromatography-Mass Spectrometer                               |
| GHG     | GreenHouse Gases   |
| GMI     | Global Modeling Initiative   |
| GPS     | Global Positioning System  |
| GWP     | Global Warming Potential   |
| HALOE   | HALogen Occultation Experiment                                     |
| HCFC    | Hydrochlorofluorocarbon  |
| HFC     | Hydrofluorocarbon  |
| IPCC    | Intergovenmental Panel on Climate Change                           |
| IR      | Infrared   |
| MAD     | Median Absolute Deviation  |
| MERRA   | Modern-Era Retrospective analysis for Research and Applications    |
| MIPAS   | Michelson Interferometer for Passive Atmospheric Sounding          |
| MLS     | Microwave Limb Sounder   |
| NASA    | National Aeronautics and Space Administrations                     |
| NH      | Northern Hemisphere  |
| NHS     | Northern Hemisphere Summer   |
| NHW     | Northern Hemisphere Winter   |
| NOAA    | National Oceanic and Atmospheric Administration                    |
| ODP     | Ozone Depleting Potential  |
| ODS     | Ozone Depleting Substance  |
| OPD     | Optical Path Difference  |
| RF      | Radiative Forcing  |

## Abbreviations

|       |  |
|-------|--|
| S/N   | Signal-to-Noise  |
| SAOD  | Scientific Assessment of Ozone Depletion                     |
| SAP   | Scientific Assessment Panel                                  |
| SH    | Southern Hemisphere  |
| SHS   | Southern Hemisphere Summer                                   |
| SHW   | Southern Hemisphere Winter                                   |
| SPARC | Stratosphere-troposphere Processes And their Role in Climate |
| T     | Tropical   |
| TH    | Time Horizon   |
| UARS  | Upper Atmosphere Research Satellite                          |
| UNEP  | United Nations Environment Programme                         |
| UV    | Ultraviolet  |
| WMO   | World Meteorological Organisation                            |

# References

Allen, N. D. C., Bernath, P. F., Boone, C. D., Chipperfield, M. P., Fu, D., Manney, G. L., Oram, D. E., Toon, G. C., and Weisenstein, D. K.: Global carbon tetrachloride distributions obtained from the Atmospheric Chemistry Experiment (ACE), *Atmos. Chem. Phys.*, 9, 7449-7459, 10.5194/acp-9-7449-2009, 2009.

Anderson, S.O., Madhava Sarma, K.: *Protecting the ozone layer: The United Nations history*, Routledge Publishers, Oxford, 63, 2002a

Anderson, S.O., Madhava Sarma, K.: *Protecting the ozone layer: The United Nations history*, Routledge Publishers, Oxford, 84, 2002b

Baker, T. R., Phillips, O. L., Malhi, Y., Almeida, S., Arroyo, L., Di Fiore, A., Erwin, T., Higuchi, N., Killeen, T.J., Laurance, S. G., Laurance, W. F., Lewis, S. L., Monteagudo, A., Neill, D. A., Vargas, P. N., Pitman, N. C. A., Silva, J. N. M., and Martinez, R. V.: Increasing biomass in Amazonian forest plots. *Philos. Trans. R. Soc. London Ser. B*, 359, 353–365. 2004:

Barry, R.G., Chorley, R.J: *Atmosphere, Weather and Climate*, Eighth Edition, Taylor & Francis, London, 25 - 28, 2007a

Barry, R.G., Chorley, R.J: *Atmosphere, Weather and Climate*, Eighth Edition, Taylor & Francis, London, 112 - 161, 2007b

Barry, R.G., Chorley, R.J: *Atmosphere, Weather and Climate*, Eighth Edition, Taylor & Francis, London, 51, 2007c

Barry, R.G., Chorley, R.J: *Atmosphere, Weather and Climate*, Eighth Edition, Taylor & Francis, London, 262, 2007d

## References

Bernath, P. F., McElroy, C. T., Abrams, M. C., Boone, C. D., Butler, M., Camy-Peyret, C., Carleer, M., Clerbaux, C., Coheur, P. F., Colin, R., DeCola, P., DeMazière, M., Drummond, J. R., Dufour, D., Evans, W. F. J., Fast, H., Fussen, D., Gilbert, K., Jennings, D. E., Llewellyn, E. J., Lowe, R. P., Mahieu, E., McConnell, J. C., McHugh, M., McLeod, S. D., Michaud, R., Midwinter, C., Nassar, R., Nichitiu, F., Nowlan, C., Rinsland, C. P., Rochon, Y. J., Rowlands, N., Semeniuk, K., Simon, P., Skelton, R., Sloan, J. J., Soucy, M. A., Strong, K., Tremblay, P., Turnbull, D., Walker, K. A., Walkty, I., Wardle, D. A., Wehrle, V., Zander, R., and Zou, J.: Atmospheric Chemistry Experiment (ACE): Mission overview, *Geophys. Res. Lett.*, 32, L15S01, 10.1029/2005gl022386, 2005a.

Bernath, P. F.: Atmospheric chemistry experiment (ACE): Analytical chemistry from orbit, *TrAC Trends in Analytical Chemistry*, 25, 647-654, 10.1016/j.trac.2006.05.001, 2006.

Bernath, Peter Atmospheric Chemistry Experiment: Spectroscopy from Orbit, *Optics & Photonics News*, Optical Society of America, 24-2, 2005b.

Boone, C. D., Nassar, R., Walker, K. A., Rochon, Y., McLeod, S. D., Rinsland, C. P., and Bernath, P. F.: Retrievals for the atmospheric chemistry experiment Fourier-transform spectrometer, *Appl. Opt.*, 44, 7218-7231, 2005.

Brown, A. T., Chipperfield, M. P., Boone, C., Wilson, C., Walker, K. A., and Bernath, P. F.: Trends in atmospheric halogen containing gases since 2004, *Journal of Quantitative Spectroscopy and Radiative Transfer*, 112, 2552-2566, 10.1016/j.jqsrt.2011.07.005, 2011.

Bujok, O., Tan, V., Klein, E., Nopper, R., Bauer, R., Engel, A., Gerhards, M.-T., Afchine, A., McKenna, D. S., Schmidt, U., Wienhold, F. G., and Fischer, H.: GHOST – A Novel Airborne Gas Chromatograph for In Situ Measurements of

## References

Long-Lived Tracers in the Lower Stratosphere: Method and Applications, *Journal of Atmospheric Chemistry*, 39, 37-64, 10.1023/a:1010789715871, 2001.

Chipperfield, M. P.: Multiannual simulations with a three-dimensional chemical transport model, *J. Geophys. Res.*, 104, 1781-1805, 10.1029/98jd02597, 1999.

Chipperfield, M. P.: New Version of the TOMCAT/SLIMCAT Off-Line Chemical Transport Model: Intercomparison of Stratospheric Tracer Experiments, *Q. J. R. Meteorol. Soc.*, 132, 1179-1203, 2006.

Cox, M. L., Sturrock, G. A., Fraser, P. J., Siems, S. T., Krummel, P. B., and O'Doherty, S.: Regional Sources of Methyl Chloride, Chloroform and Dichloromethane Identified from AGAGE Observations at Cape Grim, Tasmania, 1998–2000, *Journal of Atmospheric Chemistry*, 45, 79-99, 10.1023/a:1024022320985, 2003.

Cunnold, D. M., Weiss, R. F., Prinn, R. G., Hartley, D., Simmonds, P. G., Fraser, P. J., Miller, B., Alyea, F. N., and Porter, L.: GAGE/AGAGE measurements indicating reductions in global emissions of CCl<sub>3</sub>F and CCl<sub>2</sub>F<sub>2</sub> in 1992, *J. Geophys. Res.*, 102, 1259-1269, 10.1029/96jd02973, 1997.

Cunnold, D. M., Steele, L. P., Fraser, P. J., Simmonds, P. G., Prinn, R. G., Weiss, R. F., Porter, L. W., O'Doherty, S., Langenfelds, R. L., Krummel, P. B., Wang, H. J., Emmons, L., Tie, X. X., and Dlugokencky, E. J.: In situ measurements of atmospheric methane at GAGE/AGAGE sites during 1985 to 2000 and resulting source inferences, *J. Geophys. Res.*, 107, 4225, 10.1029/2001jd001226, 2002.

Dobson, G. M. B.: Ozone in the upper atmosphere and its relation to meteorology, *Nature*, 127, 668-672, 1931

## References

Douglass, A. R., Stolarski, R. S., Schoeberl, M. R., Jackman, C. H., Gupta, M. L., Newman, P. A., Nielsen, J. E., and Fleming, E. L.: Relationship of loss, mean age of air and the distribution of CFCs to stratospheric circulation and implications for atmospheric lifetimes, *J. Geophys. Res.*, 113, D14309, 10.1029/2007jd009575, 2008.

Dufour G, Boone C. D, Bernath P. F.: First measurements of CFC-113 and HCFC-142b from space using ACE-FTS infrared spectra. *Geophys Res Lett.* 32, 4, 2005

Dufour, G., Nassar, R., Boone, C. D., Skelton, R., Walker, K. A., Bernath, P. F., Rinsland, C. P., Semeniuk, K., Jin, J. J., McConnell, J. C., and Manney, G. L.: Partitioning between the inorganic chlorine reservoirs HCl and ClONO<sub>2</sub> during the Arctic winter 2005 from the ACE-FTS, *Atmos. Chem. Phys.*, 6, 2355-2366, 10.5194/acp-6-2355-2006, 2006.

Efron, B.: Bootstrap methods: Another look at the jackknife, *The Annals of Statistics*, 7, 1-26, 1979

Farman, J. C., Gardiner B. G., Shanklin J. D.: Large losses of total ozone in Antarctica reveal seasonal ClO<sub>x</sub>/NO<sub>x</sub> interaction. *Nature.* 315, 207-210, 1985

Feng, W., Chipperfield, M. P., Dorf, M., Pfeilsticker, K., and Ricaud, P.: Mid-latitude ozone changes: studies with a 3-D CTM forced by ERA-40 analyses, *Atmos. Chem. Phys.*, 7, 2357-2369, 10.5194/acp-7-2357-2007, 2007.

Fischer, H, Birk, M, Blom, C, Carli, B, Carlotti, M, von Clarmann, T.: MIPAS: an instrument for atmospheric and climate research. *Atmos Chem Phys.*, 8, 2151-88. 2008

Freedman, R.A., Kaufmann, W.J. III: *Universe*, Seventh edition, W H Freeman & Co, New York, 2005

## References

Froidevaux, L., Livesey, N. J., Read, W. G., Jiang, Y. B., Jimenez, C., Filipiak, M. J., Schwartz, M. J., Santee, M. L., Pumphrey, H. C., Jiang, J. H., Wu, D. L., Manney, G. L., Drouin, B. J., Waters, J. W., Fetzer, E. J., Bernath, P. F., Boone, C. D., Walker, K. A., Jucks, K. W., Toon, G. C., Margitan, J. J., Sen, B., Webster, C. R., Christensen, L. E., Elkins, J. W., Atlas, E., Lueb, R. A., and Hendershot, R.: Early validation analyses of atmospheric profiles from EOS MLS on the aura Satellite, *Geoscience and Remote Sensing, IEEE Transactions on*, 44, 1106-1121, 10.1109/tgrs.2006.864366, 2006a.

Froidevaux, L., Livesey, N. J., Read, W. G., Salawitch, R. J., Waters, J. W., Drouin, B., MacKenzie, I. A., Pumphrey, H. C., Bernath, P., Boone, C., Nassar, R., Montzka, S., Elkins, J., Cunnold, D., and Waugh, D.: Temporal decrease in upper atmospheric chlorine, *Geophys. Res. Lett.*, 33, L23812, 10.1029/2006gl027600, 2006b.

Fu, D., Boone, C. D., Bernath, P. F., Walker, K. A., Nassar, R., Manney, G. L., Global phosgene observations from the atmospheric chemistry experiment (ACE) mission. *Geophys Res Lett.* 34:5 2007.

Fu, D., Boone, C. D., Bernath, P. F., Weisenstein, D. K., Rinsland, C. P., Manney, G. L., and Walker, K. A.: First global observations of atmospheric COClF from the Atmospheric Chemistry Experiment mission, *Journal of Quantitative Spectroscopy and Radiative Transfer*, 110, 974-985, 10.1016/j.jqsrt.2009.02.018, 2009.

Greally, B.R., Manning, A.J., Reimann, S., McCulloch, A., Huang, J., Dunse, B.L., Simmonds, P.G., Prinn, R.G., Fraser, P.J., Cunnold, D.M., O'Doherty, S., Porter, L.W., Stemmler, K., Vollmer, M.K., Lunder, C.R., Schmidbauer, N., Hermansen, O., Arduini, J., Salameh, P.K., Krummel, P.B., Wang, R.H.J., Folini, D., Weiss, R.F., Maione, M., Nickless, G., Stordal F., and Derwent, R.G.: Observations of 1,1-difluoroethane (HFC-152a) at AGAGE and SOGE

## References

monitoring stations in 1994–2004 and derived global and regional emission estimates, *J. Geophys. Res.*, 112, D06308, doi: 10.1029/2006JD007527, 2007.

Gunson, M.R., Abbas, M.M., Abrams, M.C., Allen, M., Brown, L.R., Brown, T.L., Chang, A.Y., Goldman, A., Irion, F.W., Lowes, L.L., Mahieu, E., Manney, G.L., Michelsen, H.A., Newchurch, M.J., Rinsland, C.P., Salawitch, R.J., Stiller, G.P., Toon, G.C., Yung, Y.L., Zander, R.: The Atmospheric Trace Molecular Spectroscopy (ATMOS) experiment: Deployment on the ATLAS Space Shuttle Missions, *Geophys. Res. Lett.*, 23, 2333-2336, 1996

Harrison, J. J., Boone, C. D., Brown, A. T., Allen, N. D. C., Toon, G. C., and Bernath, P. F.: First remote sensing observations of trifluoromethane (HFC-23) in the upper troposphere and lower stratosphere, *J. Geophys. Res.*, 117, D05308, 10.1029/2011jd016423, 2012.

Holton, J. R.: An introduction to dynamic meteorology, Fourth Edition, Elsevier Academic Press, London, 407-445, 2004a

Holton, J. R.: An introduction to dynamic meteorology, Fourth Edition, Elsevier Academic Press, London, 50, 2004b

Höpfner, M., von Clarmann, T., Fischer, H., Funke, B., Glatthor, N., Grabowski, U., Kellmann, S., Kiefer, M., Linden, A., Milz, M., Steck, T., Stiller, G. P., Bernath, P., Blom, C. E., Blumenstock, T., Boone, C., Chance, K., Coffey, M. T., Friedl-Vallon, F., Griffith, D., Hannigan, J. W., Hase, F., Jones, N., Jucks, K. W., Keim, C., Kleinert, A., Kouker, W., Liu, G. Y., Mahieu, E., Mellqvist, J., Mikuteit, S., Notholt, J., Oelhaf, H., Piesch, C., Reddman, T., Ruhnke, R., Schneider, M., Strandberg, A., Toon, G., Walker, K. A., Warneke, T., Wetzell, G., Wood, S., and Zander, R.: Validation of MIPAS ClONO<sub>2</sub> measurements, *Atmos. Chem. Phys.*, 7, 257-281, 10.5194/acp-7-257-2007, 2007.

Irion, F. W., Gunson, M. R., Toon, G. C., Chang, A. Y., Eldering, A., Mahieu, E., Manney, G. L., Michelsen, H. A., Moyer, E. J., Newchurch, M. J.,

## References

Osterman, G. B., Rinsland, C. P., Salawitch, R. J., Sen, B., Yung, Y. L., and Zander, R.: Atmospheric Trace Molecule Spectroscopy (ATMOS) Experiment Version 3 data retrievals, *Appl. Opt.*, 41, 6968-6979, 2002.

Jacob D.J.: *Introduction to Atmospheric Chemistry*, Princeton University Press, New Jersey, 79, 1999

Johnston, H. S., Serang, O., and Podolske, J.: Instantaneous Global Nitrous Oxide Photochemical Rates, *J. Geophys. Res.*, 84, 5077-5082, 10.1029/JC084iC08p05077, 1979.

Keim, C, Liu, G. Y., Blom, C. E., Fischer, H., Gulde, T., Höpfner, M., Piesch, C., Ravegnani, F., Roiger, A., Schlager, H. and Sitnikov, N.: Vertical profile of peroxyacetyl nitrate (PAN) from MIPAS-STR measurements over Brazil in February 2005 and its contribution to tropical UT NO<sub>y</sub> partitioning, *Atmos. Chem. Phys.*, 8, 4891–4902, 2008

Ko, M. K., Newman, P. A., Reimann, S., and Strahan, S. E.: Lifetime of halogen source gases, In Preparation.

Kuttippurath, J., Lefèvre, F., Pommereau, J. P., Roscoe, H. K., Goutail, F., Pazmiño, A., and Shanklin, J. D.: Antarctic ozone loss in 1979–2010: first sign of ozone recovery, *Atmos. Chem. Phys.*, 13, 1625-1635, 10.5194/acp-13-1625-2013, 2013.

Lary, D. J., Waugh, D. W., Douglass, A. R., Stolarski, R. S., Newman, P. A., and Mussa, H.: Variations in stratospheric inorganic chlorine between 1991 and 2006, *Geophys. Res. Lett.*, 34, L21811, 10.1029/2007gl030053, 2007.

Lary, D. J, Aulov, O.: Space-based measurements of HCl: Intercomparison and historical context. *J Geophys Res-Atmos.* 113, 10, 2008

Laube, J. C., Engel, A. Keil, H. Bönisch, M. J. Bolder, T. Röckmann, and W. T. Sturges, Observation-based assessment of stratospheric fractional release, lifetimes, and Ozone Depletion Potentials of ten important source gases,

## References

Atmos. Chem. Phys. Discuss., 12, 28525–28557, doi:10.5194/acpd-12-28525, 2013.

Lide, D.: Handbook of Chemistry and Physics, in, Chemical Rubber Publishing Company, USA, 9-109, 1990.

Lovelock, J.E., Maggs, R.J., and Wade, R.J.: Halogenated Hydrocarbons in and over the Atlantic, *Nature*, 241, 1973.

Mäder, J. A., Staehelin, J., Peter, T., Brunner, D., Rieder, H. E., and Stahel, W. A.: Evidence for the effectiveness of the Montreal Protocol to protect the ozone layer, *Atmos. Chem. Phys.*, 10, 12161-12171, 10.5194/acp-10-12161-2010, 2010.

Mahieu, E., Zander, R., Duchatelet, P., Hannigan, J. W., Coffey, M. T., Mikuteit, S., Hase, F., Blumenstock, T., Wiacek, A., Strong, K., Taylor, J. R., Mittermeier, R. L., Fast, H., Boone, C. D., McLeod, S. D., Walker, K. A., Bernath, P. F., and Rinsland, C. P.: Comparisons between ACE-FTS and ground-based measurements of stratospheric HCl and ClONO<sub>2</sub> loadings at northern latitudes, *Geophys. Res. Lett.*, 32, L15S08, 10.1029/2005gl022396, 2005.

Mahieu, E., Duchatelet, P., Demoulin, P., Walker, K. A., Dupuy, E., Froidevaux, L., Randall, C., Catoire, V., Strong, K., Boone, C. D., Bernath, P. F., Blavier, J. F., Blumenstock, T., Coffey, M., De Mazière, M., Griffith, D., Hannigan, J., Hase, F., Jones, N., Jucks, K. W., Kagawa, A., Kasai, Y., Mebarki, Y., Mikuteit, S., Nassar, R., Notholt, J., Rinsland, C. P., Robert, C., Schrems, O., Senten, C., Smale, D., Taylor, J., Tétard, C., Toon, G. C., Warneke, T., Wood, S. W., Zander, R., and Servais, C.: Validation of ACE-FTS v2.2 measurements of HCl, HF, CCl<sub>3</sub>F and CCl<sub>2</sub>F<sub>2</sub> using space-, balloon- and ground-based instrument observations, *Atmos. Chem. Phys.*, 8, 6199-6221, 10.5194/acp-8-6199-2008, 2008.

## References

Mahieu, E., Zander, R., Bernath, P., Boone, C., and Walker, K.: Recent Trend Anomaly of Hydrogen Chloride (HCl) at Northern Mid-Latitudes Derived from Jungfraujoch, HALOE and ACE-FTS Infrared Solar Observations, The Atmospheric Chemistry Experiment ACE at 10: A Solar Occultation Anthology, P. Bernath (editor), A. Deepak Publishing, Hampton, VA, USA, 239-249, 2013

McHugh, M., Magill, B., Walker, K. A., Boone, C. D., Bernath, P. F., and Russell, J. M., III: Comparison of atmospheric retrievals from ACE and HALOE, *Geophys. Res. Lett.*, 32, L15S10, 10.1029/2005gl022403, 2005.

McIntyre, M.E., Palmer, T.N.: Breaking planetary waves in the stratosphere, *Nature*, 305, 593 – 600, 10.1038/305593a0, 1983

McNeill, J. R.: Something new under the Sun: An environmental history of the twentieth-century world, W. W. Norton & Company, London, 2001

Mikuteit, S.: Trendbestimmung stratosphärischer Spurengase mit Hilfebodengebundener FTIR-Messungen - dissertation, FZK Report No. 7385, GERMANY, 2008.

Miller, B.R, Rigby, M., Kuijpers, L.J.M., Krummel, P.B., Steele, L.P., Leist, M., Fraser, P.J., McCulloch, A., Harth, C., Salameh, P., Mühle, J., Weiss, R.F., Prinn, R.G., Wang, R.H.J., O'Doherty, S., Grealley, B.R., and Simmonds, P.G., HFC-23 (CHF<sub>3</sub>) emission trend response to HCFC-22 (CHClF<sub>2</sub>) production and recent HFC-23 emission abatement measures, *Atmos. Chem. Phys.*, 10 (16), 7875-7890, doi: 10.5194/acp-10-7875-2010, 2010.

Minschwaner, K., Carver, R. W., Briegleb, B. P., and Roche, A. E.: Infrared radiative forcing and atmospheric lifetimes of trace species based on observations from UARS, *J. Geophys. Res.*, 103, 23243-23253, 10.1029/98jd02116, 1998.

## References

Molina, M. J., Rowland, F. S.: Stratospheric sink for chlorofluoromethanes - chlorine atomic-catalysed destruction of ozone. *Nature*, 249, 810-2, 1974

Monge-Sanz, B. M., Chipperfield, M. P., Simmons, A. J., and Uppala, S. M.: Mean age of air and transport in a CTM: Comparison of different ECMWF analyses, *Geophys. Res. Lett.*, 34, L04801, 10.1029/2006gl028515, 2007.

Montzka, S. A., Hall, B. D., and Elkins, J. W.: Accelerated increases observed for hydrochlorofluorocarbons since 2004 in the global atmosphere, *Geophys. Res. Lett.*, 36, L03804, 10.1029/2008gl036475, 2009.

Montzka, S. A., Reimann, S., (Coordinating Lead Authors), Engel, A., Krüger, K., O'Doherty, S., Sturges, W. T., Blake, D., Dorf, M., Fraser, P., Froidevaux, L., Jucks, K., Kreher, K., Kurylo, M. J., Mellouki, A., Miller, J., Nielsen, O.-J., Orkin, V. L., Prinn, R. G., Rhew, R., Santee, M. L., Stohl, A., and Verdonik, D.: Ozone-Depleting Substances (ODSs) and Related Chemicals, Chapter 1 in *Scientific Assessment of Ozone Depletion: 2010, Global Ozone Research and Monitoring Project—Report No. 52*, World Meteorological Organization, Geneva, Switzerland, 2011a.

Montzka, S. A., Reimann, S., (Coordinating Lead Authors), Engel, A., Krüger, K., O'Doherty, S., Sturges, W. T., Blake, D., Dorf, M., Fraser, P., Froidevaux, L., Jucks, K., Kreher, K., Kurylo, M. J., Mellouki, A., Miller, J., Nielsen, O.-J., Orkin, V. L., Prinn, R. G., Rhew, R., Santee, M. L., Stohl, A., and Verdonik, D.: Ozone-Depleting Substances (ODSs) and Related Chemicals, Chapter 5 in *Scientific Assessment of Ozone Depletion: 2010, Global Ozone Research and Monitoring Project—Report No. 52*, World Meteorological Organization, Geneva, Switzerland, 2011b.

Muhle J, Ganesan AL, Miller BR, Salameh PK, Harth CM, Grealley BR, et al. Perfluorocarbons in the global atmosphere: tetrafluoromethane,

## References

hexafluoroethane, and octafluoropropane. *Atmos Chem Phys Discuss.*10:6485-536. 2010

Nassar, R., Bernath, P. F., Boone, C. D., Clerbaux, C., Coheur, P. F., Dufour, G., Froidevaux, L., Mahieu, E., McConnell, J. C., McLeod, S. D., Murtagh, D. P., Rinsland, C. P., Semeniuk, K., Skelton, R., Walker, K. A., and Zander, R.: A global inventory of stratospheric chlorine in 2004, *J. Geophys. Res.*, 111, D22312, 10.1029/2006jd007073, 2006a.

Nassar, R., Bernath, P. F., Boone, C. D., McLeod, S. D., Skelton, R., Walker, K. A., Rinsland, C. P., and Duchatelet, P.: A global inventory of stratospheric fluorine in 2004 based on Atmospheric Chemistry Experiment Fourier transform spectrometer (ACE-FTS) measurements, *J. Geophys. Res.*, 111, D22313, 10.1029/2006jd007395, 2006b.

Neu, J.L , and Plumb, R.A.: Age of air in a “leaky pipe” model of stratospheric transport, *J. Geophys. Res.*, 104, 19243-19255, 1999

O'Doherty, S., Cunnold, D. M., Manning, A., Miller, B. R., Wang, R. H. J., Krummel, P. B., Fraser, P. J., Simmonds, P. G., McCulloch, A., Weiss, R. F., Salameh, P., Porter, L. W., Prinn, R. G., Huang, J., Sturrock, G., Ryall, D., Derwent, R. G., and Montzka, S. A.: Rapid growth of hydrofluorocarbon 134a and hydrochlorofluorocarbons 141b, 142b, and 22 from Advanced Global Atmospheric Gases Experiment (AGAGE) observations at Cape Grim, Tasmania, and Mace Head, Ireland, *J. Geophys. Res.*, 109, D06310, 10.1029/2003jd004277, 2004.

Plumb, R. A., and Ko, M. K. W.: INTERRELATIONSHIPS BETWEEN MIXING RATIOS OF LONG-LIVED STRATOSPHERIC CONSTITUENTS, *J. Geophys. Res.*, 97, 10145-10156, 10.1029/92jd00450, 1992.

Plumb, R. A.: A tropical pipe model of stratospheric transport, *J. Geophys. Res.*, 101, 3957-3972, 10.1029/95jd03002, 1996.

## References

Plumb, R. A.: Stratospheric Transport, *Journal of Meteorological Society of Japan*, 80, 793-809, 2002.

Plumb, R. A.: Tracer interrelationships in the stratosphere, *Rev. Geophys.*, 45, RG4005, 10.1029/2005rg000179, 2007.

Prinn, R., Cunnold, D., Rasmussen, R., Simmonds, P., Alyea, F., Crawford, A., Fraser, P., and Rosen, R.: Atmospheric Emissions and Trends of Nitrous Oxide Deduced From 10 Years of ALE/GAGE Data, *J. Geophys. Res.*, 95, 18369-18385, 10.1029/JD095iD11p18369, 1990.

Prinn, R. G., Weiss, R. F., Fraser, P. J., Simmonds, P. G., Cunnold, D. M., Alyea, F. N., O'Doherty, S., Salameh, P., Miller, B. R., Huang, J., Wang, R. H. J., Hartley, D. E., Harth, C., Steele, L. P., Sturrock, G., Midgley, P. M., and McCulloch, A.: A history of chemically and radiatively important gases in air deduced from ALE/GAGE/AGAGE, *J. Geophys. Res.*, 105, 17751-17792, 10.1029/2000jd900141, 2000.

Prinn, R. G., Huang, J., Weiss, R. F., Cunnold, D. M., Fraser, P. J., Simmonds, P. G., McCulloch, A., Harth, C., Salameh, P., O'Doherty, S., Wang, R. H. J., Porter, L., and Miller, B. R.: Evidence for Substantial Variations of Atmospheric Hydroxyl Radicals in the Past Two Decades, *Science*, 292, 1882-1888, 10.1126/science.1058673, 2001.

Prinn, R. G., Zander, R., (Coordinating Lead Authors), Cunnold, D. M., Elkins, J. W., Engel, A., Fraser, P. J., Gunson, M. R., Ko, M. K. W., Mahieu, E., Midgley, P. M., Russell III, J. M., Volk, C.M., and Weis, R.F.: Long-Lived Ozone-Related Compounds, Chapter 1 in *Scientific Assessment of Ozone Depletion: 1998*, Global Ozone Research and Monitoring Project–Report No. 52, World Meteorological Organization, Geneva, Switzerland, 1999.

Ravishankara, A.R, Sheperd, T.G (Coordinating Lead Authors), Chipperfield, M.P., Haynes, P.H., Kawa, S.R., Peter, T., Plumb, R.A., Portmann, R.W.,

## References

Randel, W.J., Waugh, D.W., Worsnop, D.R.,: Lower Stratospheric Processes, Chapter 7 in Scientific Assessment of Ozone Depletion: 1998, Global Ozone Research and Monitoring Project–Report No. 44, World Meteorological Organization, Geneva, Switzerland, 1999.

Randel, W. J., and Wu, F.: Cooling of the Arctic and Antarctic Polar Stratospheres due to Ozone Depletion. *Journal of Climate*, 12, 1467–1479, 1999

Rigby, M., Prinn, R. G., Fraser, P. J., Simmonds, P. G., Langenfelds, R. L., Huang, J., Cunnold, D. M., Steele, L. P., Krummel, P. B., Weiss, R. F., O'Doherty, S., Salameh, P. K., Wang, H. J., Harth, C. M., Mühle, J., and Porter, L. W.: Renewed growth of atmospheric methane, *Geophys. Res. Lett.*, 35, L22805, 10.1029/2008gl036037, 2008.

Rinsland, C. P., Boone, C., Nassar, R., Walker, K., Bernath, P., Mahieu, E., Zander, R., McConnell, J. C., and Chiou, L.: Trends of HF, HCl, CCl<sub>2</sub>F<sub>2</sub>, CCl<sub>3</sub>F, CHClF<sub>2</sub> (HCFC-22), and SF<sub>6</sub> in the lower stratosphere from Atmospheric Chemistry Experiment (ACE) and Atmospheric Trace Molecule Spectroscopy (ATMOS) measurements near 30°N latitude, *Geophys. Res. Lett.*, 32, L16S03, 10.1029/2005gl022415, 2005.

Rinsland, C. P., Mahieu, E., Zander, R., Nassar, R., Bernath, P., Boone, C.: Long-term stratospheric carbon tetrafluoride (CF<sub>4</sub>) increase inferred from 1985-2004 infrared space-based solar occultation measurements. *Geophys Res Lett.* 2006;33:4.

Rinsland, C. P., Dufour, G., Boone, C. D., Bernath, P. F., Chiou, L., Coheur, P.-F., Turquety, S., and Clerbaux, C.: Satellite boreal measurements over Alaska and Canada during June-July 2004: Simultaneous measurements of upper tropospheric CO, C<sub>2</sub>H<sub>6</sub>, HCN, CH<sub>3</sub>Cl, CH<sub>4</sub>, C<sub>2</sub>H<sub>2</sub>, CH<sub>3</sub>OH, HCOOH, OCS,

## References

and SF<sub>6</sub> mixing ratios, *Global Biogeochem. Cycles*, 21, GB3008, 10.1029/2006gb002795, 2007.

Rinsland, C. P., Nassar, R., Boone, C. D., Bernath, P., Chiou, L., Weisenstein D. K.: Spectroscopic detection of COClF in the tropical and mid-latitude lower stratosphere. *Journal of Quantitative Spectroscopy & Radiative Transfer*. 105, 467-75, 2007

Russell, J. M., Luo, M., Cicerone, R. J., and Deaver, L. E.: Satellite confirmation of the dominance of chlorofluorocarbons in the global stratospheric chlorine budget, *Nature*, 379, 526-529, 1996.

Santee, M. L., MacKenzie, I. A., Manney, G. L., Chipperfield, M. P., Bernath, P. F., Walker, K. A., Boone, C. D., Froidevaux, L., Livesey, N. J., and Waters, J. W.: A study of stratospheric chlorine partitioning based on new satellite measurements and modeling, *J. Geophys. Res.*, 113, D12307, 10.1029/2007jd009057, 2008.

Sen, B., Toon, G. C., Blavier, J. F., Fleming, E. L., and Jackman, C. H.: Balloon-borne observations of midlatitude fluorine abundance, *J. Geophys. Res.*, 101, 9045-9054, 10.1029/96jd00227, 1996.

Sen, B., Osterman, G. B., Salawitch, R. J., Toon, G. C., Margitan, J. J., Blavier, J. F., Chang, A. Y., May, R. D., Webster, C. R., Stimpfle, R. M., Bonne, G. P., Voss, P. B., Perkins, K. K., Anderson, J. G., Cohen, R. C., Elkins, J. W., Dutton, G. S., Hurst, D. F., Romashkin, P. A., Atlas, E. L., Schauffler, S. M., and Loewenstein, M.: The budget and partitioning of stratospheric chlorine during the 1997 Arctic summer, *J. Geophys. Res.*, 104, 26653-26665, 10.1029/1999jd900245, 1999.

Shindell, D. T., Rind, D., and Lonergan, P.: Increased polar stratospheric ozone losses and delayed eventual recovery owing to increasing greenhouse-gas concentrations, *Nature*, 392, 589-592, 1998.

## References

Simmonds, P., Derwent, R., Manning, A., Fraser, P., Krummel, P., O'Doherty, S., Prinn, R., Cunnold, D., Miller, B., Wang, H., Ryall, D., Porter, L., Weiss, R., and Salameh, P.: AGAGE Observations of Methyl Bromide and Methyl Chloride at Mace Head, Ireland, and Cape Grim, Tasmania, 1998–2001, *Journal of Atmospheric Chemistry*, 47, 243-269, 10.1023/B:JOCH.0000021136.52340.9c, 2004.

Simmonds, P. G., Cunnold, D. M., Weiss, R. F., Prinn, R. G., Fraser, P. J., McCulloch, A., Alyea, F. N., and O'Doherty, S.: Global trends and emission estimates of CCl<sub>4</sub> from in situ background observations from July 1978 to June 1996, *J. Geophys. Res.*, 103, 16017-16027, 10.1029/98jd01022, 1998.

Smith, R. C., Prezelin, B. B., Baker, K. S., Bidigare, R. R., Boucher, N. P., Coley, T., Karentz, D., MacIntyre, S., Matlick, H. A., Menzies, D., Ondrusck, M., Wan, Z., Waters, K. J.: Ozone Depletion: Ultraviolet Radiation and Phytoplankton Biology in Antarctic Waters, *Science*, 255, 952-959, 1992

Solomon, S., Qin, D., Manning, M., Alley, R. B., Berntsen, T., Bindoff, N. L., Chen, Z., Chidthaisong, A., Gregory, J. M., Hegerl, G. C., Heimann, M., Hewitson, B., Hoskins, B. J., Joos, F., Jouzel, J., Kattsov, V., Lohmann, U., Matsuno, T., Molina, M., Nicholls, N., Overpeck, J., Raga, G., Ramaswamy, V., Ren, J., Rusticucci, M., Somerville, R., Stocker, T. F., Whetton, P., Wood, R. A., Wratt, D.: *Climate Change 2007: The Physical Science Basis. Contribution of Working Group I to the Fourth Assessment Report of the Intergovernmental Panel on Climate Change*, Cambridge University Press, Cambridge, 2007.

Stohl, A., Seibert, P., Arduini, J., Eckhardt, S., Fraser, P., Grealley, B.R., Lunder, C., Maione, M., Mühle, J., O'Doherty, S., Prinn, R.G., Reimann, S., Saito, T., Schmidbauer, N., Simmonds, P.G., Vollmer, M.K., Weiss, R.F., and Yokouchi, Y.: An analytical inversion method for determining regional and global emissions of greenhouse gases: Sensitivity studies and application to

## References

halocarbons, *Atmos. Chem. Phys.*, 9 (5), 1597-1620, doi: 10.5194/acp-9-1597-2009, 2009

Solomon, S., Rosenlof, K. H., Portmann, R. W., Daniel, J. S., Davis, S.M., Sanford, T. J., Plattner, G. K.: Contribution of stratospheric water vapour to decadal changes in the rate of global warming, *Science*, 327, 1219, 2010

Sonkaew, T., von Savigny, C., Eichmann, K. U., Weber, M., Rozanov, A., Bovensmann, H., Burrows, J. P., and Grooß, J. U.: Chemical ozone losses in Arctic and Antarctic polar winter/spring season derived from SCIAMACHY limb measurements 2002–2009, *Atmos. Chem. Phys.*, 13, 1809-1835, 10.5194/acp-13-1809-2013, 2013.

Tressaud, A.: *Fluorine and the Environment: Atmospheric Chemistry, Emissions, & Lithosphere*, Elsevier, 2006.

UNEP: *Handbook for the Montreal Protocol on Substances that Deplete the Ozone Layer 8ed.*, Secretariat for The Vienna Convention for the Protection of the Ozone Layer & The Montreal Protocol on Substances that Deplete the Ozone Layer, Kenya, 2009.

Velazco, V. A., Toon, G. C., Blavier, J.-F. L., Kleinböhl, A., Manney, G. L., Daffer, W. H., Bernath, P. F., Walker, K. A., and Boone, C.: Validation of the Atmospheric Chemistry Experiment by noncoincident MkIV balloon profiles, *J. Geophys. Res.*, 116, D06306, 10.1029/2010jd014928, 2011.

Velders, G. J. M., Andersen, S. O., Daniel, J. S., Fahey, D. W., and McFarland, M.: The importance of the Montreal Protocol in protecting climate, *Proceedings of the National Academy of Sciences*, 104, 4814-4819, 10.1073/pnas.0610328104, 2007.

## References

Velders, G. J. M., Fahey, D. W., Daniel, J. S., McFarland, M., Andersen, S. O.: The large contribution of projected HFC emissions to future climate forcing. *Proceedings of the National Academy of Sciences*. 2009.

Volk, C. M., Elkins, J. W., Fahey, D. W., Dutton, G. S., Gilligan, J. M., Loewenstein, M., Podolske, J. R., Chan, K. R., and Gunson, M. R.: Evaluation of source gas lifetimes from stratospheric observations, *J. Geophys. Res.*, 102, 25543-25564, 10.1029/97jd02215, 1997.

Waugh, D. W., and Hall, T. M.: Age of stratospheric air: Theory, observations, and models, *Rev. Geophys.*, 40(4), 1010, doi: 10.1029/2000RG000101, 2002.

Wayne, R. P., *Chemistry of the Atmospheres: Third Edition*, Oxford University Press, Oxford, 403, 2000a

Wayne, R. P., *Chemistry of the Atmospheres: Third Edition*, Oxford University Press, Oxford, 12, 2000b

Wayne, R. P., *Chemistry of the Atmospheres: Third Edition*, Oxford University Press, Oxford, 219, 2000c

Wayne, R. P., *Chemistry of the Atmospheres: Third Edition*, Oxford University Press, Oxford, 224, 2000d

Wayne, R. P., *Chemistry of the Atmospheres: Third Edition*, Oxford University Press, Oxford, 245, 2000e

Zander, R., Gunson, M. R., Farmer, C. B., Rinsland, C. P., Irion, F. W., and Mahieu, E.: The 1985 chlorine and fluorine inventories in the stratosphere based on ATMOS observations at 30° north latitude, *Journal of Atmospheric Chemistry*, 15, 171-186, 10.1007/bf00053758, 1992.

Zander, R., Mahieu, E., Gunson, M. R., Abrams, M. C., Chang, A. Y., Abbas, M., Aellig, C., Engel, A., Goldman, A., Irion, F. W., Kämpfer, N., Michelson, H.

## References

A., Newchurch, M. J., Rinsland, C. P., Salawitch, R. J., Stiller, G. P., and Toon, G. C.: The 1994 northern midlatitude budget of stratospheric chlorine derived from ATMOS/ATLAS observations, *Geophys. Res. Lett.*, 23, 2357-2360, 10.1029/96gl01792, 1996.